[redacted]

REFERENCE NO. 63 1467

C/30 COPIES

SINGLE COPY ONLY

LUNAR ORBIT RENDEZVOUS REFERENCE TRAJECTORY DATA PACKAGE (U)

PREPARED UNDER CONTRACT NO. 10001
TO BELLCOMM, INC.

C7-257

SUMMARY AND REFERENCE TRAJECTORY DATA EXHIBITS

ISSUE I
VOLUME 1

JUNE 30, 1963
8408-6013-RC-000

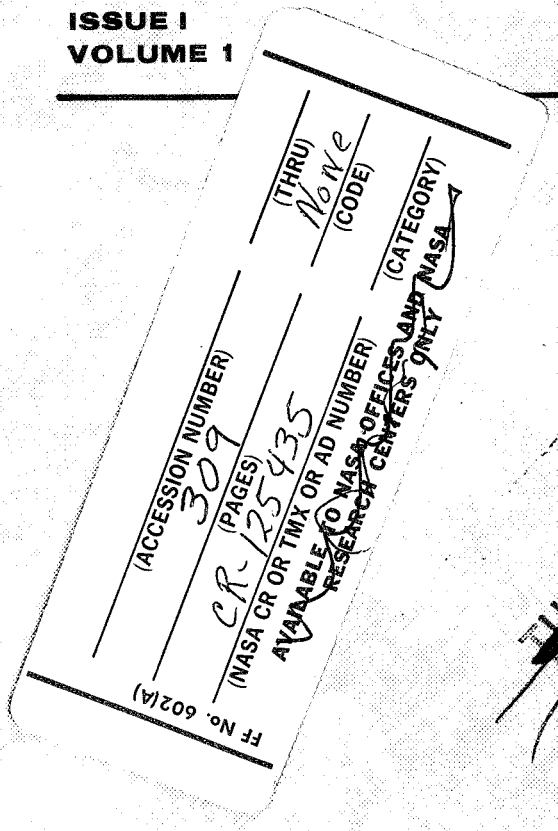

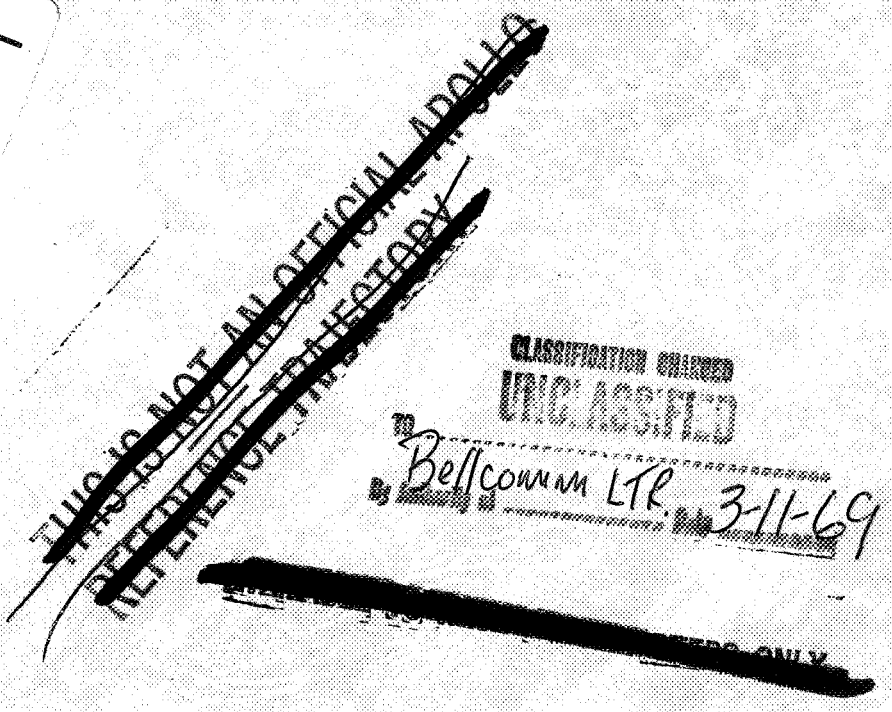

[redacted]

SPACE TECHNOLOGY LABORATORIES, INC.
a subsidiary of Thompson Ramo Wooldridge Inc.
ONE SPACE PARK • REDONDO BEACH, CALIFORNIA

(NASA-CR-125435) LUNAR ORBIT RENDEZVOUS REFERENCE TRAJECTORY DATA PACKAGE. VOLUME 1, ISSUE 1: SUMMARY AND REFERENCE TRAJECTORY DATA EXHIBITS (Space Technology Labs., Inc.) 309 p

N79-71925

Unclas
00/13 12163

[redacted]

[redacted] ERENCE NO. 63 1467

30 COPIES

LUNAR ORBIT RENDEZVOUS REFERENCE TRAJECTORY DATA PACKAGE (U)

PREPARED UNDER CONTRACT NO. 10001
TO BELLCOMM, INC.

SUMMARY AND REFERENCE TRAJECTORY DATA EXHIBITS

[redacted] THIS IS NOT AN OFFICIAL APOLLO [redacted]

ISSUE I

VOLUME I

June 30, 1963

8408-6013-RC-000

Edward M Boughton

E. M. Boughton
Project Manager

Approved: R M Page

R. M. Page
Manager,
Systems Analysis Department

[redacted]

Space Technology Laboratories, Inc.
One Space Park
Redondo Beach, California

[redacted] CONFIDENTIAL [redacted]

CONTENTS

ACKNOWLEDGEMENTS

INTRODUCTION AND SUMMARY

REFERENCE TRAJECTORY DATA PACKAGE

1.0 Mission Profile

- 1.1 Introduction
- 1.2 Earth Launch and Translunar Injection
- 1.3 Translunar Flight
- 1.4 Hyperbolic Deboost and LEM Descent Operations
- 1.5 LEM Ascent and Rendezvous Operations
- 1.6 Transearth Injection
- 1.7 Transearth Flight
- 1.8 Re-entry and Landing

2.0 Sequence of Trajectory Events

- 2.1 Introduction
- 2.2 Events Schedule

3.0 Summary of Input Information

- 3.1 Introduction
- 3.2 System Configuration
  - 3.2.1 Launch Vehicle
  - 3.2.2 Spacecraft
  - 3.2.3 Ground Stations
- 3.3 System Constraints
  - 3.3.1 Launch Vehicle
  - 3.3.2 Spacecraft
  - 3.3.3 Ground Stations
  - 3.3.4 Trajectory

4.0 Summary of Trajectory Ground Rules

- 4.1 Introduction
- 4.2 Launch
- 4.3 Parking Orbit and Translunar Injection
- 4.4 Translunar Trajectory
- 4.5 Circumlunar Trajectory
- 4.6 LEM Operations
- 4.7 Transearth Injection
- 4.8 Transearth Trajectory
- 4.9 Re-entry and Landing
- 4.10 General

5.0 Summary of Trajectory Data

5.1 Introduction
5.2 Earth Launch and Translunar Injection
5.3 Translunar Flight
5.4 Hyperbolic Deboost and Equiperiod Maneuver
5.5 LEM Descent and Ascent
5.6 Rendezvous
5.7 Transearth Injection and Return
5.8 Re-entry

6.0 Launch Windows and Vehicle Performance Studies

6.1 Introduction
6.2 Free Return Launch Opportunities
6.3 Lunar Landing, LOR, and the Constrained Return Problem
6.4 Powered Flight Optimization
6.5 Launch Window Duration and Effects of Powered Flight Performance
6.6 Re-entry Studies

7.0 Range Safety Maps

7.1 Introduction
7.2 Graphical Data

8.0 Communication and Tracking Data

8.1 Introduction
8.2 Graphical Data

9.0 Earth and Lunar Landing Site Maps

9.1 Introduction
9.2 Graphical Data

10.0 Midcourse Sensitivities and Guidance Analysis Coefficients

10.1 Introduction
10.2 Tabular Data

APPENDIX

REFERENCES

ACKNOWLEDGEMENTS

The following personnel have contributed to the preparation of this report:

Austgen, D. M.
Bahrke, W. P.
Baker, F. L.
Boughton, E. M.
De Salvio, A. J.
Dethlefsen, D.
Erwin, D. B.
Furtkamp, D. C.
Hanson, G. J.
Herbaugh, J. A.
Hite, R. E.
Johnson, R.
King, G.
Lipinski, P. R.
Penzo, P. A.
Peterson, N. W.
Poppe, R. M.
Sands, T. A.
Senda, O.
Shinkle, R. D.
Stableford, C. V.
Werts, D. D.

INTRODUCTION AND SUMMARY

In accordance with the schedule of deliverable items under Contract 10001 to Bellcomm, Inc., Space Technology Laboratories, Inc., is pleased to submit a second Apollo mission reference trajectory and associated documentation. This document, the second quarterly publication of the LOR RTDP (Lunar Orbit Rendezvous Reference Trajectory Data Package), consists of four volumes:

Volume 1 - Summary and Reference Trajectory Data Exhibits

Volume 2 - Printout Key and Reference Trajectory Listing

Volume 3 - Reference Trajectory Listing Continued

Volume 4 - Reference Trajectory Listing Concluded

The LOR RTDP is to include at each issue, current knowledge of the Apollo mission systems, the incorporation of that data into computer program development, an Apollo trajectory calculation, and the exhibition of trajectory output data. Concurrent with LOR RTDP development, various studies of mission definition and trajectory analysis are extending quantitative knowledge about the Apollo system. Results of these studies, relative to the reference trajectory environment, are and will be supporting trajectory development.

Volume 1 of Issue 1 includes a mission profile narrative, a tabular sequence of major trajectory events, system configuration, constraints, and ground rule data, graphical exhibits of some reference trajectory parameters, and a complete section of mission analysis. The mission analysis presentation examines the range of given launch dates (in this case, January 29 through February 3, 1968), vehicle performance capability, and earth-moon geometries, to show the relationships among these parameters and the launch window; subject to the major constraint that all outbound trajectories "free return" to earth with acceptable re-entry conditions. From this assembly of permissible conditions, the documented reference trajectory has been chosen. The Issue 1

national defense of the United States within the meaning of the espionage laws, Title 18, U.S.C., Sections 793 and 794. The transmission or the revelation of its contents in any manner to an unauthorized person is prohibited by law.

reference trajectory is approximately in middle ground between the least and most ambitious mission with respect to vehicle performance required.

Volumes 2, 3, and 4 include the printout key and machine listing of the reference trajectory. Since publication of Issue 0, the printout format has been revised both in complexion and content. Although two different computer programs are used in the simulation (SNS program and MVNS program), their printout formats are essentially identical. Secondly, the print logic has been modified so that certain parameters which become unimportant or meaningless in certain trajectory phases, are arranged in blocks and automatically deleted from the print. The net result of these modifications is a more tractable and compressed output without loss of informational content.

The Issue 1 reference trajectory differs from the previous publication in two basic areas. First, the outbound leg has been targeted in such a way that it returns to earth with acceptable re-entry conditions. As shown in Section 6.0, this criterion permits an infinity of acceptable outbound trajectory profiles as long as the earth landing site is not specified. The second major change is that the prescribed lunar landing site has been removed from the equator to 3 degree South latitude. Longitude remains the same at 28 degree West. The non-equatorial landing site specification introduces a number of complications which an equatorial site obviates. Since yaw steering is not permitted in either the equiperiod maneuver or the LEM descent to the lunar surface, the circular lunar orbit produced by the Service Module must be so arranged that its plane contains the landing site at approximately the moment of LEM touchdown. But since this condition is fulfilled by an infinity of certain combinations of circular orbit node and inclination, it remains to adopt that combination which results in a modest velocity demand on the SM during the circularization phase and also during the maneuver to return to earth. In other words, whereas an equatorial landing site requires only one spatial orientation of the circular orbit, a non-equatorial site allows many possible orientations from which to choose.

Two notable flight profile changes have been made from the Issue 0 reference trajectory; first, in the Saturn V second and third stage treatment and second, in the LEM descent profile to the lunar surface. At Saturn V

second stage ignition a vehicle attitude is determined such that, in combination with an inertial pitch rate equal in both the second and third stages, a maximum burnout weight is injected into the parking orbit. The previous trajectory was optimized by not changing the second stage ignition attitude and determining differing pitch rates in the upper stages. The LEM descent profile is now shaped so as to satisfy velocity and vehicle attitude constraints at altitudes of 10000, 1000, 200 and zero feet. Previously, the trajectory was constrained only at 300 and zero feet. Other notable features of the Issue 1 reference trajectory are:

1. In the absence of detailed flight profile constraints data (e.g., aerodynamic pressure and heating limits) and guidance equations, all powered flight operations were optimized with respect to the flight profile for maximum burnout weight.

2. Liftoff time at Cape Canaveral and coast time in earth parking orbit were chosen so as to satisfy given mission constraints including free return and result in a hyperbolic orbit with respect to the moon which has a selenographic inclination of approximately 171.48 degrees.

3. Yaw steering in the SM deboost phase and LEM rendezvous phase was employed to land at the lunar site (latitude 3^{o}S, longitude 28^{o}W) and effect coincidence with the CM/SM orbit, respectively.

4. LEM stay time on the moon of approximately 8 hours was used to allow acceptable geometry to develop between the CM/SM orbit and the earth landing site at Woomera, Australia.

5. Earth re-entry conditions were targeted such that landing occurs at Woomera, Australia without the necessity of midcourse trajectory adjustments.

1.0 Mission Profile

1.1 Introduction

The paragraphs below present a general description of the three-man Apollo lunar orbit rendezvous mission profile. Each major phase of the reference trajectory, as currently designed to accomplish the mission, is discussed in chronological order and related to the manner in which the Saturn V and its spacecraft are operated. Because the mission profile has been accommodated without knowledge of guidance and attitude control modes, the mission description is largely the result of a mathematically satisfactory solution to the Apollo LOR problem. Specifically, stage flight profiles were generated so as to comply with intermediate constraints and boundary conditions in an approximately optimal fashion. Attitude control system experience, except where an assumed fluids budget was specified, is unknown, and does not appear in the mission profile description. This is particularly true of vehicle operations during lunar deboost, rendezvous and return injection, where out-of-plane maneuvers have been simulated without knowledge of guidance constraints. Therefore, all mission phases have been accomplished within the known mission constraints and capabilities of major propulsion systems.

1.2 Earth Launch and Translunar Injection

The earth launch and translunar injection portions of the LOR reference trajectory consist of S-V vehicle powered flight and a parking orbit (Figure 1.2-1).

Powered flight consists of four separate burn phases: the S-IC, S-II, and S-IVB first and second burns. The S-IC burn period is initiated at a prescribed time of day and begins with a twelve second vertical ascent followed by an instantaneous rotation of the body axis and velocity vector. A gravity turn trajectory profile is flown from pitch over to the burnout of the S-IC stage (prescribed by propellant depletion).

The S-II burn phase is initiated 1.5 seconds after S-IC engine shut-down and is characterized by an instantaneous rotation upward of the body axis

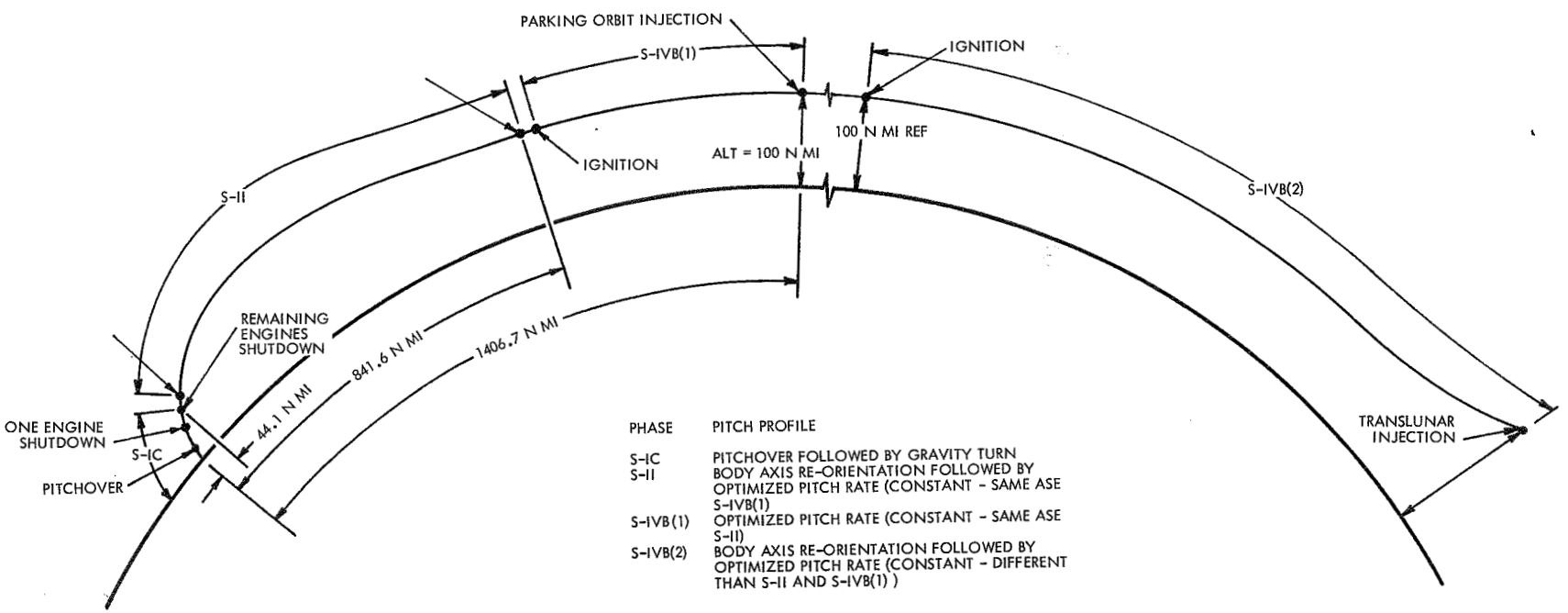

Figure 1.2-1. Earth Launch to Translunar Injection

followed by a constant pitch rate for the burning duration of the S-II stage (prescribed by propellant depletion). At predetermined times after S-II ignition, the launch escape system and the SIC/S-II interstage are jettisoned.

The S-IVB first burn phase is initiated 1.5 seconds after S-II engine shutdown and is flown at the same constant pitch rate as that of the S-II stage. The S-IVB first burn is terminated at achievement of 100 nautical mile circular parking orbit conditions.

The parking orbit duration, which is constrained to be greater than 1.5 revolutions, is terminated for realization of satisfactory conditions at approach to the moon. The parking orbit is characterized by a body axis orientation pitch profile which retains the body axis aligned along the velocity vector.

The S-IVB second burn is initiated at termination of the parking orbit and the duration of the burn is dictated by the mission constraints and the position of the moon. This burn phase begins with a reorientation of the body axis to a particular attitude and a constant pitch rate program is then flown for the remainder of the phase. The S-IVB stage is jettisoned 3 hours after injection.

1.3 Translunar Flight

After achieving S-IVB burnout conditions which result in a lunar approach hyperbola having a pericynthion altitude of approximately 80 nautical miles, the free flight trajectory proceeds to the moon. Three hours after injection the S-IVB stage is jettisoned and 2 hours later the first midcourse correction is made. Although the reference trajectory does not nominally require midcourse corrections, SM propellant is jettisoned non-impulsively at three different times in order to simulate the weight loss which would have occurred. At approximately 73.4 hours from injection, the spacecraft is prepared for deboost into a circular lunar orbit. The uncorrected translunar trajectory, when integrated through pericynthion passage, "free returns" to earth with a re-entry angle of 96.6 degrees at 400,000 feet.

1.4 Hyperbolic Deboost and Equiperiod Maneuver

The salient trajectory features of this phase of the mission are presented schematically in Figures 1.4-1 and 1.4-2. A reasonably accurate scale is maintained in the diagram.

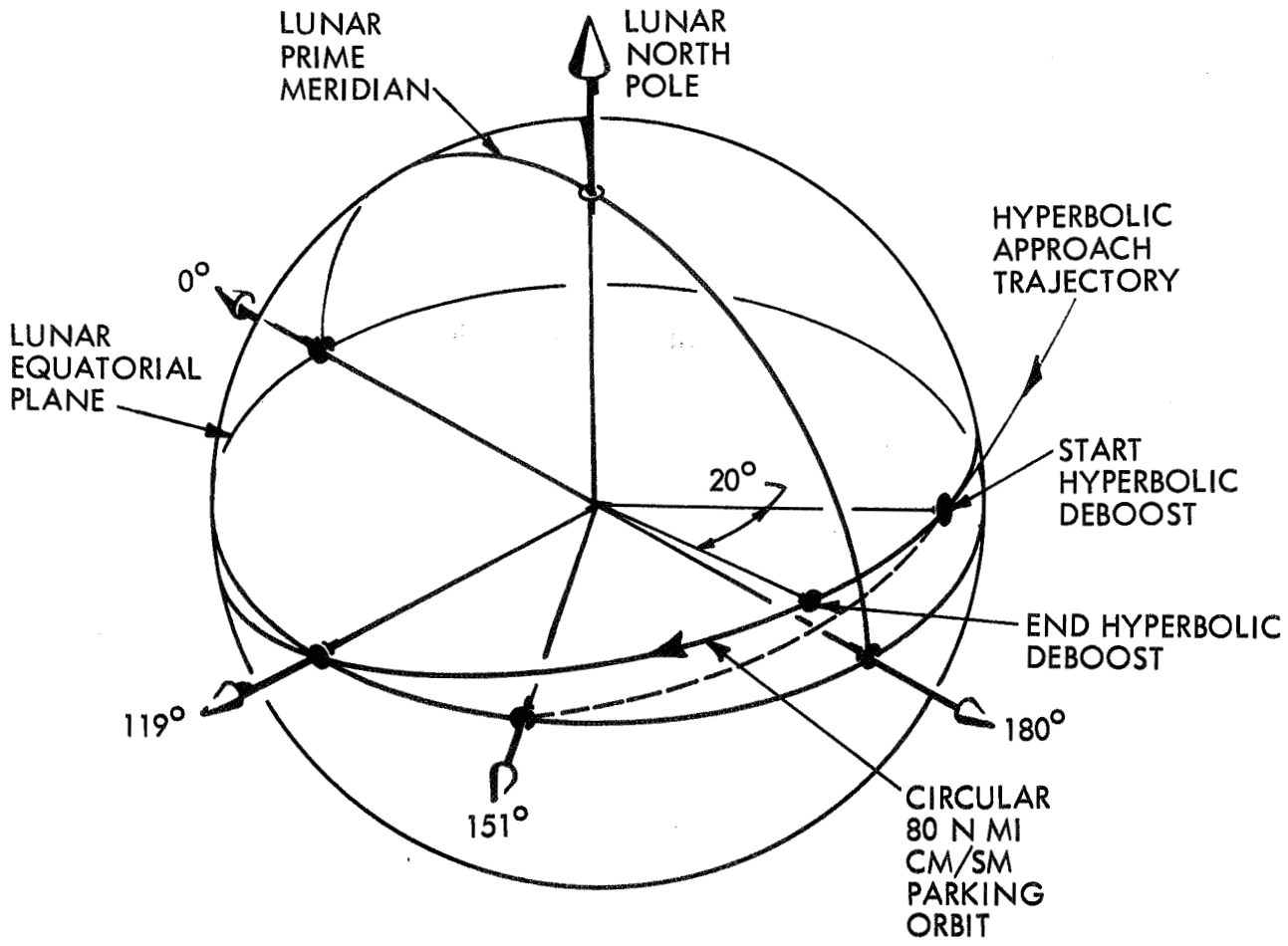

Figure 1.4-1. Hyperbolic Deboost Phase

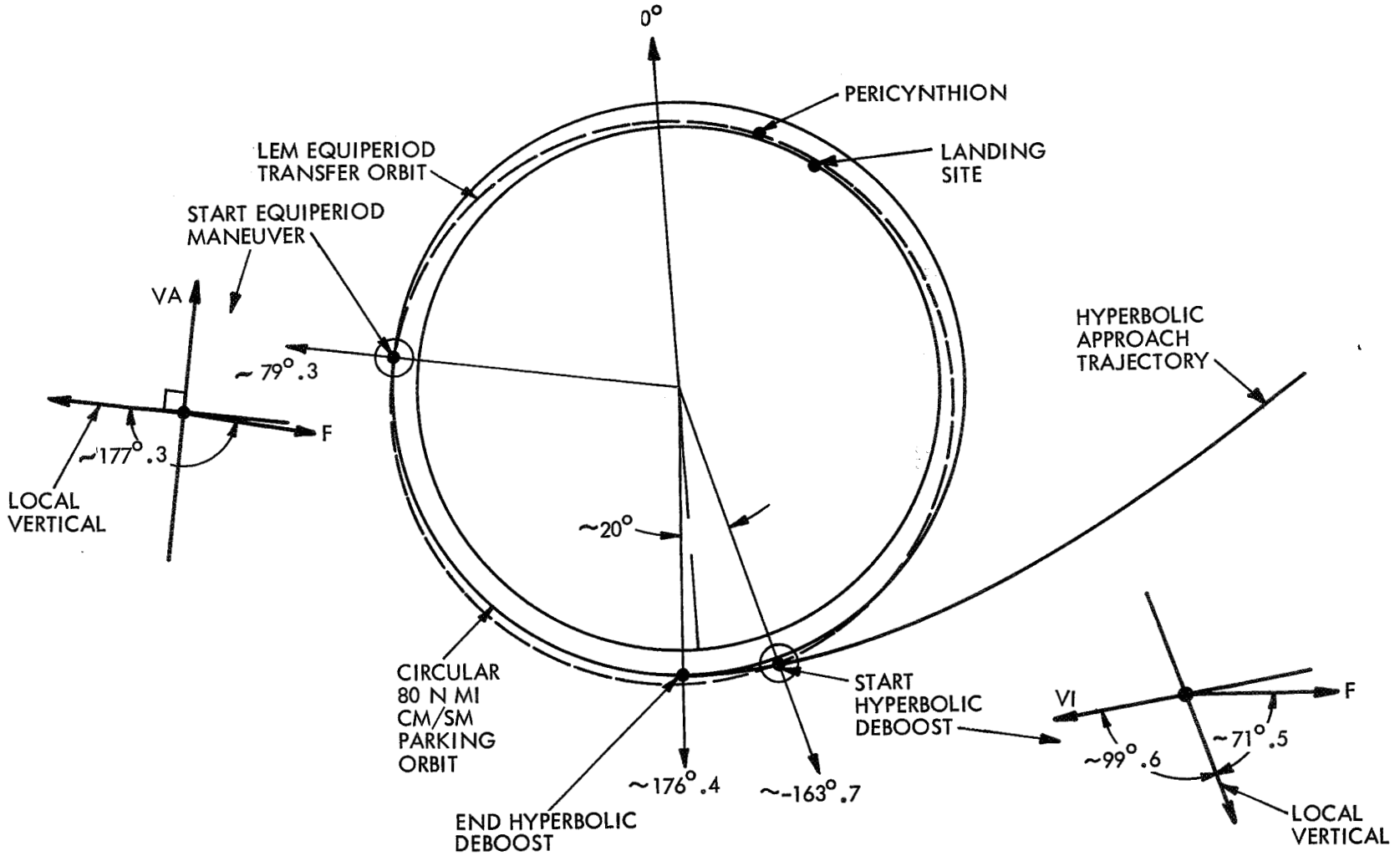

Figure 1.4-2. Hyperbolic Deboost and Equiperiod Maneuver - Projection in CM/SM Orbital Plane

In general terms, the profile consists of deboost from the hyperbolic approach trajectory to an 80 nautical mile circular parking orbit, coast in the parking orbit, injection of the LEM into an elliptical transfer orbit with a pericynthion altitude of 50,000 feet and a period equal to that of the circular parking orbit, and LEM coast in the equiperiod orbit. Subsequent to these maneuvers is the final LEM descent to the surface, which is constrained to be an in-plane descent from pericynthion of the equiperiod orbit. The actual descent profile is established outside of the reference trajectory; and it is considered to be constant, except for fine adjustments due to small variations in the initial conditions. It follows, then, that the maneuvers leading up to the descent must establish the correct geometrical situation to insure a landing at the prescribed lunar site (28°W, 3°S).

The hyperbolic approach trajectory is inclined approximately 171.5 degrees to the lunar equator, but its node is so placed that an in-plane deboost will not permit landing at the specified site. In order to achieve an 80 nautical mile circular parking orbit which passes directly over the landing site during LEM descent, it is necessary to make a plane change of nearly 5 degrees during hyperbolic deboost. (A ground track of the resulting orbit is given in Figure 5.4-8. It should be noted that this orbit passes directly over the landing site on the third revolution.) The plane change is accomplished with a constant yaw attitude, while the initial pitch attitude, initiation point, and burning time are controlled to meet the circular orbit conditions at burnout ($h \doteq 80$ n. mi., $\gamma = 0$, $\frac{rv^2}{\mu} = 1$).

The spacecraft coasts in the circular parking orbit in excess of one revolution prior to LEM separation making one pass across the visible side of the moon. The subsequent equiperiod maneuver places the LEM in an elliptical transfer orbit. The initial pitch attitude and burning time are controlled to meet the pericynthion altitude and equiperiod constraints. The exact time to initiate the equiperiod maneuver is treated as a targeting parameter along with the yaw attitude during hyperbolic deboost. These two quantities are controlled to achieve the correct orientation of the established descent profile and, hence, the prescribed landing site coordinates. The yaw attitude directly affects the

landing site latitude; whereas the equiperiod initiation time shifts the descent profile in the plane of the parking orbit thereby affecting the landing site longitude.

Following equiperiod injection, the LEM coasts in the transfer orbit in excess of one revolution, making one pass over the landing site at close range.

I. 5 LEM Descent and Ascent

The salient trajectory features of this phase of the mission are presented schematically in Figures I. 5-1, I. 5-2, and I. 5-3. A reasonably accurate scale is maintained in the diagrams.

Given the initial conditions (altitude and relative velocity at pericynthion of the equiperiod orbit), a descent profile is established which not only reduces the altitude and velocity to zero within the fuel capabilities of the LEM descent stage, but also meets certain vehicle and velocity constraints imposed at selected altitudes. A throttling capability is assumed and is, in fact, applied in order to satisfy the constraints. The descent proceeds in a series of steps, and a description of each follows.

Step 1 is a descent from pericynthion at a constant pitch rate and maximum thrust level (10, 400 pounds). The initial pitch attitude, pitch rate, and burning time are controlled to achieve a vehicle attitude of 70 degrees to the local vertical at an altitude of 10, 000 feet, with the further restriction that the relative velocity be in the neighborhood of 700 ft/sec (corresponding to a radial component of $\sim$165 ft/sec and a tangential component of $\sim$675 ft/sec).

Step 2 is a descent from 10, 000 feet at a constant pitch attitude and reduced thrust level. The initial pitch attitude, thrust level, and burning time are controlled to reduce the radial velocity component to $\sim$0 ft/sec and the tangential component to $<$75 ft/sec at an altitude of 1000 feet.

Step 3 is a descent from 1000 feet at a constant pitch rate and reduced thrust level. The pitch rate, thrust level, and burning time are controlled to achieve a vertical vehicle attitude and to reduce the tangential velocity component to $\sim$0 ft/sec at an altitude of 400 feet.

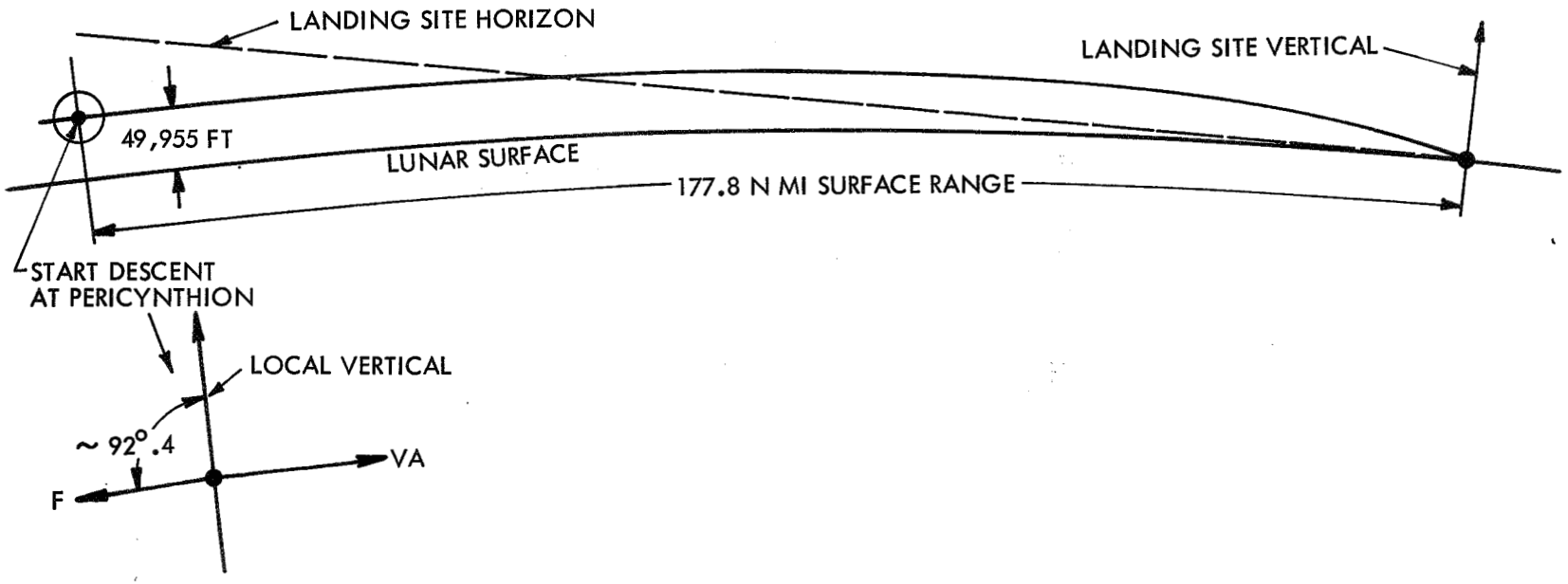

Figure 1.5-1. Descent Phase

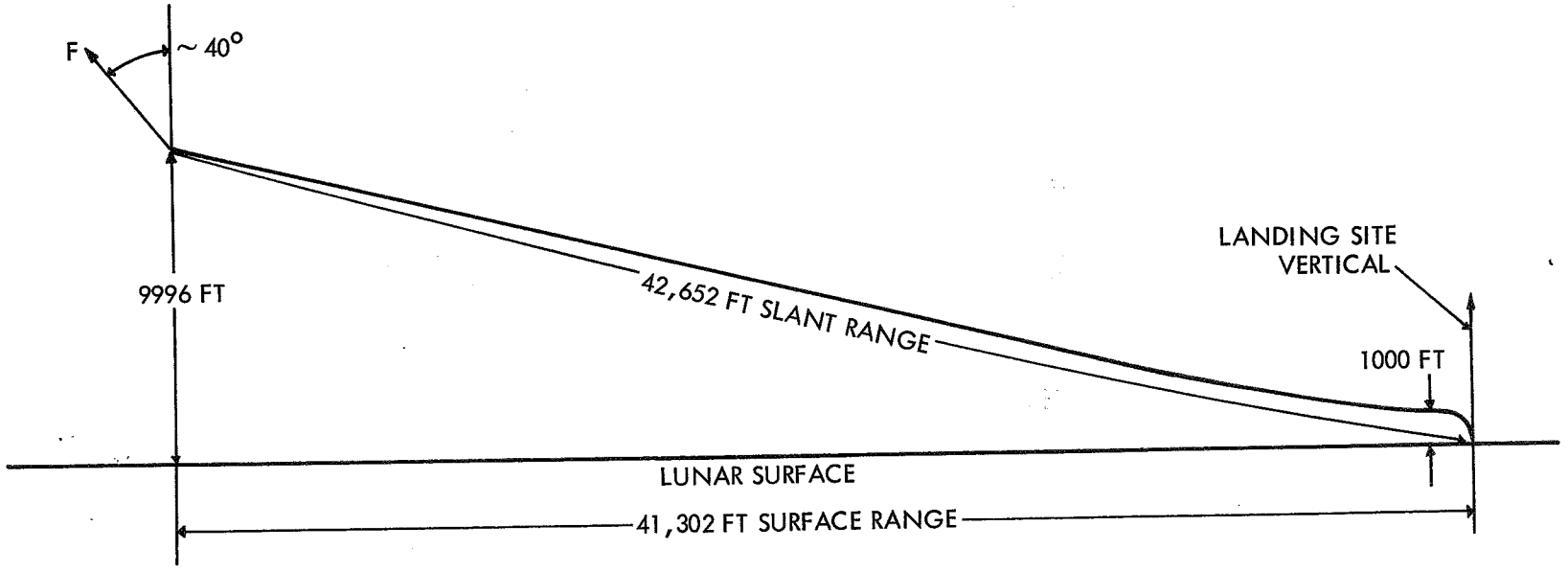

Figure 1.5-2. Descent Phase

CONFIDENTIAL

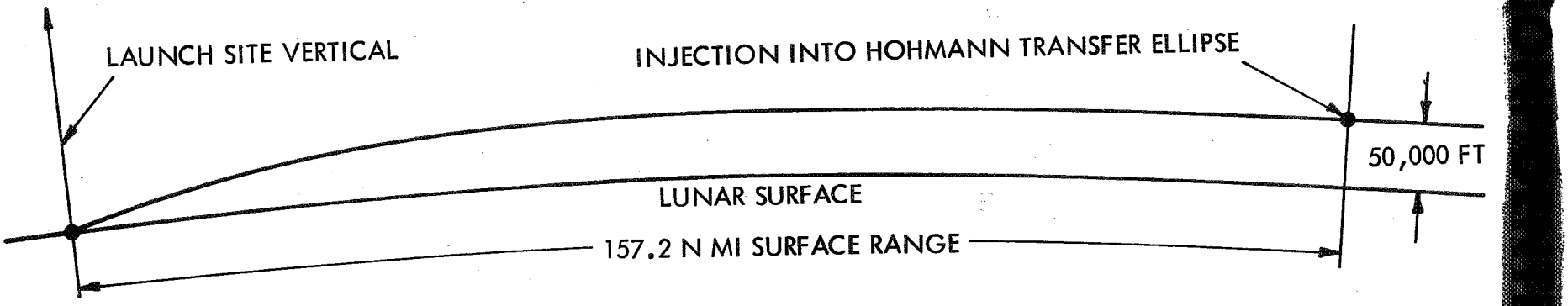

Figure 1.5-3. Ascent Phase - Projection in CM/SM Orbital Plane

Step 4 is a descent from 400 feet at a constant vertical pitch attitude and slightly increased thrust level. The thrust level and burning time are controlled to reduce the radial velocity component to ~0 ft/sec at an altitude of 200 feet.

Step 5 is a descent from the hover condition at 200 feet to touchdown. In order to achieve a landing velocity of ~0 ft/sec, two thrust levels are used within this step, subject to the overall time restriction of ~45 seconds.

In addition to the above restrictions, approximately 2 minutes are allowed for the descent from 1000 feet to touchdown.

The ascent phase consists of the LEM powered flight to an altitude of 50,000 feet, subsequent injection into a Hohmann transfer ellipse with an apocynthion altitude approximately equal to the CM/SM orbital altitude, and LEM coast in the transfer ellipse.

Liftoff from the surface occurs after a stay time of approximately 8 hours (determined from earth return considerations). During this time the landing site has rotated over 4 degrees from the plane of the CM/SM orbit. As a result, a plane change of nearly 2 degrees must be made during ascent in order to make the planes of the CM/SM orbit and Hohmann transfer ellipse coincident.

The LEM powered ascent includes a 1 second vertical rise, a constant high pitch rate program (3 deg/sec), and a combined constant low pitch rate and yaw rate program. The launch azimuth and yaw rate are controlled to reduce to ~0 the out of plane coordinates of the LEM relative to the CM/SM at burnout. This insures coincidence of the orbital planes; and, as it turns out, the out of plane coordinates remain within tolerable limits during the subsequent coast.

The duration of the high pitch rate program, the magnitude of the low pitch rate and burning time are controlled to achieve circular orbit condition ($\frac{rv^2}{\mu}$ = 1) at an altitude of 50,000 feet. The subsequent short burning time increment adds approximately 100 ft/sec to the circular orbit velocity and directly affects the apocynthion altitude of the transfer ellipse. After injection the LEM coasts in the transfer orbit to apocynthion where the rendezvous maneuver

is initiated. The conditions at the termination of this maneuver depend to a large extent upon two quantities at the beginning of the ascent. The burning time increment at 50,000 feet is controlled to reduce the radial coordinate of the LEM relative to the CM/SM and the exact liftoff time is controlled to reduce the tangential coordinate to within a tolerable limit (200 feet). Neither of these quantities have any appreciable effect on the powered ascent profile, so that the simulation is easily facilitated.

1.6 Rendezvous

The salient trajectory features of this phase of the mission are presented schematically in Figures 1.6-1 and 1.6-2. A reasonably accurate scale is maintained in the diagrams.

A short powered flight maneuver is initiated at apocynthion of the Hohmann transfer ellipse with the subsequent injection of the LEM into the CM/SM orbit. The ascent phase parameters are controlled to reduce the relative radial, tangential, and out of plane coordinates to within tolerable limits at the termination of the rendezvous maneuver. The pitch and yaw attitudes and burning time during rendezvous are controlled to reduce the relative velocity components to within tolerable limits (1 ft/sec).

Once rendezvous conditions have been achieved, 30 minutes is allowed for the docking procedure (which is not simulated). At this time it is assumed that the astronauts have been transferred back to the CM. The CM/SM then continued to coast in its parking orbit for a minimum of 100 minutes prior to transearth injection.

1.7 Transearth Injection and Return

It is required that the CM/SM be injected into transearth orbit no sooner than 100 minutes after completion of docking, but as soon as possible thereafter. However, the CM/SM arrives at the injection point considerably sooner than this; and, hence, it must make one more complete orbital revolution, before the start of transearth injection (Figure 1.7-1).

The simulation of the powered flight transearth injection maneuver essentially consists of a constant thrust attitude in the pitch and yaw planes. No other steering is performed during the burn phase.

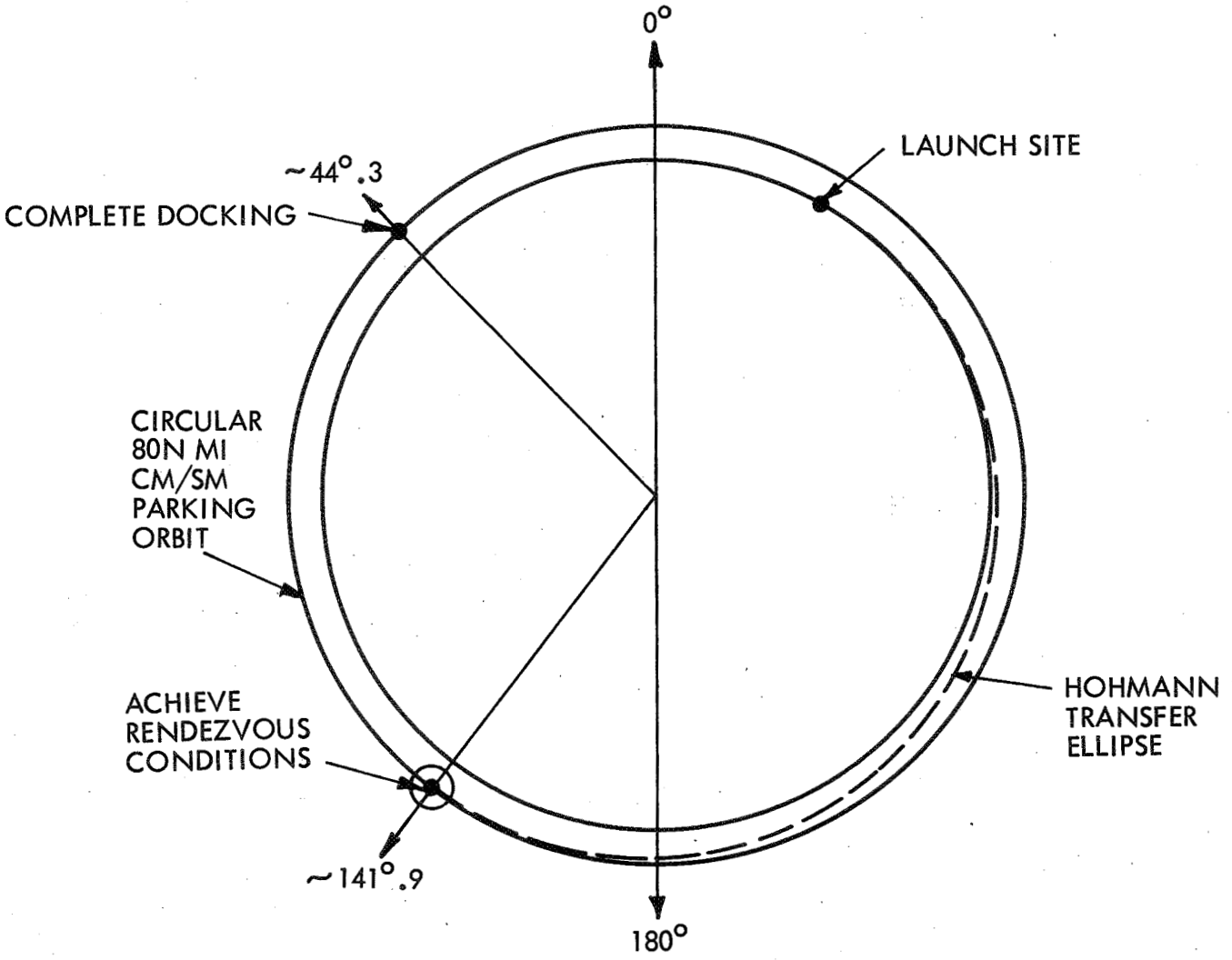

Figure 1.6-1. Rendezvous Phase - Projection in CM/SM Orbital Plane

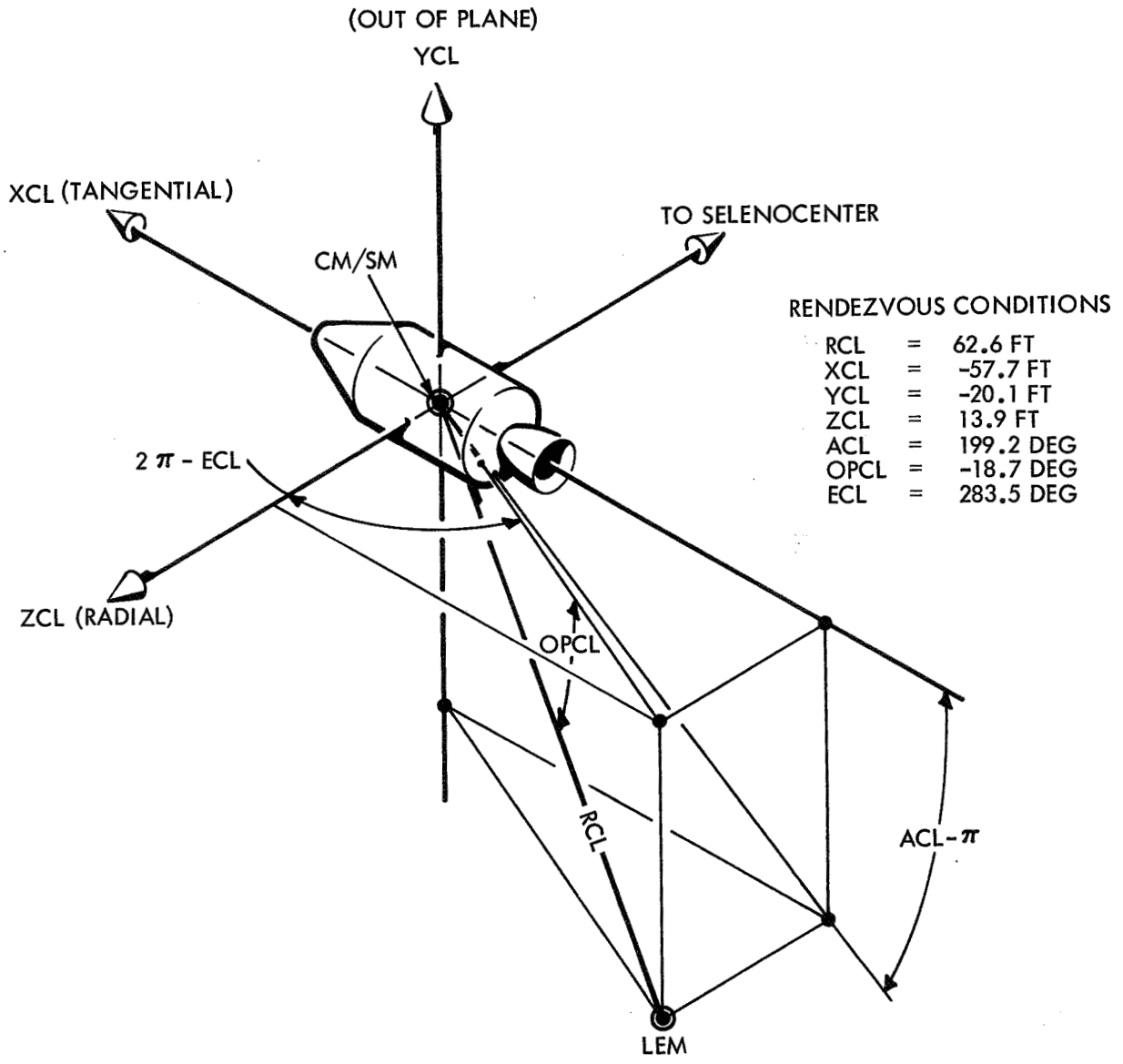

Figure 1.6-2. Rendezvous Phase - Relative Coordinate System

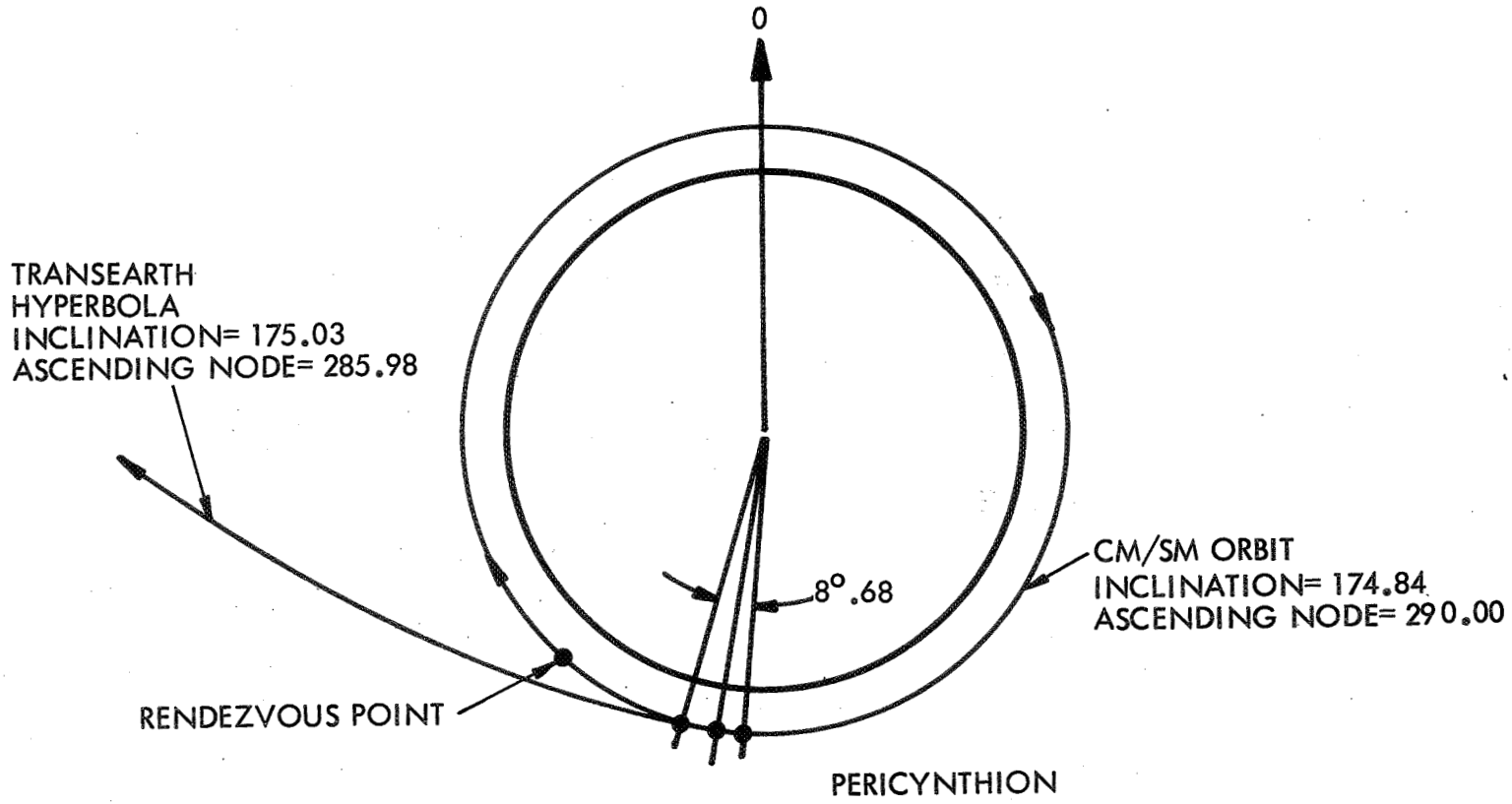

Figure 1.7-1. Transearth Injection

The return phase of the LOR reference trajectory consists of the free flight phase from lunar injection to earth atmospheric re-entry at 400,000 feet altitude. This phase is characterized by a non-impulsive weight loss equivalent to three midcourse maneuvers at predetermined times during the transearth free flight trajectory.

1.8 Re-entry to Landing

Entry is defined to begin at 400,000 feet altitude with a nominal inertial flight path angle of 6.4 degrees below the local horizontal (but not restricted to this angle). Inertial velocity is approximately 36,180 feet per second. A maximum lift of +0.4 times drag during the initial phase causes a maximum deceleration of 5.5 g's at the pull-up. This is well below the 10 g limit, as is the maximum deceleration of 7.9 g's during the final phase of re-entry. The L/D ratio is held at a constant value of +0.017736 from the pull-up to landing, giving a total maneuver angle during re-entry of 41 degrees.

2.0 Sequence of Trajectory Events

2.1 Introduction

A sequence of trajectory events in tabular form has been prepared which denotes the major mission events and important trajectory simulation occurrences. By comparing the date and GMT with those in the trajectory printout, one may rapidly locate the trajectory history corresponding to any desired mission event. A third time base has been added to this table to show elapsed time in each of the powered flight phases. The trajectory data graphs in Section 5.0 use this convention for reporting time.

2.2 Events Schedule

Table 2.2-I. Sequence of Trajectory Events

Date	GMT	Time From Liftoff (min)	Reference Time (sec)	Event
Earth Launch and Translunar Injection				
3 Feb 1968	$2^h\ 54^m\ 23.0^s$	0.00	0.0	Liftoff in vertical ascent
3 Feb 1968	$2^h\ 54^m\ 35.0^s$	0.20	12.0	Pitch over and start S-IC gravity turn pitch program
3 Feb 1968	$2^h\ 56^m\ 49.0^s$	2.43	146.0	Shutdown inboard S-IC engine
3 Feb 1968	$2^h\ 56^m\ 53.1^s$	2.50	150.1	Shutdown remaining S-IC engines - start coast period
3 Feb 1968	$2^h\ 56^m\ 54.6^s$	2.53	151.6	Jettison S-IC; start S-II ignition. Body axis reorientation. Begin constant pitch rate program
3 Feb 1968	$2^h\ 57^m\ 4.6^s$	2.69	161.6	Jettison launch escape system
3 Feb 1968	$2^h\ 57^m\ 9.6^s$	2.78	166.6	Jettison S-IC/S-II interstage
3 Feb 1968	$3^h\ 3^m\ 28.5^s$	9.09	545.6	Shutdown S-II engines. Begin coast period

Table 2.2-I. Sequence of Trajectory Events (Continued)

Date	GMT	Time From Liftoff (min)	Reference Time (sec)	Event
3 Feb 1968	$3^h\ 3^m\ 30.0^s$	9.12	547.1	Jettison S-II stage; S-IVB first ignition. Continue constant pitch rage program (same as S-II phase)
3 Feb 1968	$3^h\ 6^m\ 6.5^s$	11.73	703.5	Shutdown S-IVB engine. Begin circular parking orbit. Begin body axis orientation pitch rate
3 Feb 1968	$3^h\ 23^m\ 44.5^s$	29.36	1761.5	First parking orbit venting
3 Feb 1968	$3^h\ 41^m\ 22.5^s$	46.99	2819.5	Second parking orbit venting
3 Feb 1968	$3^h\ 59^m\ 0.5^s$	64.63	3877.5	Third parking orbit venting
3 Feb 1968	$4^h\ 16^m\ 38.5^s$	82.26	4935.5	Fourth parking orbit venting
3 Feb 1968	$4^h\ 34^m\ 16.5^s$	99.89	5993.5	Fifth parking orbit venting
3 Feb 1968	$4^h\ 51^m\ 54.5^s$	117.53	7051.5	Sixth parking orbit venting
3 Feb 1968	$5^h\ 9^m\ 32.5^s$	135.16	8109.5	Seventh parking orbit venting
3 Feb 1968	$5^h\ 27^m\ 10.5^s$	152.79	9167.5	Eighth parking orbit venting
3 Feb 1968	$5^h\ 44^m\ 48.5^s$	170.43	10225.5	Ninth parking orbit venting
3 Feb 1968	$6^h\ 2^m\ 26.5^s$	188.06	11283.5	Tenth parking orbit venting
3 Feb 1968	$6^h\ 20^m\ 4.5^s$	205.69	12341.5	Eleventh parking orbit venting
3 Feb 1968	$6^h\ 26^m\ 54.3^s$	212.52	12751.3	S-IVB second ignition S-IVB body axis reorientation to 95.57^o. Begin new constant pitch rate program

Table 2.2-I. Sequence of Trajectory Events (Continued)

Date	GMT	Time From Liftoff (min)	Reference Time (sec)	Event
3 Feb 1968	$6^h\ 32^m\ 16.2^s$	217.89	13073.2	S-IVB engine shutdown. Translunar injection achieved
Translunar Flight				
3 Feb 1968	$8^h\ 32^m\ 16^s$	337.89	20273.2	S-IVB stage separation and jettison
3 Feb 1968	$11^h\ 32^m\ 16^s$	517.89	31073.2	First midcourse (jettison propellant equivalent to 1/3 midcourse delta velocity correction)
3 Feb 1968	$18^h\ 32^m\ 16^s$	937.89	56273.2	Second midcourse (jettison propellant equivalent to 1/3 midcourse delta velocity correction)
4 Feb 1968	$0^h\ 32^m\ 16^s$	1297.89	77873.2	Third midcourse (jettison propellant equivalent to 1/3 midcourse delta velocity correction)
Hyperbolic Deboost and Equiperiod Maneuver				
6 Feb 1968	$7^h\ 58^m\ 27.26^s$	4624.071	0.00	SM ignition/start hyperbolic deboost to circular orbit
6 Feb 1968	$8^h\ 3^m\ 44.85^s$	4629.364	317.58	End hyperbolic deboost/start coast in circular orbit
6 Feb 1968	$10^h\ 38^m\ 50.36^s$	4784.456	9623.10	Separate CM/SM and LEM/transfer 2 astronauts to LEM
6 Feb 1968	$10^h\ 38^m\ 50.36^s$	4784.456	0.00	LEM ignition/start equiperiod maneuver
6 Feb 1968	$10^h\ 39^m\ 19.54^s$	4784.942	29.18	End equiperiod maneuver/start coast in transfer orbit

Table 2.2-I. Sequence of Trajectory Events (Continued)

Date	GMT	Time From Liftoff (min)	Reference Time (sec)	Event
6 Feb 1968	$11^h\ 8^m\ 20.20^s$	4813.953	1769.82	First pericynthion arrival in equiperiod transfer orbit
6 Feb 1968	$13^h\ 10^m\ 50.71^s$	4936.461	9120.30	Second pericynthion arrival in equiperiod transfer orbit
LEM Descent and Ascent				
6 Feb 1968	$13^h\ 10^m\ 50.71^s$	4936.461	0.00	LEM ignition/start final descent to surface with constant pitch rate
6 Feb 1968	$13^h\ 12^m\ 0.18^s$	4937.619	69.48	Enter landing site visibility sphere
6 Feb 1968	$13^h\ 16^m\ 1.17^s$	4941.635	310.44	Change thrust level and vehicle attitude at 10,000 ft/continue descent with constant thrust attitude
6 Feb 1968	$13^h\ 17^m\ 46.23^s$	4943.386	415.50	Achieve hover condition (radial velocity = 0) at 1000 ft/change thrust level/continue descent with constant pitch rate
6 Feb 1968	$13^h\ 18^m\ 28.22^s$	4944.086	457.50	Achieve vertical attitude at 400 ft/ change thrust level/ start constant attitude vertical descent
6 Feb 1968	$13^h\ 18^m\ 49.69^s$	4944.444	478.98	Achieve hover condition at 200 ft/ change thrust level/ continue vertical descent
6 Feb 1968	$13^h\ 19^m\ 14.35^s$	4944.855	503.64	Change thrust level at 75 ft/ continue vertical descent
6 Feb 1968	$13^h\ 19^m\ 29.69^s$	4945.111	519.00	Touchdown on lunar surface

Table 2.2-I. Sequence of Trajectory Events (Continued)

Date	GMT	Time From Liftoff (min)	Reference Time (sec)	Event
6 Feb 1968	$21^h\ 25^m\ 19.65^s$	5430.944	0.00	LEM ignition/ liftoff from lunar surface
6 Feb 1968	$21^h\ 25^m\ 20.65^s$	5430.961	1.00	End vertical rise/ start constant high pitch rate program
6 Feb 1968	$21^h\ 25^m\ 38.39^s$	5431.257	18.78	Continue ascent with constant low pitch rate and yaw rate program
6 Feb 1968	$21^h\ 31^m\ 57.37^s$	5437.573	397.74	End pitch and yaw program at 50,000 ft/ start transfer to Hohmann ellipse
6 Feb 1968	$21^h\ 32^m\ 2.34^s$	5437.656	402.72	End powered ascent/ start coast in Hohmann transfer ellipse
6 Feb 1968	$22^h\ 30^m\ 1.54^s$	5495.643	3881.94	Apocynthion arrival in transfer ellipse
Rendezvous				
6 Feb 1968	$22^h\ 30^m\ 1.54^s$	5495.643	0.00	LEM ignition/ start transfer to CM/SM orbit
6 Feb 1968	$22^h\ 30^m\ 6.29^s$	5495.722	4.75	End powered transfer maneuver/ achieve rendezvous conditions/ start docking procedure
6 Feb 1968	$23^h\ 3^m\ 16.18^s$	5528.886	1994.58	Complete docking/ jettison LEM/ continue coast in CM/SM parking orbit
7 Feb 1968	$0^h\ 43^m\ 16.18^s$	5628.886	7994.58	End minimum stay in parking orbit

Table 2.2-I. Sequence of Trajectory Events (Continued)

Date	GMT	Time From Liftoff (min)	Reference Time (sec)	Event
Transearth Injection and Return				
7 Feb 1968	$2^h\ 23^m\ 21.9^s$	5728.98	0.00	Start burn for injection into transearth orbit
7 Feb 1968	$2^h\ 25^m\ 40.7^s$	5731.29	138.7	Injection into transearth orbit
7 Feb 1968	$2^h\ 25^m\ 40.7$	5731.29	138.7	SM/CM engine shutdown-transearth injection
7 Feb 1968	$7^h\ 25^m\ 41^s$	6031.29	18138.7	First midcourse (jettison propellant equivalent to 1/3 midcourse delta velocity correction)
7 Feb 1968	$14^h\ 25^m\ 41^s$	6451.29	43338.7	Second midcourse (jettison propellant equivalent to 1/3 midcourse delta velocity correction)
7 Feb 1968	$20^h\ 25^m\ 41^s$	6811.29	64938.7	Third midcourse (jettison propellant equivalent to 1/3 midcourse delta velocity correction)
Re-entry to Landing				
9 Feb 1968	$22^h\ 2^m\ 19.9^s$	9787.95	0.00	Re-entry into earth atmosphere
9 Feb 1968	$22^h\ 3^m\ 40.1^s$	9789.28	80.22	First advent of horizontal flight
9 Feb 1968	$22^h\ 7^m\ 35.35^s$	9793.21	315.47	Second advent of horizontal flight
9 Feb 1968	$22^h\ 16^m\ 5.1^s$	9801.70	825.20	Impact

3.0 Summary of Input Information

3.1 Introduction

The summary of input information appearing in this section is based exclusively on data contained in References (1) through (6) as amended by certain minor unpublished changes agreed upon during technical coordination meetings between Bellcomm and STL. The data are divided between system configuration and system constraint information.

System configuration data include all quantitative specifications on vehicle, spacecraft, and ground station operating characteristics. The vehicle weight data given in Table 3.2.1-I essentially represent design goals and not current design status. The degree of detail given is derived as being appropriate for current trajectory simulation purposes and consonant with present evaluation of the system. A deliberate attempt has been made with all configuration data to avoid detail which would suggest an unreasonable system definition accuracy at this point in time. Other system mass characteristics such as centers of gravity and moments of inertia do not appear as input data for several reasons. First, center of gravity data can normally be incorporated in an open loop-trajectory simulation to establish the degree of thrust misalignment required to null upsetting moments caused by c.g. offset and any aerodynamic forces which may be acting. However, since the boost trajectory was specified to be a gravity turn (zero lift), only the effect of drag force coupled with c.g. offset needs to be counteracted. It was decided by Bellcomm and STL that this need not be included in the trajectory since the effect would be small and since there was some question whether the c.g. data available were consistent with the vehicle configuration and weight history to be used. Similar remarks are true in connection with spacecraft operation. Moment and product of inertia data are not included since the trajectory simulation is not concerned with the dynamic response of the vehicle to commanded angular acceleration or velocity. Although somewhat more detailed propulsion data were available, the trajectory has been calculated using nominal values of thrust and specific impulse which have been corrected for atmospheric effects. The effects of thrust buildup and decay and thrust or specific impulse variation in vacuum or at sea level have been neglected by mutual agreement. The

amount of propellant consumed during thrust transient phenomena has been used in mainstage operation. Fluid expenditure by other propulsion subsystems has not been differentiated from mainstage consumption and hence contributes directly to nominal stage performance. Due to considerations noted above the only aerodynamic force evident in the boost trajectory simulation is drag. Normal force coefficient and center of pressure data are obviated by the adoption of a zero lift trajectory. A wind profile during the launch phase was not specified. Data on ground station operating characteristics is thought to be descriptive of current station capabilities but the number and location of stations, together with their performance, is expected to change markedly during the years prior to the Apollo launch schedule.

System constraint data given in paragraph 3.3 are limited to those items which are expected to be representative of all Apollo LOR missions. A separate Section (4.0) has been used to list simulation ground rules which are in effect for this particular reference trajectory.

3.2 System Configuration Data

3.2.1 Launch Vehicle

Between Issue 0 and Issue 1, minor changes have been made in data describing the launch vehicle. Notably, specified stage operating durations have been replaced by useable propellant allocations and stage jettison weights. Further detail has been made available on the composition of vehicle weights as shown in Table 3.2.1-I.

Weight Data

Table 3.2.1-I. Weight Data

			Weight (lb)
1.	S-V Vehicle at Ignition		6,070,907
2.	S-IC hold-down fluid expended		-70,907
	Total	(70,907)	
	Mainstage prop.	70,907	

Table 3.2.1-I. Weight Data (Continued)

				Weight (lb)
3.	S-V Vehicle at liftoff[1]			6,000,000
4.	S-IC fluids consumed			-4,247,690
	Total		(4,247,690)	
	Mainstage prop.	4,227,613		
	Center eng. decay[2]	4,015		
	Outer engs. decay[2]	16,062		
5.	S-V at S-IC burnout			1,752,310
6.	S-IC jettison weight			-363,205
	Total		(363,205)	
	S-IC dry weight	287,000		
	Interstage	500		
	Trapped prop.	45,705		
	Prop. reserves	30,000		
7.	S-V at S-II ignition			1,389,105
8.	S-II fluids consumed[3]			-941,355
	Total		(941,355)	
	Mainstage prop.	919,755		
	Start prop.[4]	4,550		
	Stop prop.[5]	450		
	LES jettison wt.	6,600		
	S-IC/S-II interstage	10,000		
9.	S-V at S-II burnout			447,750
10.	S-II jettison weight			-87,305
	Total		(87,305)	

Table 3.2.1-I. Weight Data (Continued)

			Weight (lb)
	S-II dry weight	72,000	
	Retrorockets	1,500	
	Trapped prop.	8,110	
	Prop. reserves	1,695	
	S-II/S-IVB interstage	4,000	
11.	S-V at S-IVB first ignition		360,445
12.	S-IVB fluids consumed		-231,259
	Total	(231,259)	
	Mainstage prop.	224,495	
	Start prop.[4] (390 + 355 + 316)	1,061	
	Stop prop.[5] (100 + 100)	200	
	Parking orbit boiloff[6]	2,750	
	Parking orbit venting[6]	756	
	Parking orbit attitude cont.[6]	77	
	Roll cont. (13 + 27)	40	
	Launch window prop. allowance	1,880	
13.	S-V at S-IVB second burnout		129,186
14.	S-IVB jettison weight		-31,709
	Total	(31,709)	

Table 3.2.1-I. Weight Data (Continued)

		Weight (lb)
S-IVB dry weight	20,500	
Trapped prop.	750	
Prop. reserves	4,195	
S-IVB/spacecraft interstage	2,750	
Unused att. cont. prop.	14	
Instrument unit	3,500	
15. Allowable spacecraft weight[7]		97,477

Notes:

(1) The trajectory simulation begins at this point in the vehicle weight history.

(2) These amounts of propellant are burned at nominal stage thrust and specific impulse levels.

(3) Includes the weight of the LES and S-IC/S-II interstage which are jettisoned during S-II mainstage operation.

(4) S-II and S-IVB start propellant is assumed to be used at full impulse. S-IVB stage uses 390 lb of propellant during first start. During second start, 355 lb of propellant are used plus 316 lb for engine chilldown.

(5) S-II and S-IVB stop propellant is assumed to be used at full impulse. S-IVB stage uses 100 lb of propellant in both shutdown sequences.

(6) Weight allocations for fluids consumed during the parking orbit are for three revolutions. Actual consumption during the reference trajectory is proportioned according to the time spent.

(7) Based on stipulated vehicle weight at liftoff and not indicative of vehicle performance for the LOR mission. Useful spacecraft weight of 86,500 lb is the design goal and has been used in the reference trajectory.

Propulsion Data

Table 3.2.1-II. Stage Propulsion Data

Stage	Thrust (lbf)	Specific Impulse (lbf-sec/lbm)	Flow Rate[1] (lbm/sec)
S-IC[2]	7.5×10^6 [3]	263.6[3]	28452.200
S-II[2]	1.0×10^6 [4]	426.0[4]	2347.4178
S-IVB	2.0×10^5 [4]	426.0[4]	469.48356

Notes:

[1] Flow rate calculated from given thrust and specific impulse and used as input to the reference trajectory computer program.

[2] Five engines operating - total nozzle exit area of 531.6 ft^2 - sea level atmospheric pressure 14.696 lbf/in^2.

[3] Sea level value

[4] Vacuum value

Aerodynamic Data

The axial force coefficient at zero angle-of-attack is presented in Figure 3.2.1-1. Vehicle reference area is 855.3 ft^2. No other aerodynamic data are used per the discussion in paragraph 3.1.

Atmosphere

The atmosphere model used for establishing S-IC thrust variation with altitude is the ARDC 1959 model.

Launch Vehicle Configuration

A sketch of the Saturn S-V launch vehicle is shown in Figure 3.2.1-2.

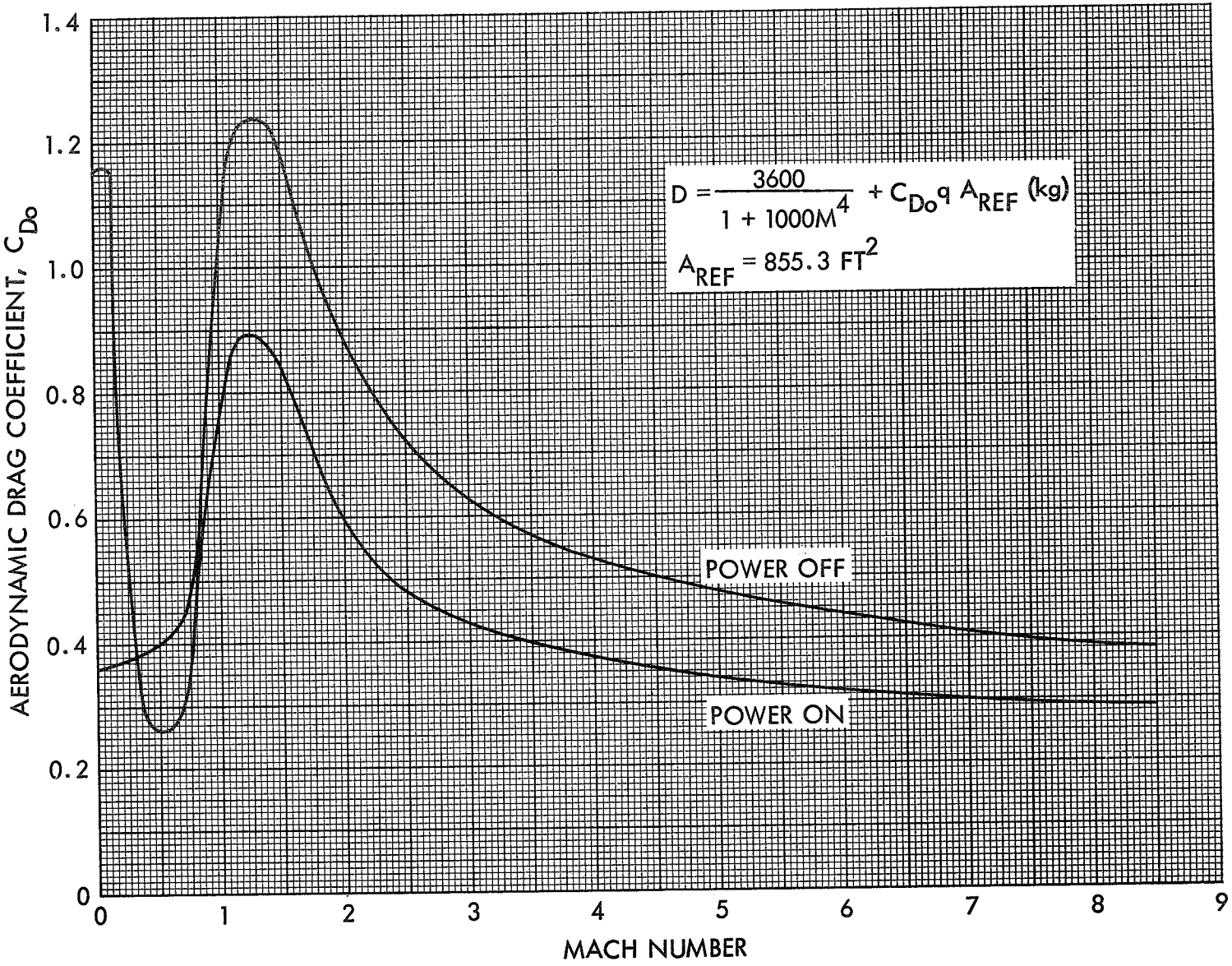

Figure 3.2.1-1. S-V Powered Flight Phase – Zero Angle of Attack Drag Coefficient

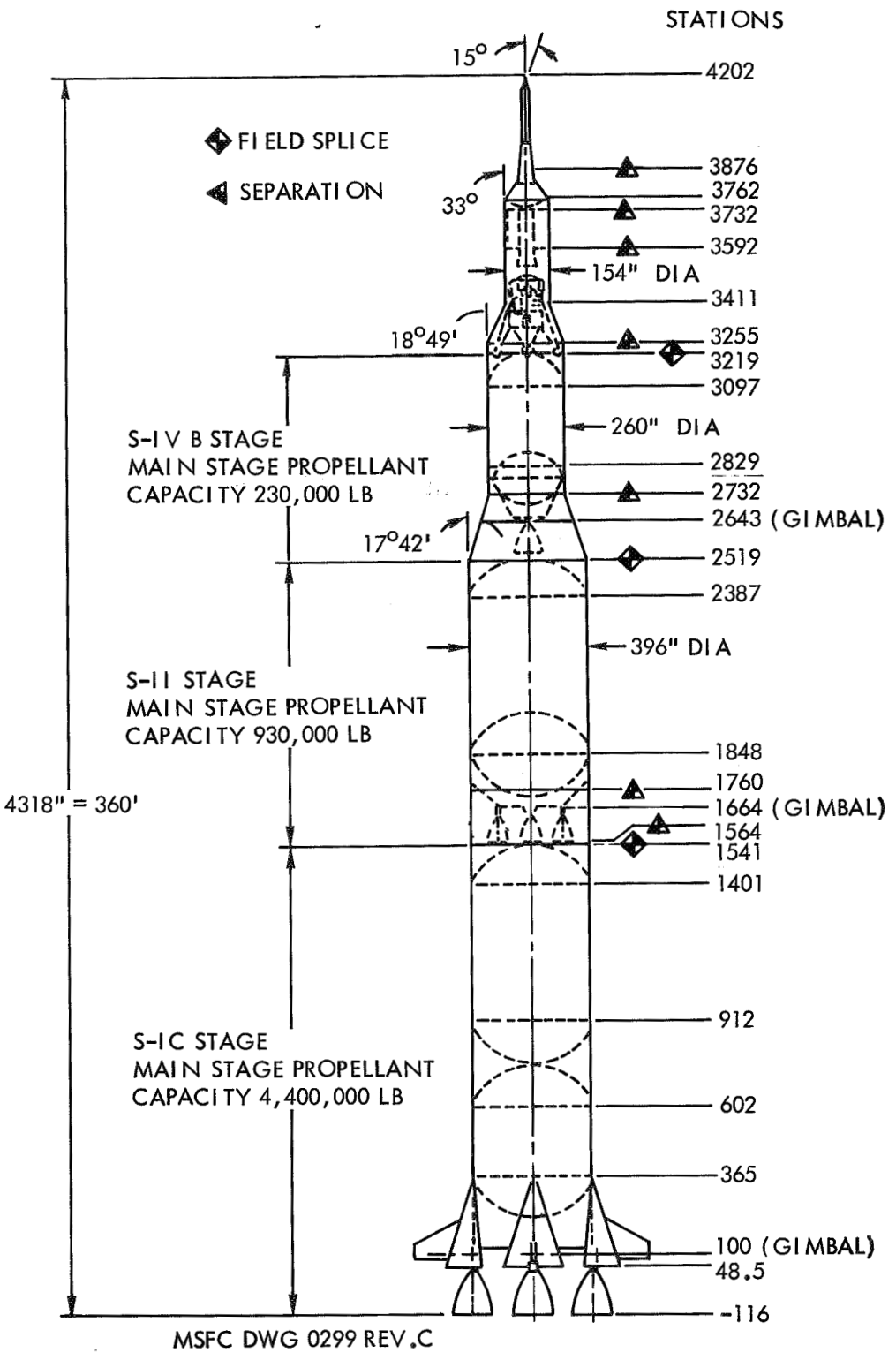

Figure 3.2.1-2. S-V Vehicle Reference Dimensions

CONFIDENTIAL
Title law.

Launch Site Location

Although Reference (5) specifies three potential Saturn V launch pads at Cape Canaveral complex 39:

Pad	Latitude	Longitude	Altitude
A	28° 36'. 4N	80° 36'. 25 W	---
B	28° 37'. 5 N	80° 36'. 25 W	---
C	28° 38'. 5 N	80° 38'. 2 W	---

the launch site coordinates used in Issue 0 have been carried over to Issue I. They are latitude = 28° 37'. 5333 N, longitude = 80° 37'. 2166, altitude = 133. 75 feet.

3. 2. 2 Spacecraft

Spacecraft configuration data has changed somewhat from Issue 0. Useable spacecraft weight has increased by 500 pounds due to addition of weight in the Command Module (+80 pound) and Service Module (+420 pound). Service Module specific impulse was reduced from 318. 7 to 315. 0 lbf-sec/lbm reflecting the nominal minimum value to be expected by using an ablative thrust chamber. Thrust level of the SM was reduced by 500 lbf.

Weight Data

Table 3. 2. 2-I. Weight Data

Module	Item	Weight (lbm)
CM	Structure	8, 840
	Three men @ 176 and equipment @ 44[1]	+660
	Re-entry configuration	9, 500
	Fluid used prior to re-entry	+80
	Liftoff configuration	9, 580
SM	Structure	8, 420
	Residual propellant	+2, 500
	Burnout configuration	10, 920

Table 3.2.2-I. Weight Data (Continued)

Module	Item	Weight (lbm)
	Useful propellant	+39,500
	Liftoff configuration	50,420
LEM	Ascent stage structure	3,800
	Ascent useful propellant	+4,250
	Total ascent stage(1)	8,050
	Descent stage structure	+3,700
	Minimum lunar landing weight(1)	11,750
	Descent stage propellant	+14,750
	Total module weight(1)	26,500
Spacecraft	CM	9,580
	SM	50,420
	LEM	26,500
	Total spacecraft weight	86,500

Note:

(1) In the trajectory simulation, when the LEM separates from the CM/SM, two men and their equipment (440 lbm) are transferred to the LEM and its subtotal weights are increased accordingly.

Propulsion Data

Table 3.2.2-II. Spacecraft Propulsion Data

Module	Thrust (lbf)	Specific Impulse (lbf-sec/lbm)	Flow Rate(1) (lbm/sec)
SM	21,500	315.0	68.253968
LEM			
Descent stage	10,400	310.0	33.548387
Ascent stage	3,000	325.0	9.2307692
CM	---	---	---

Note:

(1) Flow rate calculated from given thrust and specific impulse and used as input to the reference trajectory computer program.

Re-entry Data

CM weight at re-entry = 9500 lb

L/D = 0.4 (in plane and continuously variable)

W/C_DA = 57 lb/ft^2

Re-entry altitude = 400,000 ft

3.2.3 Ground Stations

The Apollo mission will be supported by the Mercury, AMR and DSIF (Deep Space Instrumentation Facility) network stations. The precise complement of stations, their ultimate locations, operating characteristics, and such related data are unknown in the Apollo mission context. The following data are assumed to be applicable at this time.

Station Data

Tracking station locations and performance characteristics, of current interest to the Apollo mission, are listed in Table 3.2.3-I. Performance data have been taken from unpublished memoranda of both STL and Bellcomm and represent present best estimates. However, since station operating data are continually changing and improving, these specifications must be considered tentative.

Earth Figure

The station coordinates given above were computed from the figure of the earth as determined by Fischer. The figure is described by:

a = semimajor axis = 6378.166 km

b = semiminor axis = 6356.784 km

f = flattening = 1/298.3

The altitude is referenced to mean sea level and does not include geodial separation.

3.3 System Constraint Data

This subsection contains all known constraint data on the launch vehicle, spacecraft, ground stations and trajectory. [redacted]

[redacted]

NOMINAL STATION LOCATION	DESIGNATION	RADAR EQUIPMENT	LATITUDE GEODETIC (deg)	LATITUDE GEOCENTRIC (deg)	LONGITUDE (deg)	HEIGHT ABOVE M. S. L. (ft)	MAXIMUM RANGE (n mi)	MINIMUM ELEVATION ANGLE (deg)	MAXIMUM RATES AZIMUTH (deg/sec)	MAXIMUM RATES ELEVATION (deg/sec)
Cape Canaveral, Fla.	MERC. (1)/AMR(1-16)	FPS-16	28.481761	28.320766	-80.576514	44.78	1000	+3	40	30
Grand Bahama Island, B. W. I.	MERC. (1a)/AMR(XN-2)	FPS-16/TPQ-18	26.615781	26.461969	-78.347852	45.93	1000/32000	↓	40/28	30/28
San Salvador Island, B. W. I.	MERC. (1b)/AMR(5-16)	FPS-16	24.118986	23.975795	-74.504078	42.65	1000	↓	40	30
Bermuda	MERCURY (2)	FPS-16	32.347528	32.173843	-64.653556	65.38	1000	↓	40	30
Bermuda	MERCURY (2)	VERLORT	32.347306	32.173621	-64.656861	59.94	6000	↓	50	50
Grand Canary Island	MERCURY (4)	VERLORT	27.735522	27.577320	-15.600006	54.23	5000	↓	50	50
Muchea, Australia	MERCURY (8)	VERLORT	-31.599536	-31.428067	115.927986	298.52	5000	↓	50	50
Woomera, Australia	MERCURY (9)	FPS-16	-30.819311	-30.650278	136.836739	420.04	1000	↓	40	30
Kauai, Hawaii	MERCURY (12)	FPS-16	22.125278	21.991347	-159.671000	3789.36	1000	↓	40	30
Kauai, Hawaii	MERCURY (12)	VERLORT	22.128056	21.994111	-159.670389	3779.52	5000	↓	50	50
Point Arguello, Cal.	MERCURY (13)	FPS-16	34.582903	34.403302	-120.561153	2170.56	1000	↓	40	30
Point Arguello, Cal.	MERCURY (13)	S-BAND	34.581489	34.401891	-120.572014	1586.84		↓		
Guaymas, Mexico	MERCURY (14)	S-BAND	27.958400	27.799352	-110.720794	75.46		↓		
White Sands, N. M.	MERCURY (15)	FPS-16	32.358217	32.184501	-106.369567	4048.87	1000	↓	40	30
Corpus Christi, Tex.	MERCURY (16)	VERLORT	27.655392	27.497499	-97.380256	42.65	5000	↓	50	50
Eglin AFB, Fla.	MERCURY (17)	FPS-16	30.421764	30.254021	-86.798117	91.37	1000	+3	40	30
Goldstone, Cal. (pioneer)	DSIF (1)		35.389628	35.208158	-116.848773	1037.54	> Moon	+5	1	1
Johannesburg, South Africa*	DSIF (5)		-25.887350	-25.736520	27.684780	1381.92	> Moon	+5	1	1
Woomera, Australia	DSIF		-31.382870	-31.212065	136.885020	150.79	> Moon	+5	1	1
Ascension Island, B. W. I.*	AMR (12-16)	FPS-16/TPQ-18	-7.952109	-7.899557	-14.412604	295.88	1000/32000	+3	40/28	30/28
Antigua, B. W. I.	AMR (91-26)	MPS-26/FPQ-16	17.143463	17.035379	-61.792566	124.77	32000/32000	↓	/28	/28
Carnarvan, Australia		MPQ-25	-24.875000	-24.728475	113.708333	246.06		↓		
Carter Cay, Grand Bahama I.	AMR (3A-16)	FPS-16/MPS-25	27.087533	26.931843	-78.000860	37.88	1000/500	↓	40/	30/
Eleuthera Island, B. W. I.	AMR (4.1)	MOD II S-BAND	25.268172	25.119953	-76.312942	123.09	400	↓		
Grand Turk Island, B. W. I.	AMR (7.1)	MOD II/TPQ-18	21.434035	21.303467	-71.145111	82.83	400/32000	↓	/28	/28
Patrick AFB, Fla.	AMR (XN-1)	FPS-16/FPQ-16	28.226908	28.066855	-80.599244	27.13	1000/32000	↓	40/28	30/28
Pretoria, South Africa*	AMR (13-16)	FPS-16/TPQ-18	-25.943107	-25.792045	28.360919	5197.00	1000/32000	↓	40/28	30/28
San Juan, Puerto Rico	AMR (92-16)	FPS-16	18.475230	18.359885	-66.179545	98.30	32000	↓	40	30
Wallops Island, Va.		FPS-16	37.841308	37.655043	-75.485094	40.67	1000	+3	40	30

*Accuracy of coordinates is in doubt.

Table 3.2.3-I. Radar Tracking Station Data

3.3.1 Launch Vehicle

Roll Rate

Maximum roll rate during vertical rise is 1 deg/second initiated 8 seconds after liftoff. Maximum allowable roll angle is 30 degrees.

Acceleration

S-V vehicle sensed acceleration limits are 5.0 g's axially and 1.0 g laterally.

General

Vehicle constraints have not been stipulated for aerodynamic heating and loads limits or pitch rate limits. No staging criteria have been established except at prescribed time intervals following nominal stage propellant depletion.

3.3.2 Spacecraft

Issue 0 of the LOR RTDP included a detailed ΔV budget of allowances for all portions of SM and LEM powered flight operation. These budgets have been deleted from Issue 1 and replaced by the total ideal velocity capability of the modules with their present useful propellant weight and engine performance data. These ideal velocity figures are not to be interpreted as constraints but are merely included as a point of reference for the trajectory and mission analysis discussion.

Table 3.3.2-I. Ideal Velocity Capabilities

Module	ΔV_{ideal} (ft/sec)
SM[1]	---
LEM	
Descent stage	7909.3
Ascent stage	7260.1

Note:

[1] Since the total ΔV available from the SM is dependent on whether or not the LEM is attached, there is no convenient way of stating its capability.

Re-entry Data

The nominal inertial flight path angle at the re-entry altitude is -6.4 degrees.

Re-entry altitude is defined to be 400,000 feet.

At no point in the re-entry trajectory is the acceleration to exceed 10 g.

At no point in the re-entry trajectory is the altitude to exceed 400,000 feet.

The re-entry trajectory is not to exceed a surface range of 5000 nautical miles.

3.3.3 Ground Stations

Applicable constraints on ground station operating characteristics are noted in paragraph 3.2.3.

3.3.4 Trajectory

The following constraints are applicable to the noted trajectory phases although segregation of trajectory constraints and ground rules (see Section 4.0) has been somewhat arbitrary. The constraints listed here are though to be dictated more by vehicle system considerations than by assumptions made to facilitate calculation of a reasonable reference trajectory. Most, but not all, of these constraints are planned to be in effect for all Apollo LOR missions. The reader is invited to consult Section 4.0 for additional information relative to the trajectory.

Launch

a) Launch shall be assumed to take place during the week of January 28 - February 3, 1968, such that the trajectory will provide lunar landing and stay during earth shine.
(Reference trajectory launch takes place on February 3).

b) The minimum acceptable earth launch window is 3 hours.
(Reference trajectory launch window is approximately 4.5 hours).

c) The launch azimuth out of Cape Canaveral shall be between 72 and 108 degrees with desirable values being ≤ 90 degrees.
(The chosen launch azimuth is 90 degrees).

Parking Orbit and Translunar Injection

a) The parking orbit shall have the following elements:

eccentricity ≤ 0.0025

semimajor axis = 3544 n mi (h = 100 n mi)

b) Parking orbit duration shall be between 1 and 3 revolutions.

Translunar Trajectory

a) The nominal trajectory shall be targeted so as to require no mid-course corrections. This trajectory shall circumnavigate the moon and return, uncorrected, to earth with acceptable re-entry conditions.

b) The S-IVB stage shall be jettisoned after CM/SM turnaround.

c) Pericynthion altitude of the uncorrected translunar trajectory shall be 80 nautical miles.

Circumlunar Trajectory

a) The CM/SM/LEM shall pass at least once across the visible side of the moon prior to LEM descent.

b) The CM/SM circular lunar orbit shall have the following elements:

eccentricity < 0.0025

semimajor axis = 1019 n mi (h = 80 n mi)

LEM Operations

a) Pericynthion altitude of the LEM descent orbit shall be 50,000 ± 5000 feet.

b) The LEM shall initiate descent from the CM/SM orbit no sooner than 100 minutes after injection into the circular orbit but as soon as possible thereafter.

c) The LEM shall make one pass in view of the landing site before initiating the landing.

d) LEM stay time on the moon shall be between 4 and 24 hours.

e) The LEM ascent trajectory to the rendezvous point shall be accomplished in two burns. The orbit resulting from the first burn shall not have a pericynthion altitude of less than 50,000 feet.

f) The LEM ascent launch window shall be a minimum of 10 seconds.

Transearth Injection

a) The CM/SM shall make at least one pass across the visible side of the moon after docking and prior to transearth injection.

b) The CM/SM shall be injected into transearth orbit no sooner than 100 minutes after docking but as soon as possible thereafter.

Transearth Trajectory

a) The nominal trajectory shall be targeted so as to require no midcourse corrections.

Re-entry and Landing

a) The nominal earth landing sites shall be within 100 nautical miles of San Antonio, Texas (latitude 29.48° N, longitude 99.00° W), or Woomera, Australia (latitude 29.48° S, longitude 135.00° E).

b) During re-entry (defined to begin at h = 400,000 feet), the altitude of the CM shall not exceed 400,000 feet.

c) During re-entry, deceleration shall not exceed 10 g's.

d) During re-entry, the L/D shall not exceed ±0.4.

4.0 Summary of Trajectory Ground Rules

4.1 Introduction

The included reference trajectory has been computed subject to certain ground rules as enumerated below. An attempt has been made to differentiate between ground rules and Apollo system constraints (see paragraph 3.3.4) in order to classify those assumptions which were made to facilitate or confine the trajectory calculation as compared to characteristics of Apollo system hardware. The following ground rules are applicable to the included trajectory calculation, but may be changed substantially for future issues of the LOR RTDP.

4.2 Launch

a) The S-V ascent trajectory contains no yaw turns.

b) Launch is simulated by a continuous burn.

c) Launch need not take place during daylight hours.

4.3 Parking Orbit and Translunar Injection

a) Parking orbit duration is to be between 1.5 and 2.5 revolutions. (Actual duration is approximately 2 revolutions).

b) Translunar injection is simulated by a continuous burn.

c) If possible, S-IVB injection conditions should be those which result in a free-return circumlunar trajectory.
(S-IVB injection conditions, when integrated through uncorrected circumlunar flight, result in a trajectory which returns to earth with an inertial flight path angle of -6.6 deg. at the re-entry altitude of 400,000 feet).

4.4 Translunar Trajectory

a) SM propellant is to be jettisoned in three steps equivalent to a nominal midcourse ΔV budget of 300 ft/second.

4.5 Circumlunar Trajectory

a) Injection into the circular lunar orbit is simulated by a continuous burn near pericynthion. (Initiation of the deboost maneuver occurs at a position which minimizes the velocity requirement).

b) The CM/SM does not perform orbital change maneuvers while in lunar orbit.

4.6 LEM Operations

a) The LEM is injected into a transfer orbit of period equal to that of the CM/SM orbit. This maneuver is simulated using a continuous burn of the descent stage main propulsion system.

b) Deboost from LEM orbit to lunar landing and LEM ascent are simulated by continuous burns.

c) Injection of LEM into CM/SM orbit at rendezvous is simulated using a continuous burn of the ascent stage main propulsion system.

d) A time of 30 minutes is to be allowed for docking the LEM with the CM/SM.

e) Expenditure of propellant equivalent to 50 ft/sec is allowable for midcourse correction during transfer to rendezvous. (Rendezvous targeting has been accomplished without midcourse corrections).

f) The following intermediate constraints are applicable to the LEM descent to lunar landing flight profile:

1) An "optimum" pitch program (unspecified) is to be used between the altitudes of 50,000 and 10,000 feet.

2) At 10,000 feet, residual velocity is to be approximately 165 ft/sec radially and 675 ft/sec tangentially. Thrust vector attitude is to be approximately 160 deg. counter clockwise from local horizontal.

3) From 10,000 to 1,000 feet, thrust level is to be held constant and thrust vector attitude is to be held fixed at approximately 130 deg. counter clockwise from local horizontal.

4) At 1000 feet, residual velocity is to be zero ft/sec radially and equal to or less than 75 ft/sec tangentially.

5) At 200 feet, residual velocity is to be zero ft/sec both radially and tangentially. Thrust vector attitude is to be vertical upon arrival at 200 feet.

6) The time interval from 200 feet to touchdown is to be approximately 45 seconds.

7) The time interval from 1000 feet to touchdown is to be less than 120 seconds.

(All of the above limitations on the descent flight profile have been adhered to in the reference trajectory).

g) The primary lunar landing site is to be in the vicinity of Lansberg Crater within 0.5 n mi of 3° S latitude and 332° E longitude.
(The reference trajectory landing occurred at a point approximately 200 feet from the prescribed site).

h) Rendezvous is defined to end when the LEM is within 500 feet (line of sight) of the CM/SM. Closing rate of the LEM to CM/SM is to be less than 3 ft/sec at this time.

4.7 Transearth Injection

a) Transearth injection is to be simulated by a continuous burn.

4.8 Transearth Trajectory

a) SM propellant is to be jettisoned in three steps equivalent to a nominal midcourse ΔV budget of 300 ft/second.

4.9 Re-entry and Landing

a) During re-entry, the lift vector is to be varied in the plane of the trajectory within L/D limits of ± 0.4. Resultant out-of-plane components are not to be considered at this time.

4.10 General

a) The trajectory is to be developed so as to maximize payloads within the bounds of known system constraints.

b) The exemplary trajectory is not to take advantage of any unique geometrical properties of earth-moon space except as necessary to accommodate free-return capability.

c) The total mission duration will not exceed 8 days.

d) The reference coordinate system is to be the mean equinox and equator of 1950.0 and trajectory data output will be referenced to the true equinox and equator of date.

5.0 Summary of Trajectory Data

5.1 Introduction

In trajectory and systems analysis work there is a recurring demand for quick comparisons among trajectory parameters throughout their meaningful flight histories. Many such parameters from the reference trajectory are reported in tabular and graphical form in this section.

The mission has been divided into its natural phases and the more important parameters connected with each phase have been selected for display. In order to place the graphical and tabular data in the proper context and by way of overall explanation of the material, Section 1.0, Mission Profile gives a general narrative of each trajectory phase in a chronology consistent with the data presentations.

Data reduction of range safety, communication and tracking, and landing site information can also be found in Sections 7.0, 8.0, and 9.0, respectively.

[redacted]

U.S.C., Section 793 and 794, the transmission or revelation of which in any manner to an unauthorized person is prohibited by

Table 5.2-I. Earth Launch and Translunar Injection - Discrete Events Summary

Time Since Liftoff (sec)	Altitude (ft)	Latitude (deg)	Longitude (deg)	Velocity* (ft/sec)	Flight Path* Angle (deg)	Azimuth Angle (deg)	Pitch Rate* (deg/sec)	Event
0.00	134	28.626	-80.620	1,340.45	0.00	90.00	0.00000	Liftoff
12.00	733	28.626	-80.620	1,345.72	4.76	89.99	0.34973	End Vertical Rise
146.00	188,411	28.622	-79.871	8,524.52	21.12	90.54	gravity turn	Shutdown one S-IC Engine
150.12	201,240	28.621	-79.784	8,984.60	20.63	90.59	0.00000	Shutdown Remaining S-IC Engines
151.62	205,955	28.620	-79.752	8,967.85	20.38	90.61	-12.28125 0.10144	S-II Ignition
161.62	236,458	28.618	-79.531	9,084.93	19.14	90.74	0.10144	Launch Escape System Jettison
166.62	251,173	28.616	-79.419	9,147.92	18.53	90.80	0.10144	S-IC/S-II Interstage Jettison
545.56	609,725	27.450	-64.908	22,488.77	0.38	98.45	0.10144	S-II Engines Shutdown
547.06	609,925	27.437	-64.814	22,488.49	0.35	98.50	0.10144	S-IVB Ignition First Burn
703.51	607,580	25.529	-54.529	25,581.00	0.00	103.38	0.10144	S-IVB Engine Shutdown
703.51	607,580	25.529	-54.529	25,581.00	0.00	103.38	---	Parking Orbit Initiation
12,751.32	589,945	-17.233	-10.359	25,597.71	-0.03	113.13	0.0000	Parking Orbit Termination
12,751.32	589,945	-17.233	-10.359	25,597.71	-0.03	113.13	93.5703 0.04831	S-IVB Ignition Second Burn
13,073.21	958,584	-25.512	14.421	35,675.30	6.56	103.62	0.04831	S-IVB Engine Shutdown Translunar Injection

*Inertial quantity

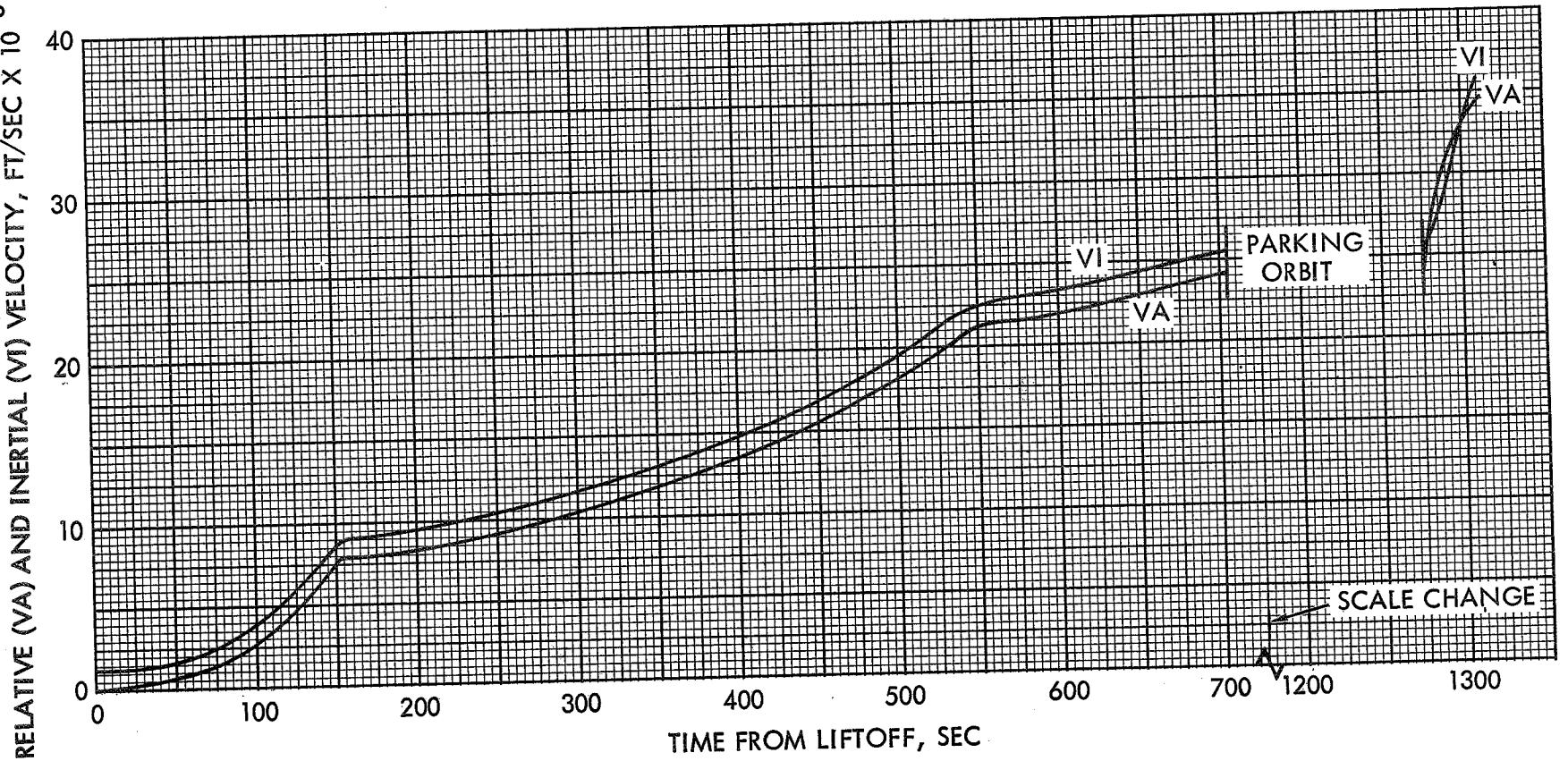

Figure 5.2-1. Earth Launch and Translunar Injection - Relative (VA) and Inertial (VI) Velocity

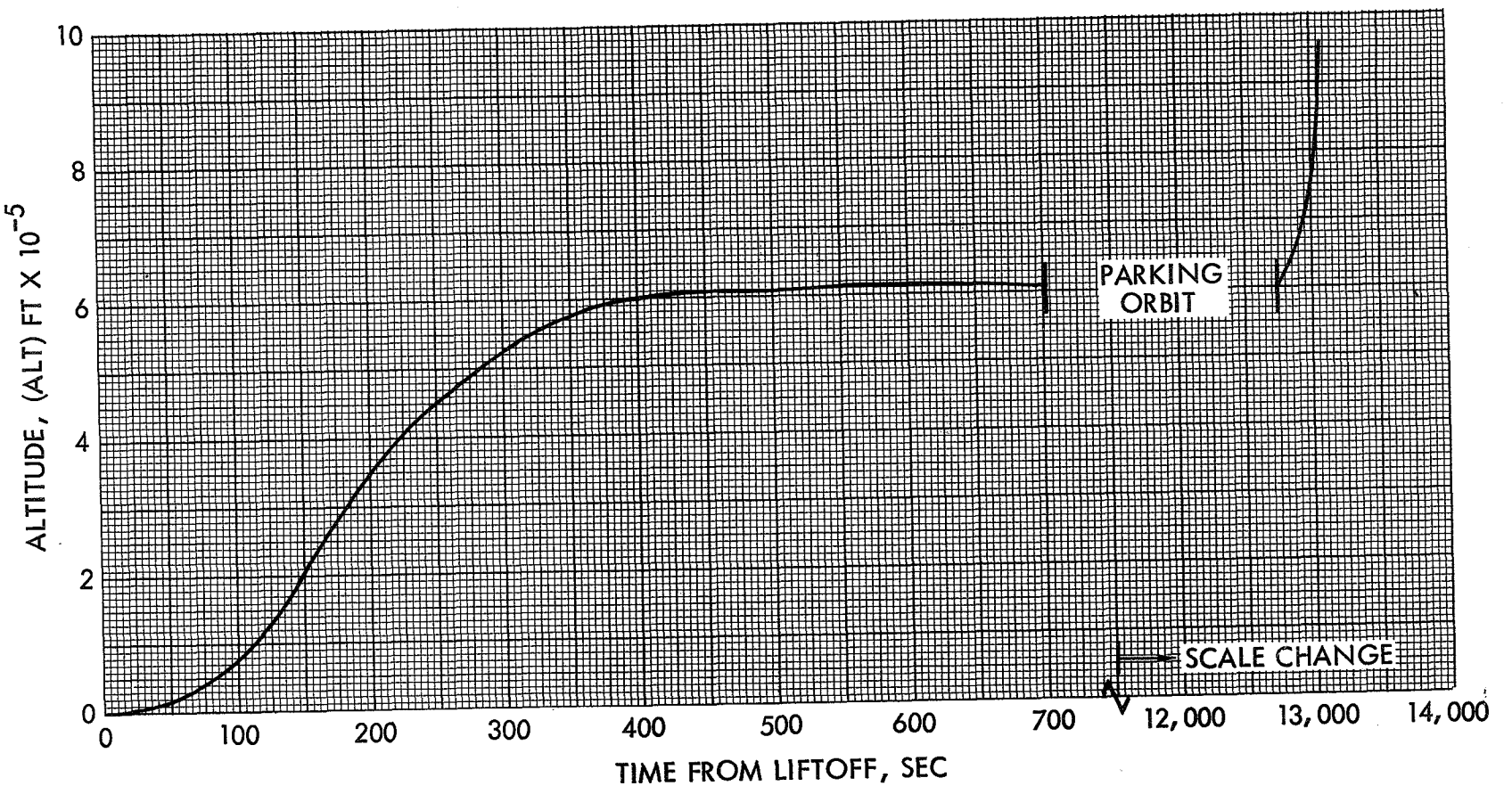

Figure 5.2-2. Earth Launch and Translunar Injection - Altitude (ALT)

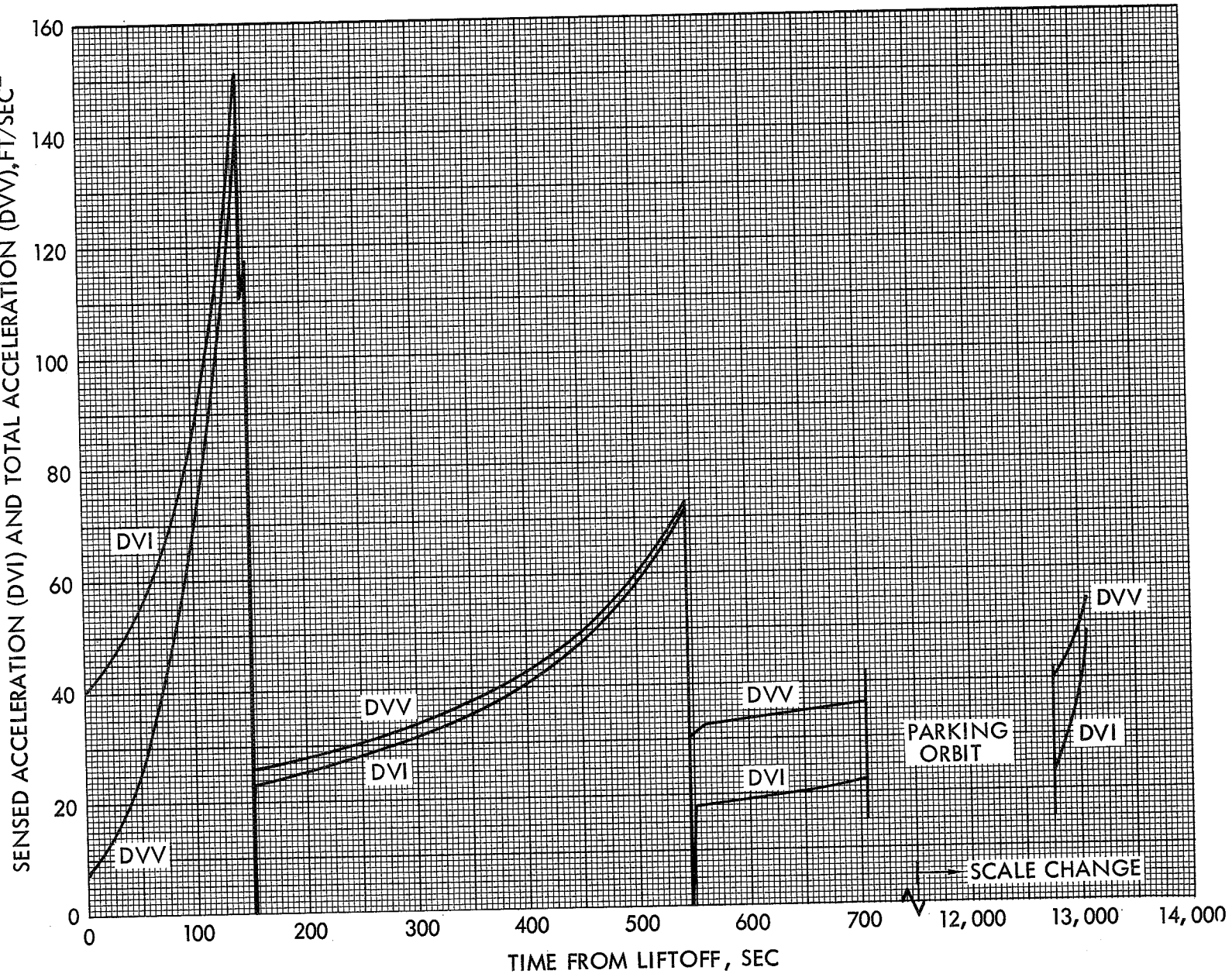

Figure 5.2-3. Earth Launch and Translunar Injection - Sensed (DVI) and Total (DVV) Acceleration

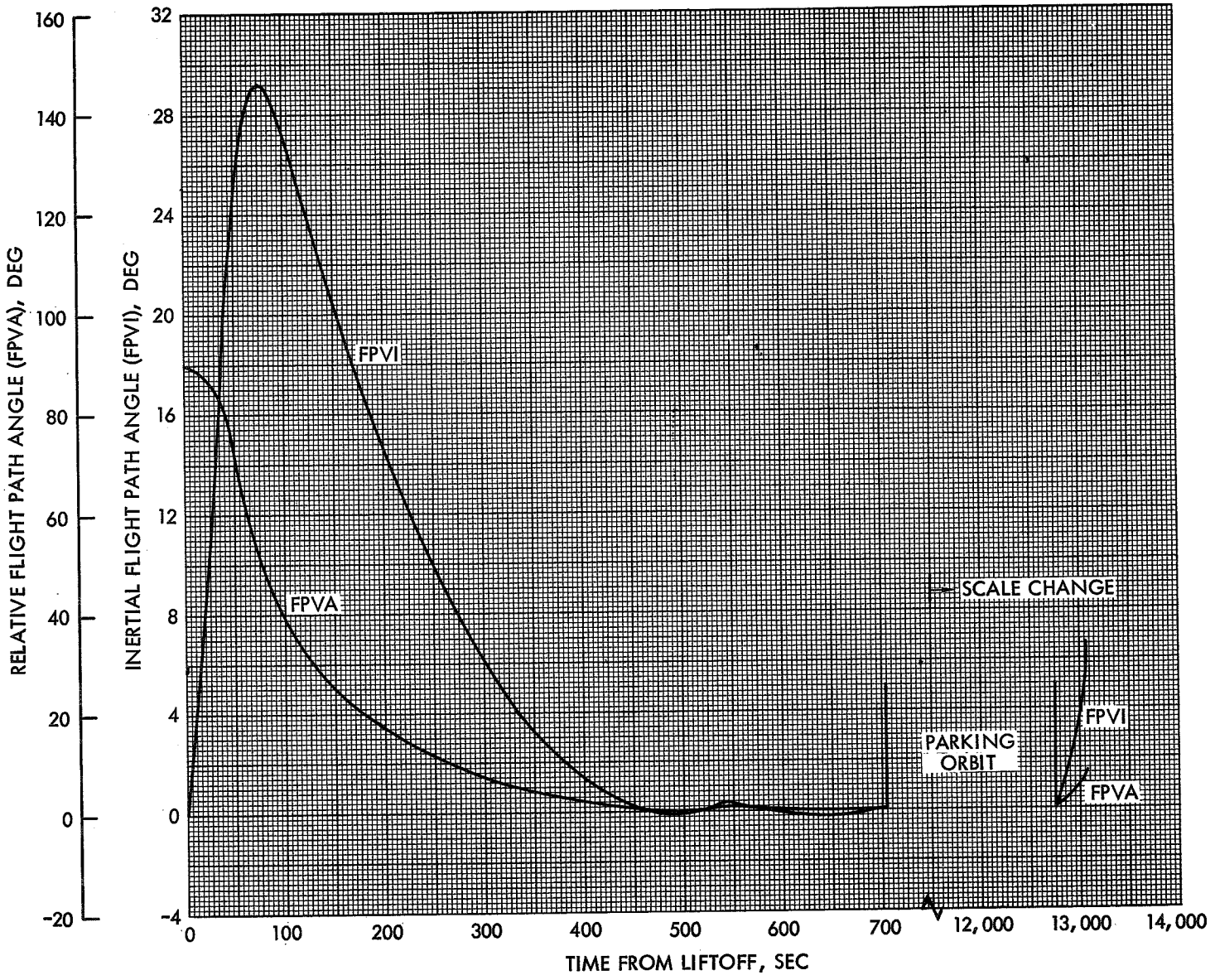

Figure 5.2-4. Earth Launch and Translunar Injection - Relative (FPVA) and Inertial (FPVI) Flight Path Angle

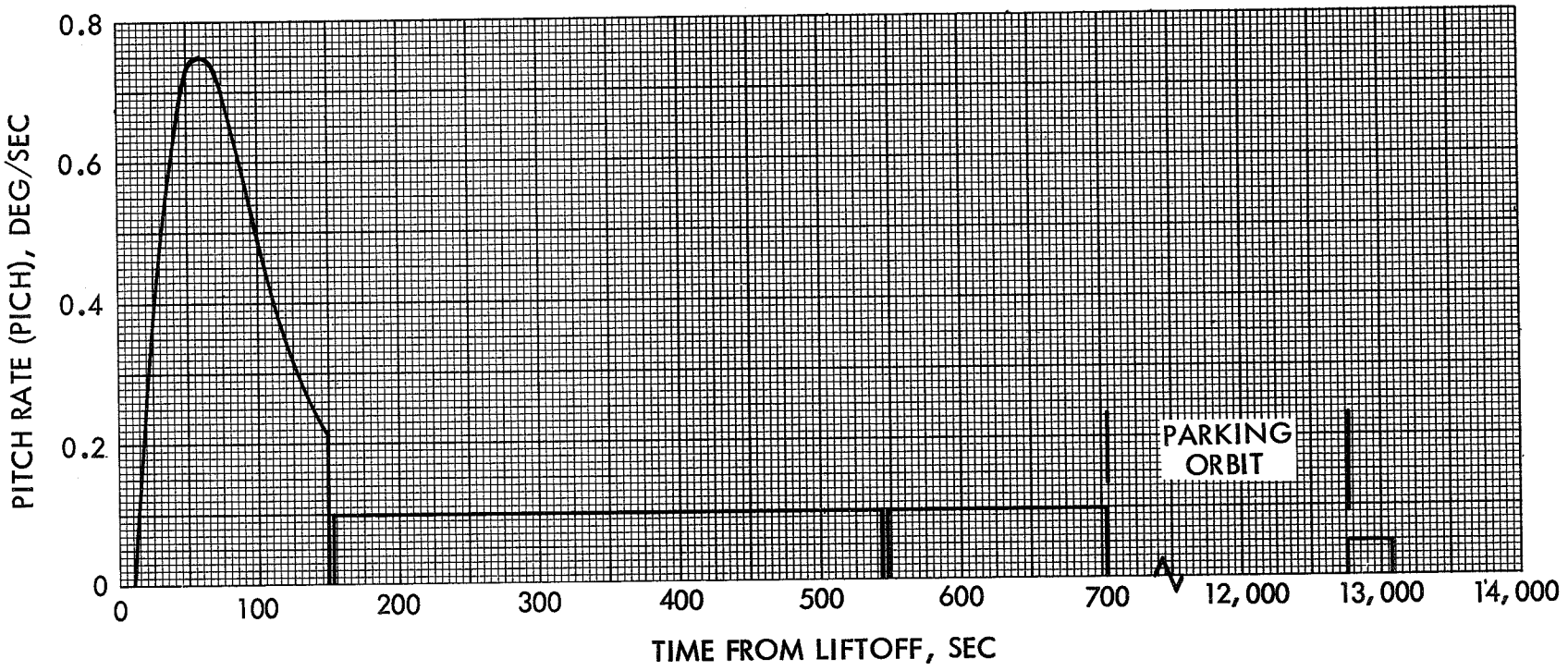

Figure 5.2-5. Earth Launch and Translunar Injection - Pitch Rate (PICH)

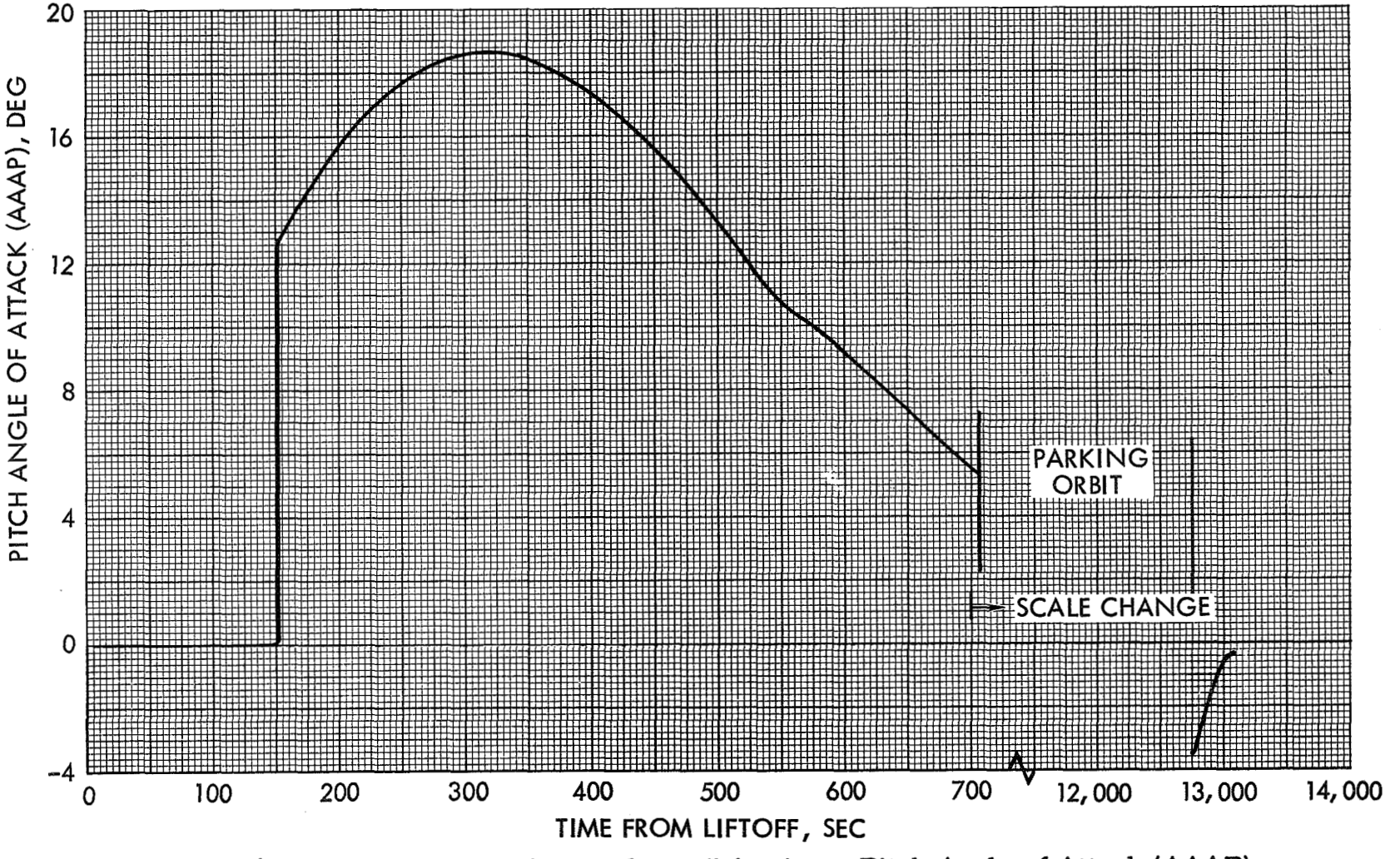

Figure 5.2-6. Earth Launch and Translunar Injection – Pitch Angle of Attack (AAAP)

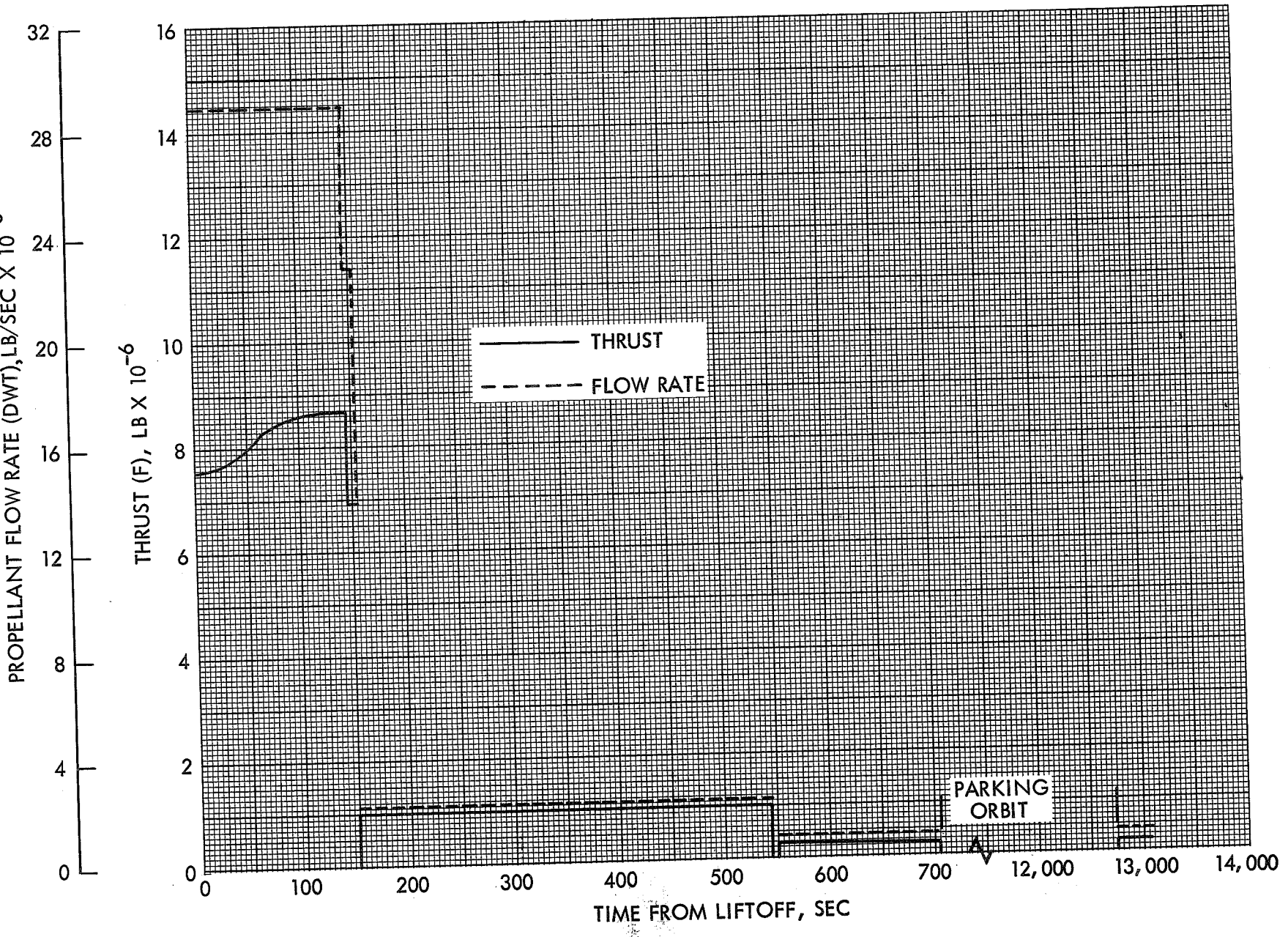

Figure 5.2-7. Earth Launch and Translunar Injection - Thrust (F) and Propellant Flow Rate (DWT)

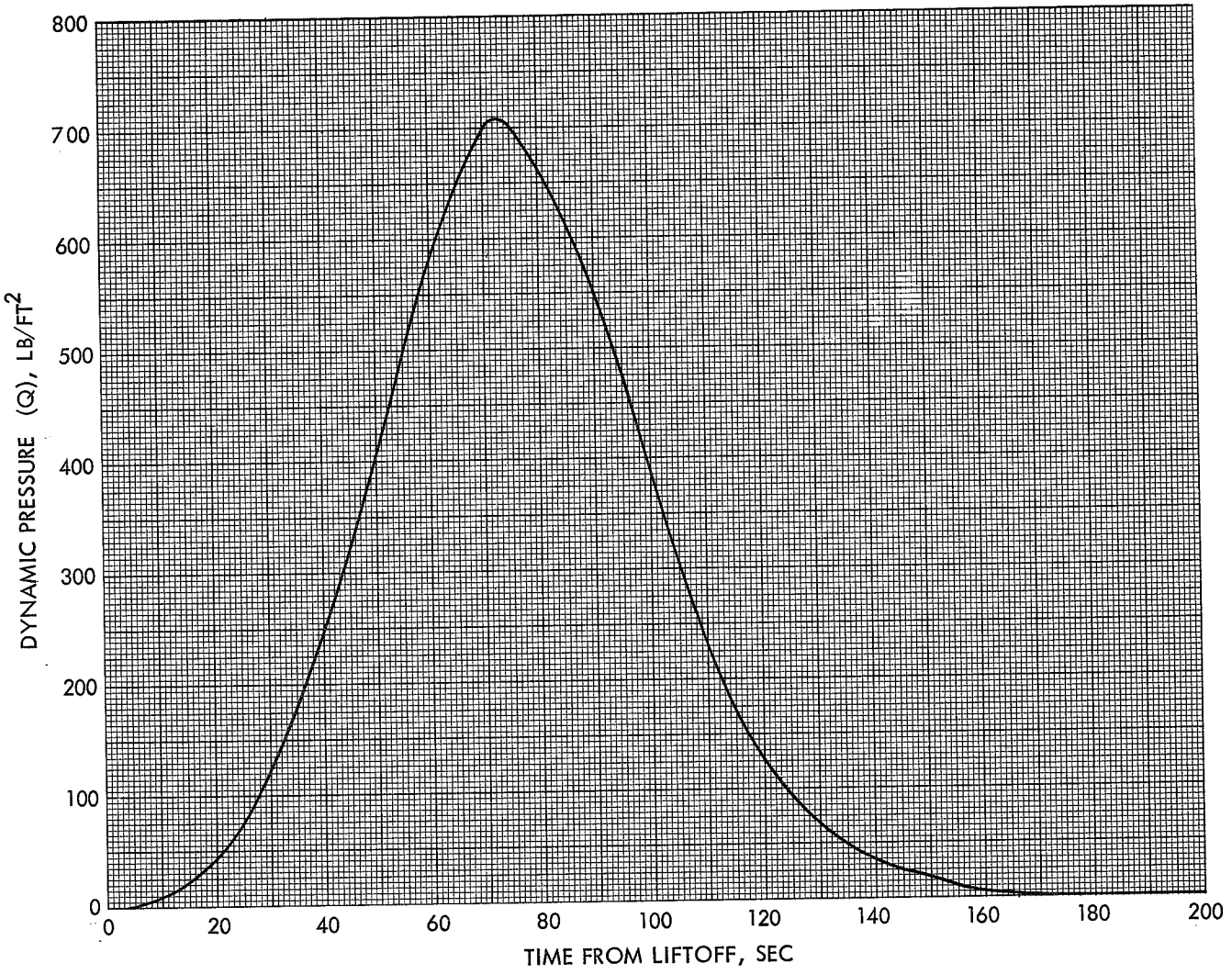

Figure 5.2-8. Earth Launch and Translunar Injection - Dynamic Pressure (Q)

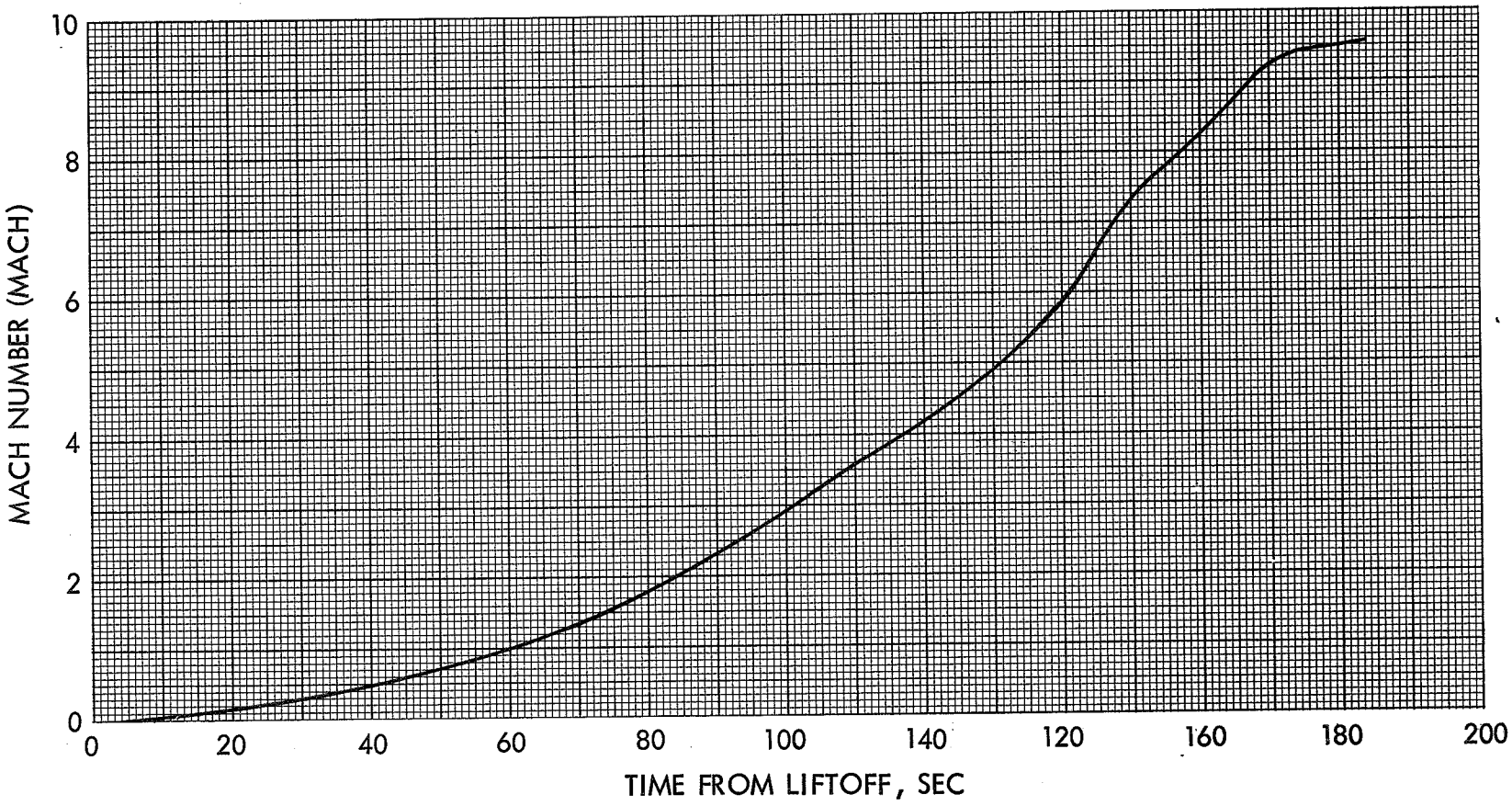

Figure 5.2-9. Earth Launch and Translunar Injection - Mach Number (MACH)

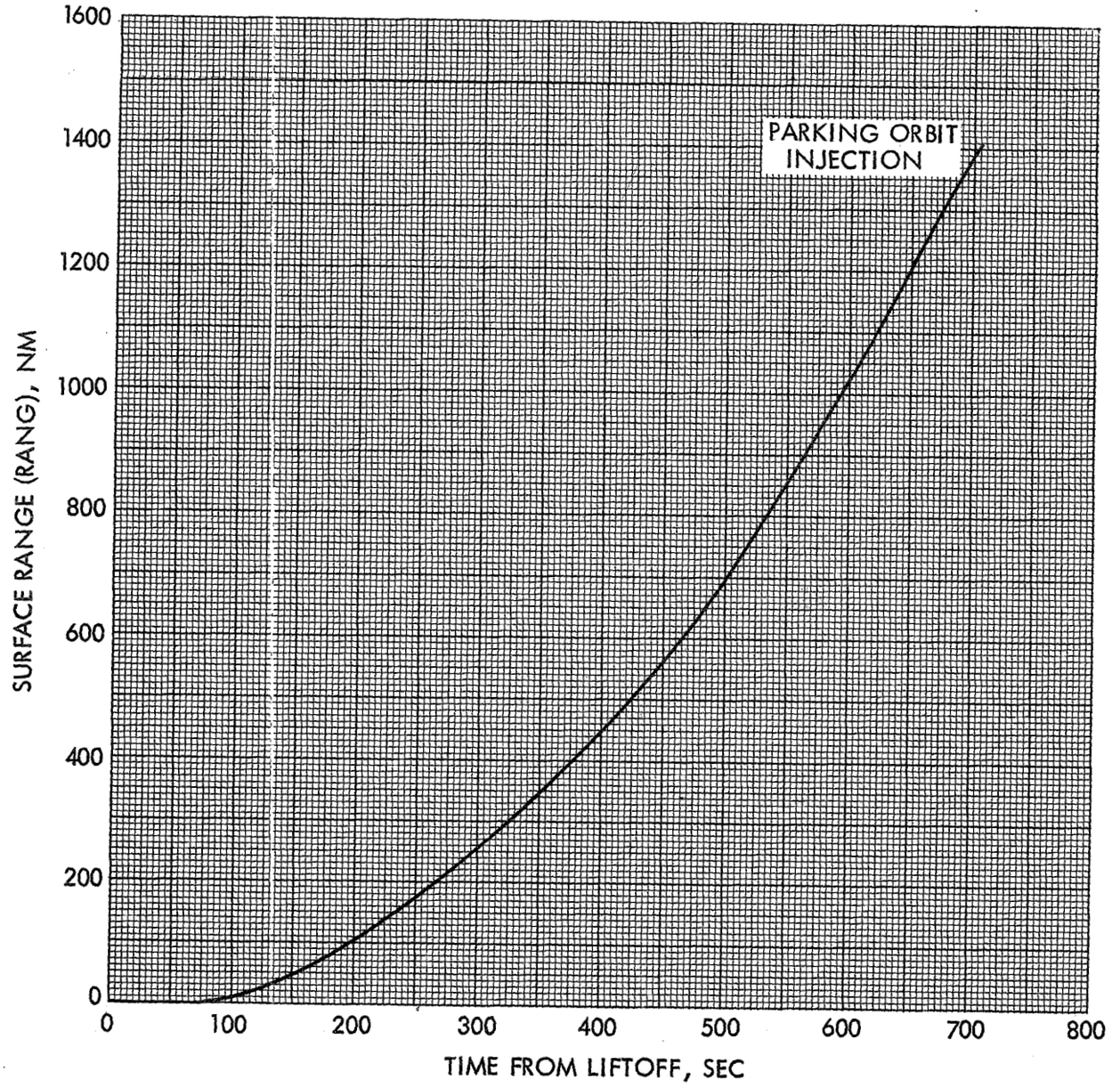

Figure 5.2-10. Earth Launch and Translunar Injection - Surface Range (RANG)

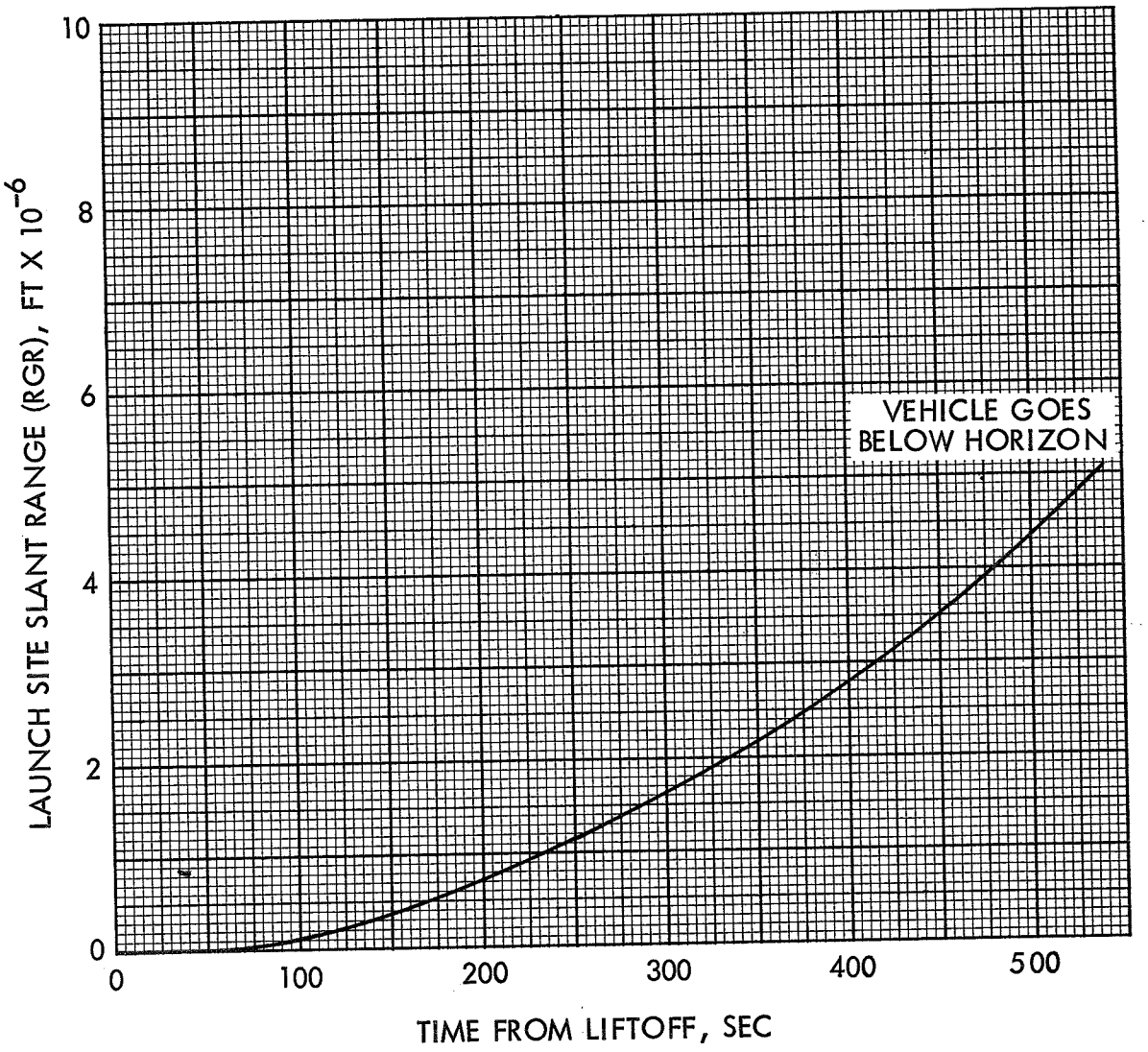

Figure 5.2-11. Earth Launch and Translunar Injection - Slant Range from Launch Site (RGR)

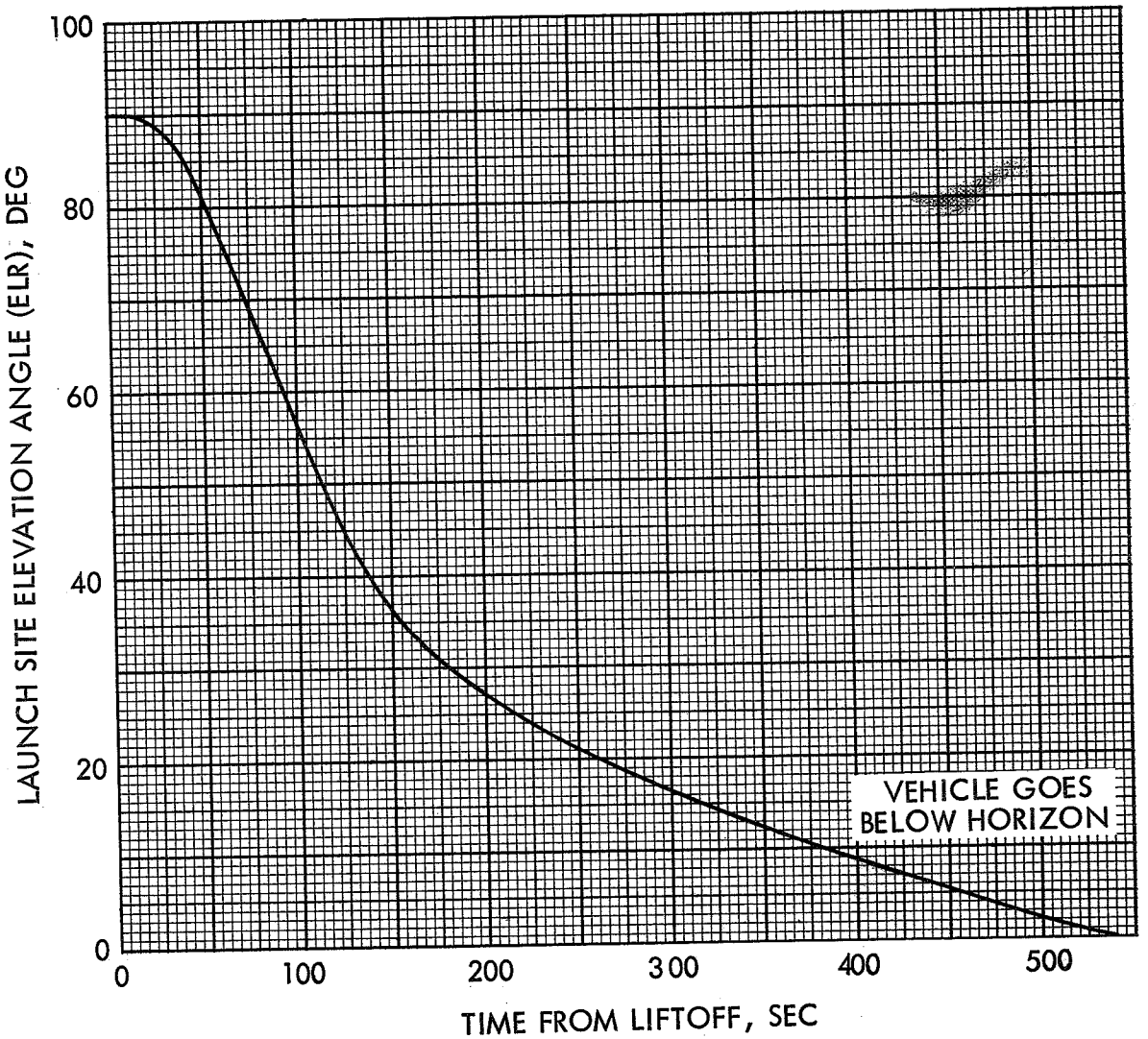

Figure 5.2-12. Earth Launch and Translunar Injection - Launch Site Radar Elevation Angle (ELR)

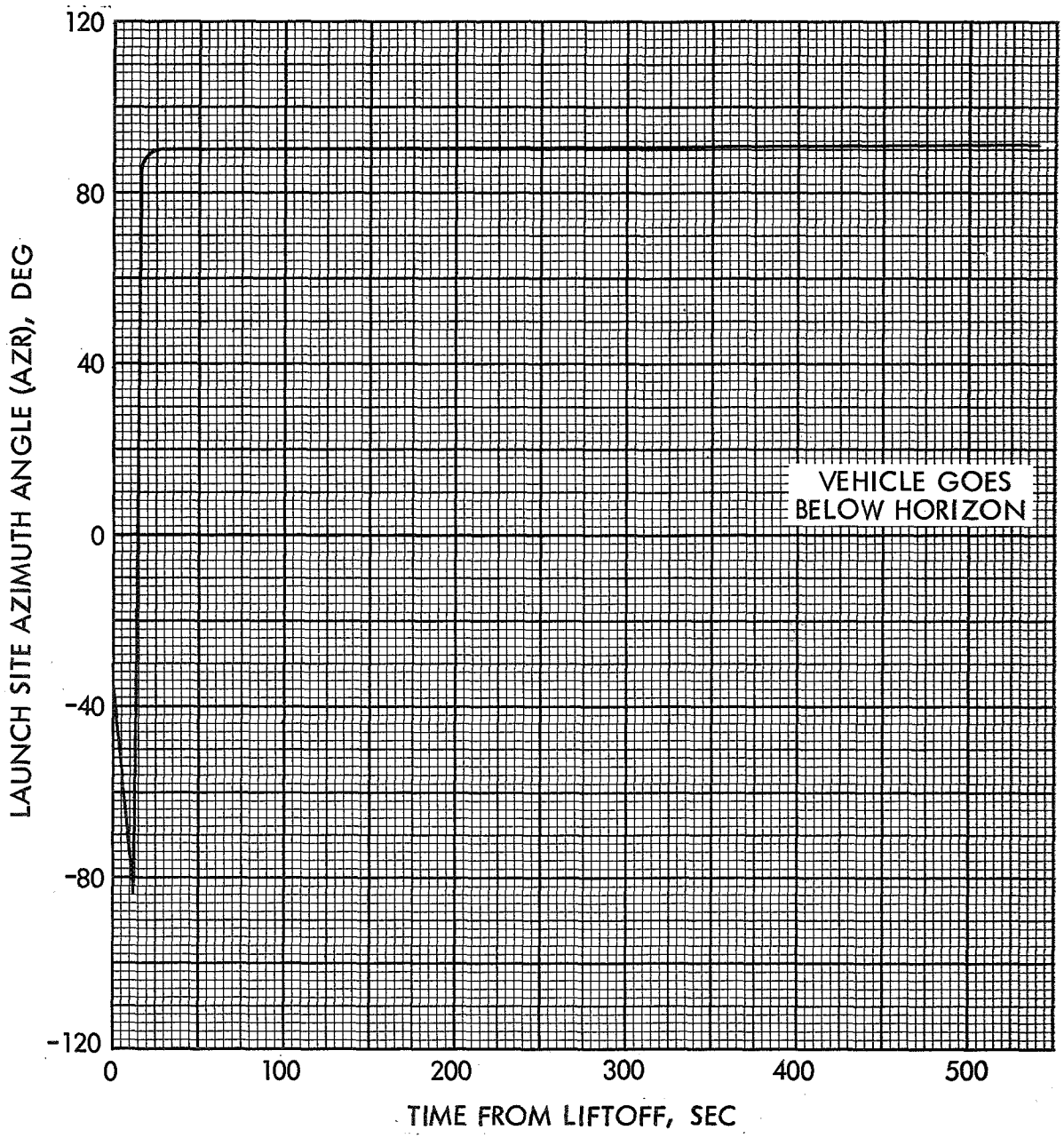

Figure 5.2-13. Earth Launch and Translunar Injection - Azimuth from Launch Site (AZR)

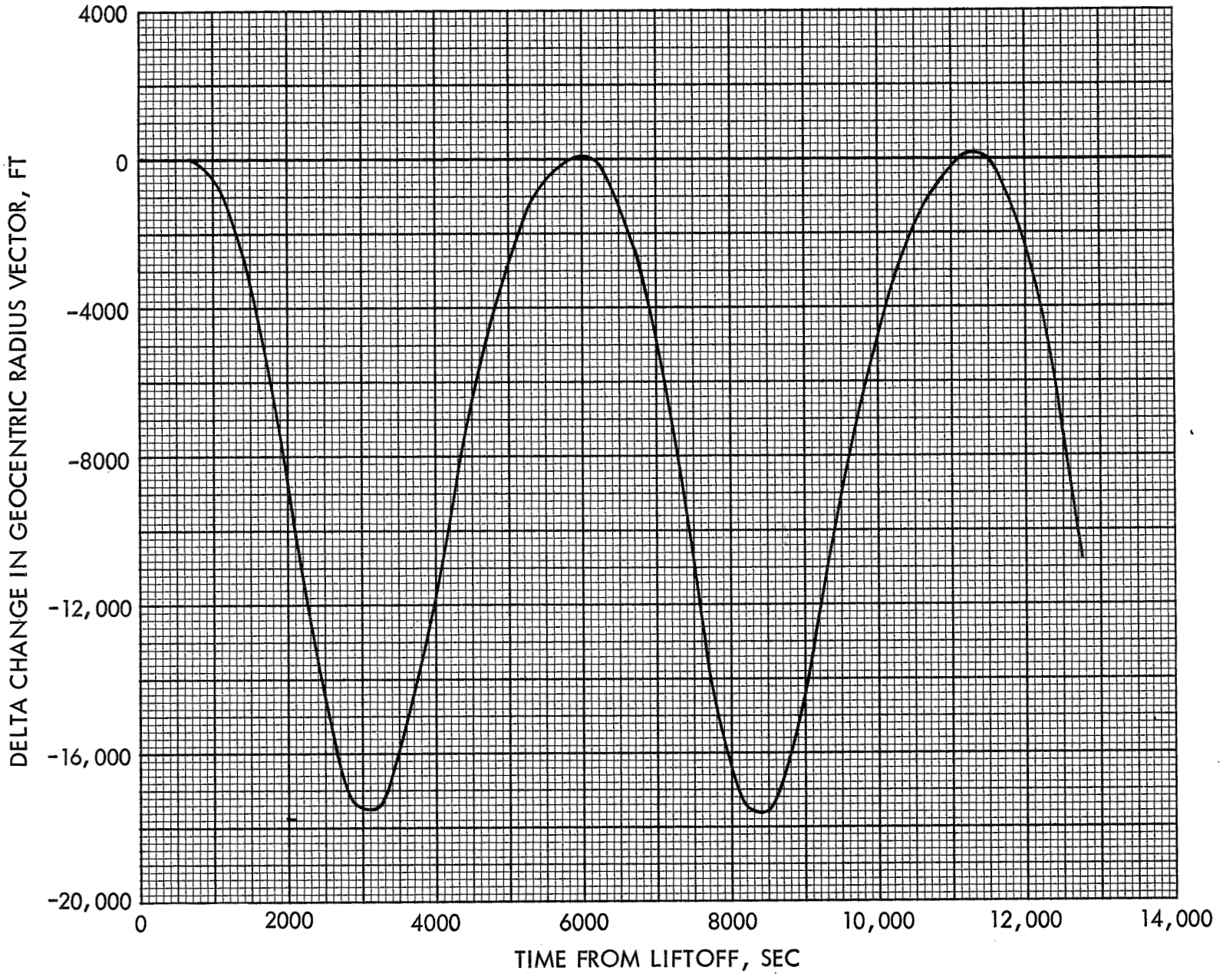

Figure 5.2-14. Earth Launch and Translunar Injection - Variation in Geocentric Radius during Parking Orbit

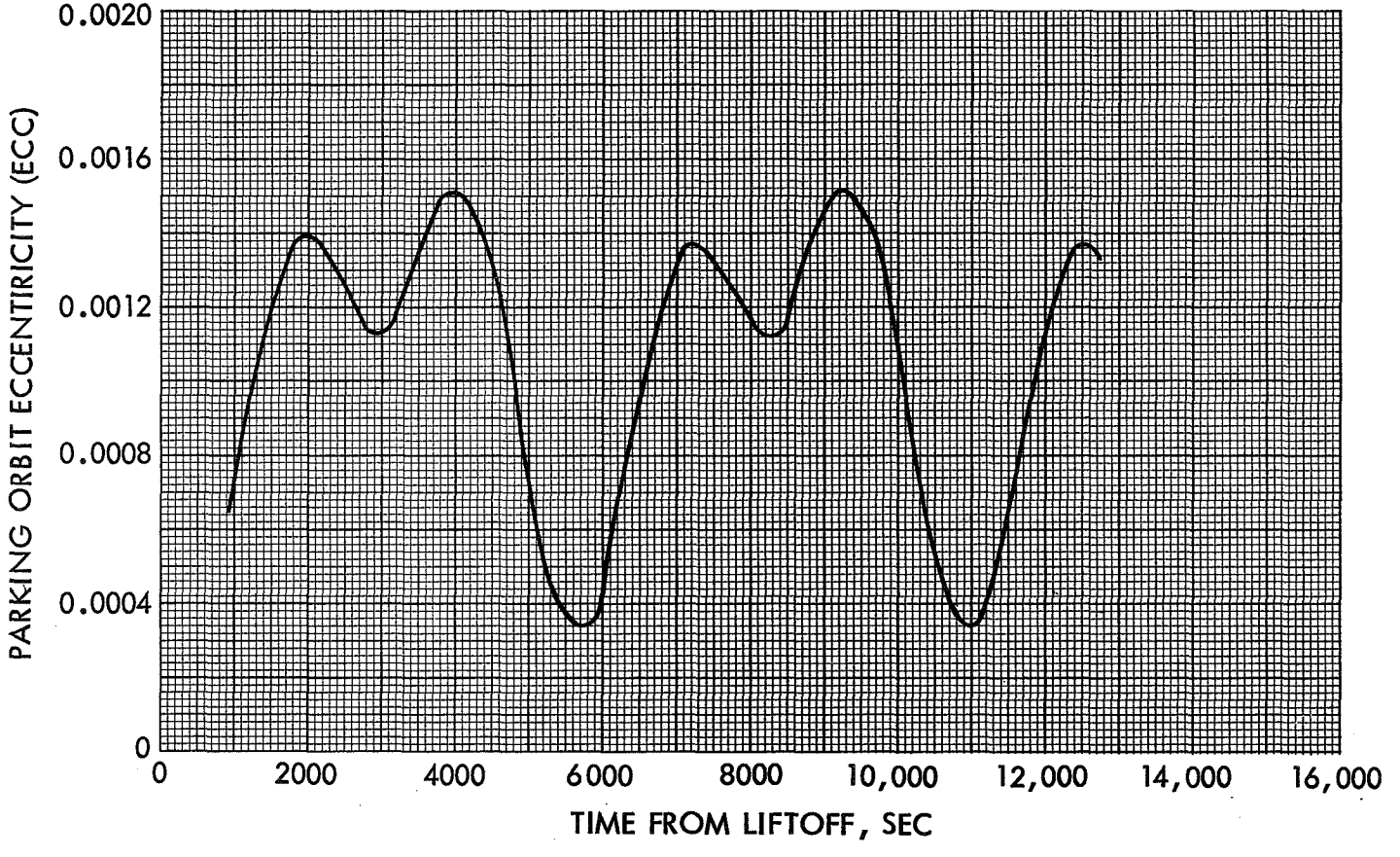

Figure 5.2-15. Earth Launch and Translunar Injection - Variation in Eccentricity during Parking Orbit

Table 5.3-I. Translunar Flight - Discrete Events Summary

Time Since Liftoff (min)	Altitude (ft x 10^{-6})	Latitude (deg)	Longitude (deg)	Velocity* (ft/sec)	Flight Path* Angle (deg)	Azimuth Angle (deg)	Event
217.89	.958584	-25.512	14.421	35,675.28	6.56	103.62	Translunar Injection
337.89	108.880	1.815	107.067	14,216.91	65.16	61.47	S-IVB Stage Separation
517.89	226.259	8.665	74.765	9,956.56	71.64	62.64	First Translunar Midcourse Correction
937.89	424.188	13.095	338.442	6,964.56	75.53	64.33	Second Translunar Midcourse Correction
1,297.89	557.316	14.682	251.636	5,827.76	76.73	65.15	Third Translunar Midcourse Correction
4,017.89	1,201.798	18.371	298.496	3,008.40	80.85	67.49	Selenocentric Phase Shift
4,627.70	1,311.542	18.321	145.512	5,075.98	0.49	245.83	Pericynthion Passage for Free Return Trajectory
5,227.70	1,204.975	18.023	355.033	2,970.58	-80.846	85.65	Geocentric Phase Shift
9,061.81	.400000	-12.914	271.084	36,139.03	-6.65	105.67	Earth Atmospheric Re-entry of Free Return Trajectory

*Inertial quantity

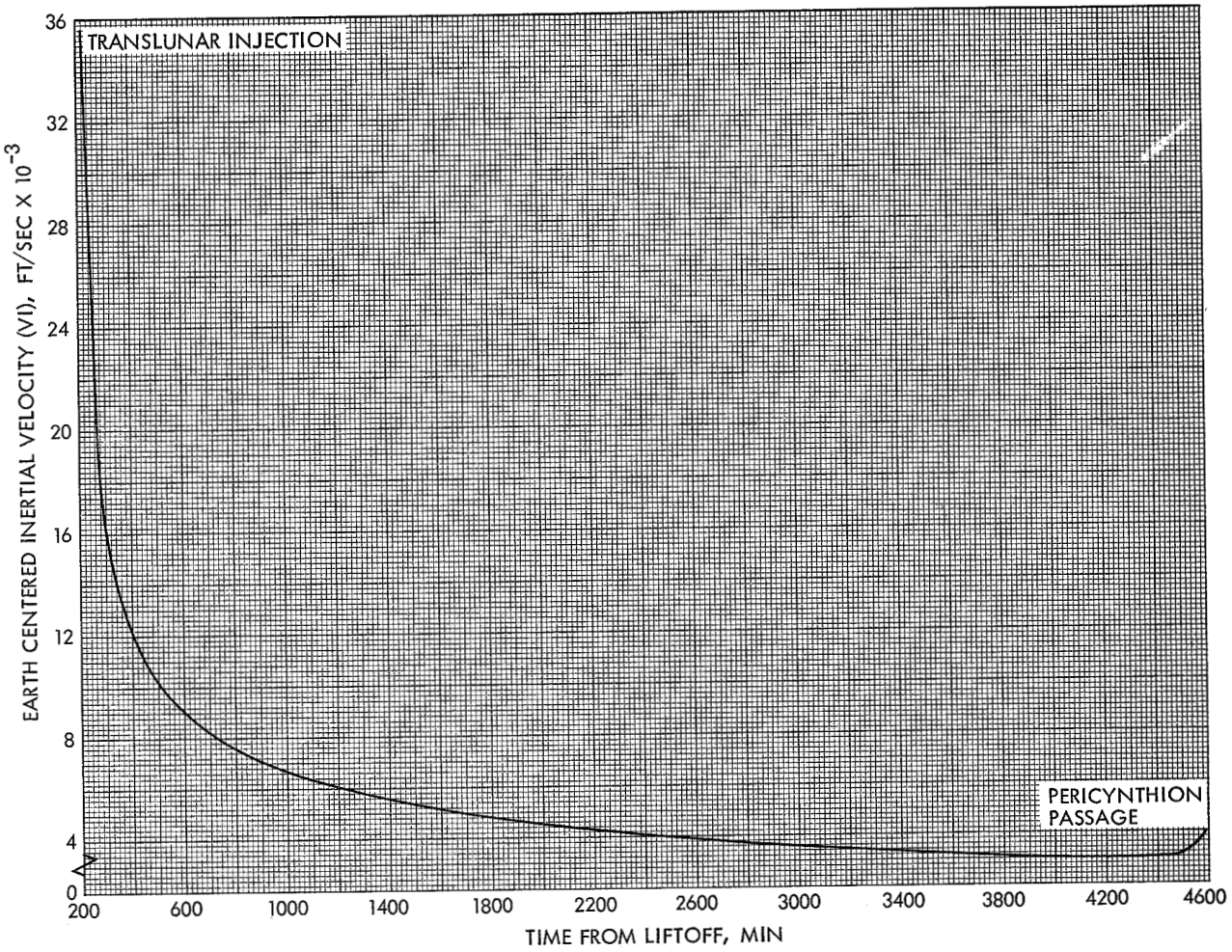

Figure 5.3-1. Translunar Flight - Earth Centered Inertial Velocity (VI)

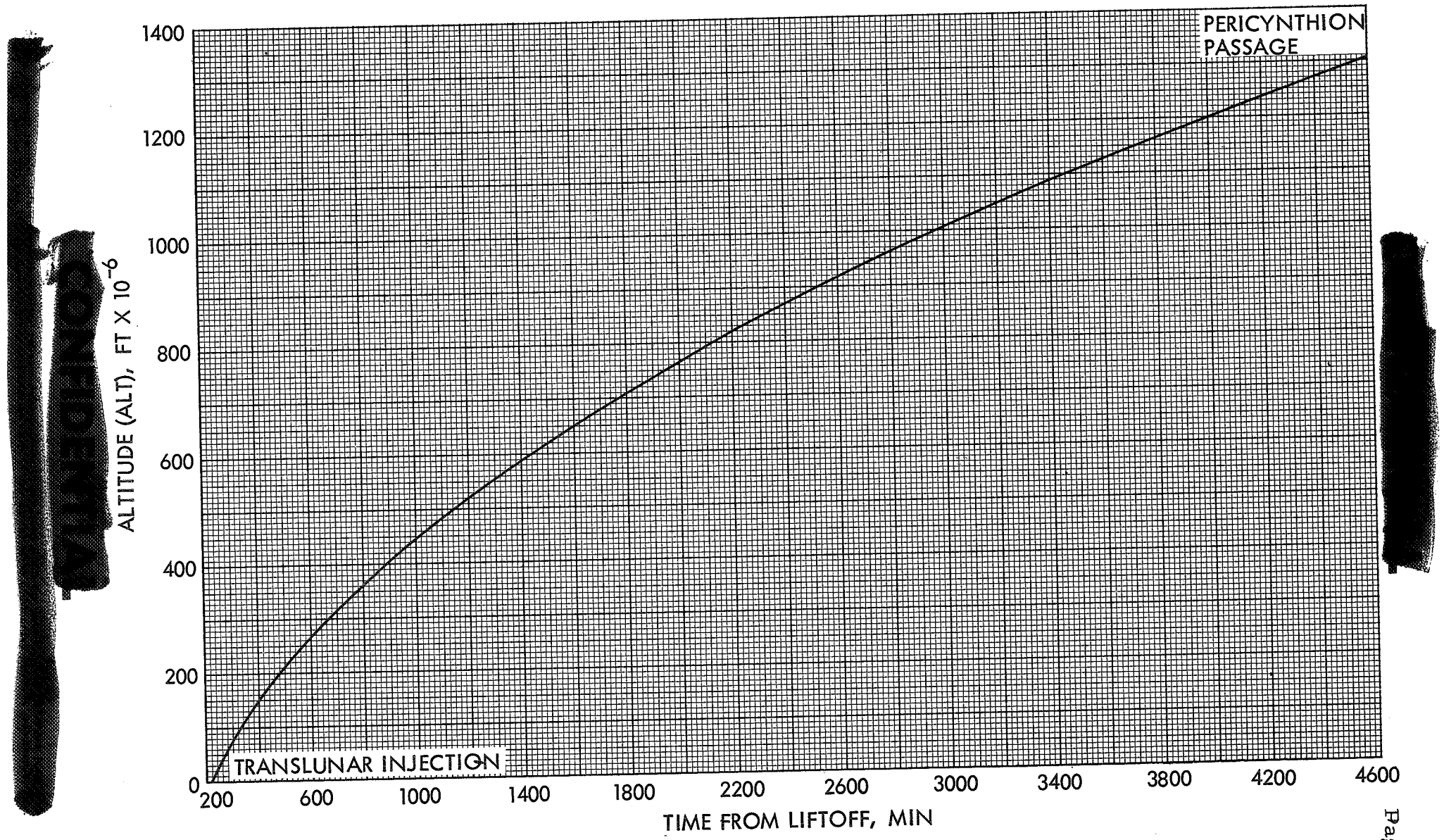

Figure 5.3-2. Translunar Flight - Altitude (ALT) Relative to Earth

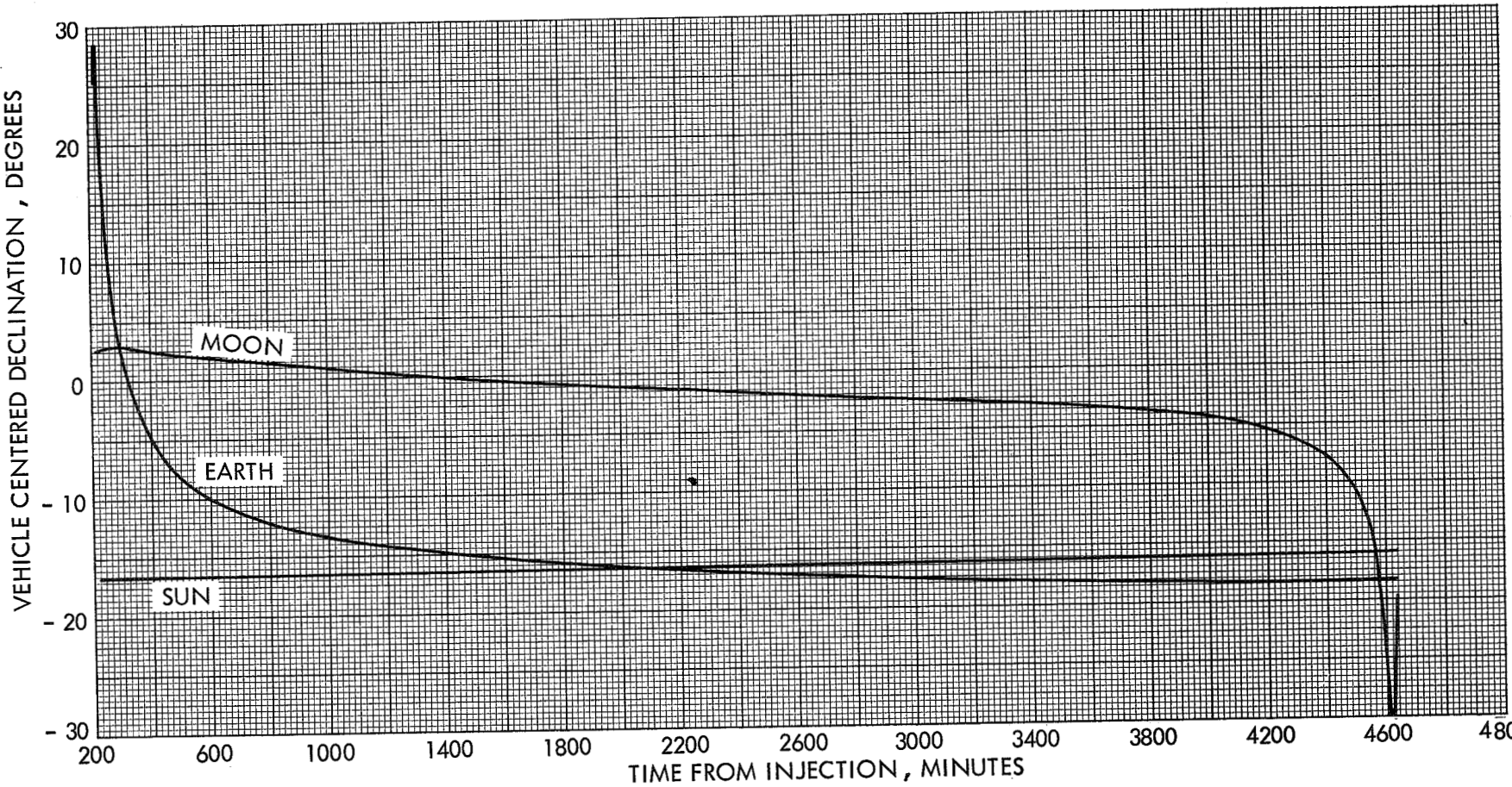

Figure 5.3-3. Translunar Flight - Vehicle Centered Declination of Earth, Sun, and Moon

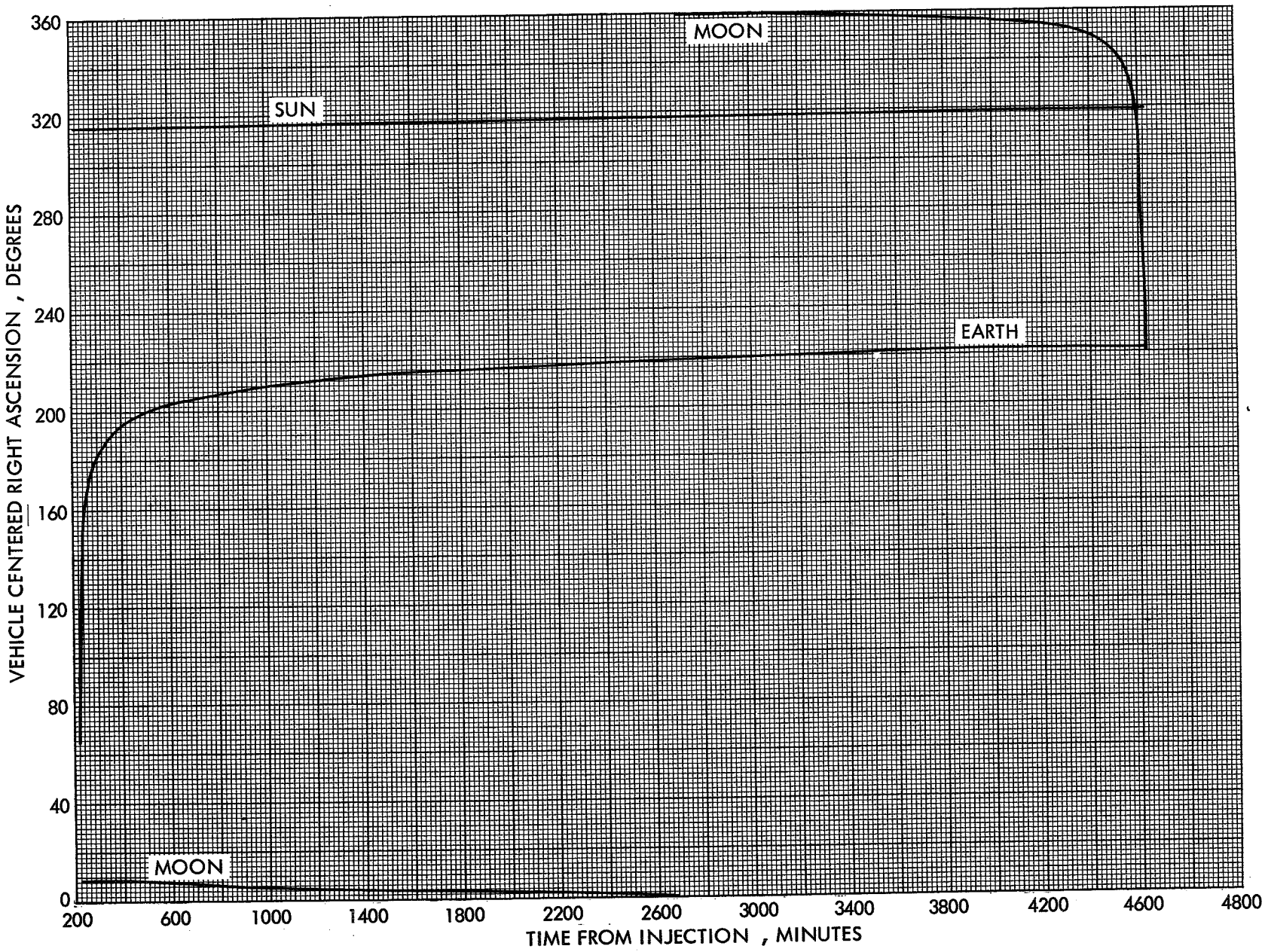

Figure 5.3-4. Translunar Flight - Vehicle Centered Right Ascension of Earth, Sun, and Moon

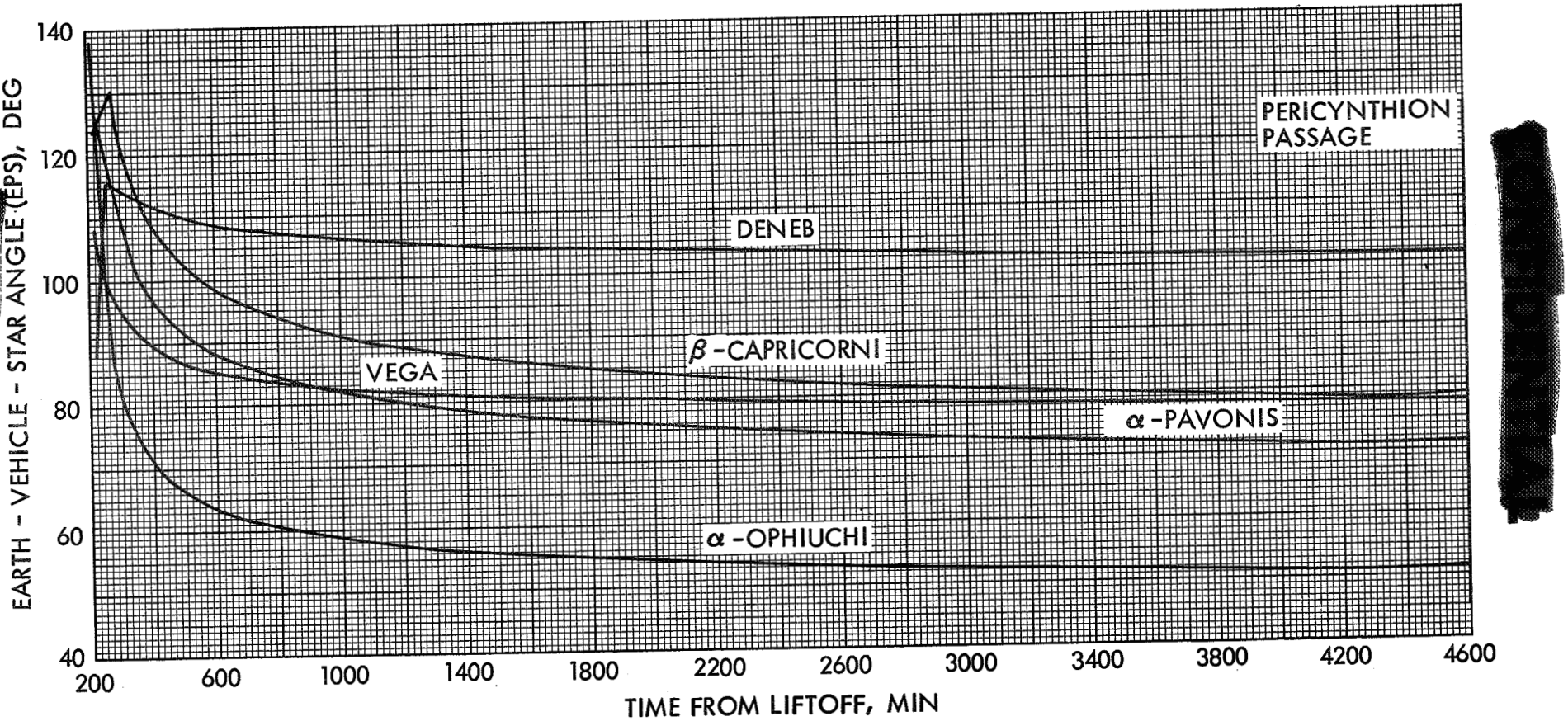

Figure 5.3-5. Translunar Flight - Earth-Vehicle-Star Angles

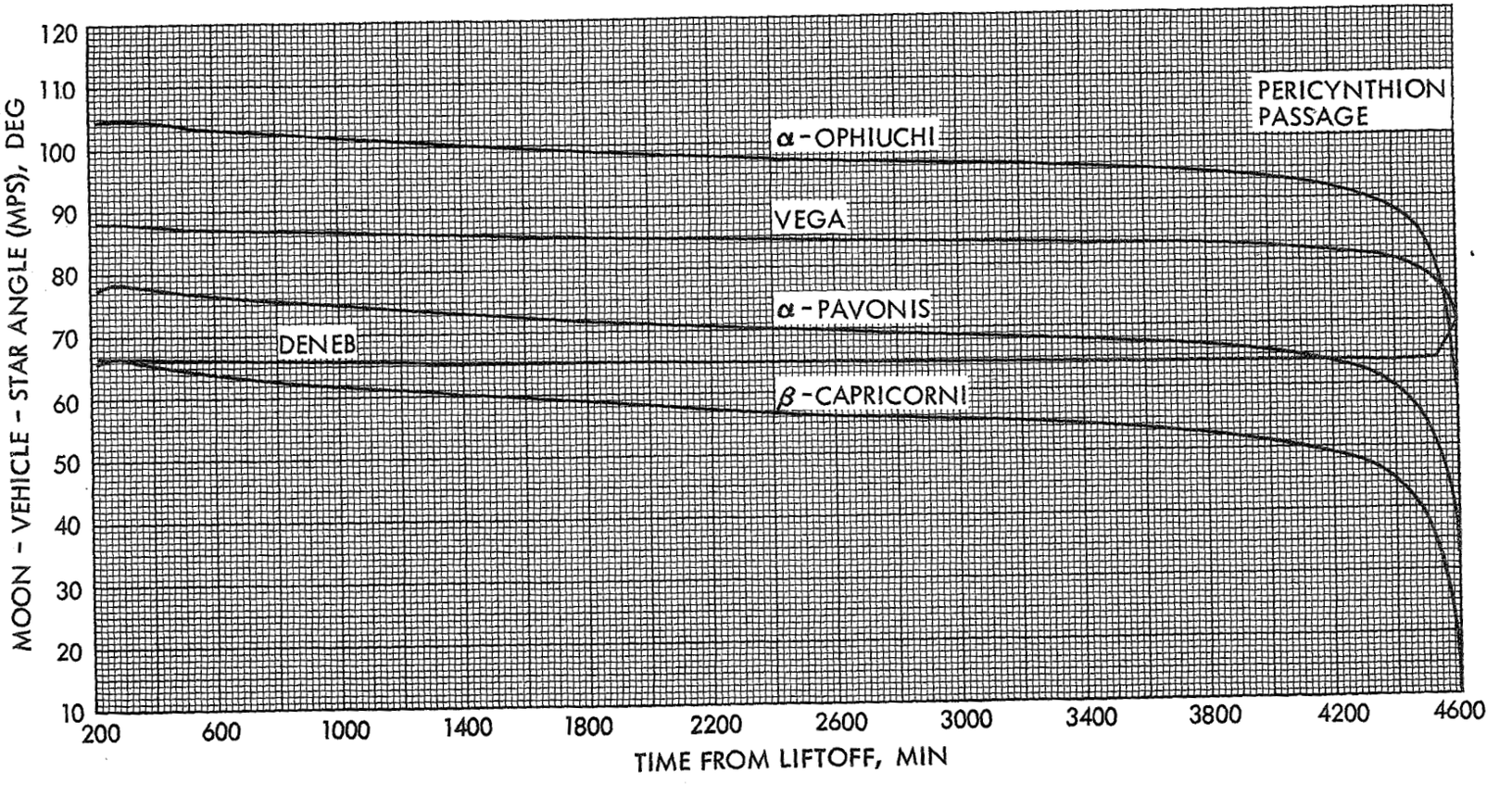

Figure 5.3-6. Translunar Flight – Moon-Vehicle-Star Angles

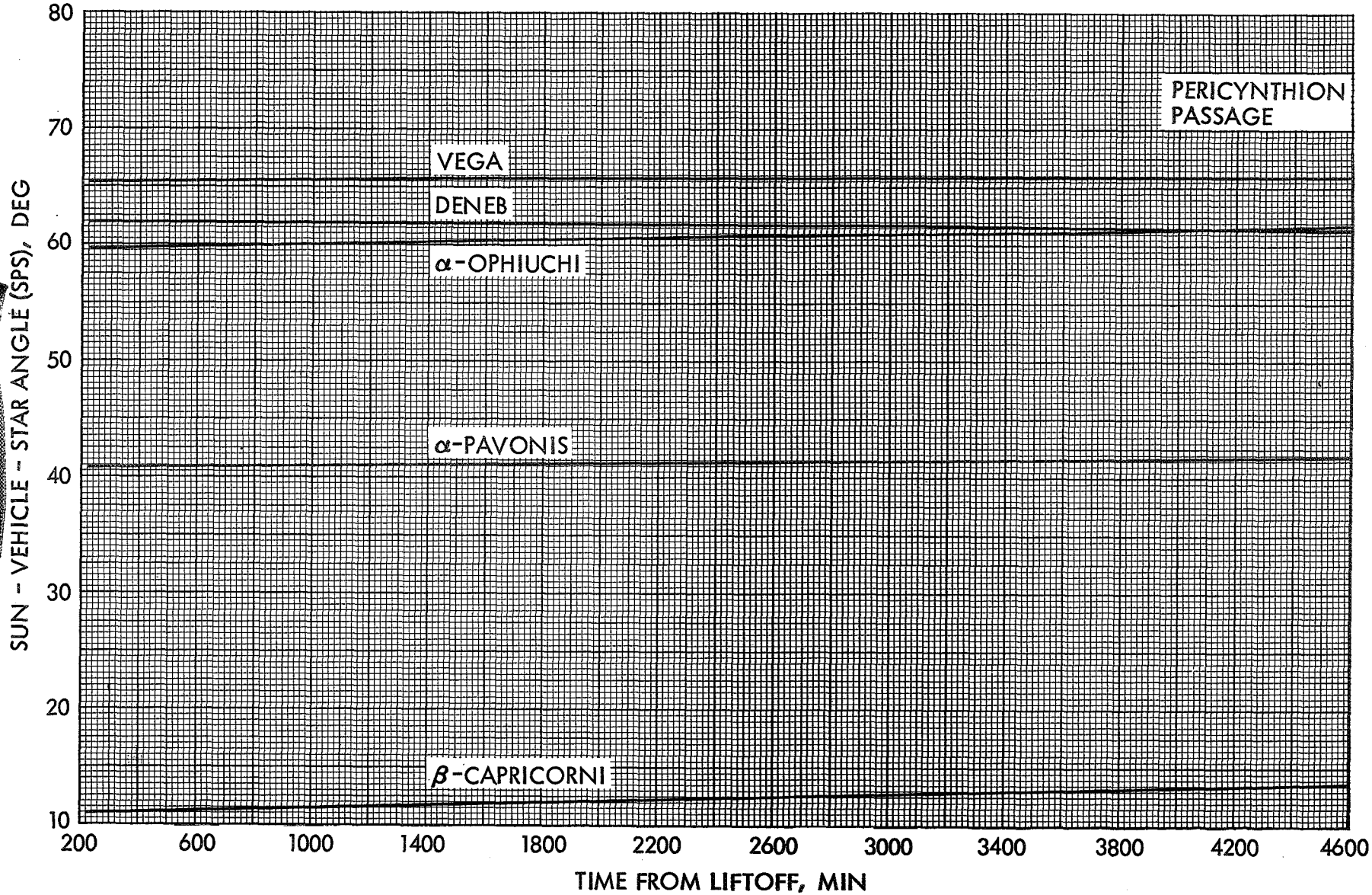

Figure 5.3-7. Translunar Flight - Sun-Vehicle-Star Angles

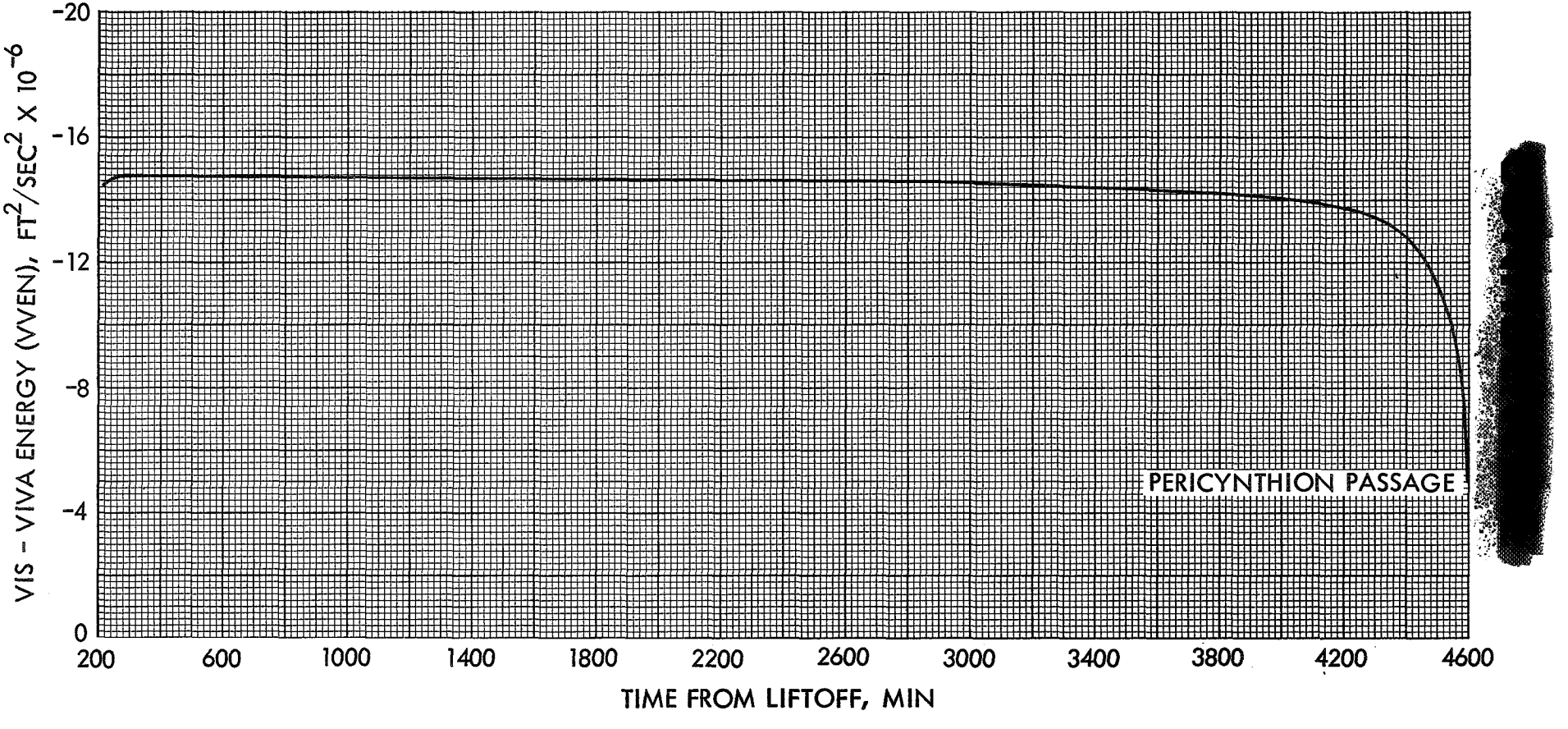

Figure 5.3-8. Translunar Flight - Vis-viva Energy (VVEN)

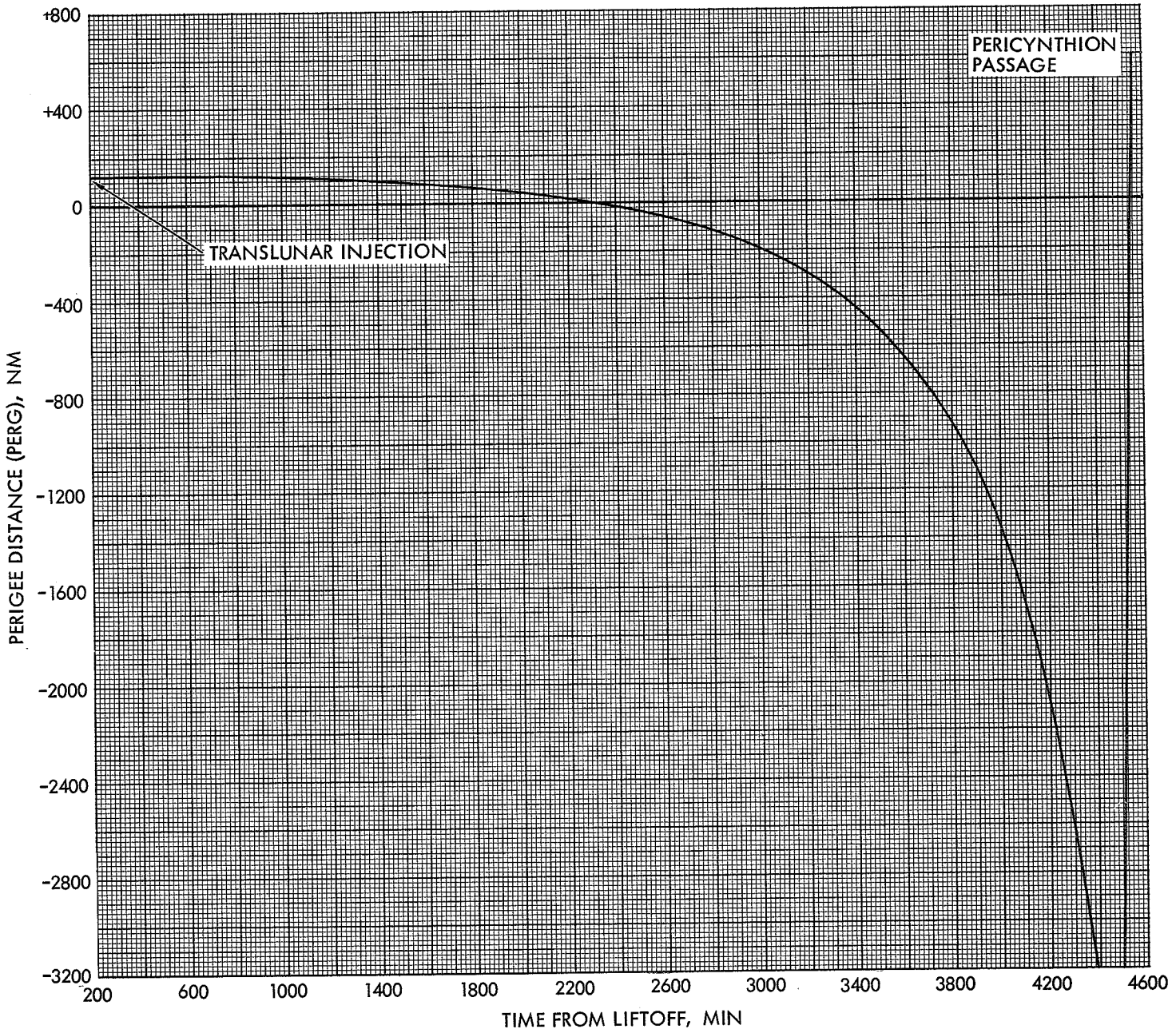

Figure 5.3-9. Translunar Flight – Perigee Distance (PERG)

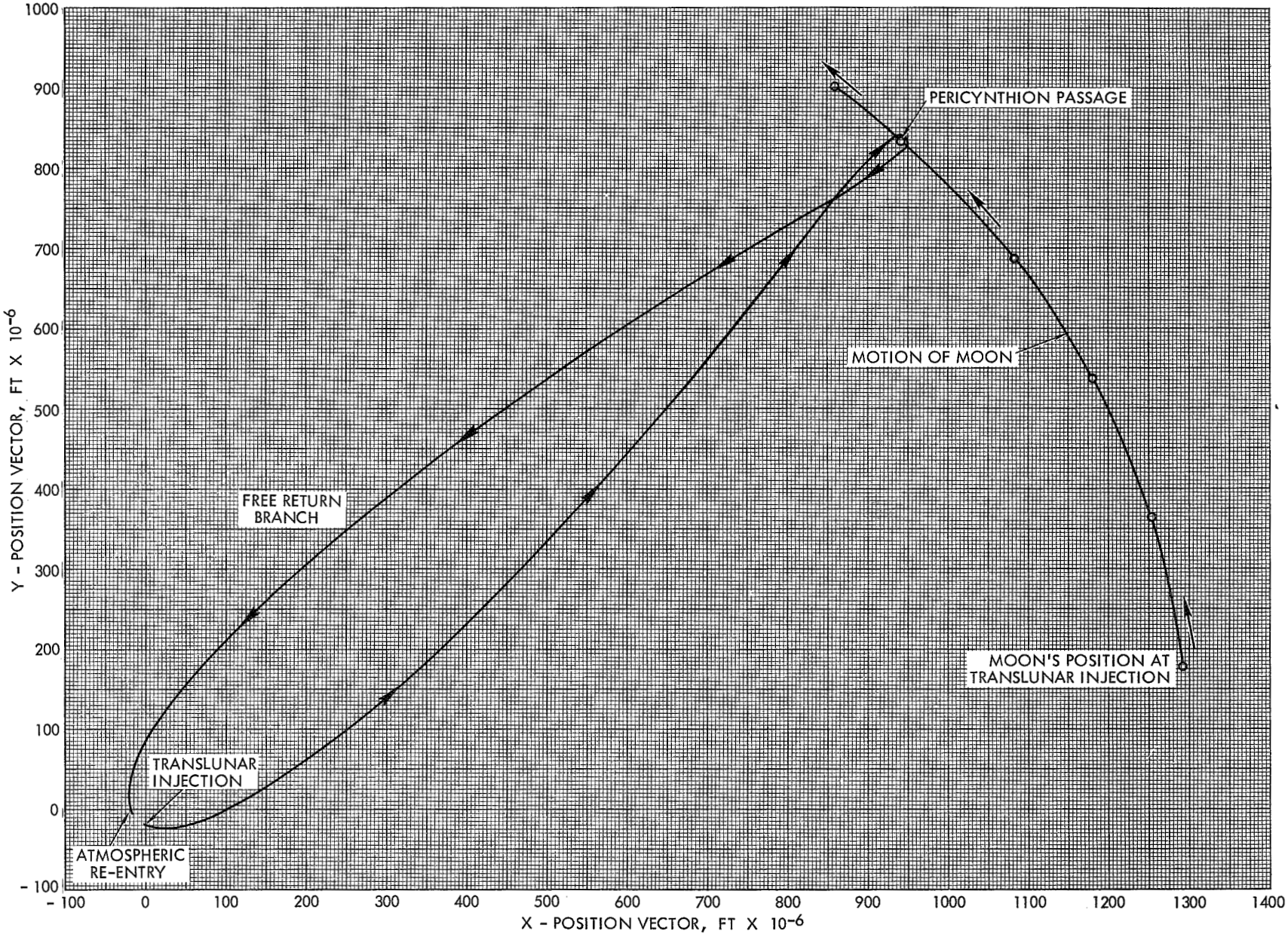

Figure 5.3-10. Translunar Flight -- Geocentric Position X versus Y

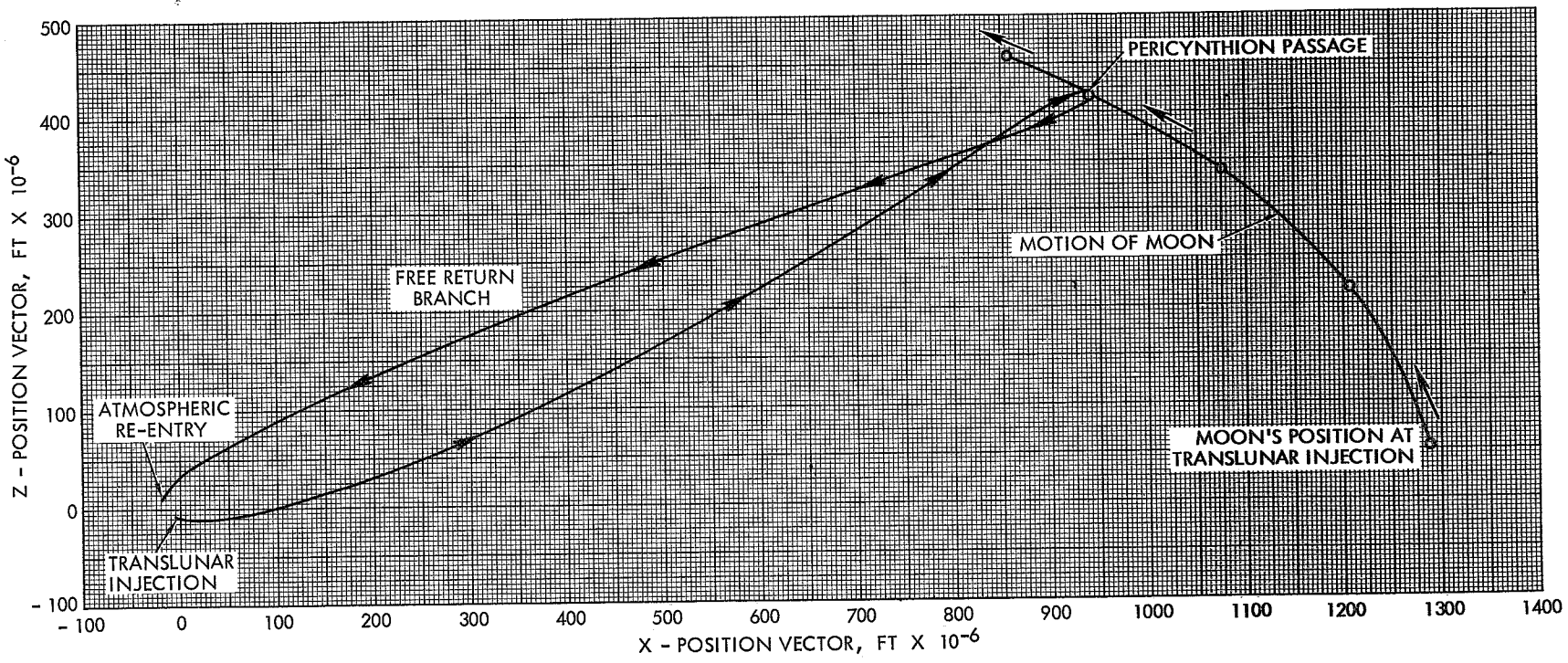

Figure 5.3-11. Translunar Flight - Geocentric Position X versus Z

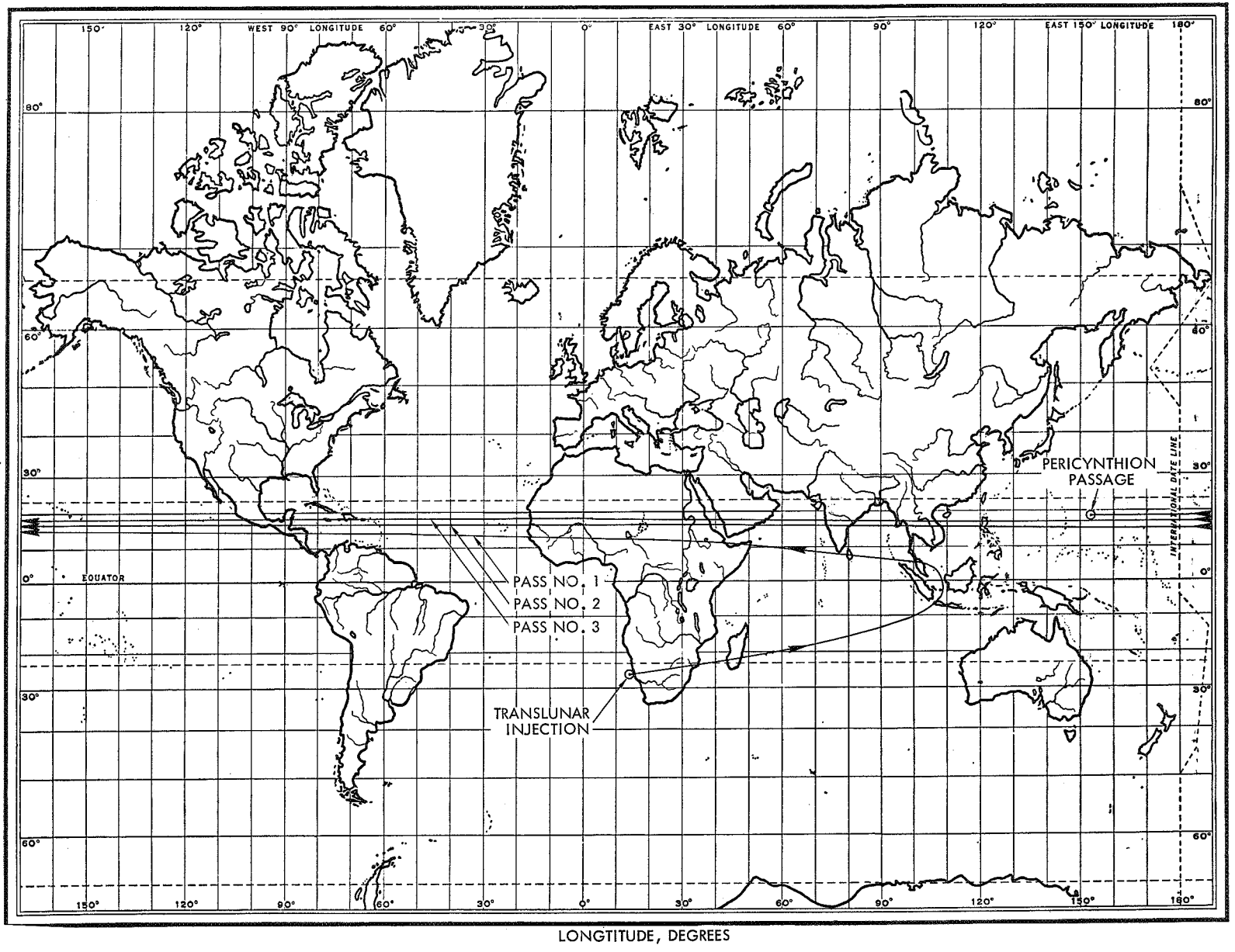

Figure 5.3-12. Translunar Flight - Earth Ground Track

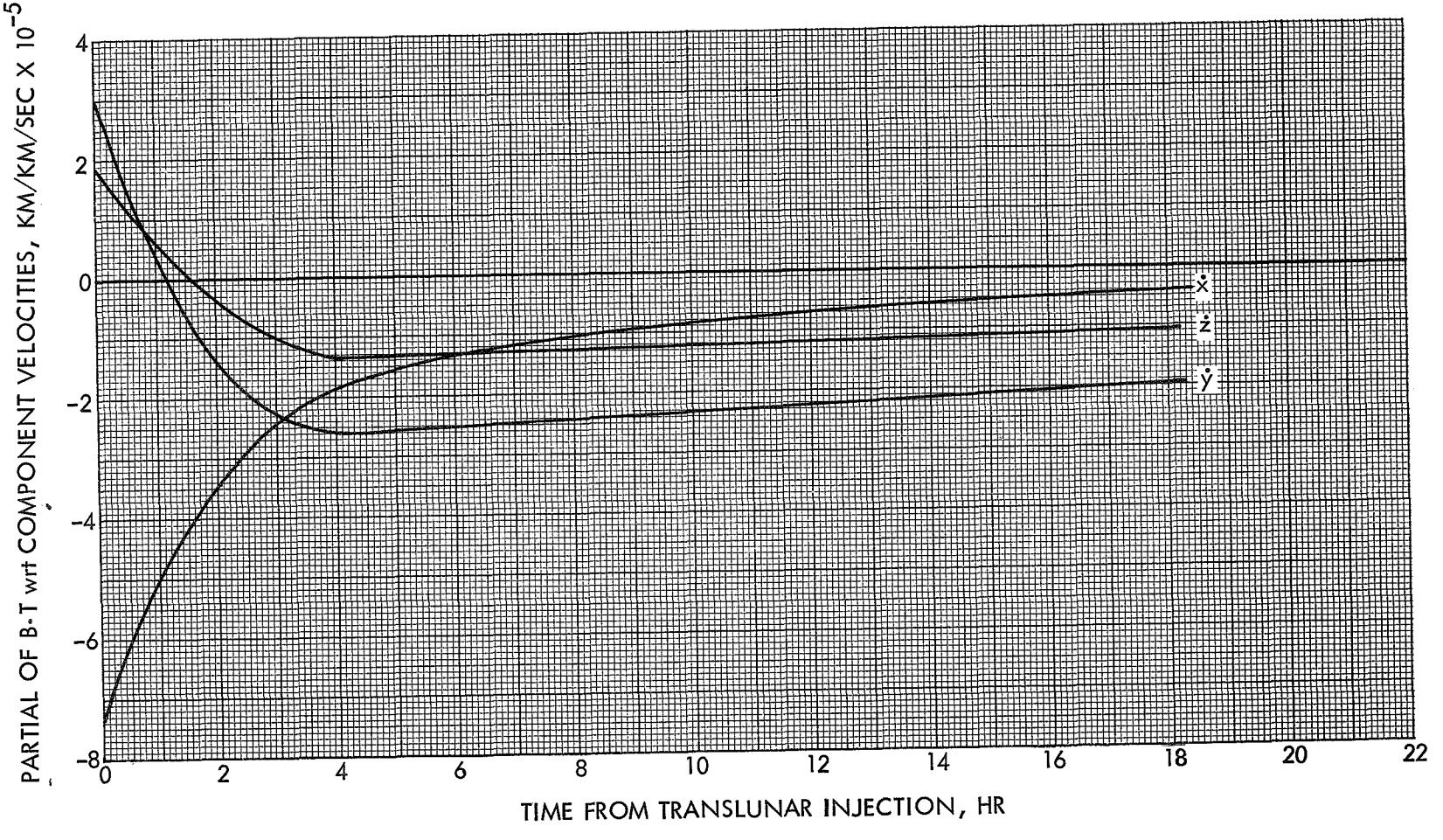

Figure 5.3-13a. Translunar Flight – Midcourse Sensitivities

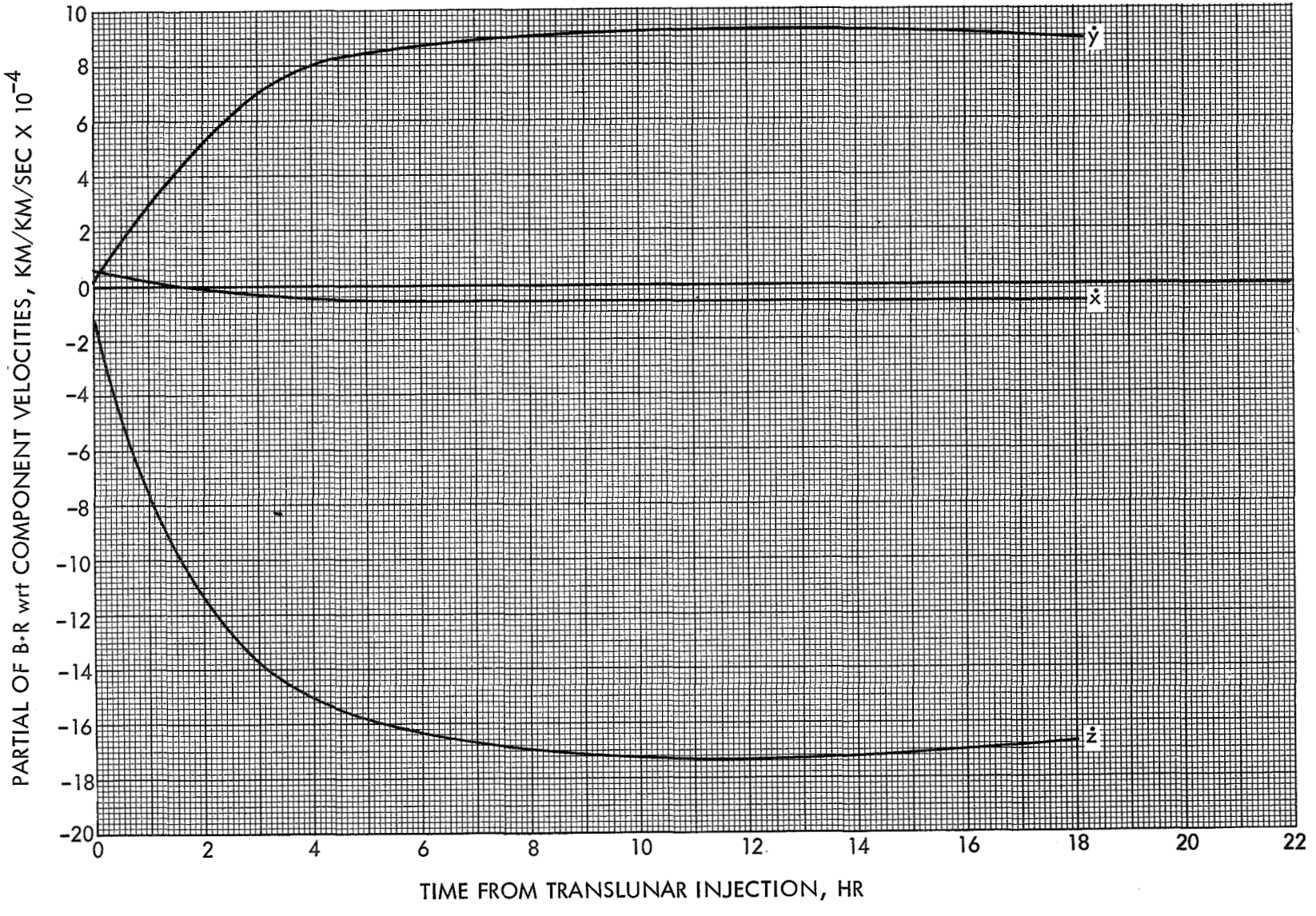

Figure 5.3-13b. Translunar Flight – Midcourse Sensitivities

CONFIDENTIAL

CONFIDENTIAL

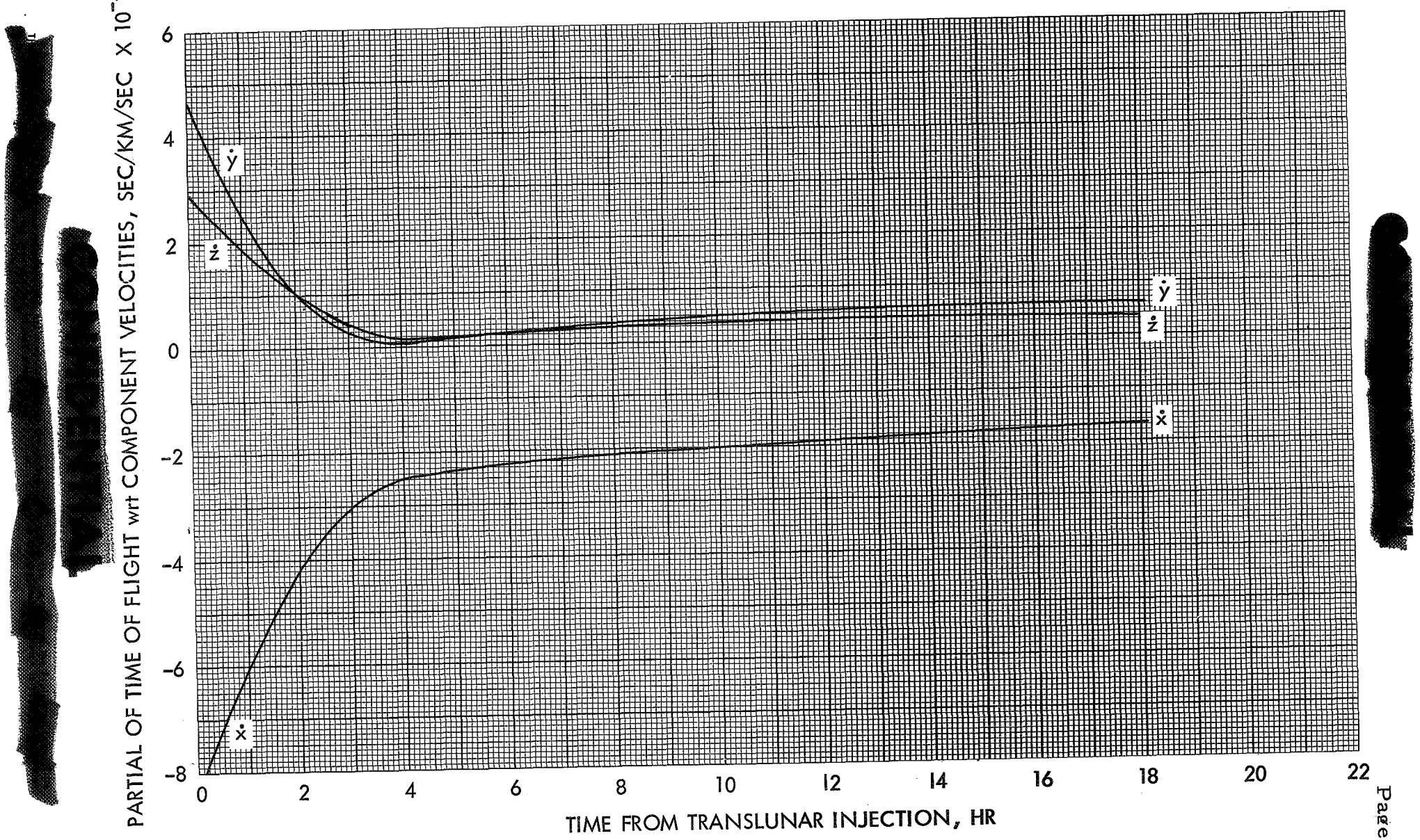

Figure 5.3-13c. Translunar Flight - Midcourse Sensitivities

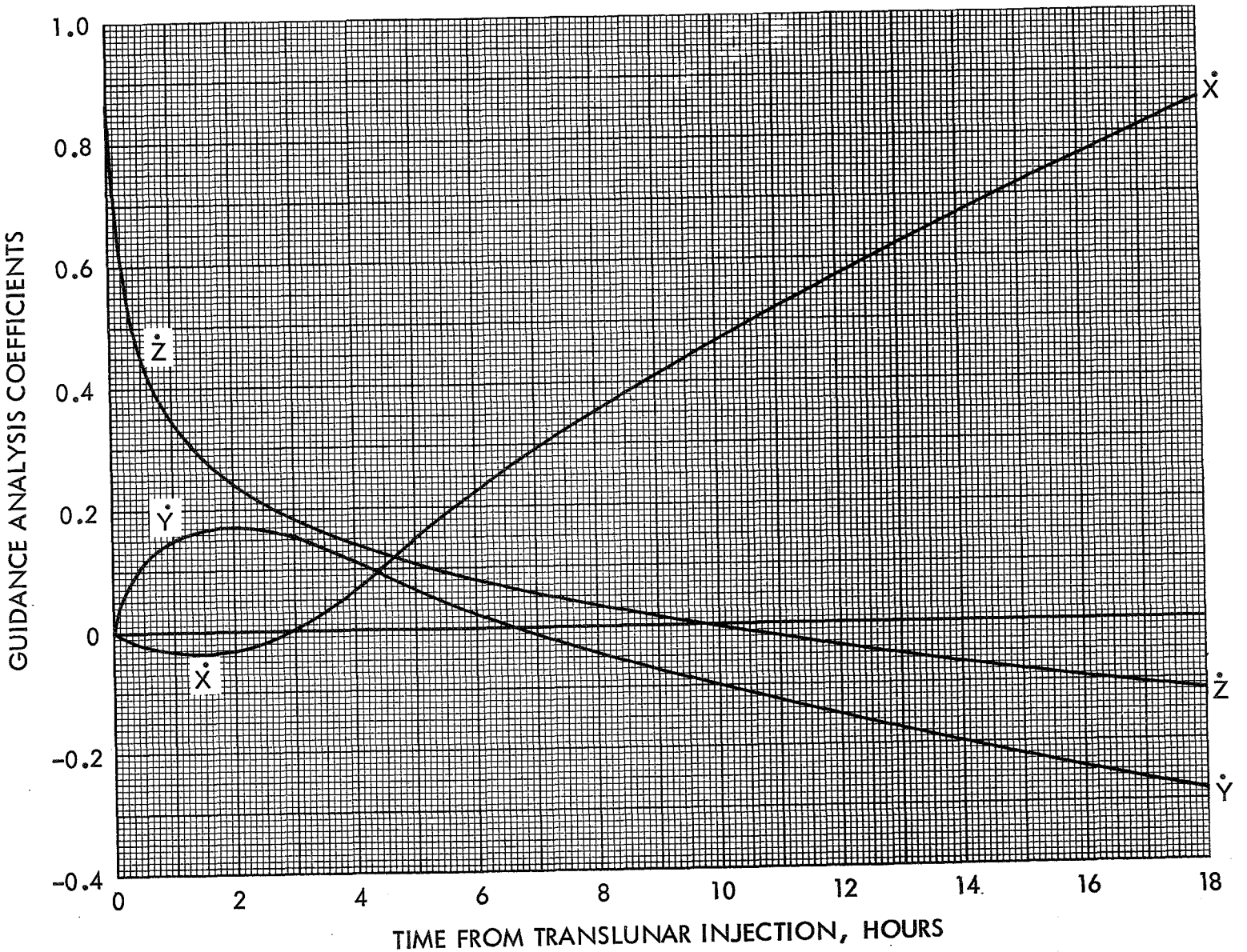

Figure 5.3-14a. Partials of the Z Component of Midcourse Velocity with Respect to the Injection Velocity Components

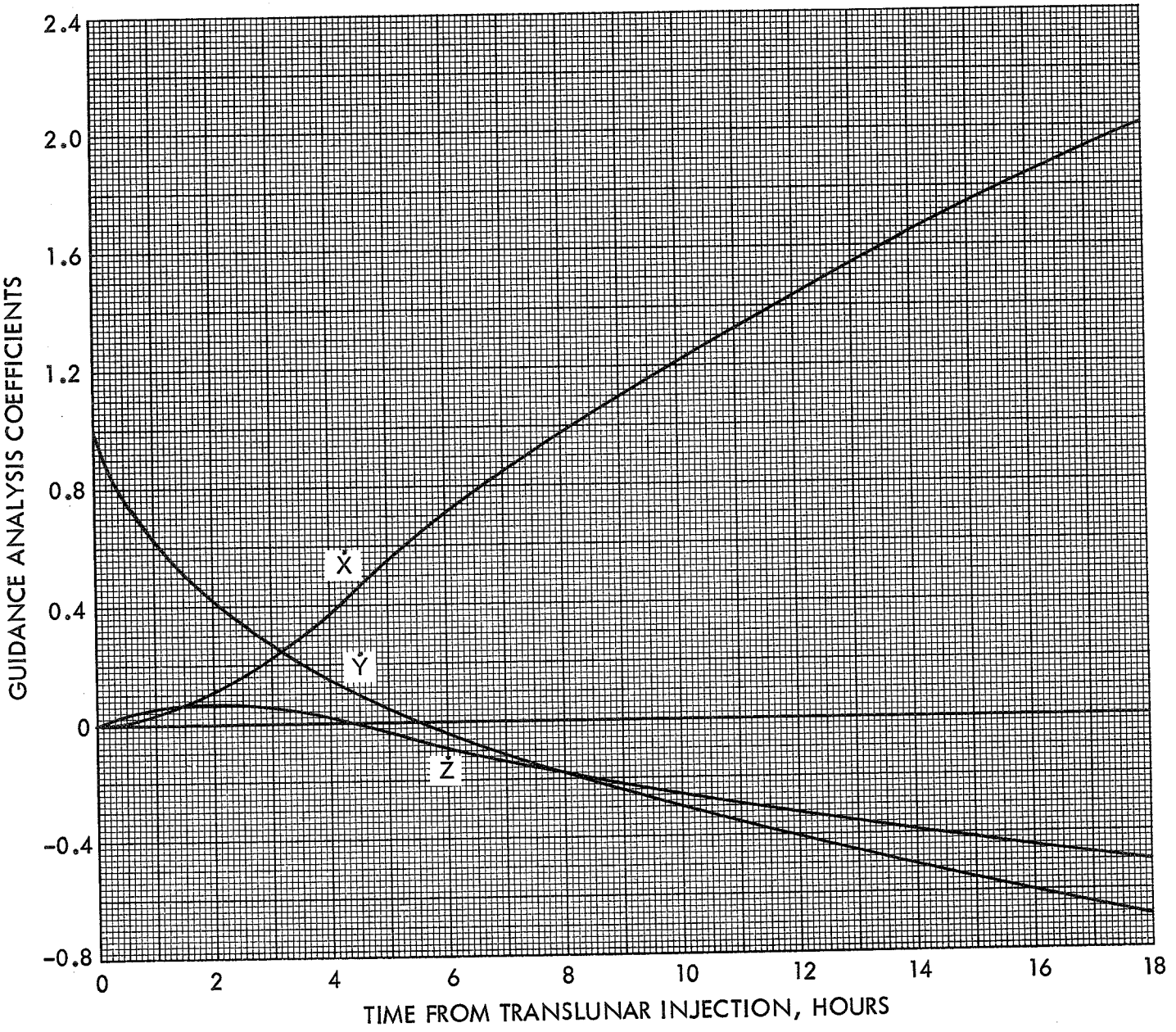

Figure 5.3-14b. Partials of the Y Component of Midcourse Velocity with Respect to the Injection Velocity Components

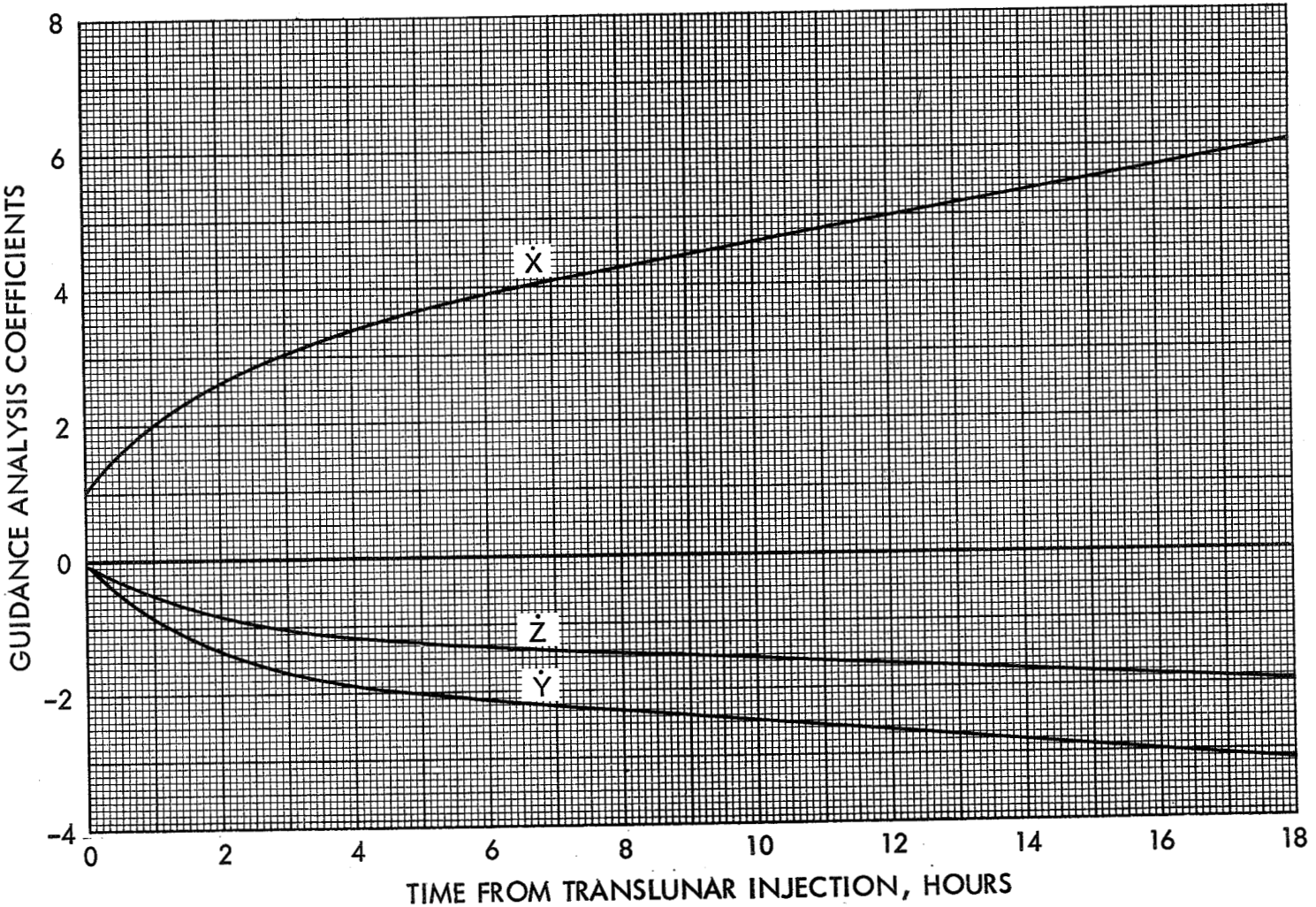

Figure 5.3-14c. Partials of the X Component of Midcourse Velocity with Respect to the Injection Velocity Components

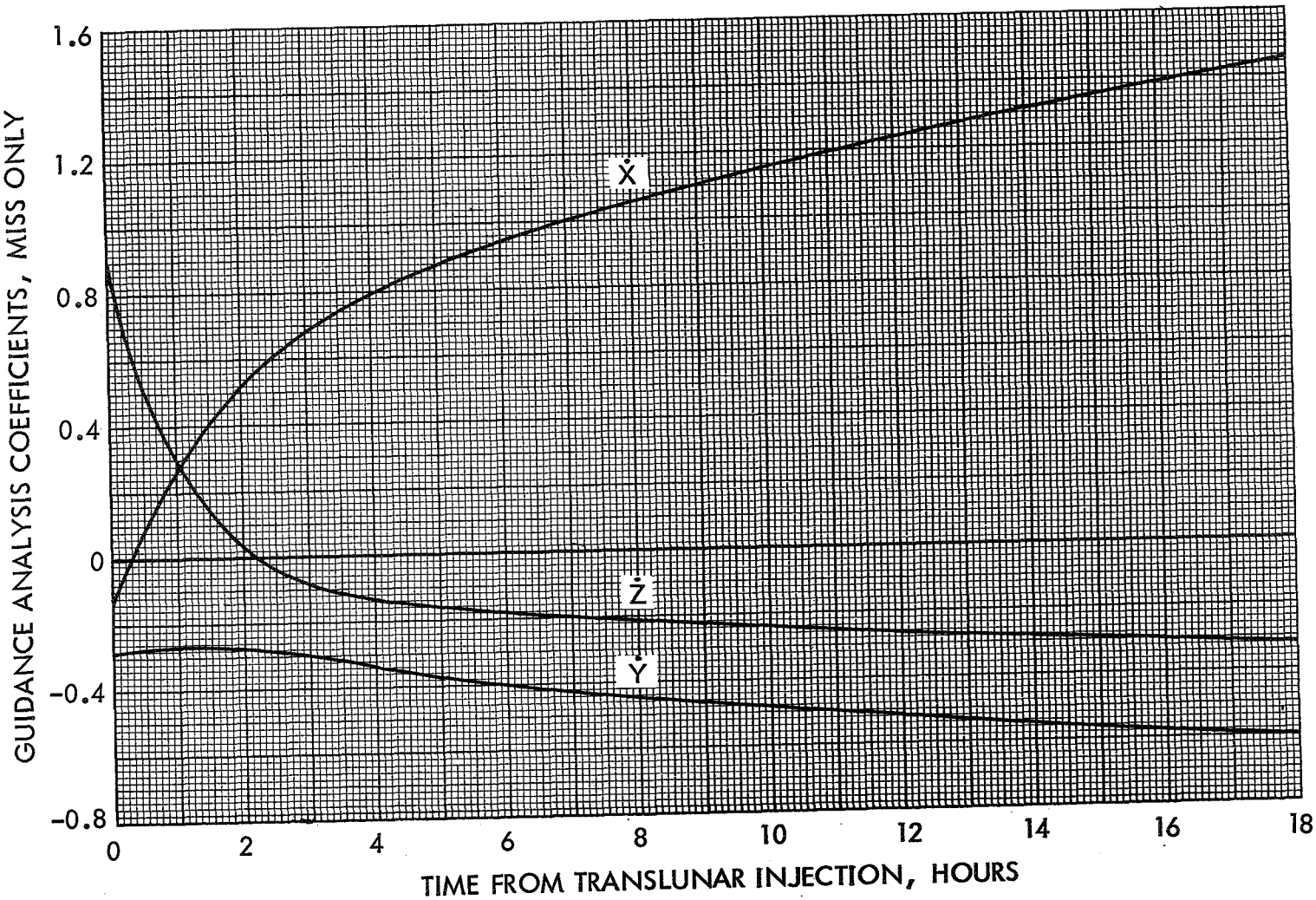

Figure 5.3-14d. Partials of the Z Component of Midcourse Velocity with Respect to the Injection Velocity Components

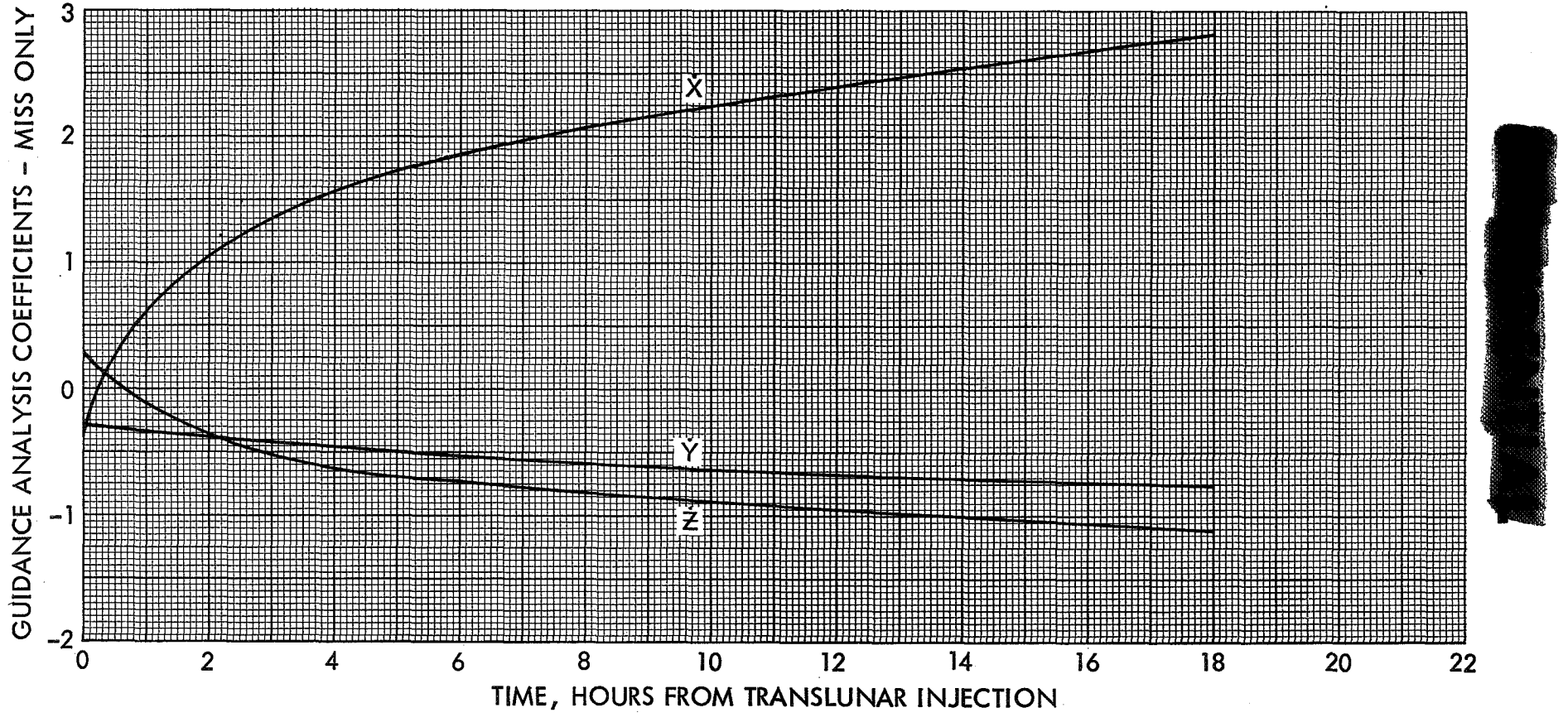

Figure 5.3-14e. Partials of the Y Component of Midcourse Velocity with Respect to the Injection Velocity Components

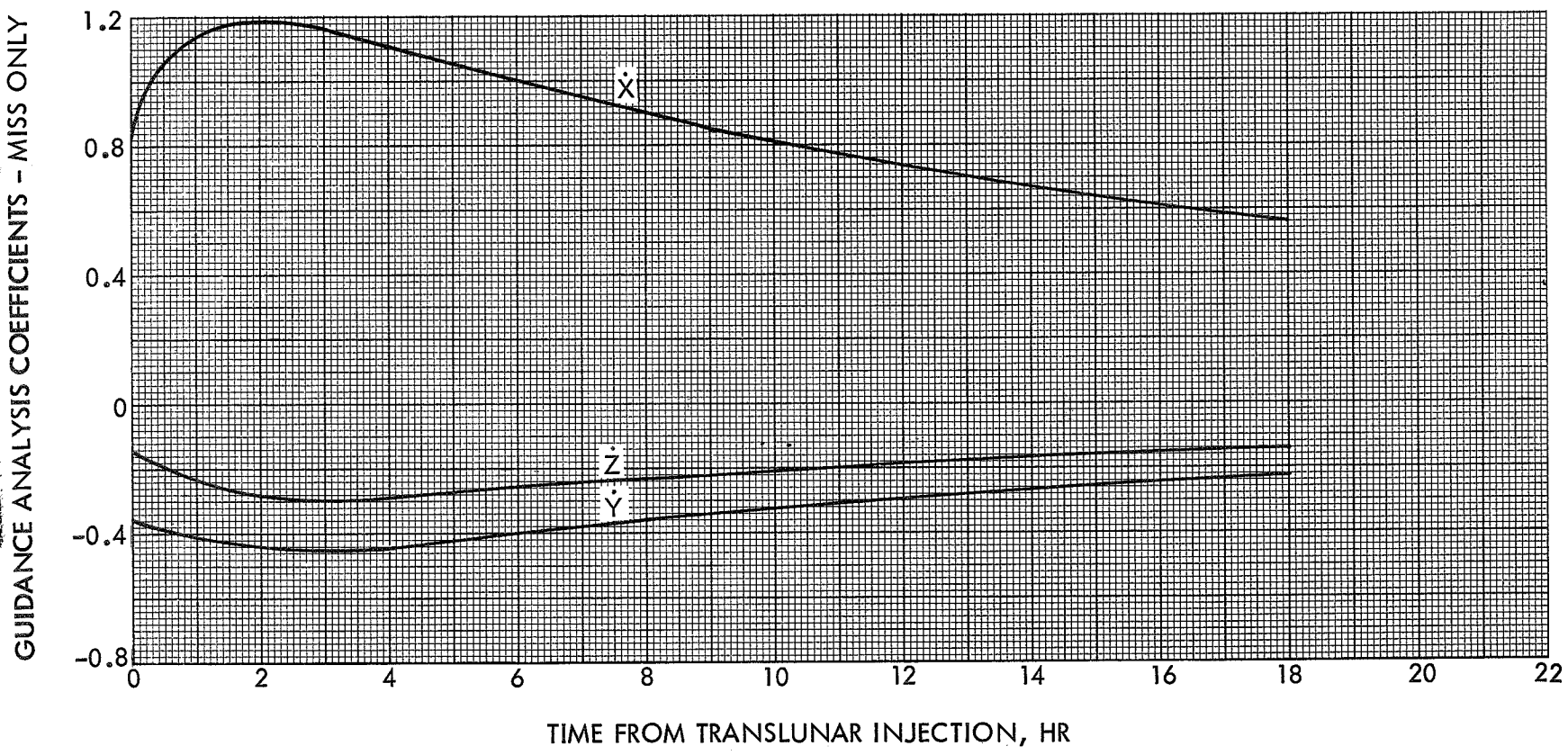

Figure 5.3-14f. Partials of the X Component of Midcourse Velocity with Respect to the Injection Velocity Components

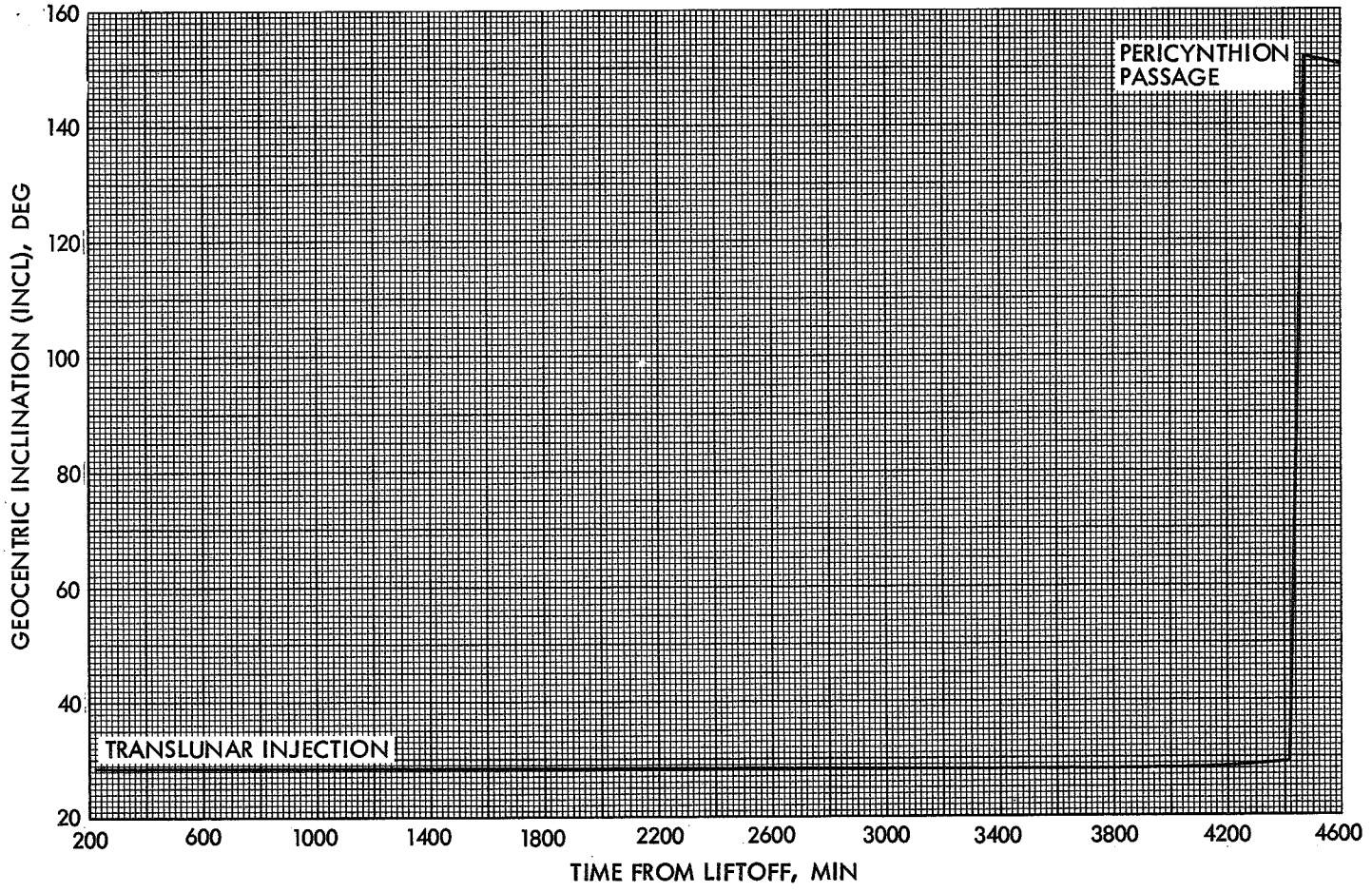

Figure 5.3-15. Translunar Flight – Geocentric Osculating Inclination (INCL)

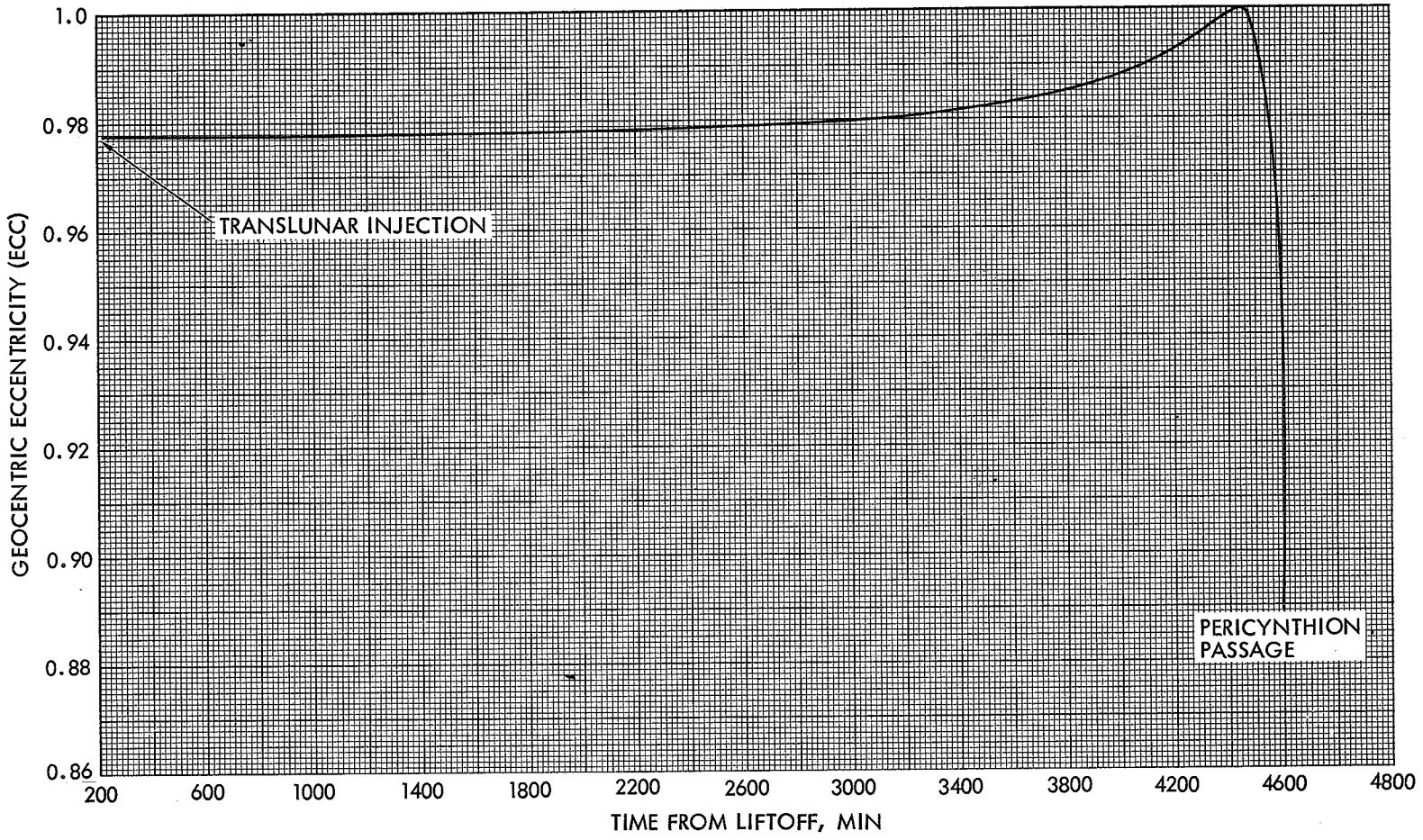

Figure 5.3-16. Translunar Flight – Geocentric Osculating Eccentricity (ECC)

Table 5.4-I. Hyperbolic Deboost and Equiperiod Maneuver - Discrete Events Summary

Time Since Liftoff (minutes)	Altitude (feet)	Latitude (degrees)	Longitude (degrees)	Velocity (feet/second)	Flight Path Angle (degrees)	Velocity Azimuth (degrees)	Pitch Rate / Yaw Rate (degrees/second)	Event
4624.071	628,563	6.084	-163.722	8162.4*	-9.6369*	264.0308*	0.0000 / 0.0000	Start hyperbolic deboost
4629.364	486,088	4.334	176.375	5287.8*	-0.9537*	267.2240*	0.0000 / 0.0000	End hyperbolic deboost/ start coast in circular orbit
4784.456	483,538	-3.205	79.334	5305.8**	-0.0201**	265.9822**	0.0000 / 0.0000	Separate CM/SM and LEM/ start equiperiod maneuver
4784.942	478,132	-3.305	77.902	5310.4**	-4.0073**	266.0631**	0.0000 / 0.0000	End equiperiod maneuver/start coast in elliptical transfer orbit
4813.953	50,000	-3.741	-15.914	5689.9**	0.0000**	273.5287**	0.0000 / 0.0000	First pericynthion arrival
4936.461	49,955	-3.729	-17.142	5689.9**	0.0000**	273.5439**	0.0000 / 0.0000	Second pericynthion arrival

Notes:

*Inertial quantities

**Relative quantities

Table 5.4-II. Hyperbolic Deboost and Equiperiod Maneuver - Spacecraft Weight History.

	CM/SM	LEM	Total
Start Hyperbolic Deboost	57,477	26,500	83,977
Deboost Propellant	-21,677		
End Hyperbolic Deboost/Start Coast in Circular Parking Orbit	35,800	26,500	62,300
Transfer two Astronauts and Equipment to LEM	-440	+440	
Start Equiperiod Maneuver	35,360	26,940	
Equiperiod Propellant		-979	
End Equiperiod Maneuver/Start Coast in Transfer Orbit	35,360	25,961	

[redacted]

[redacted] of the United States within the [redacted]

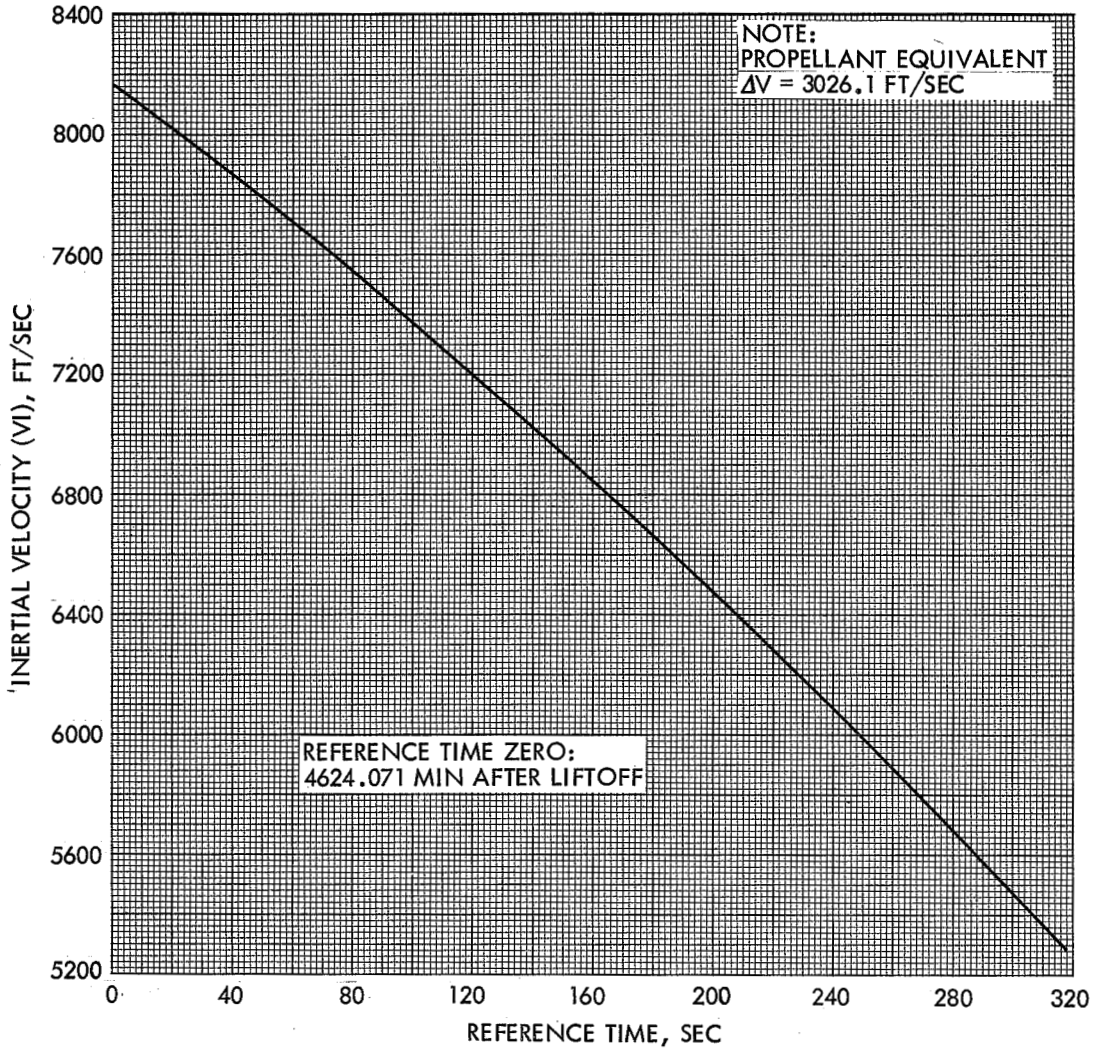

Figure 5.4-1. Hyperbolic Deboost Phase - Inertial Velocity (VI)

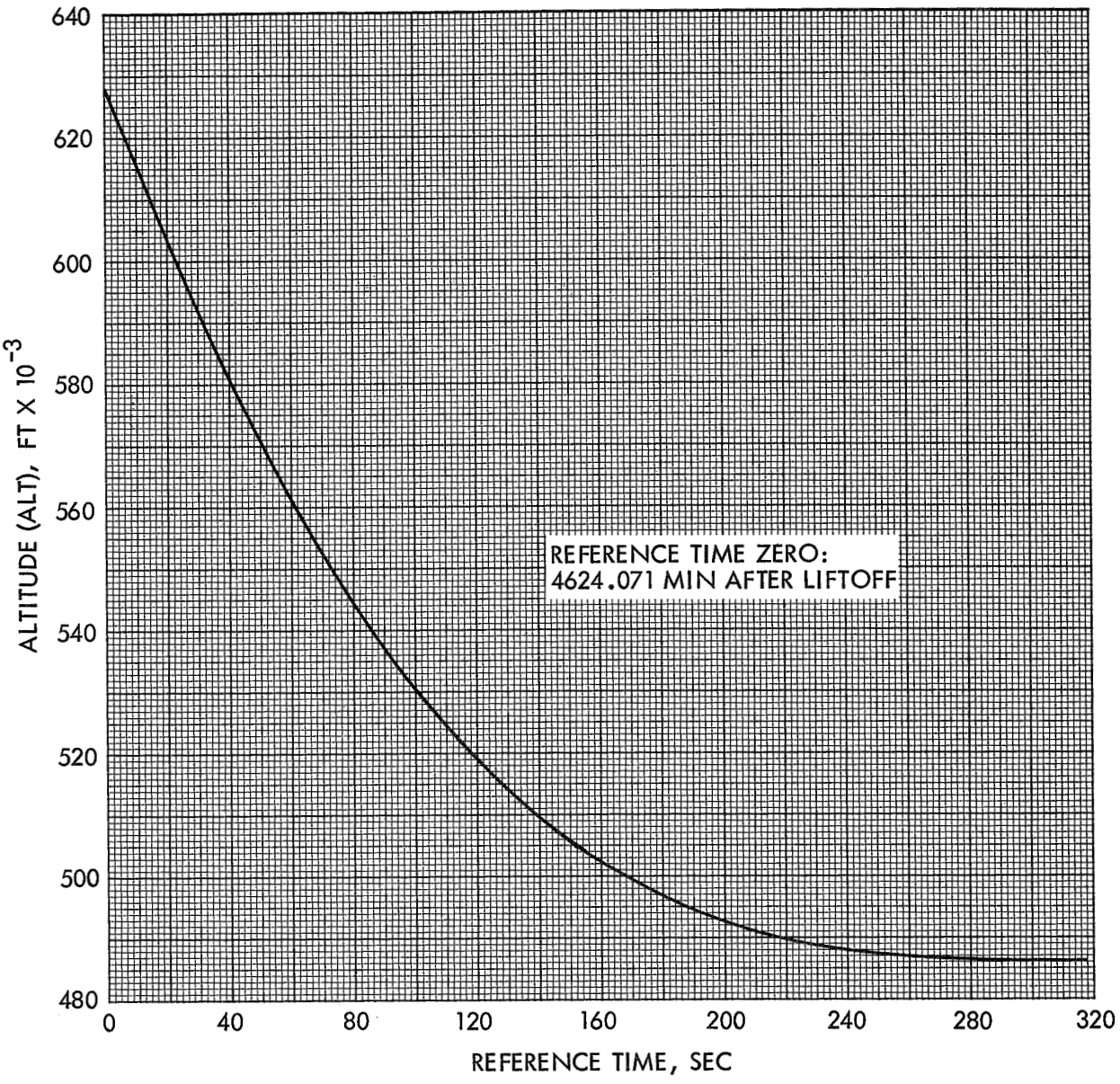

Figure 5.4-2. Hyperbolic Deboost Phase – Altitude (ALT)

Title law.

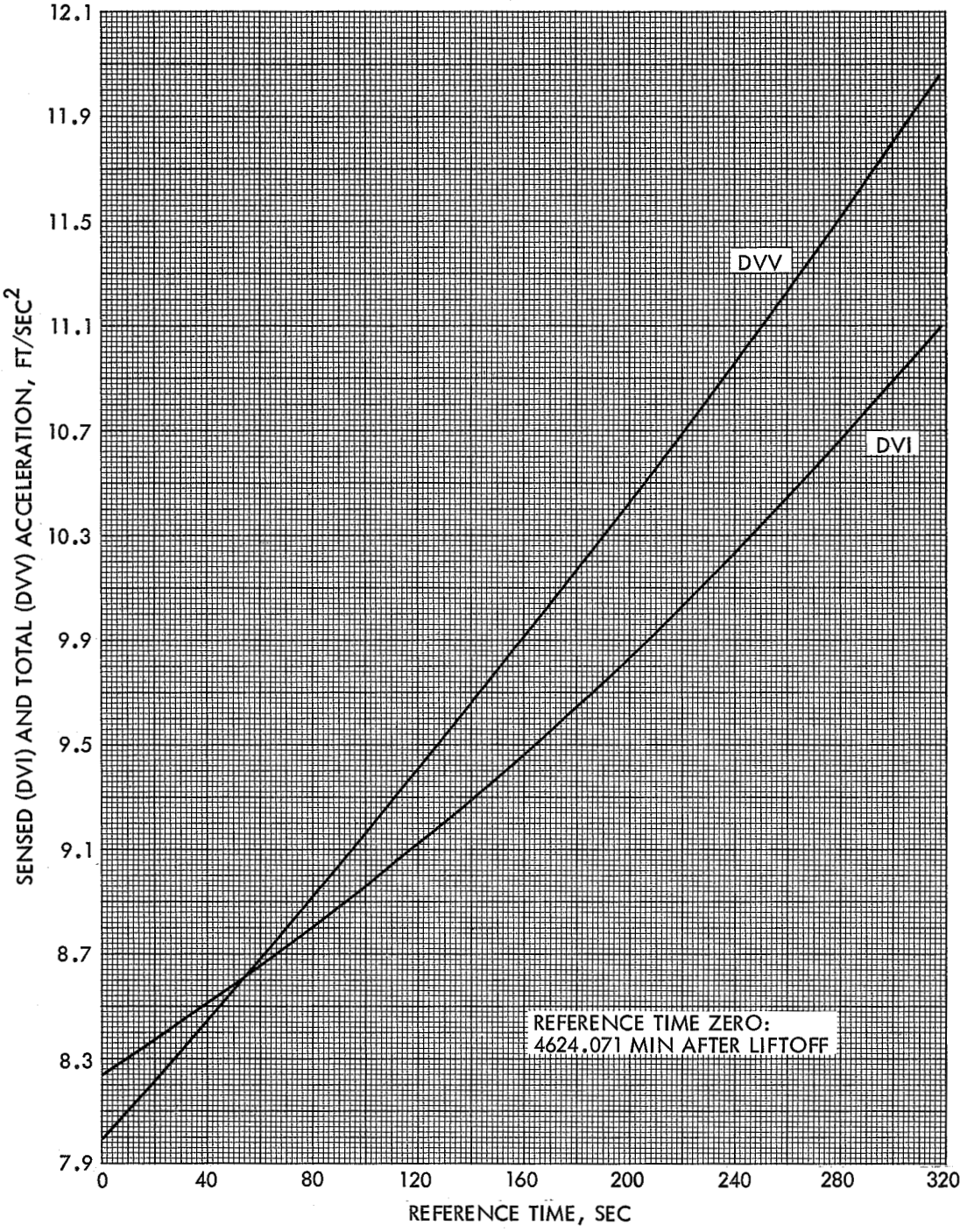

Figure 5.4-3. Hyperbolic Deboost Phase – Sensed (DVI) and Total (DVV) Acceleration

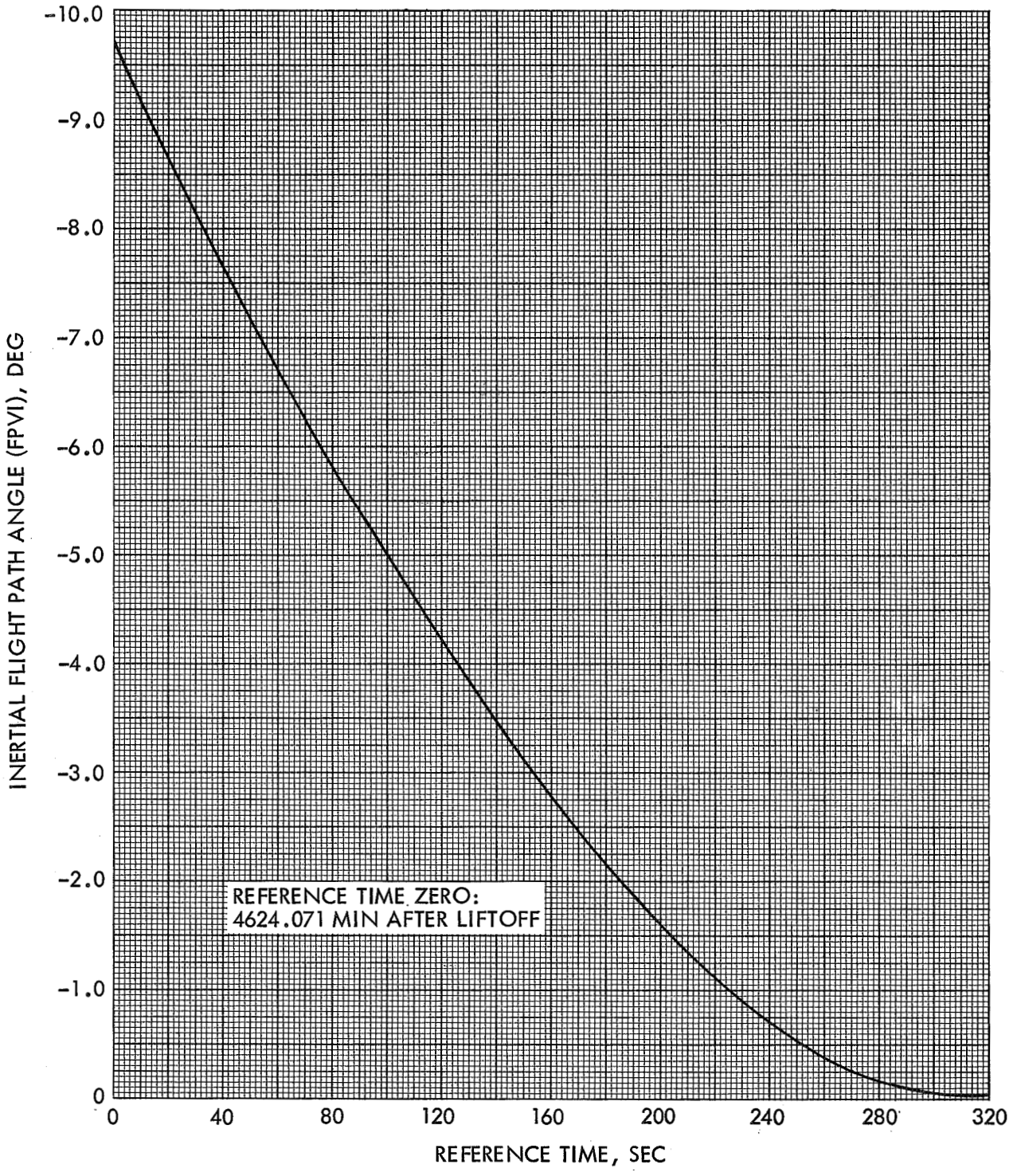

Figure 5.4-4. Hyperbolic Deboost Phase – Inertial Flight Path Angle (FPVI)

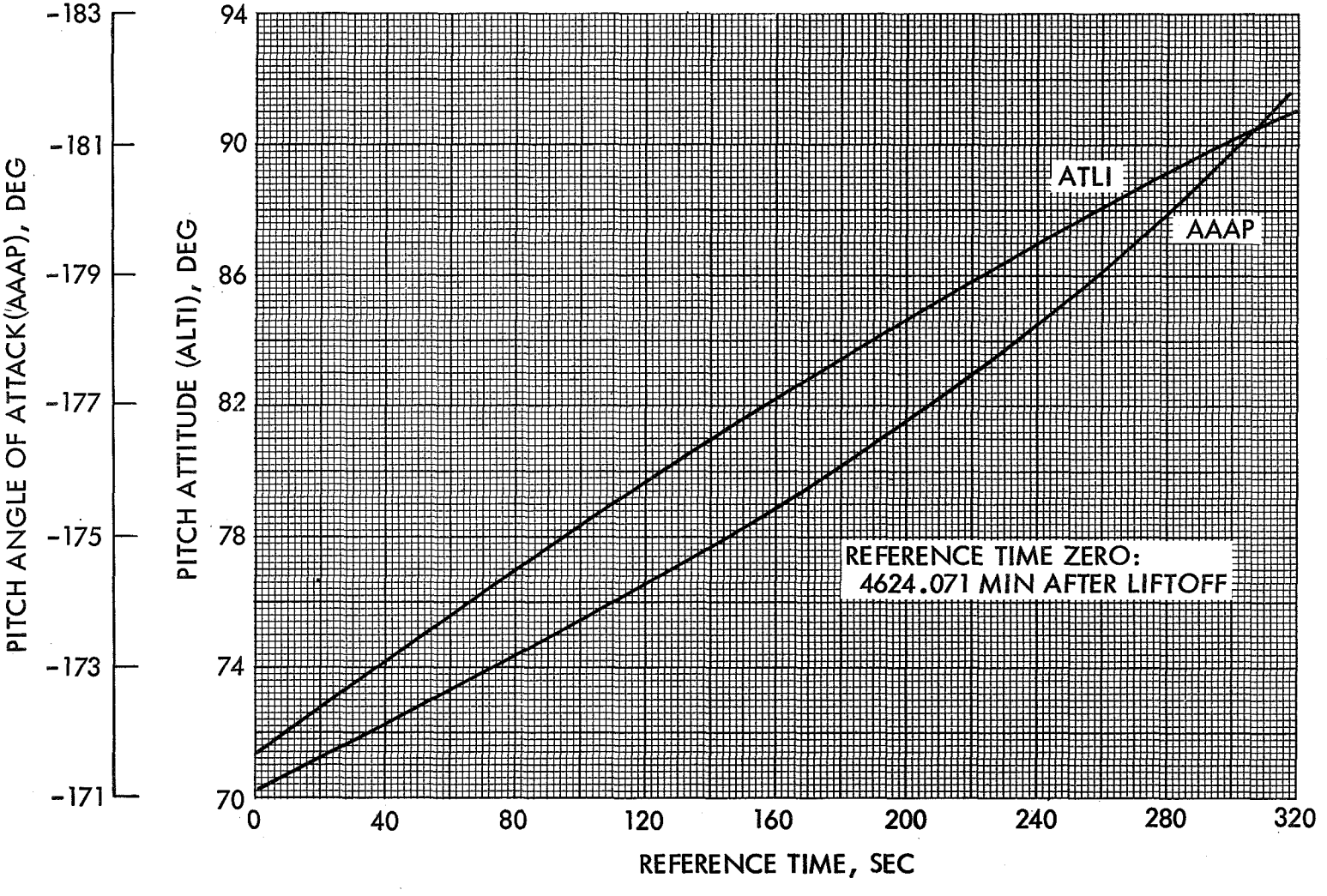

Figure 5.4-5. Hyperbolic Deboost Phase – Pitch Attitude (ATLI) and Pitch Angle of Attack (AAAP)

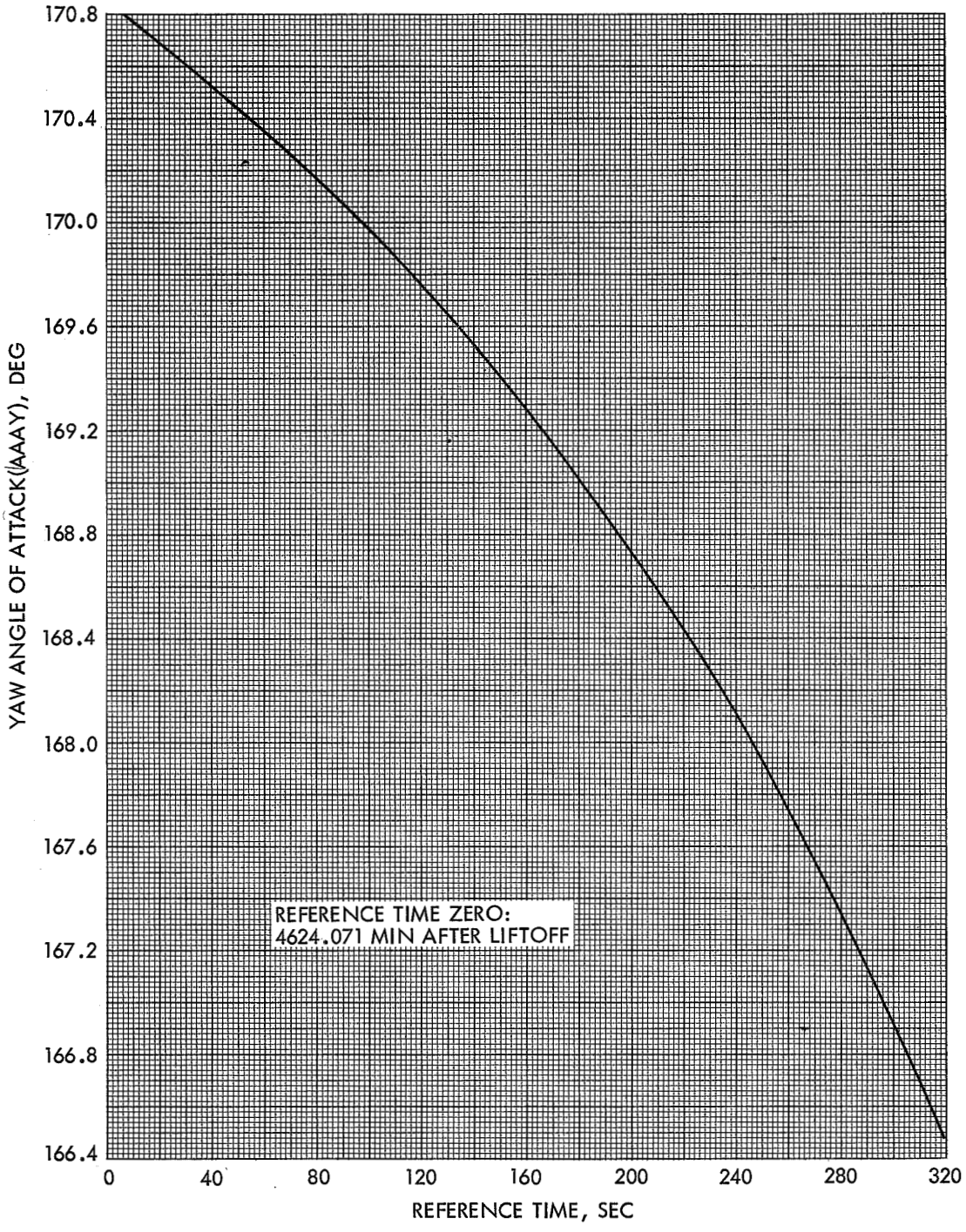

Figure 5.4-6. Hyperbolic Deboost Phase – Yaw Angle of Attack (AAAY)

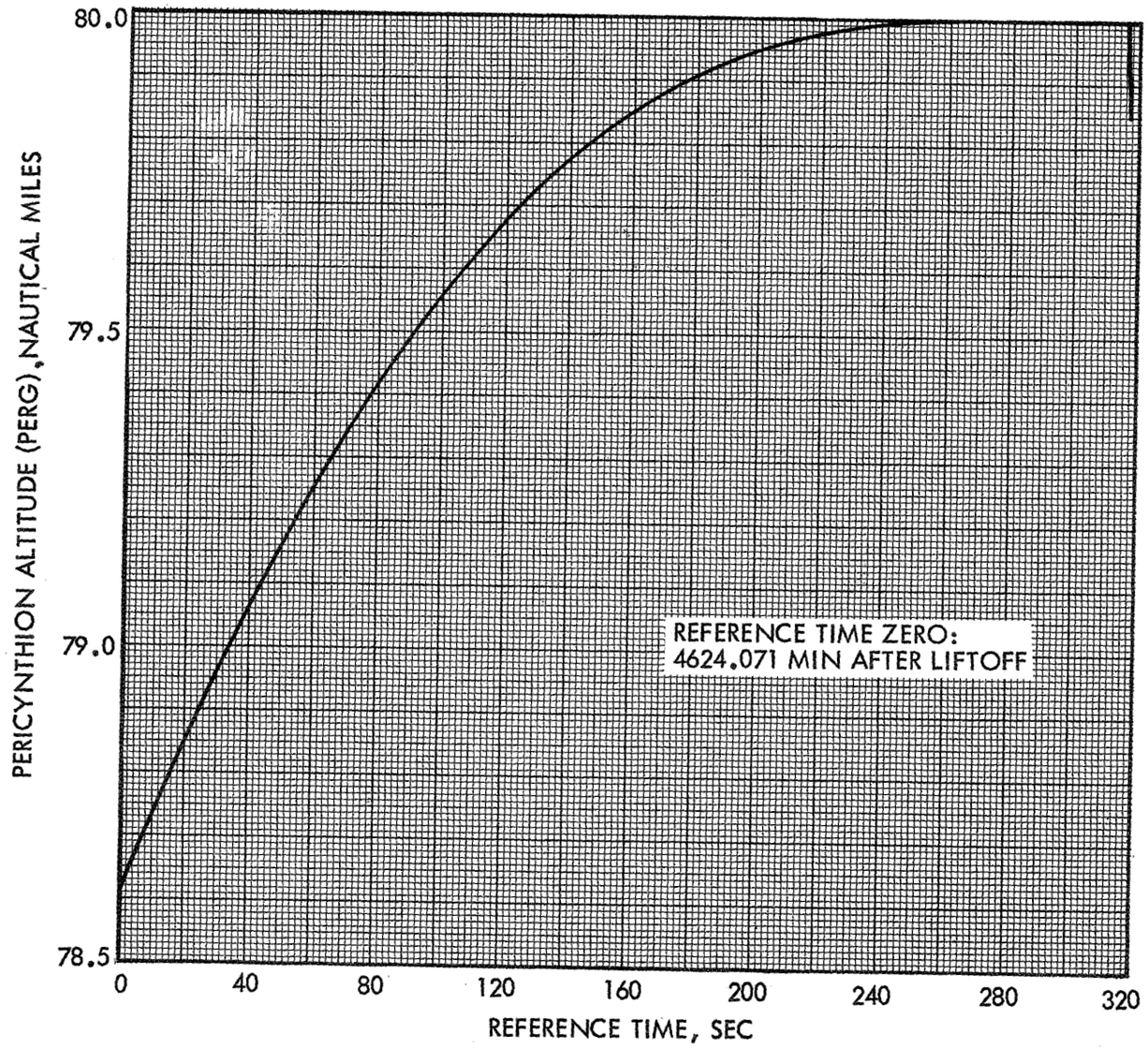

Figure 5.4-7. Hyperbolic Deboost and Equiperiod Maneuver - Predicted Pericynthion Altitude (PERG)

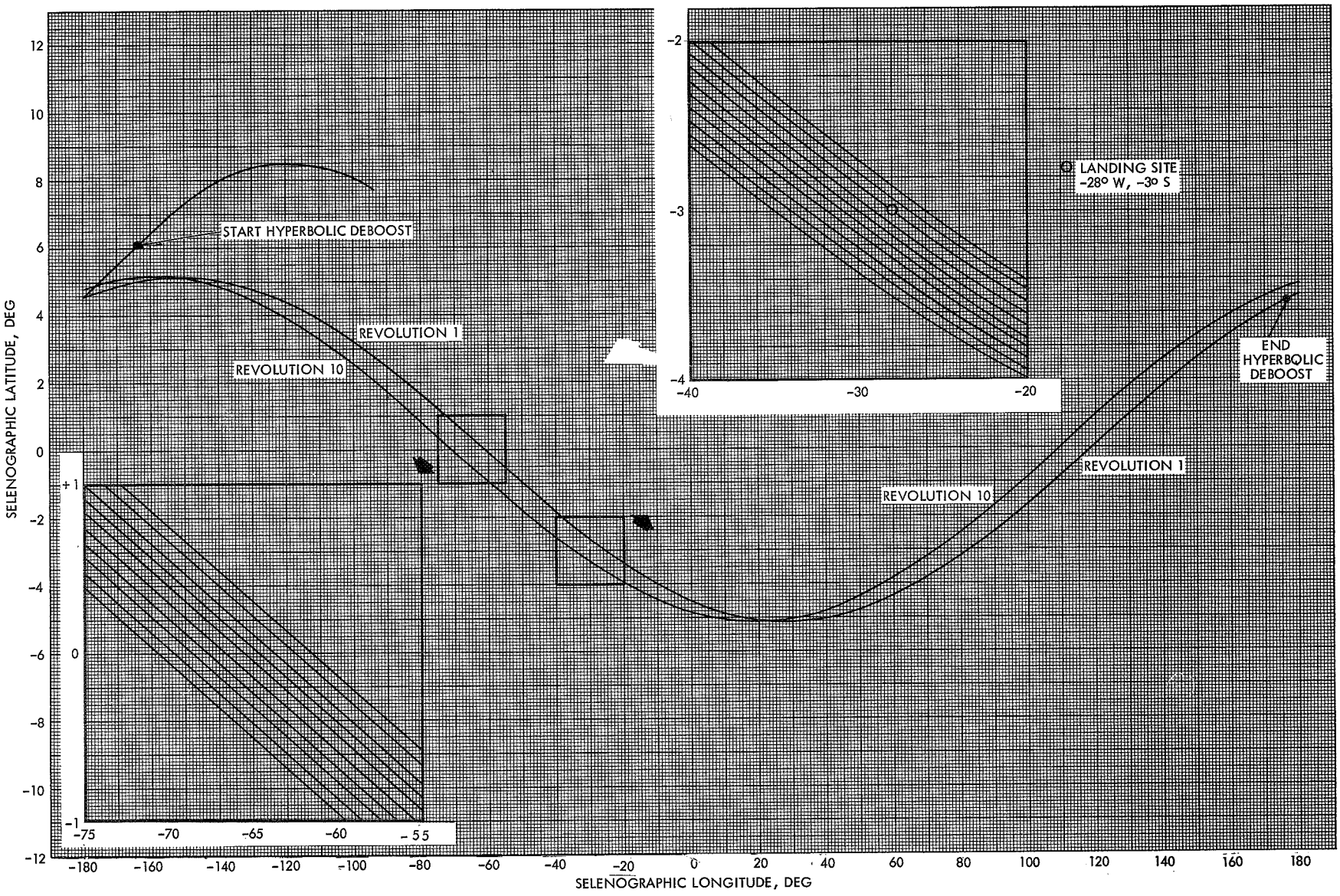

Figure 5.4-8. Hyperbolic Deboost Phase – CM/SM Lunar Ground Track

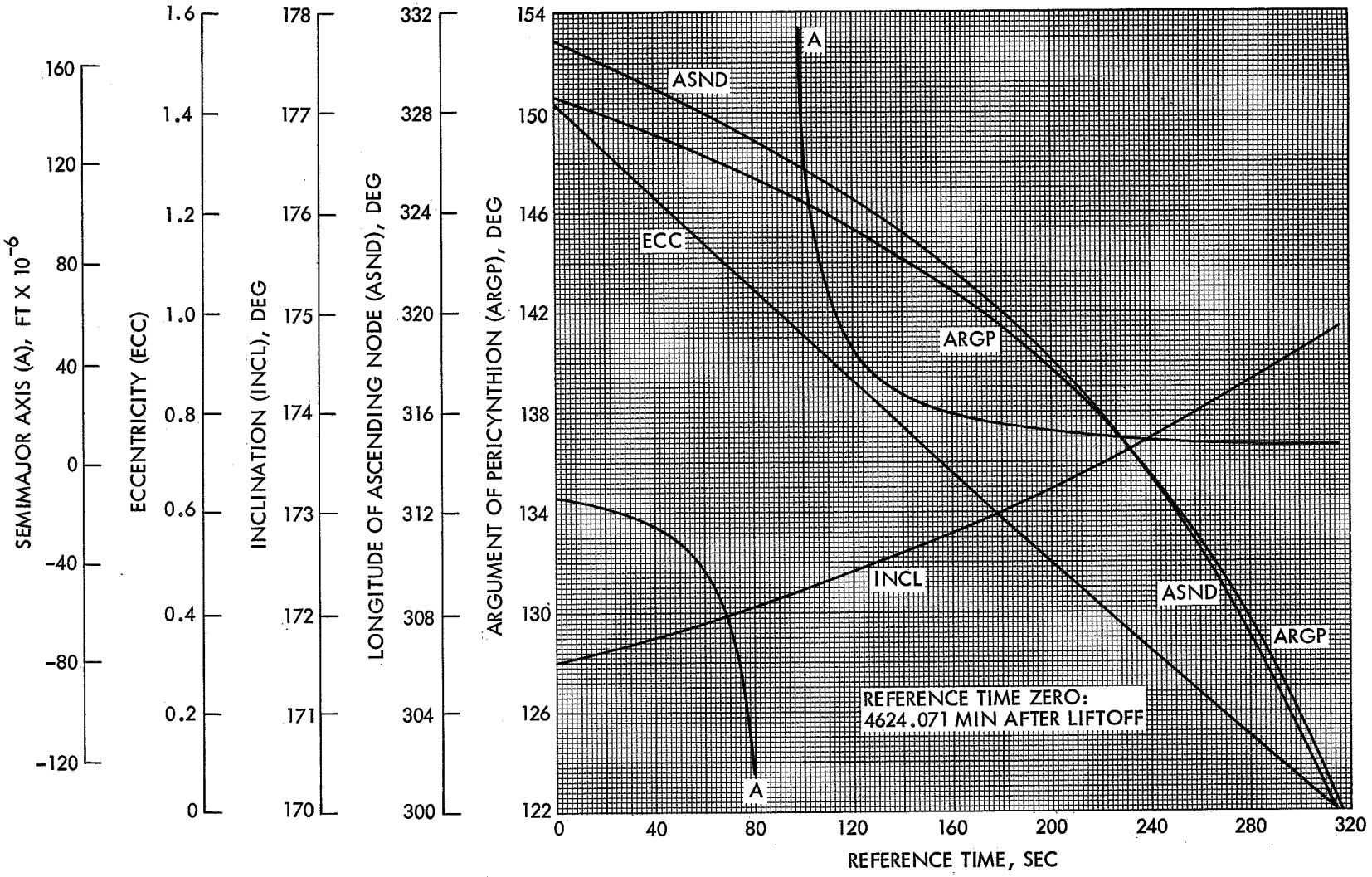

Figure 5.4-9. Hyperbolic Deboost Phase – Selenographic Orbital Elements

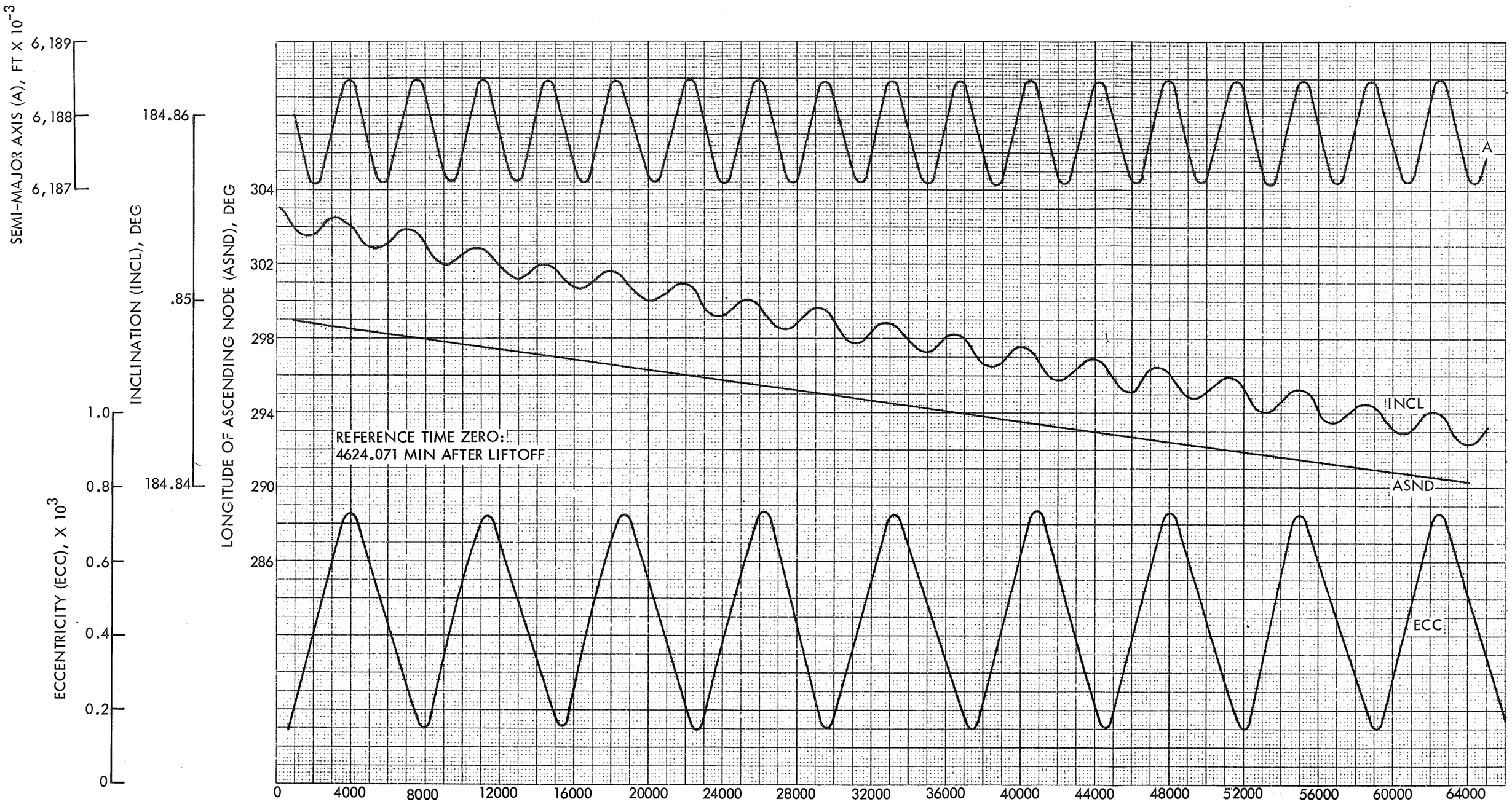

Figure 5.4-10. Hyperbolic Deboost Phase - CM/SM Orbital Elements

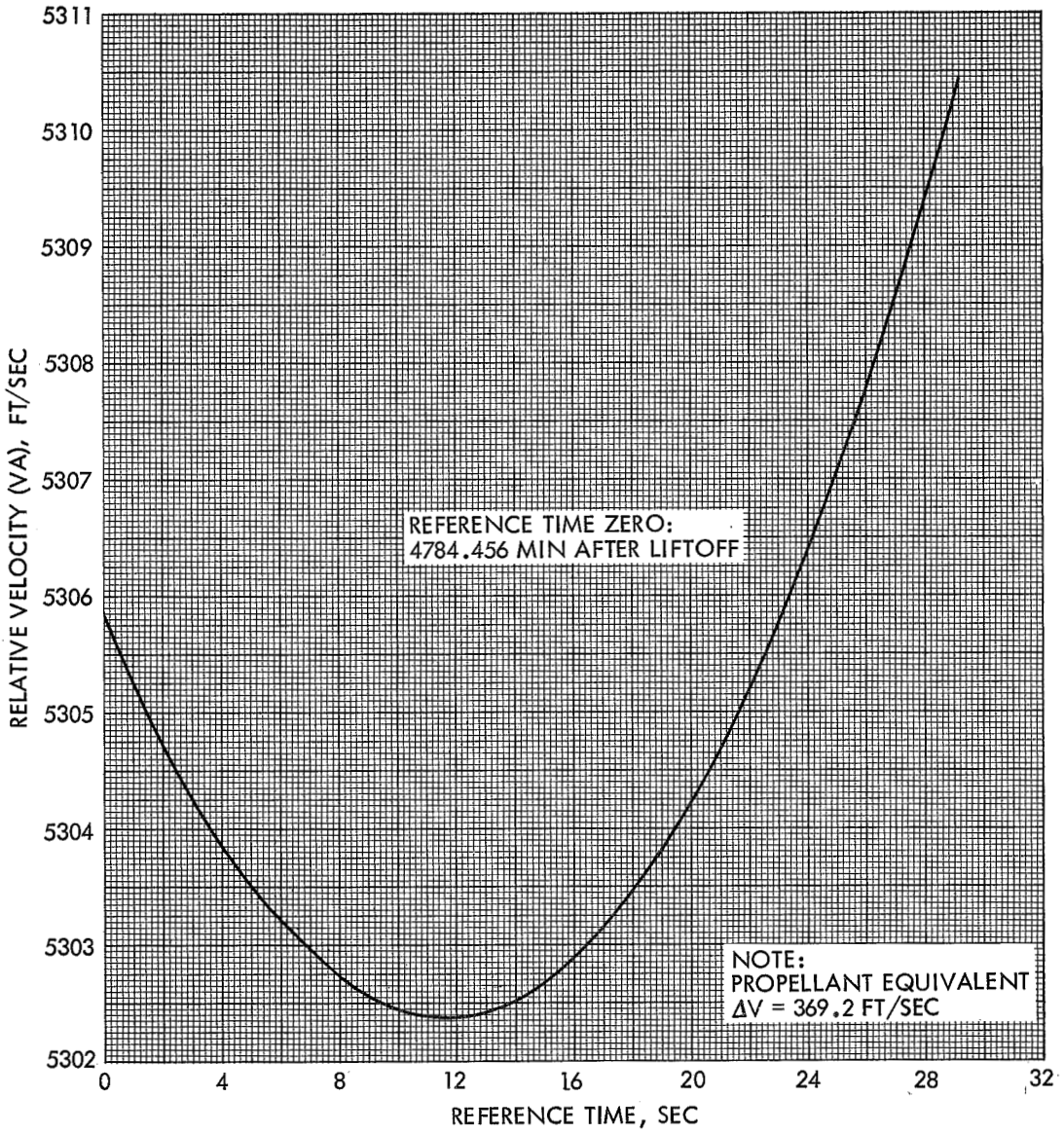

Figure 5.4-11. Equiperiod Maneuver Phase - Relative Velocity (VA)

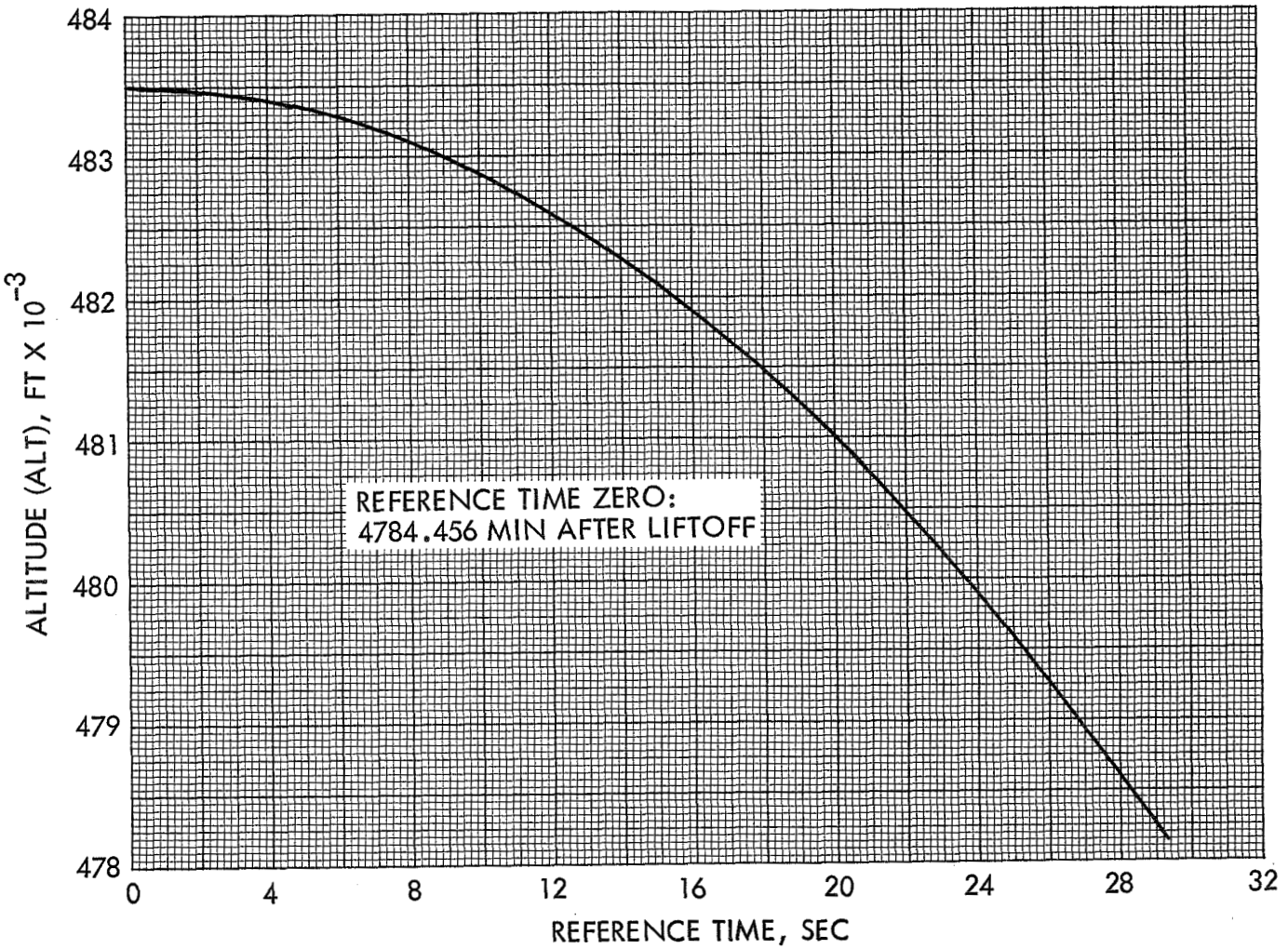

Figure 5.4-12. Equiperiod Maneuver Phase – Altitude (ALT)

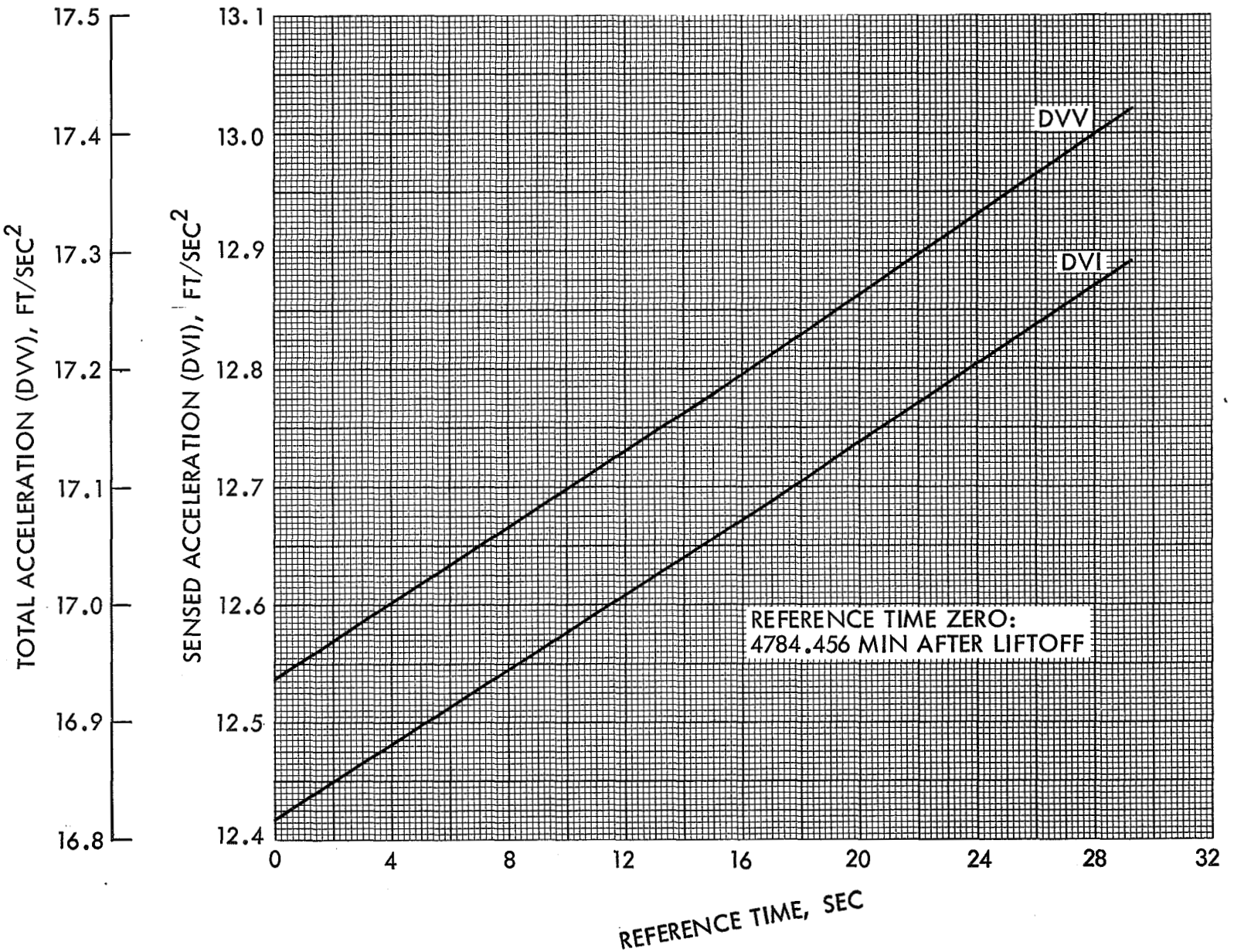

Figure 5.4-13. Equiperiod Maneuver Phase – Sensed (DVI) and Total (DVV) Acceleration

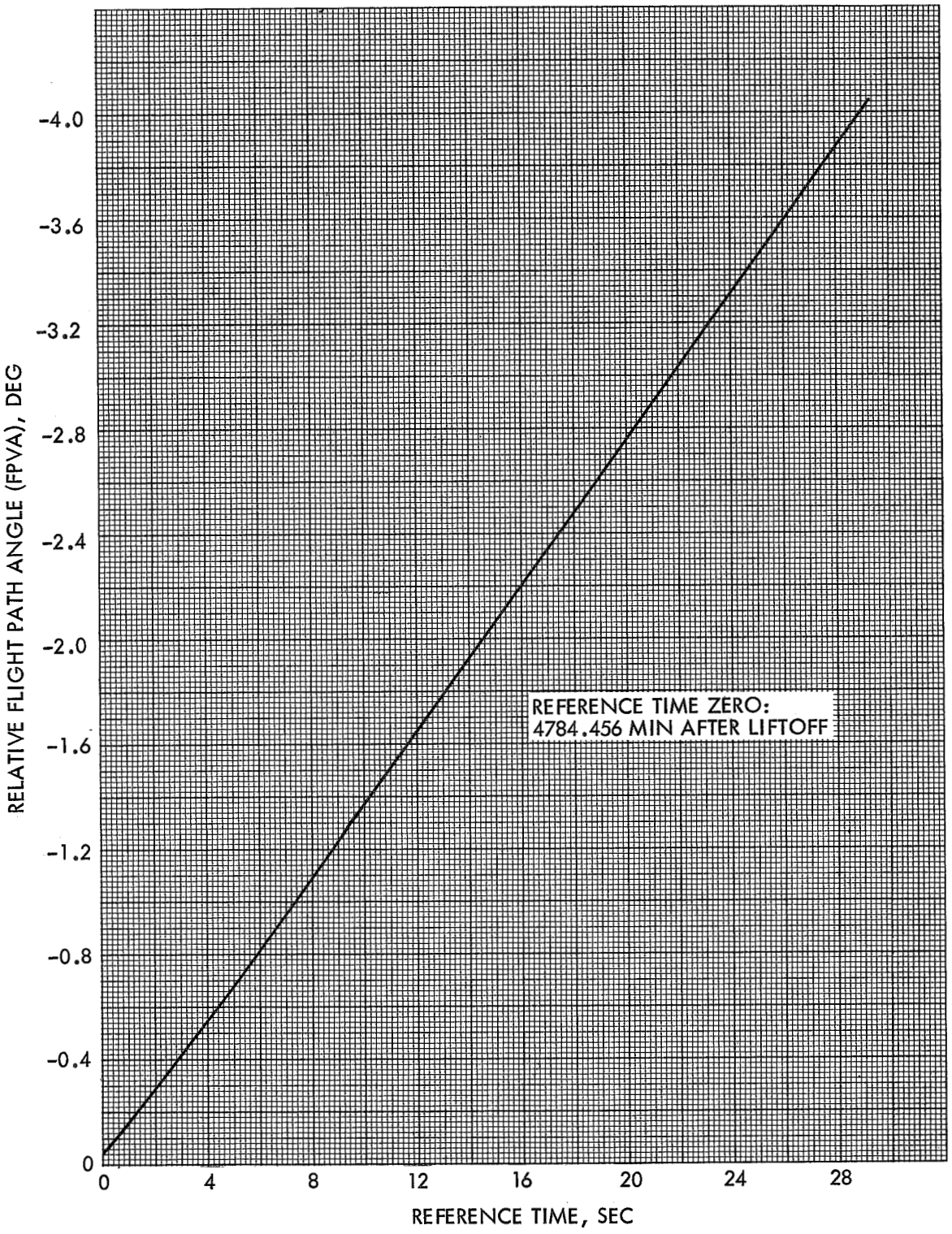

Figure 5.4-14. Equiperiod Maneuver Phase – Relative Flight Path Angle (FPVA)

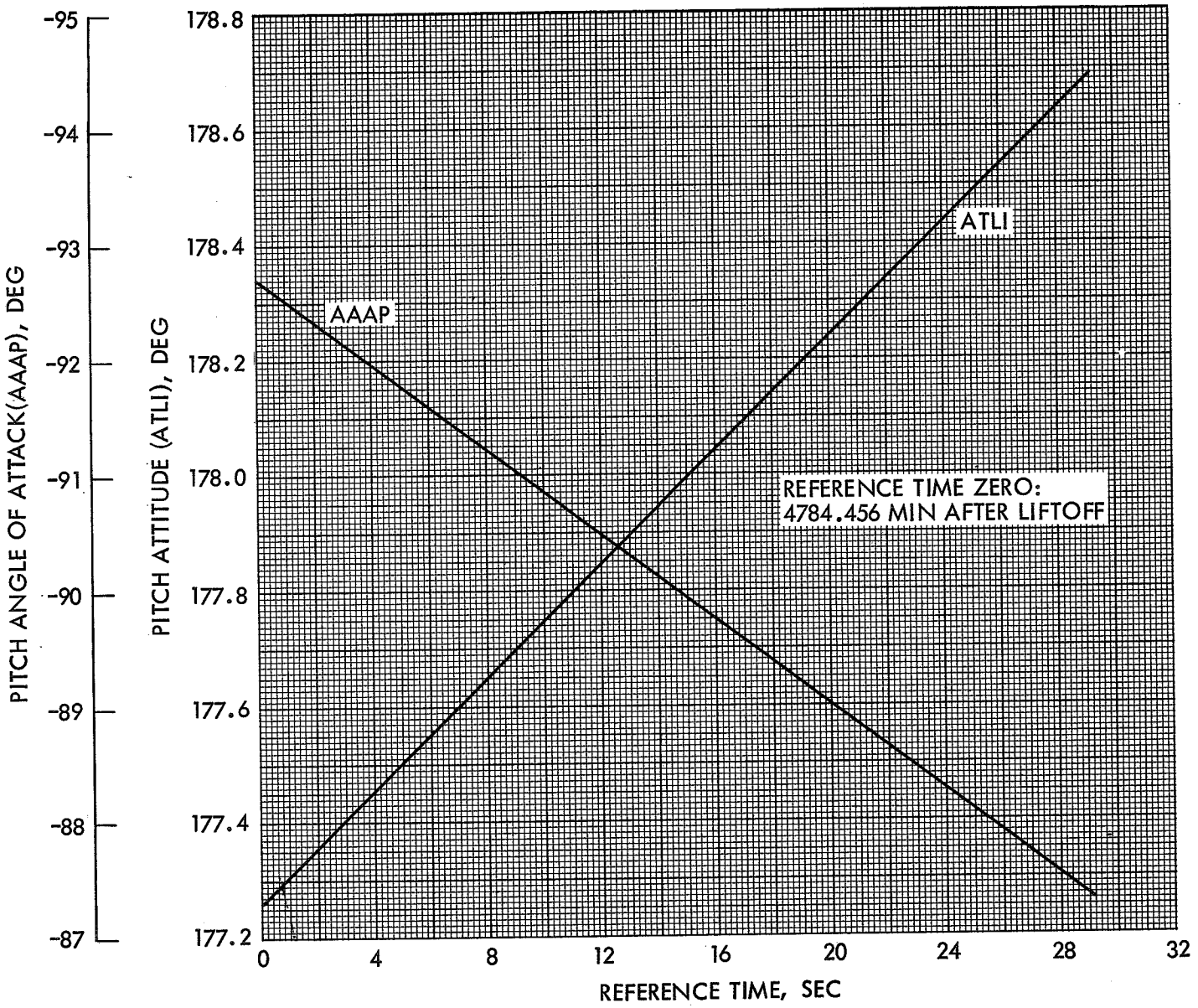

Figure 5.4-15. Equiperiod Maneuver Phase – Pitch Attitude (ATLI) and Pitch Angle of Attack (AAAP)

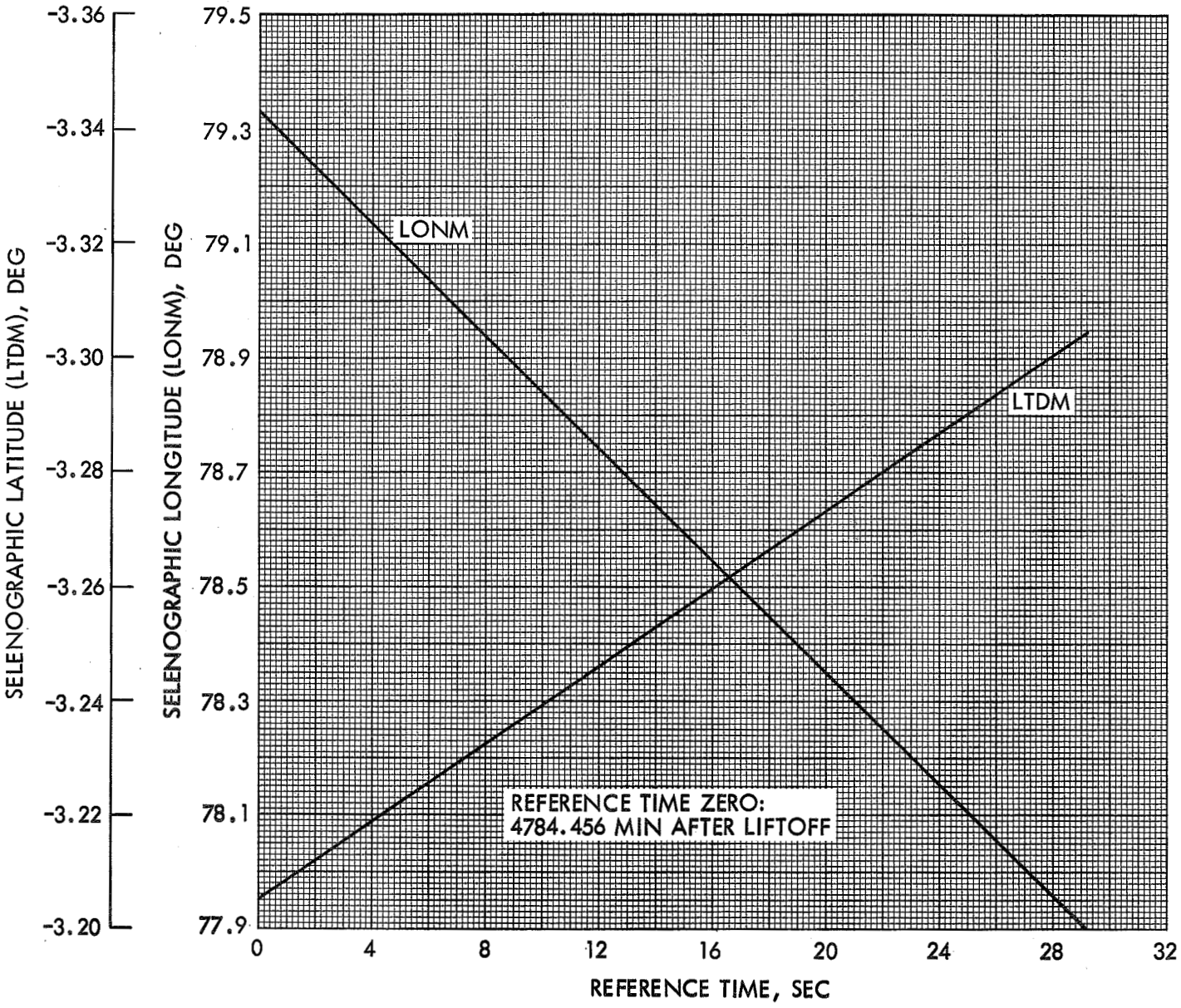

Figure 5.4-16. Equiperiod Maneuver Phase – Selenographic Latitude (LTDM) and Longitude (LONM)

Table 5.5-I. LEM Descent and Ascent - Discrete Events Summary

Time Since Liftoff (minutes)	Altitude (feet)	Latitude (degrees)	Longitude (degrees)	Velocity (feet/second)	Flight Path Angle (degrees)	Velocity Azimuth (degrees)	Pitch Rate / Yaw Rate (degrees/second)	Event
4936.461	49,955	-3.729	-17.142	5689.9	0.0000	273.5439	0.1075 / 0.0000	Start LEM powered descent to surface
4937.619	48,763	-3.498	-20.760	4753.1	-0.5295	273.7690	0.1057 / 0.0000	Enter landing site visibility sphere
4941.635	9,996	-3.027	-27.584	700.1	-13.4166	274.0811	0.0000 / 0.0000	Achieve 10,000 ft altitude
4943.386	993	-2.998	-27.988	75.0	-0.0273		0.9606 / 0.0000	Achieve hover condition
4944.086	400	-2.998	-27.999	18.6	-86.9060		0.0000 / 0.0000	Start vertical descent
4944.444	198	-2.998	-27.999	1.0	-2.1726		0.0000 / 0.0000	Achieve hover condition
4945.111	-1	-2.998	-27.999	1.0	-0.7932			Touchdown
5430.944	0	-2.998	-27.999	0.0	89.9901		0.0000 / 0.0000	Liftoff
5430.961	3	-2.998	-27.999	6.1	90.0000		3.0000 / 0.0000	Start constant high pitch rate program
5431.257	949	-2.998	-28.003	124.2	44.6515	268.5123	0.1264 / 0.0237	Start constant low pitch rate program
5437.573	50,004	-2.604	-37.325	5499.9	0.0006	274.4376	0.0000 / 0.0000	Start transfer to Hohmann ellipse
5437.656	50,006	-2.583	-37.601	5599.9	0.0079	274.4502	0.0000 / 0.0000	End powered ascent/start coast in Hohmann ellipse
5495.643	485,841	2.597	142.106	5207.7	0.0000	265.5593	0.0000 / 0.0000	Apocynthion arrival

Table 5.5-II. LEM Descent and Ascent - Spacecraft Weight History.

	CM/SM	LEM
Start Final Descent to Lunar Surface	35,360	25,961
Propellant Flow from 50,000 to 10,000 feet		-10,416
Propellant Flow from 10,000 to 1,000 feet		-1,398
Propellant Flow from 1,000 to 400 feet		-312
Propellant Flow from 400 to 200 feet		-183
Propellant Flow from 200 to 75 feet		-166
Propellant Flow from 75 to 0 feet		-122
Touchdown on Lunar Surface	35,360	13,364
Jettison LEM Descent Stage and Excess Propellant		-4,874
Liftoff from Lunar Surface	35,360	8,490
Propellant Flow in Ascent to 50,000 feet		-3,717
End Powered Ascent/Start Coast in Hohmann Transfer Ellipse	35,360	4,773

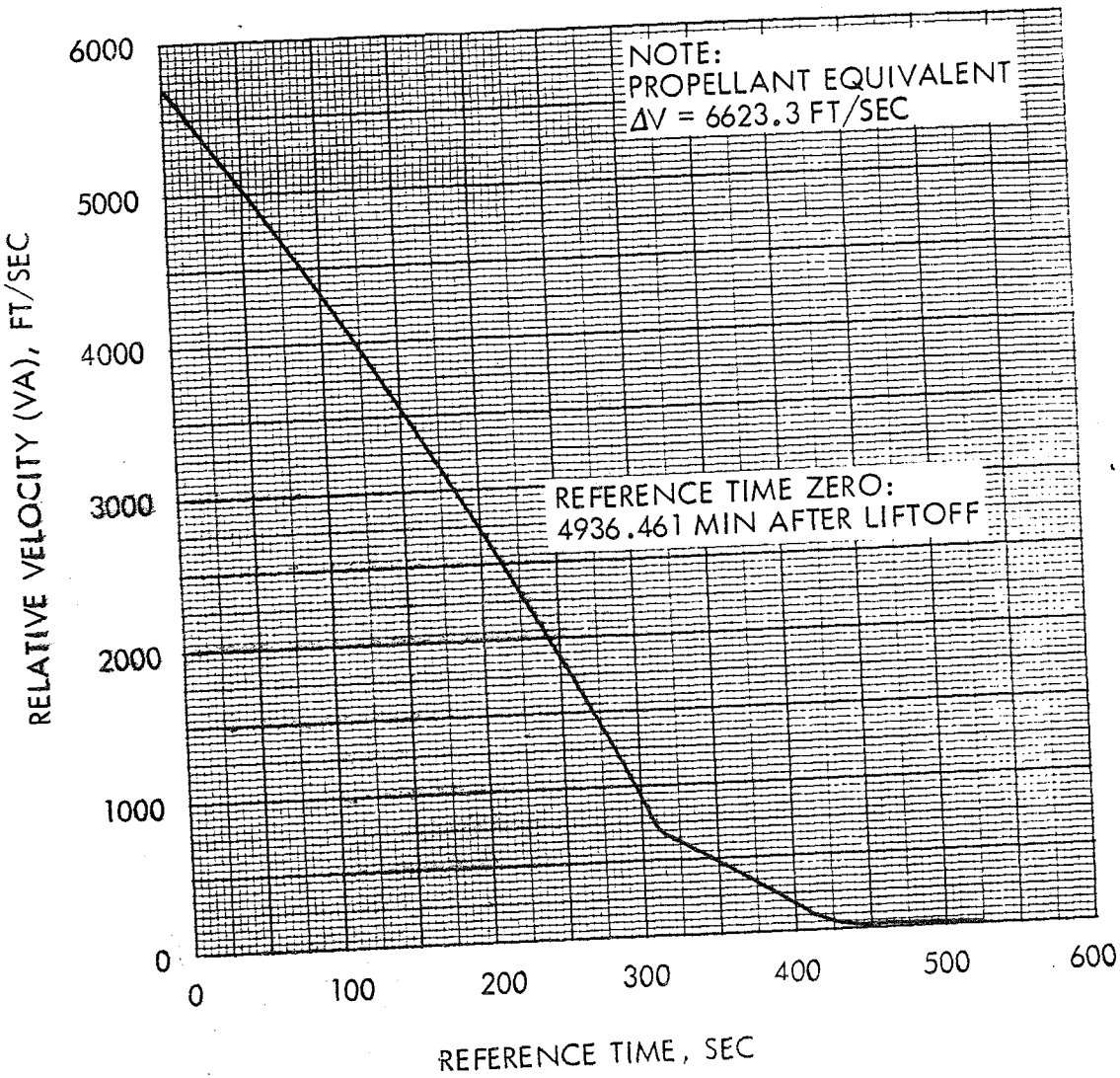

Figure 5.5-1. Descent Phase - Relative Velocity (VA)

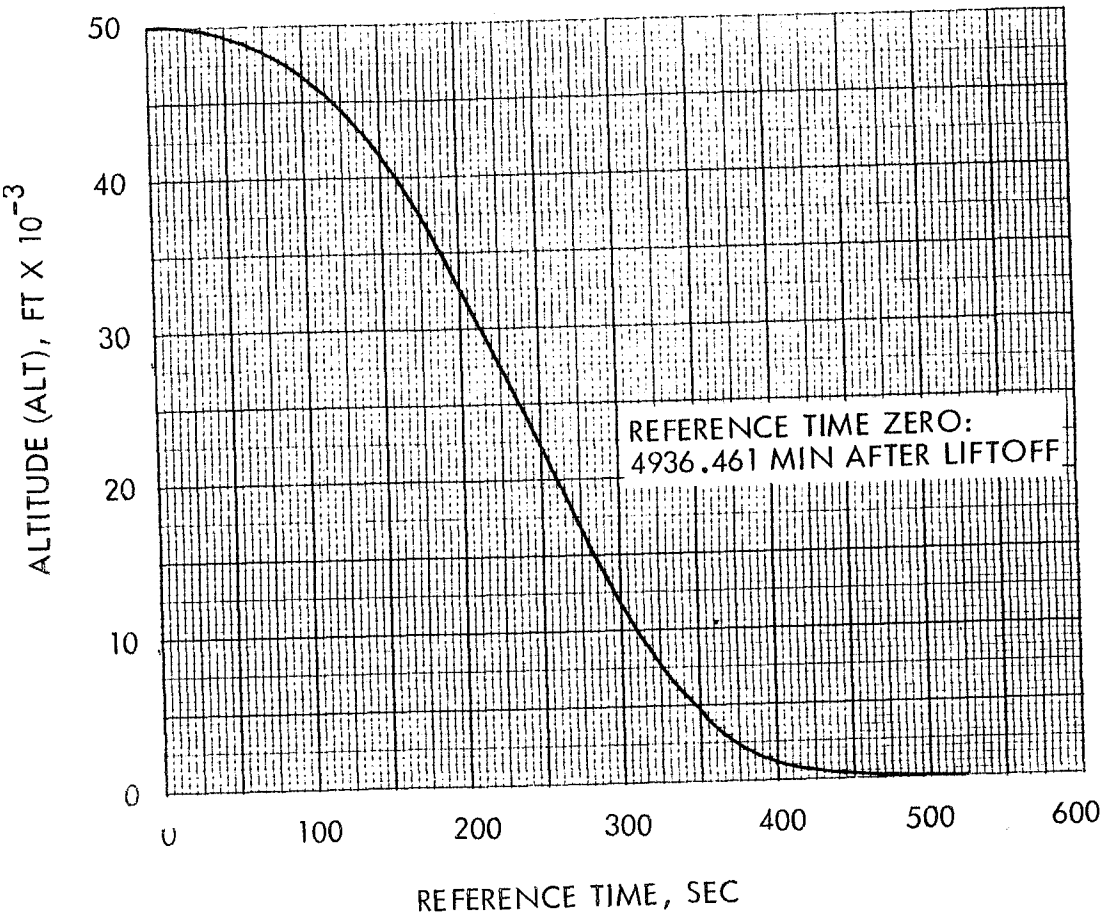

Figure 5.5-2. Descent Phase - Altitude (ALT)

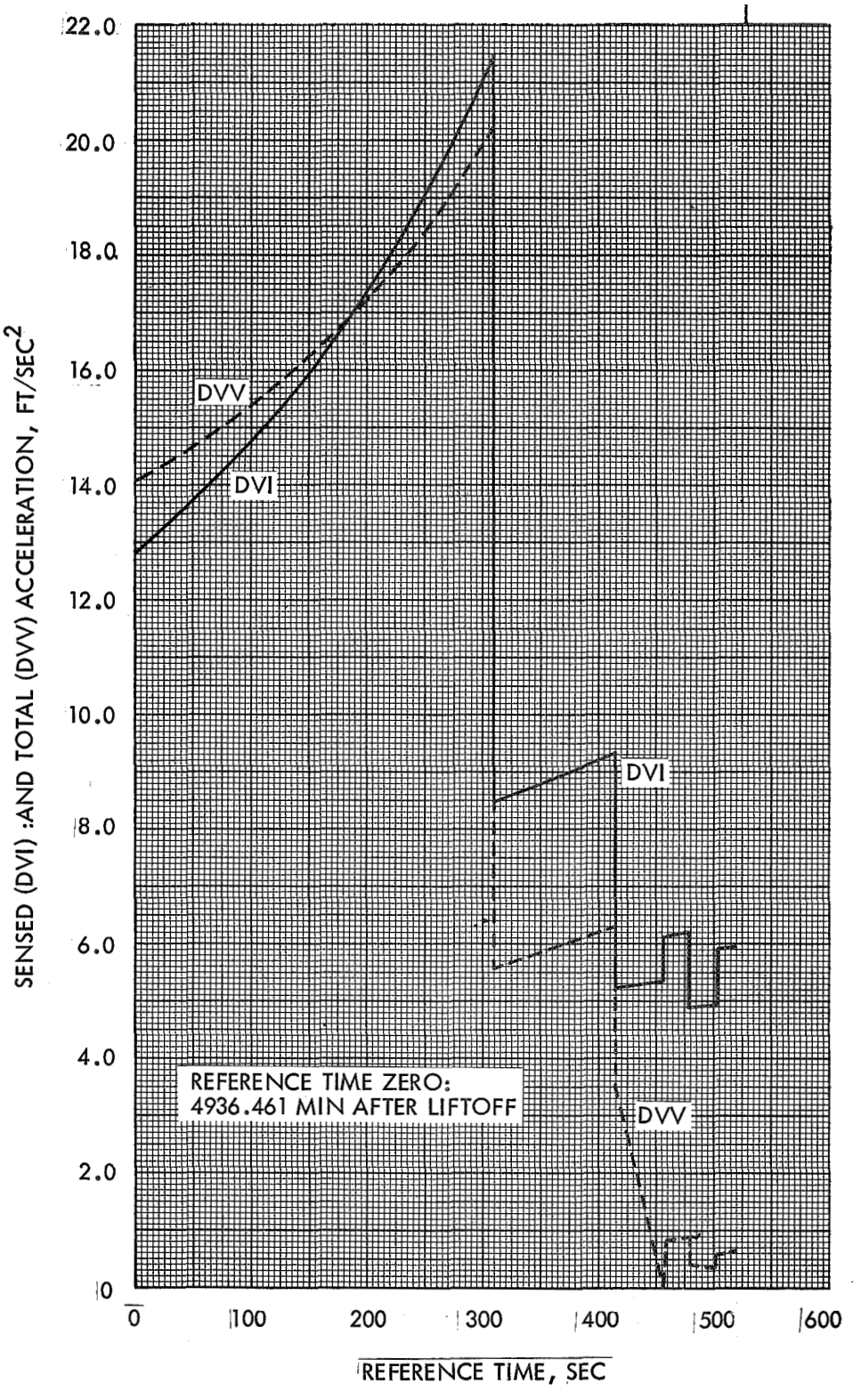

Figure 5.5-3. Descent Phase – Sensed (DVI) and Total (DVV) Acceleration

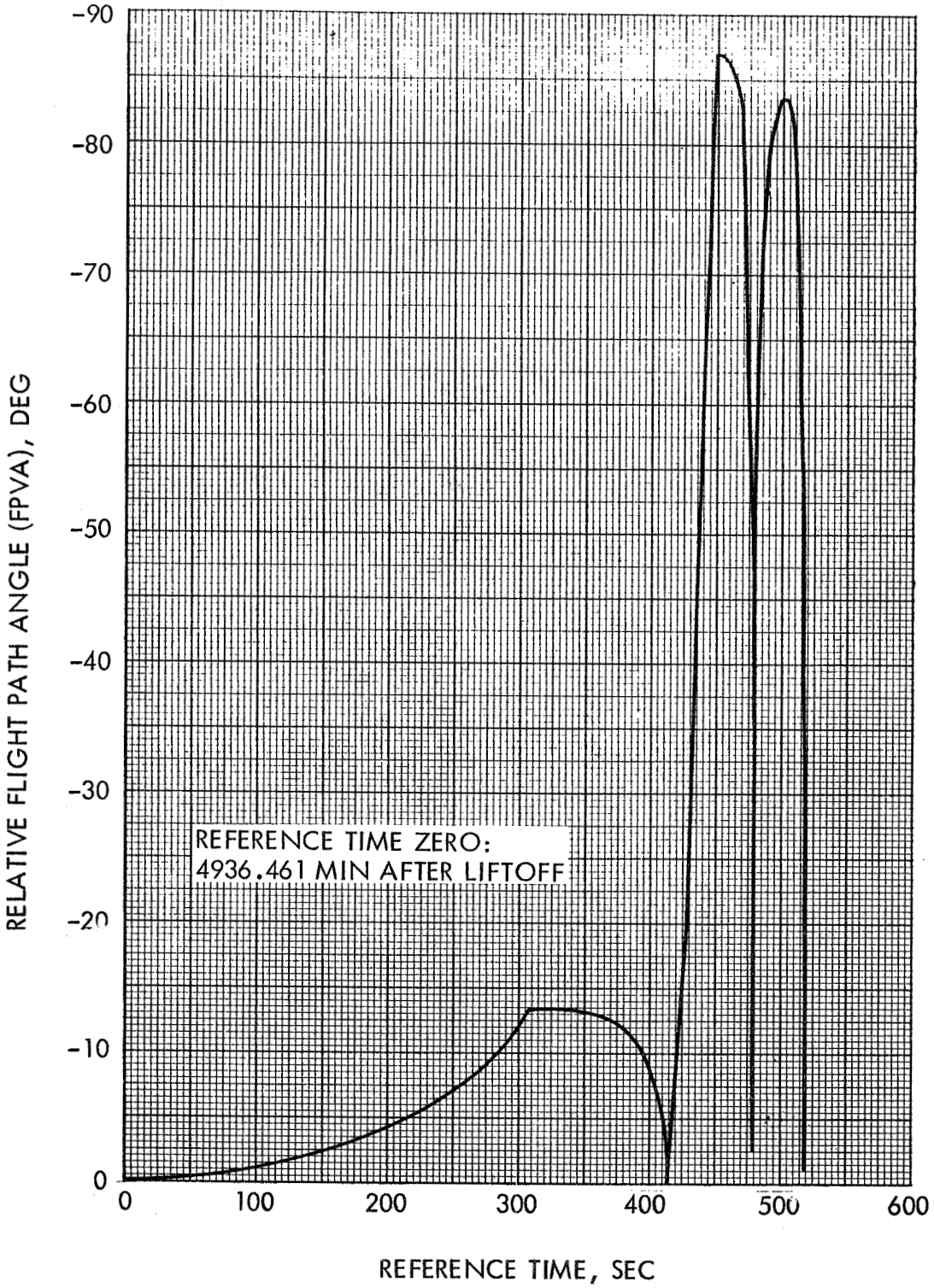

Figure 5.5-4. Descent Phase – Relative Flight Path Angle (FPVA)

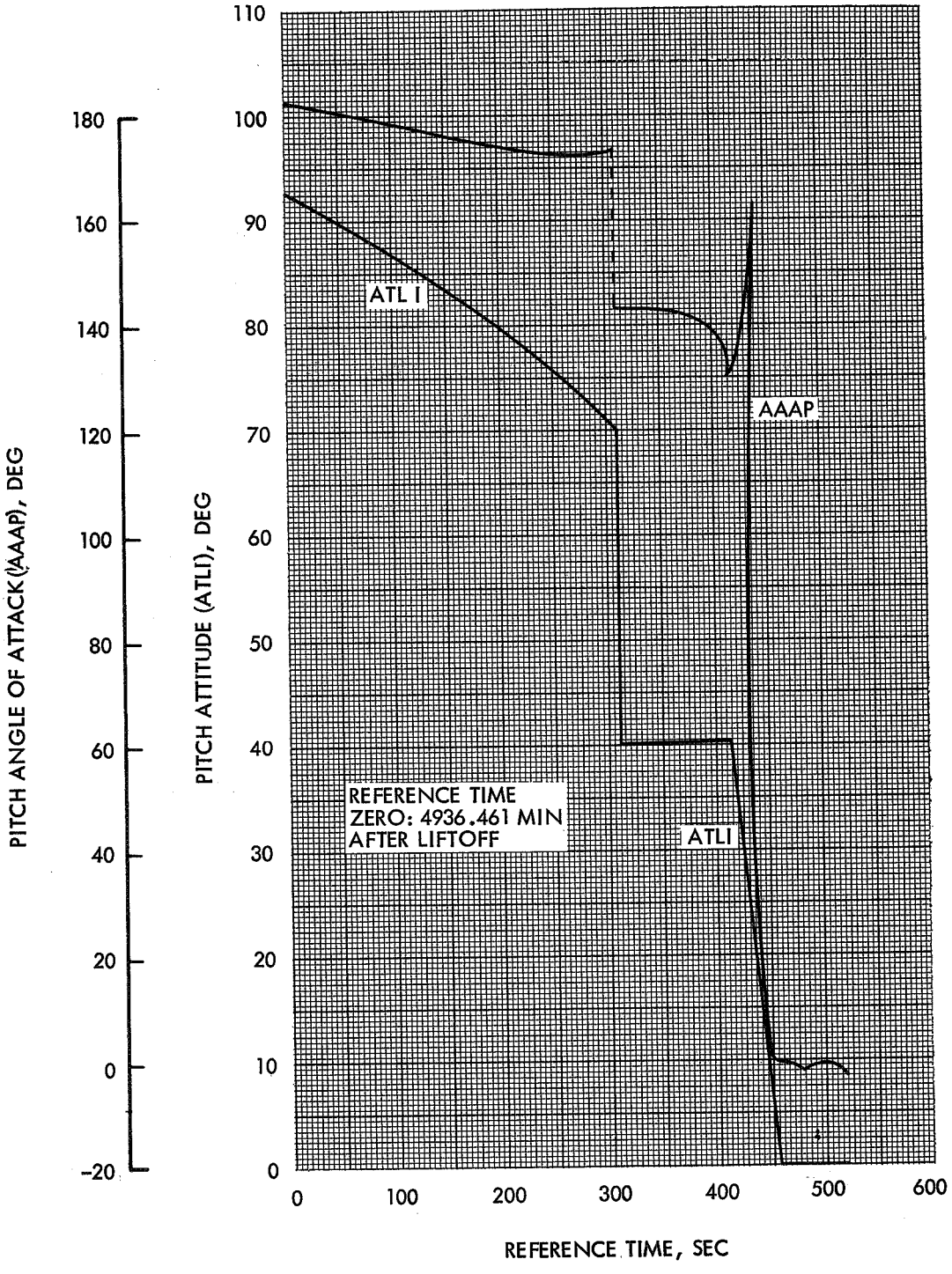

Figure 5.5-5. Descent Phase – Pitch Attitude (ALT) and Pitch Angle of Attack (AAAP)

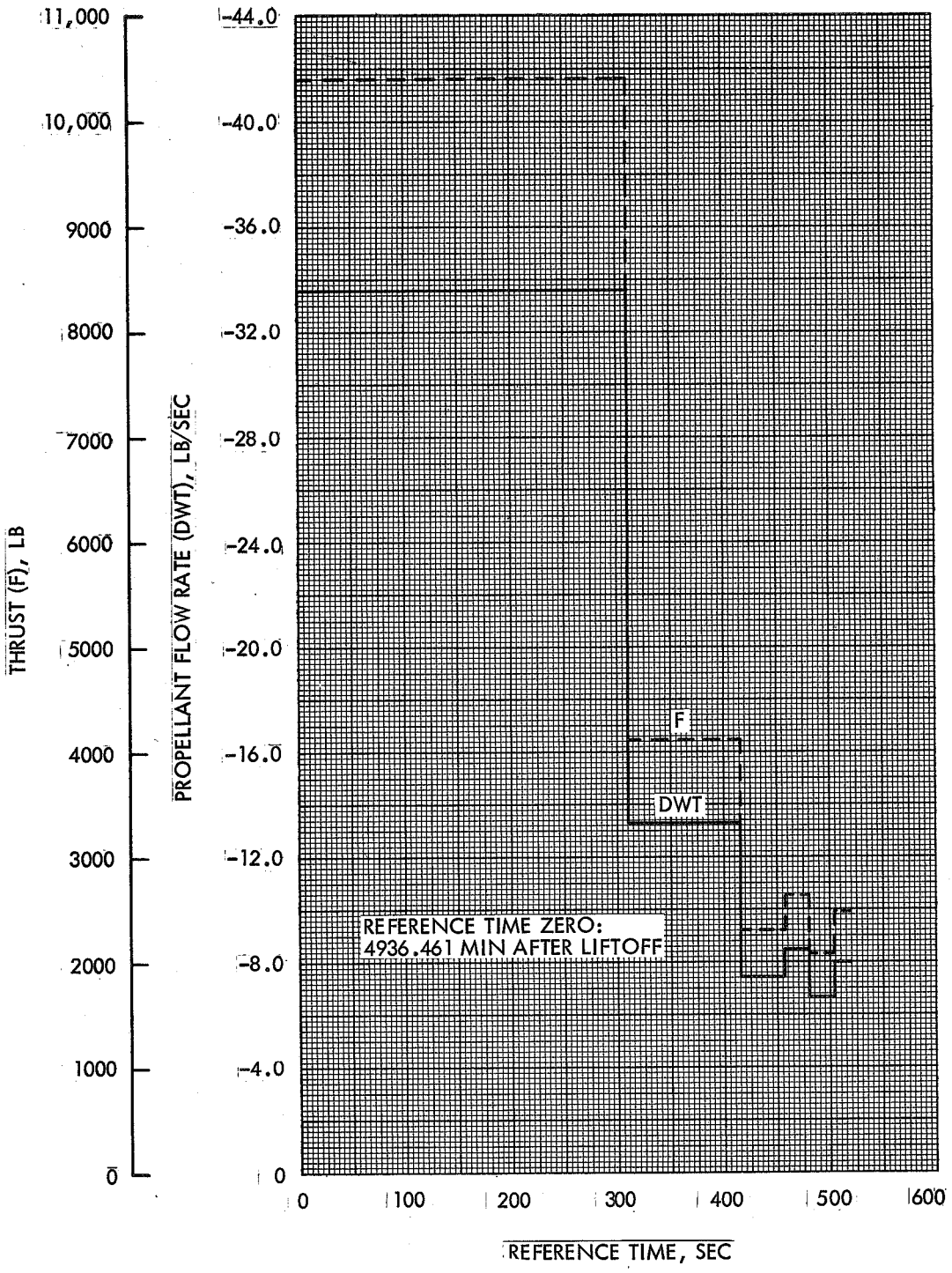

Figure 5.5-6. Descent Phase – Thrust (F) and Propellant Flow Rate (DWT)

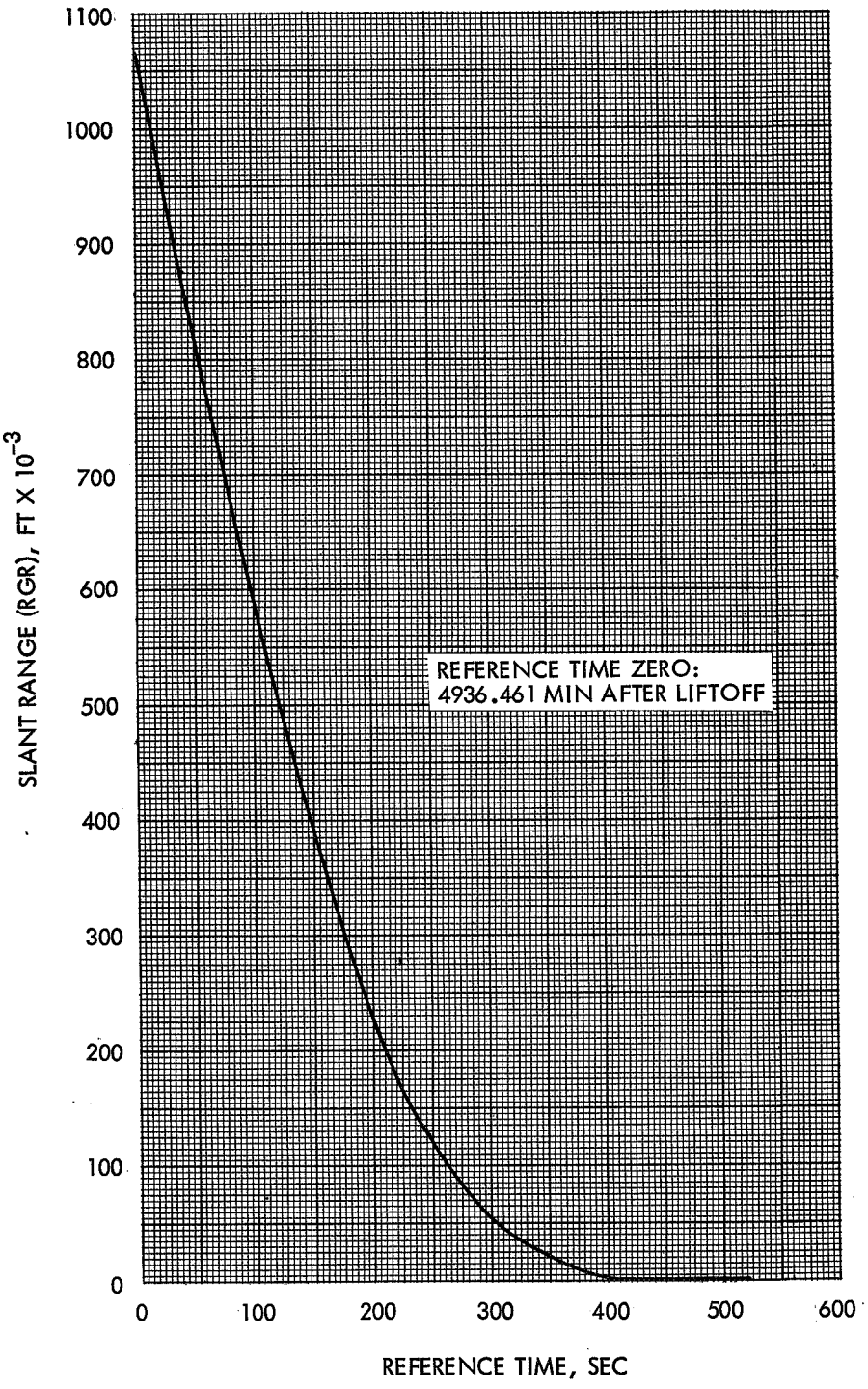

Figure 5.5-7. Descent Phase – Slant Range from Landing Site (RGR)

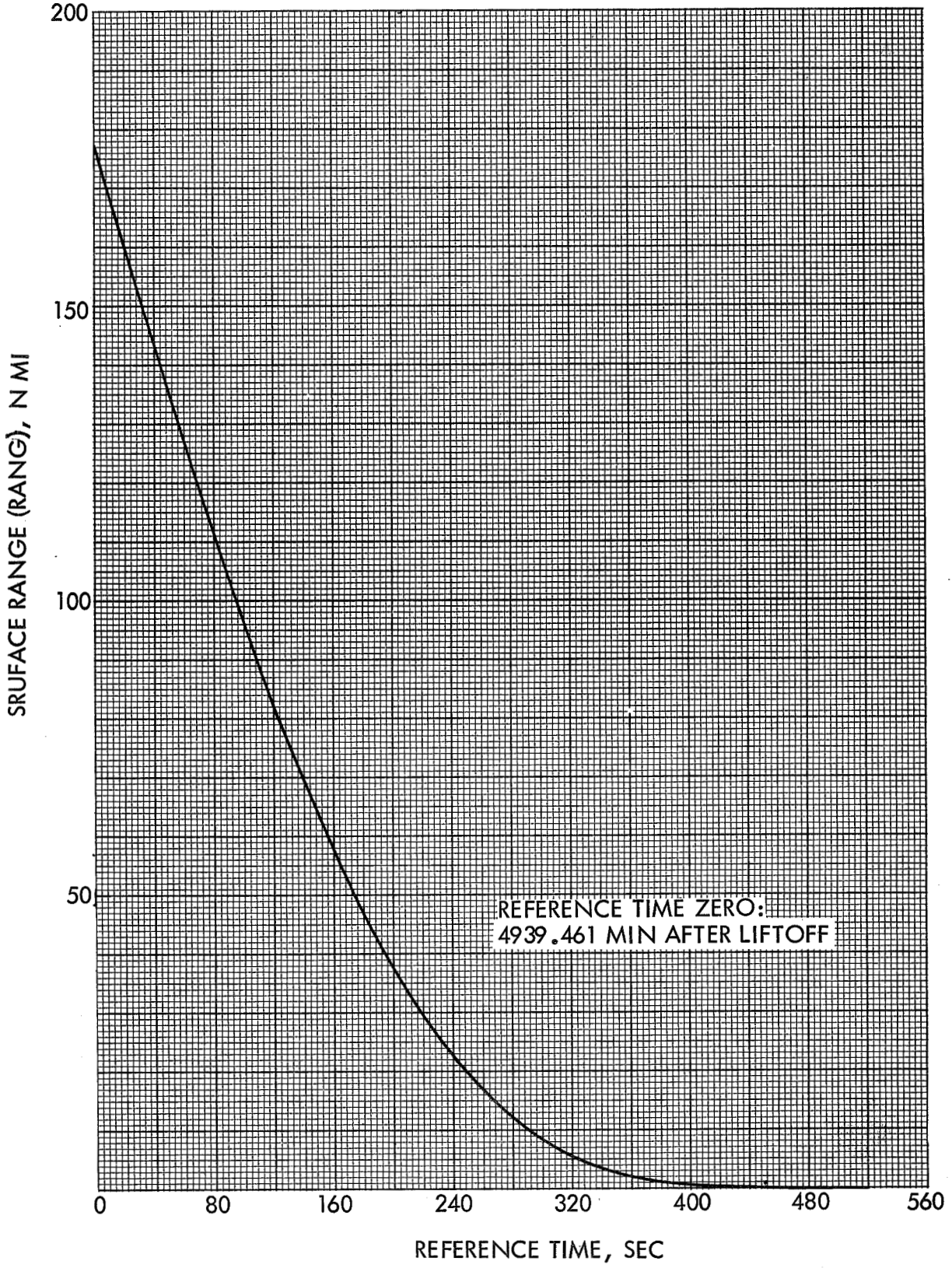

Figure 5.5-8. Descent Phase – Surface Range (RANG)

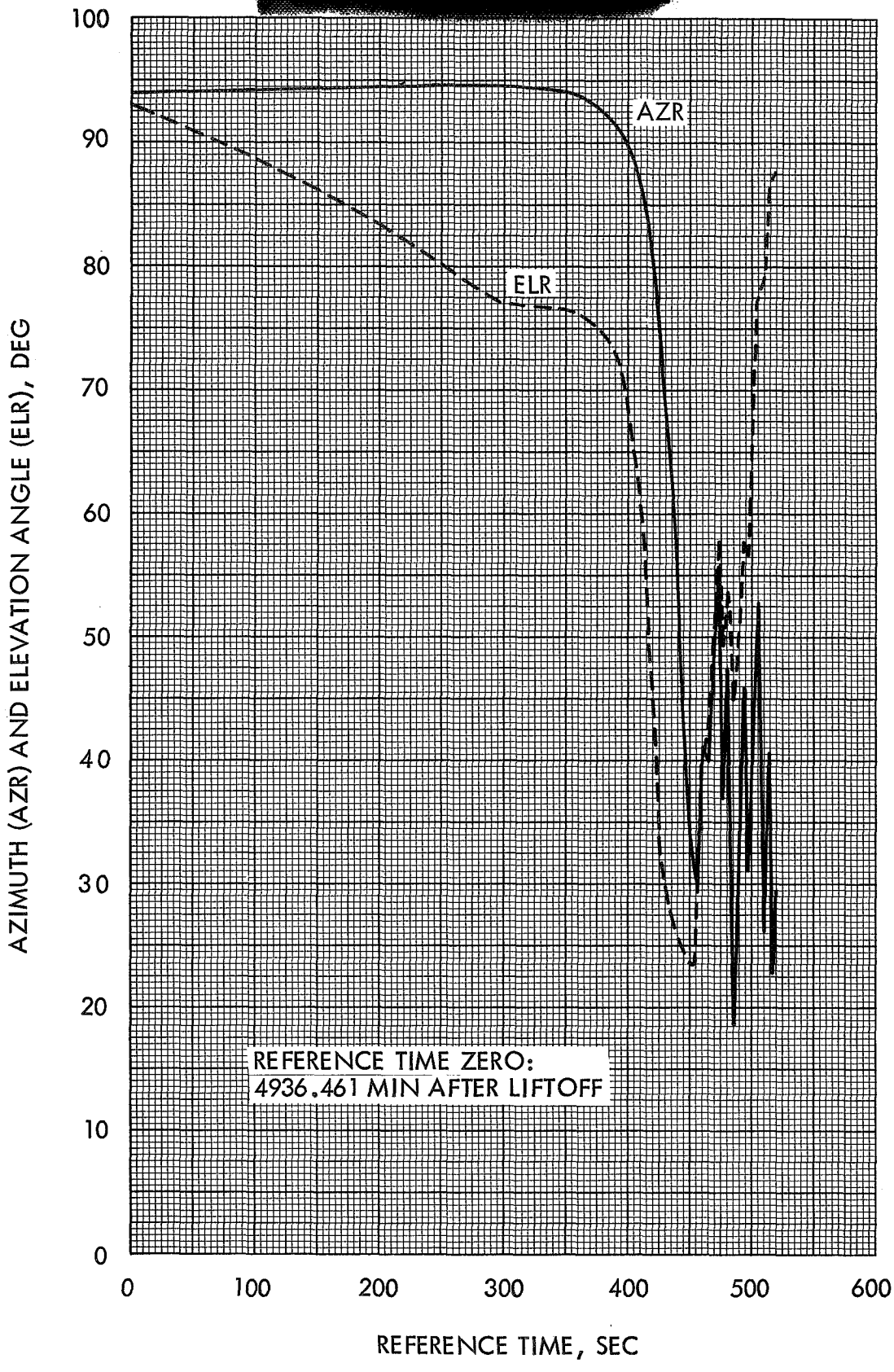

Figure 5.5-9. Descent Phase – Azimuth (AZR) and Elevation Angle (ELR) from Landing Site

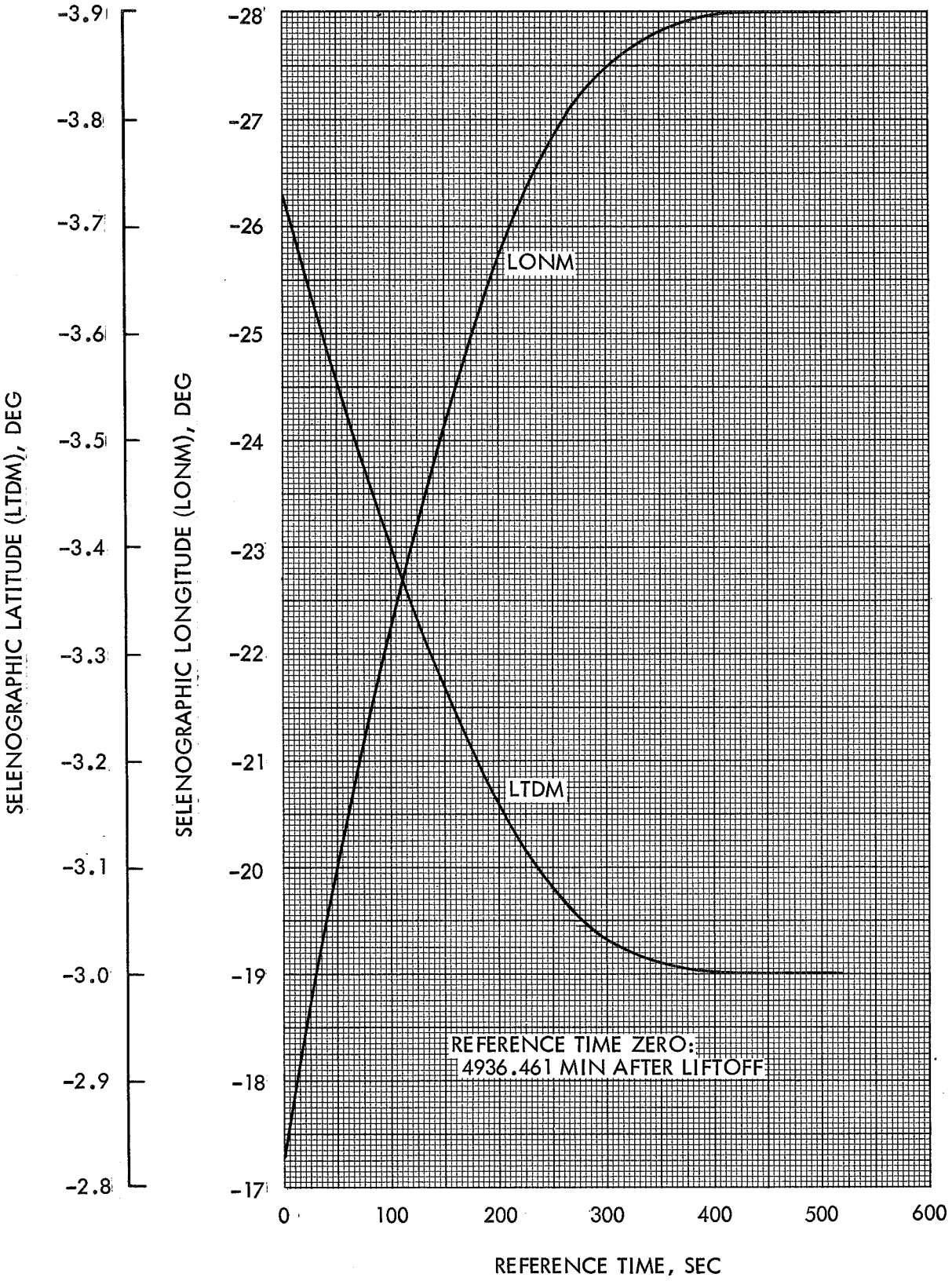

Figure 5.5-10. Descent Phase - Selenographic Latitude (LTDM) and Longitude (LONM)

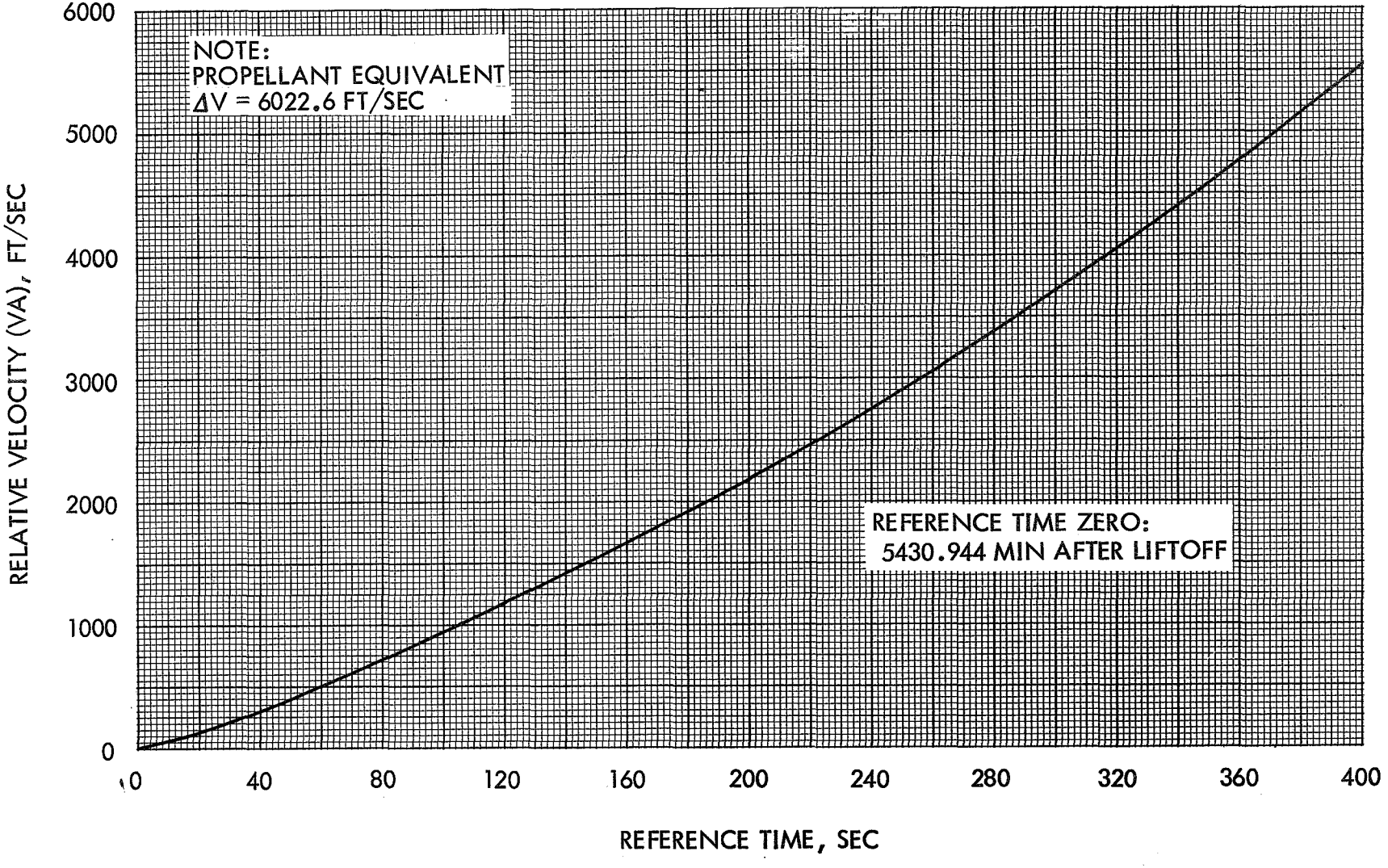

Figure 5.5-11. Ascent Phase - Relative Velocity (VA)

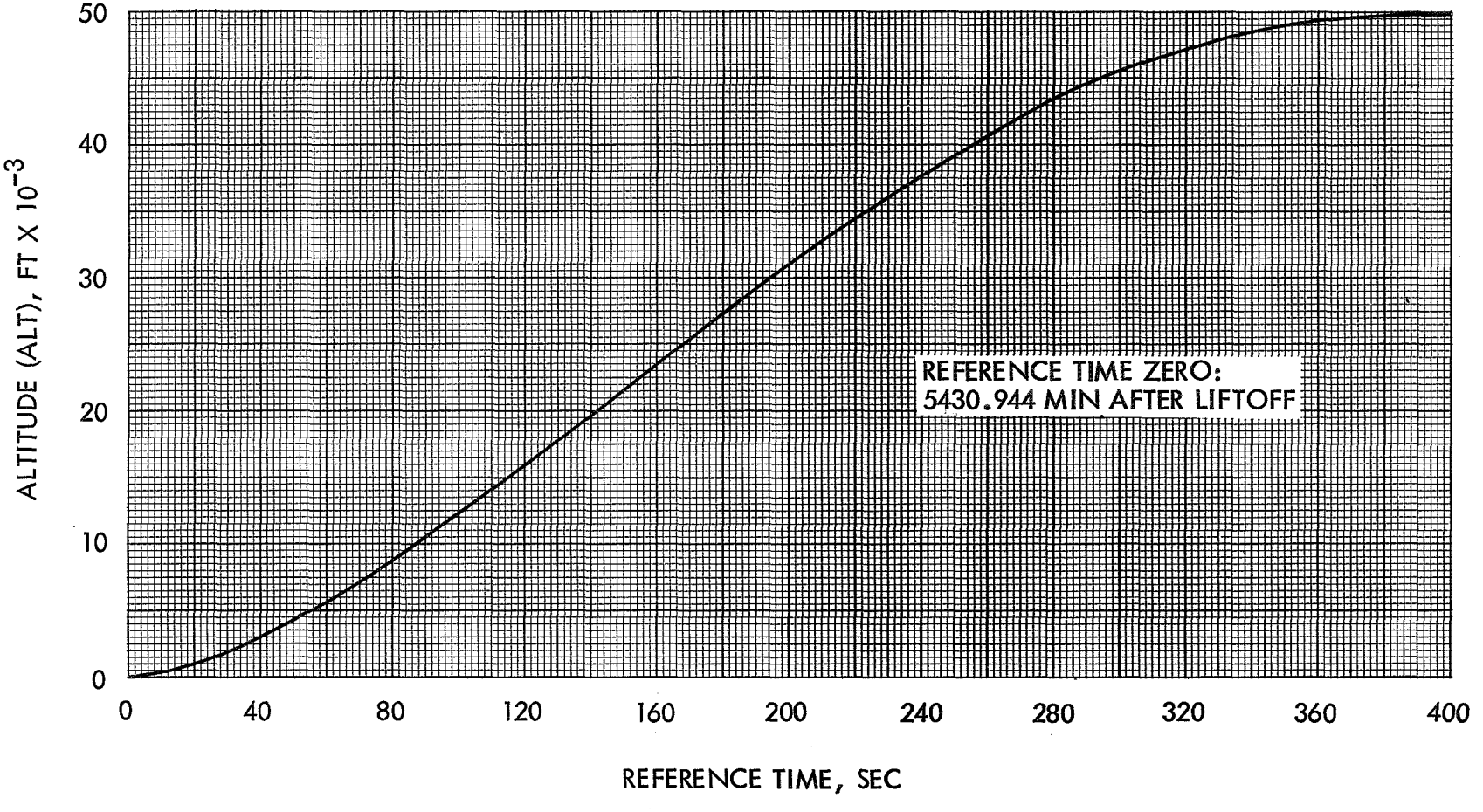

Figure 5.5-12. Ascent Phase - Altitude (ALT)

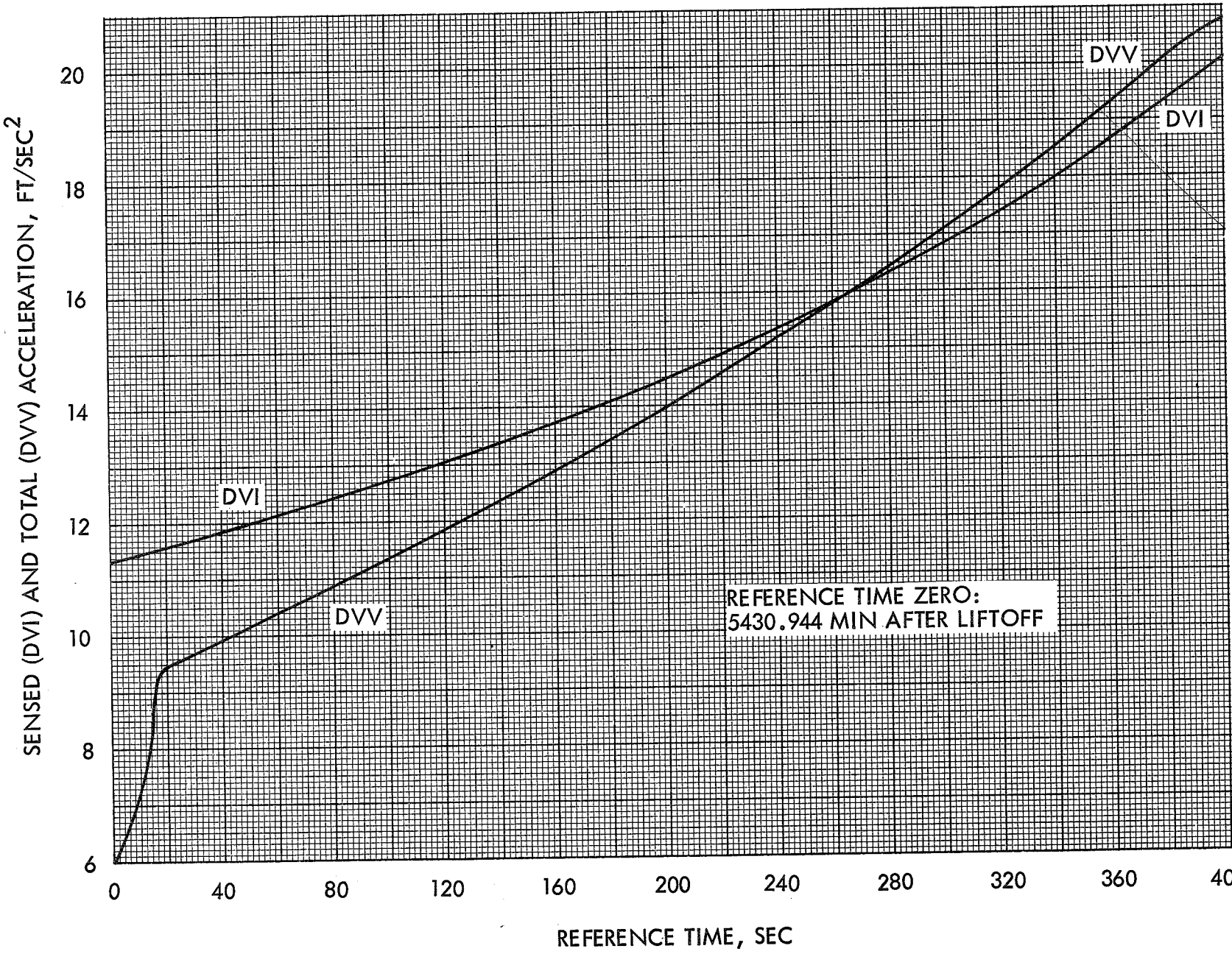

Figure 5.5-13. Ascent Phase - Sensed (DVI) and Total (DVV) Acceleration

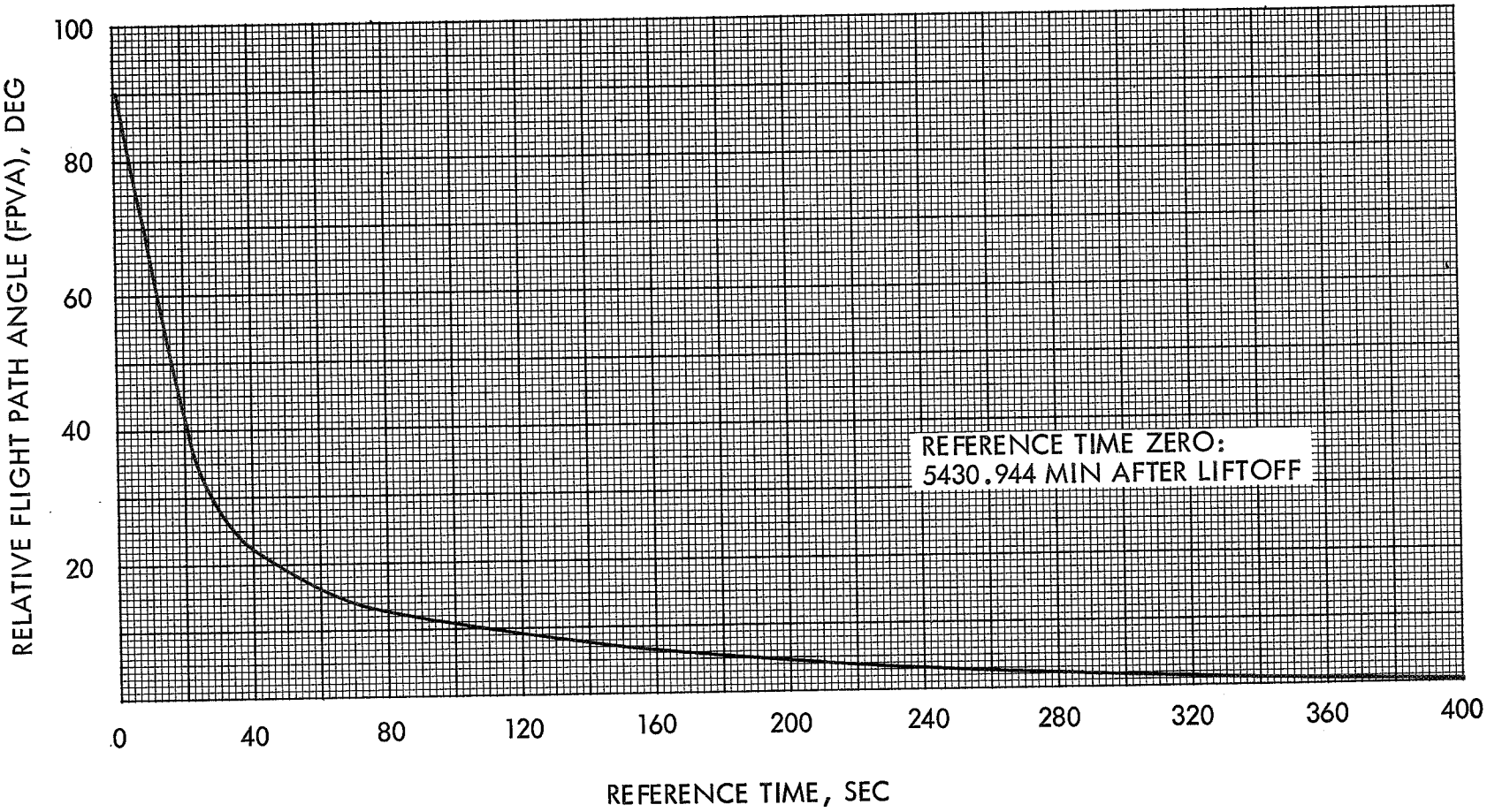

Figure 5.5-14. Ascent Phase - Relative Flight Path Angle (FPVA)

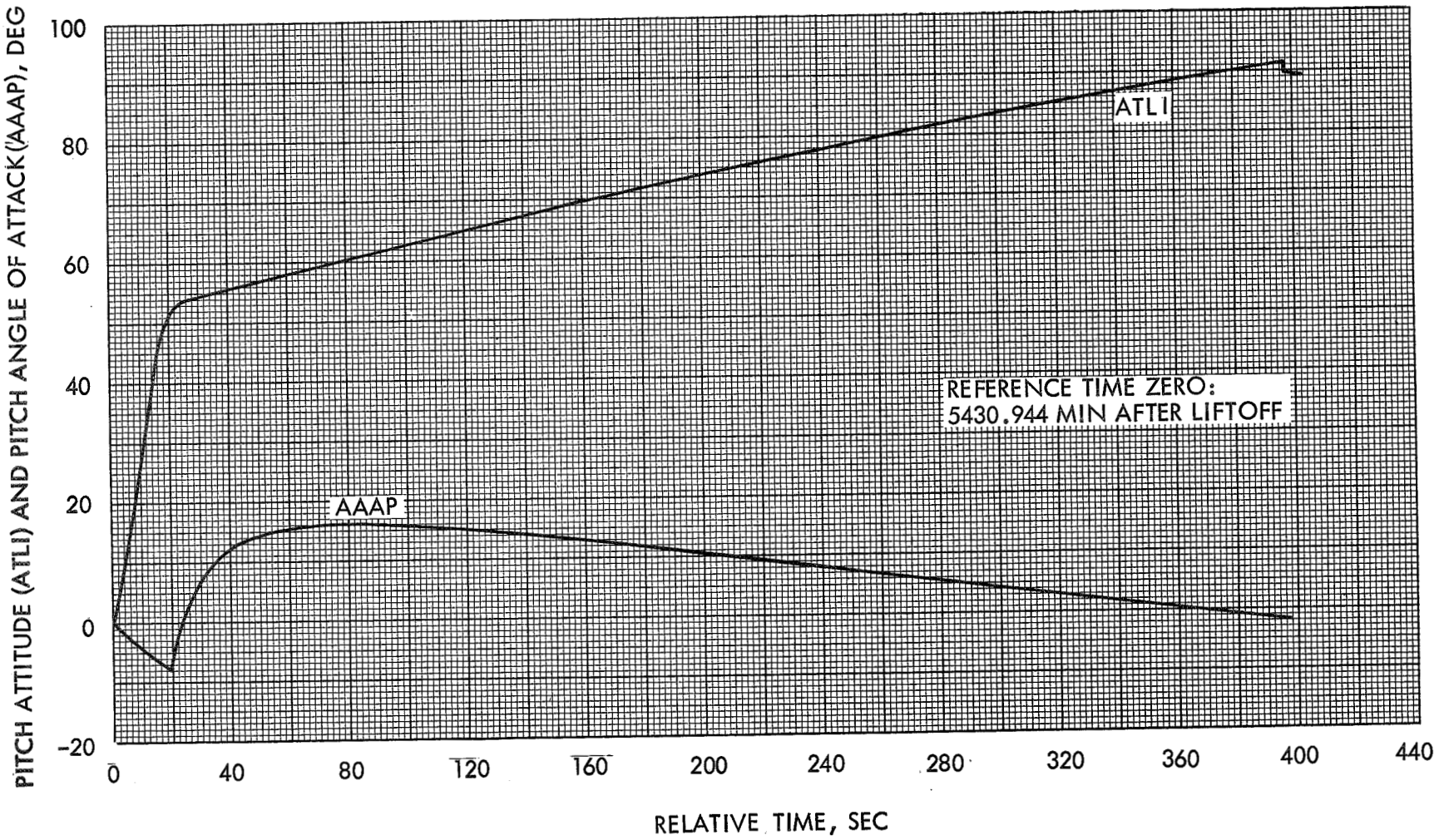

Figure 5.5-15. Ascent Phase - Pitch Attitude (ATLI) and Pitch Angle of Attack (AAAP)

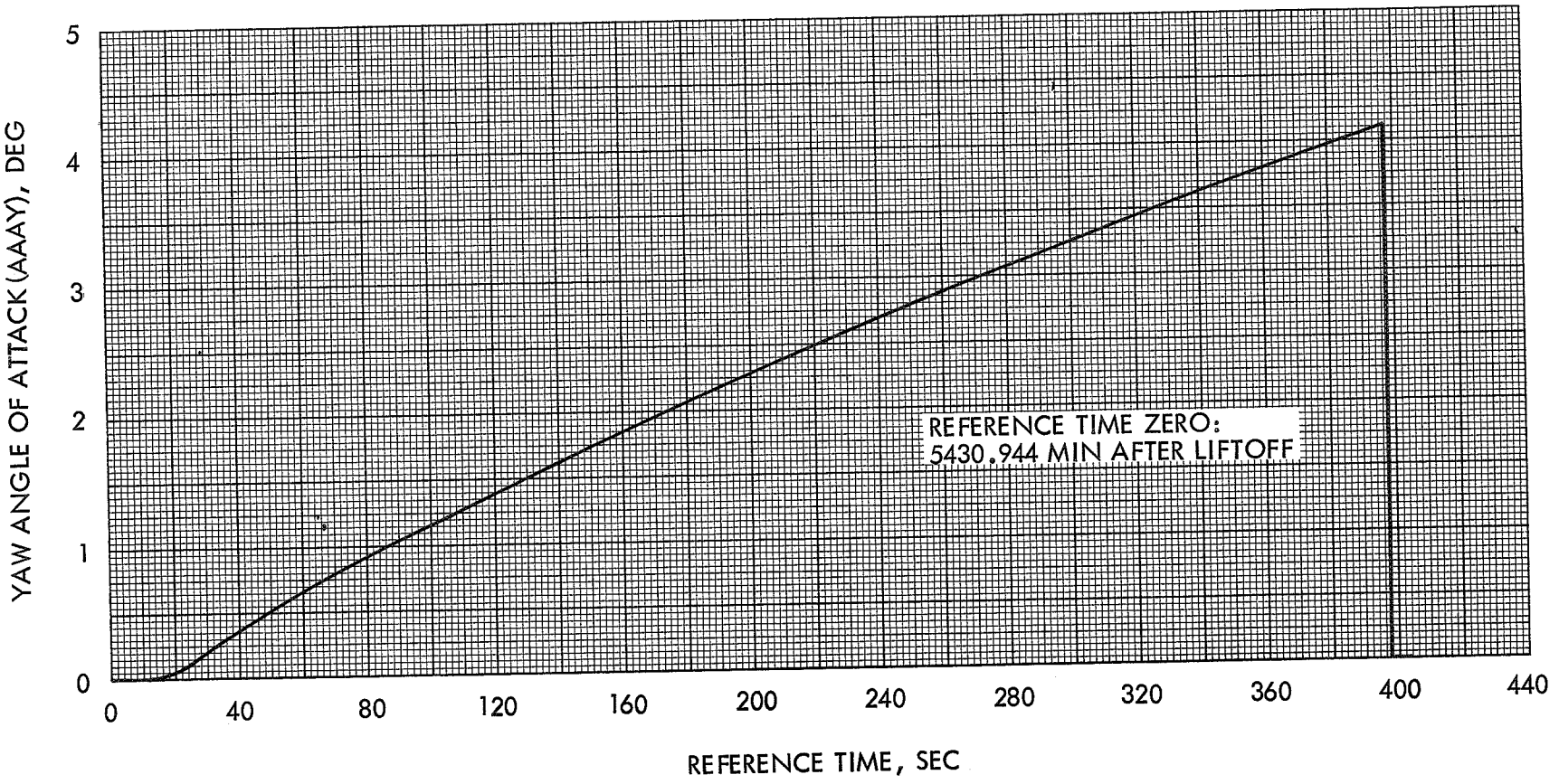

Figure 5.5-16. Ascent Phase - Yaw Angle of Attack (AAAY)

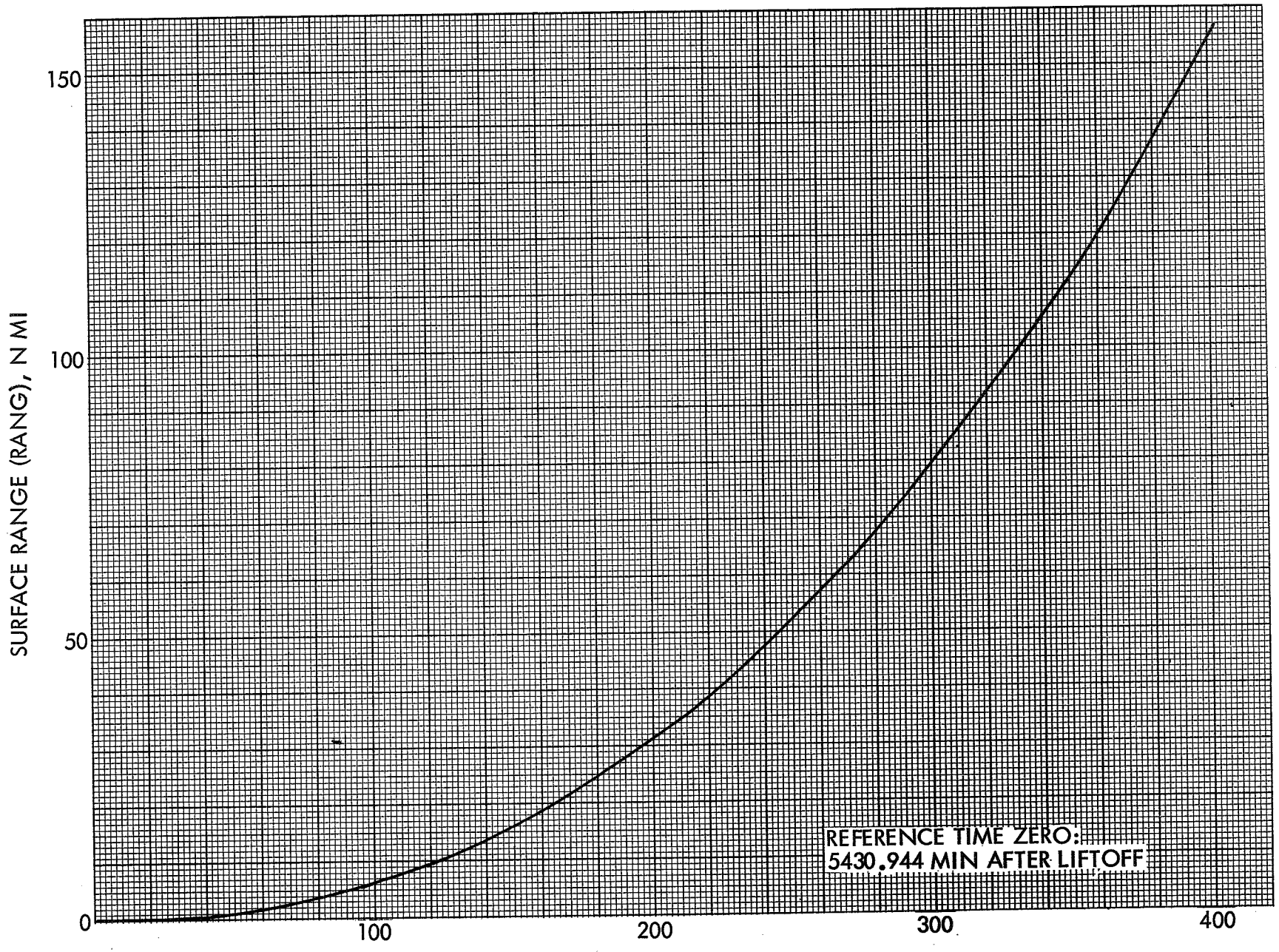

Figure 5.5-17. Ascent Phase - Surface Range (RANG)

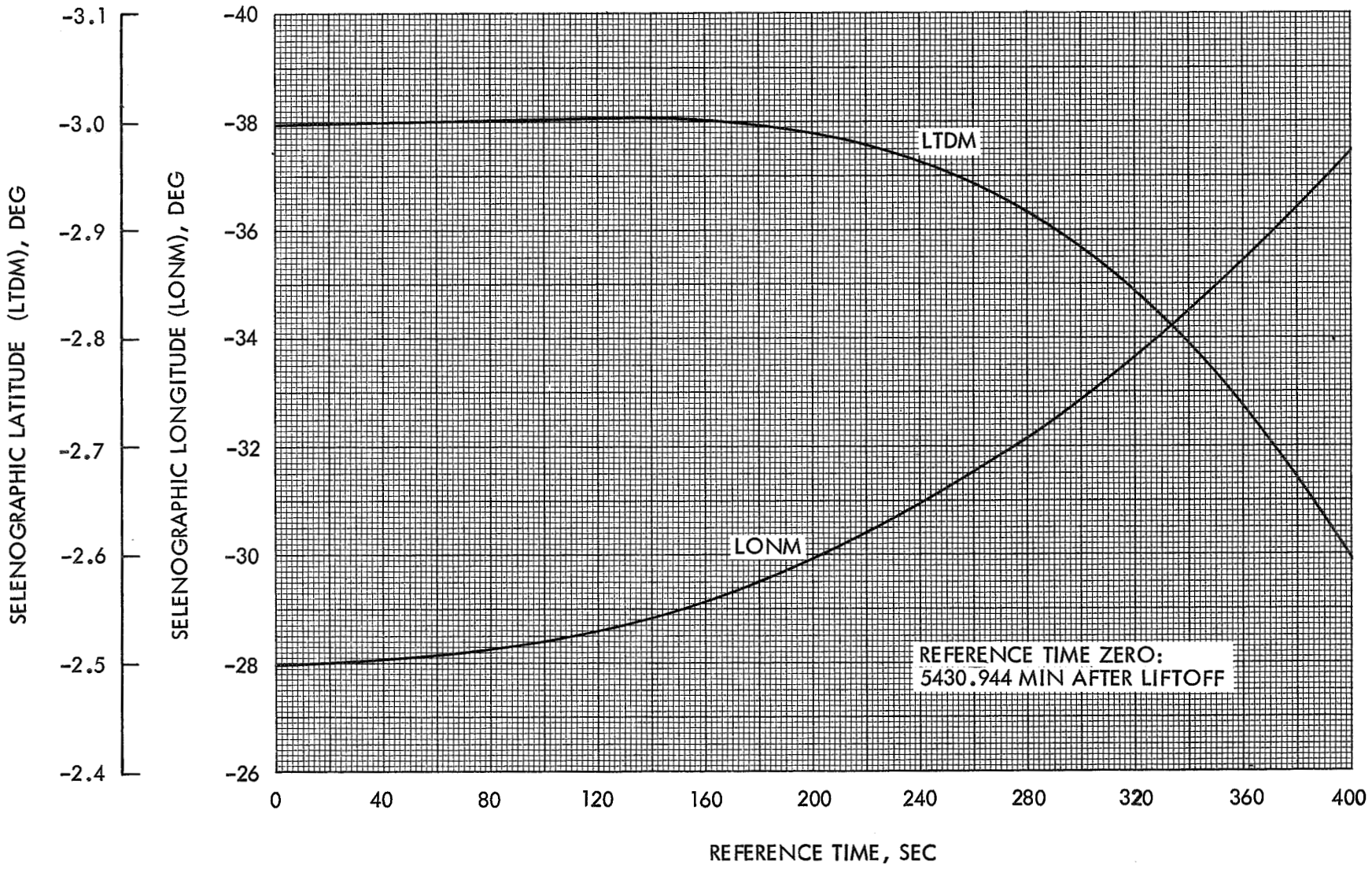

Figure 5.5-18. Ascent Phase - Selenographic Latitude (LTDM) and Longitude (LONM)

Table 5.6-I. Rendezvous - Discrete Events Summary

Time Since Liftoff (minutes)	Altitude (feet)	Latitude (degrees)	Longitude (degrees)	Velocity (feet/second)	Flight Path Angle (degrees)	Velocity Azimuth (degrees)	Pitch Rate / Yaw Rate (degrees/second)	Event
5495.643	485,841	2.597	142.106	5207.7**	0.0000**	265.5593**	0.0000 / 0.0000	Start transfer to CM/SM circular orbit
5495.722	485,838	2.579	141.876	5304.2**	-0.0131**	265.5486**	0.0000 / 0.0000	End powered transfer maneuver/ achieve rendezvous conditions/ start docking procedure
5528.886	482,582	-4.759	44.288	5290.5*	-0.0163*	268.0169*	0.0000 / 0.0000	Complete docking/ continue coast in parking orbit
5628.886	484,971	-0.132	109.353	5288.3*	-0.0180	264.8446*	0.0000 / 0.0000	End minimum stay in parking orbit

Notes:

*Inertial quantities

**Relative quantities

Table 5.6-II. Rendezvous - Spacecraft Weight History.

	CM/SM	LEM
Start Transfer Maneuver to CM/SM Orbit	35,360	4,773
Propellant Flow		-44
End Transfer Maneuver/Achieve Rendezvous Conditions/Start Docking Procedure	35,360	4,729
Transfer 2 Astronauts and Equipment to CM	+440	-440
Complete Docking	35,800	4,289
Jettison LEM Ascent Stage and Excess Propellant		-4,289
Continue Coast in CM/SM Parking Orbit	35,800	0

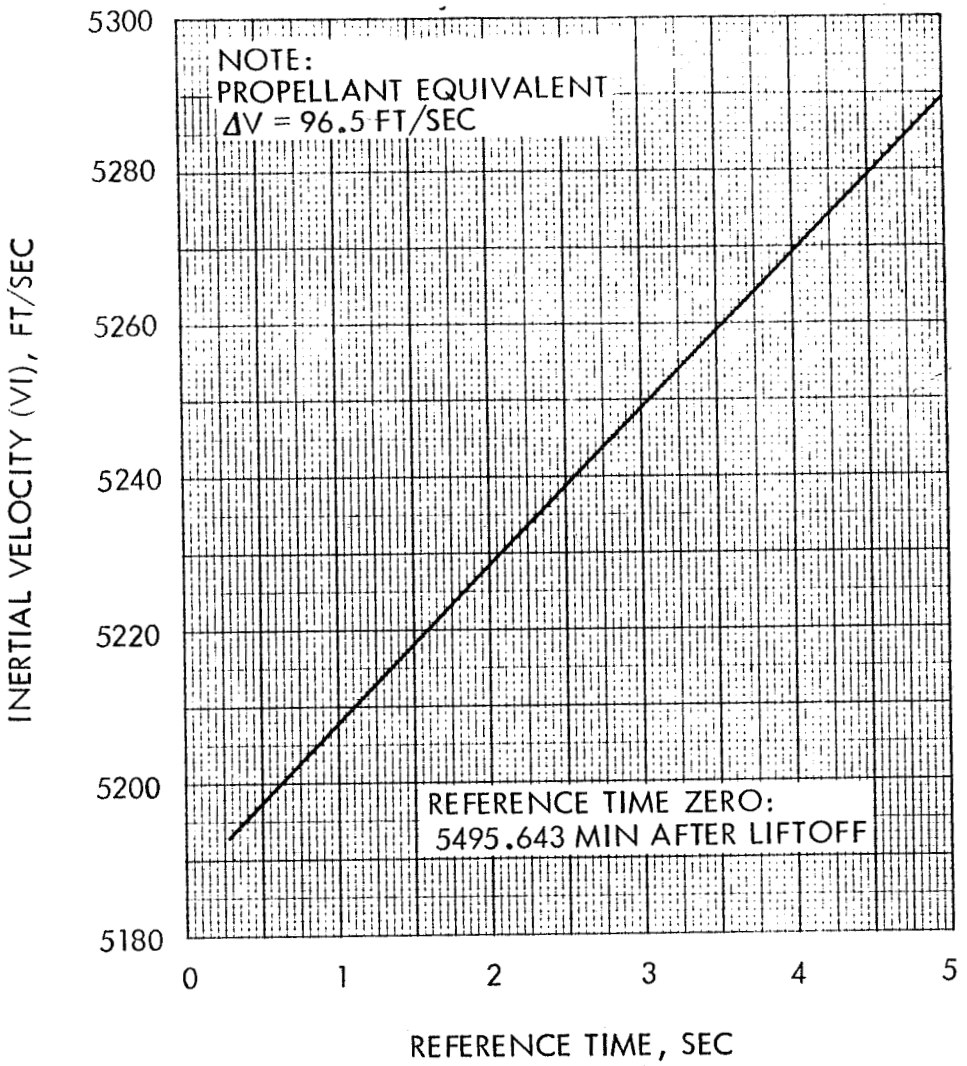

Figure 5.6-1. Rendezvous Phase - Inertial Velocity (VI)

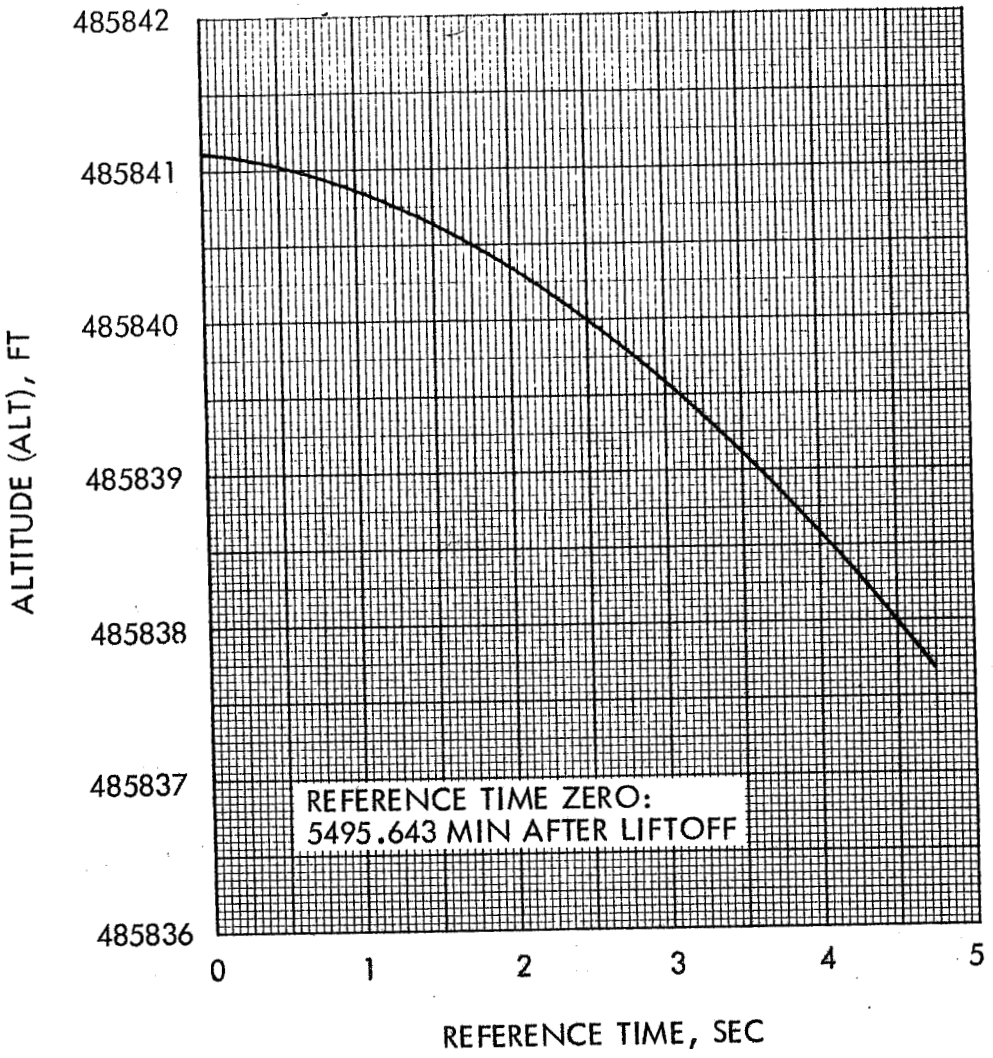

Figure 5.6-2. Rendezvous Phase - Altitude (ALT)

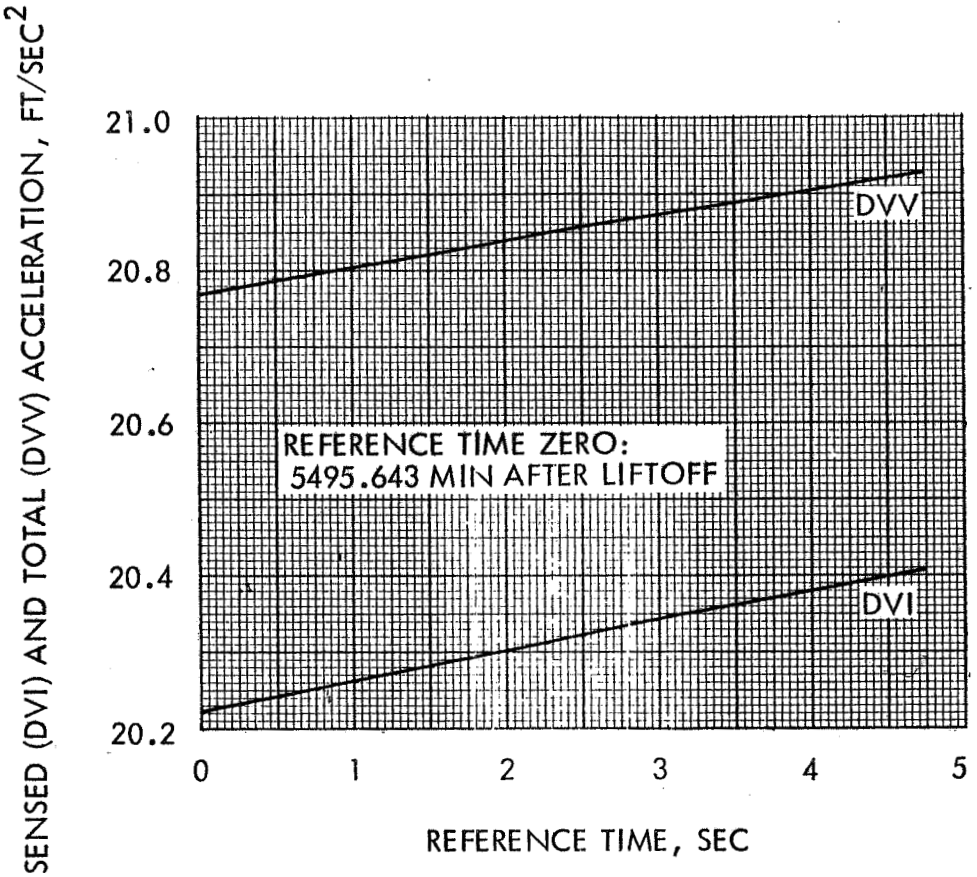

Figure 5.6-3. Rendezvous Phase - Sensed (DVI) and Total (DVV) Acceleration

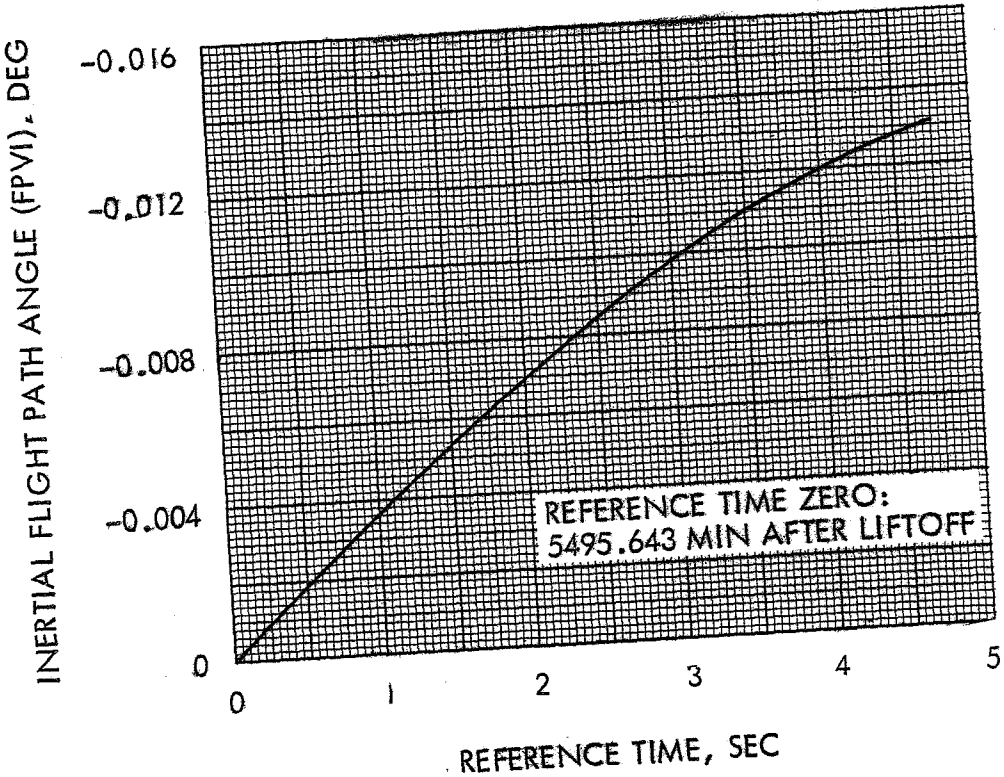

Figure 5.6-4. Rendezvous Phase - Inertial Flight Path Angle (FPVI)

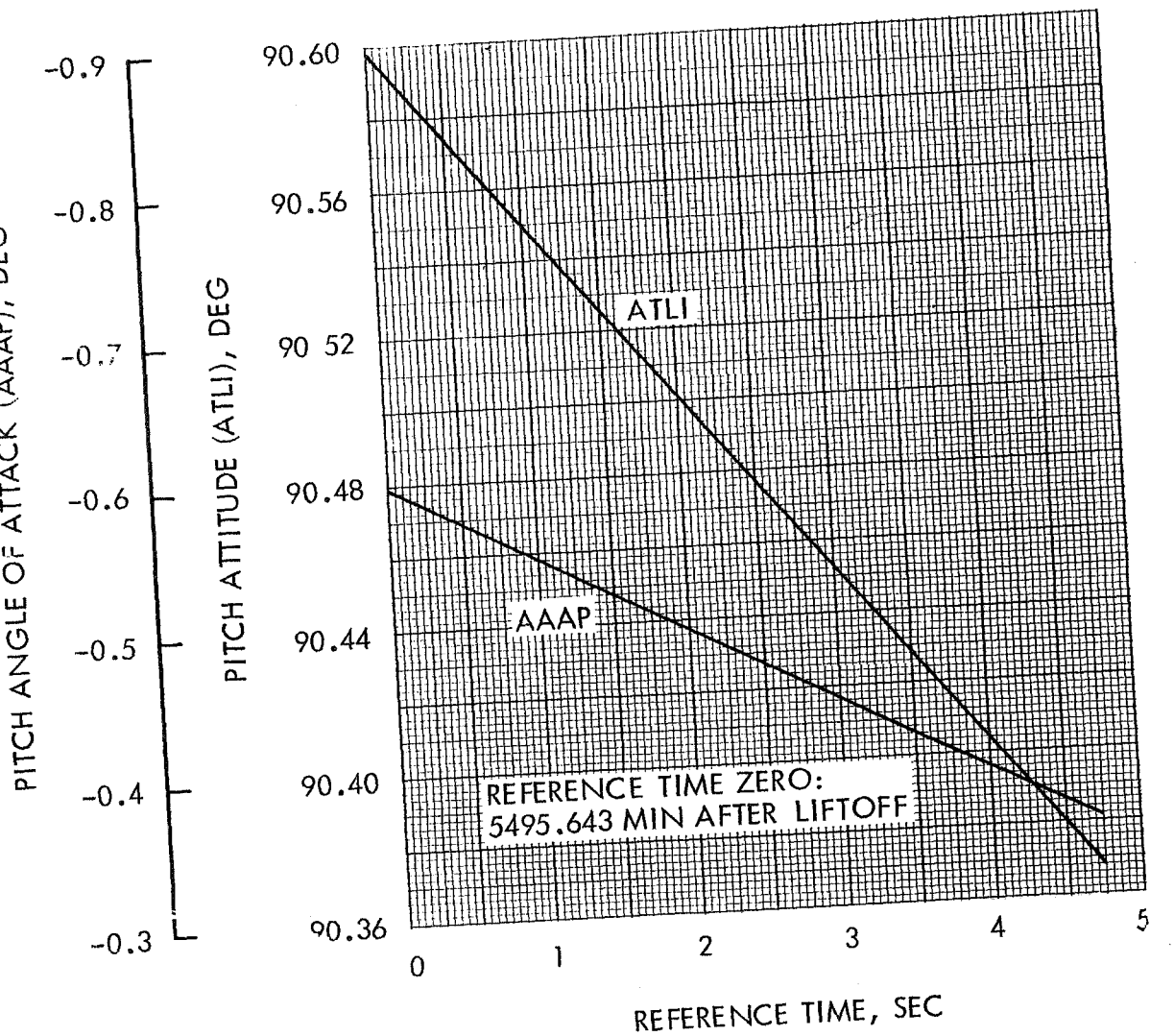

Figure 5.6-5. Rendezvous Phase - Pitch Attitude (ATLI) and Pitch Angle of Attack (AAAP)

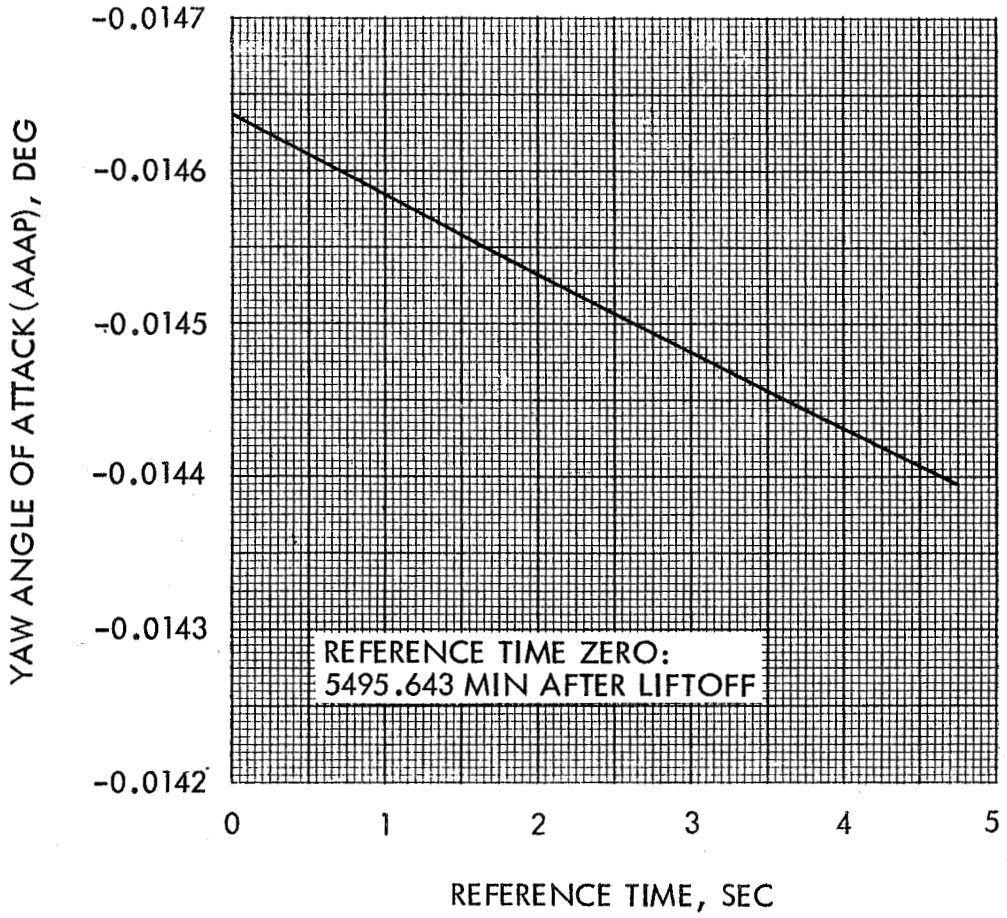

Figure 5.6-6. Rendezvous Phase - Yaw Angle of Attack (AAAY)

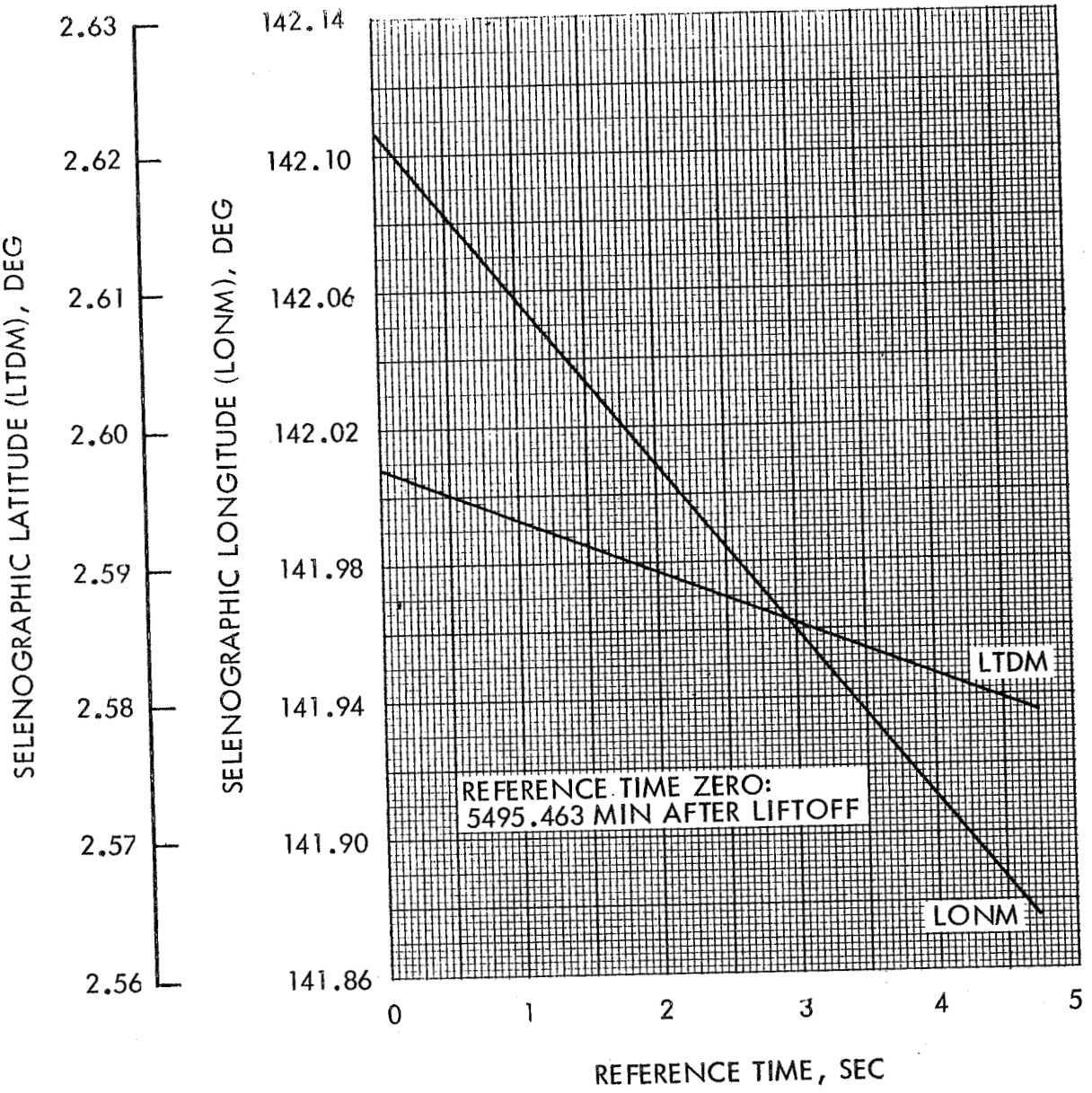

Figure 5.6-7. Rendezvous – Selenographic Latitude (LTDM) and Longitude (LONM)

Table 5.7-I. Transearth Injection and Return - Discrete Events Summary

Time Since Liftoff (min)	Altitude (ft x 10^{-6})	Latitude (deg)	Longitude (deg)	Velocity (ft/sec)	Flight Path Angle (deg)	Azimuth Angle (deg)	Pitch Orientation (deg)	Yaw Orientation (deg)	Event
5,728.98	0.486061*	4.640*	174.073*	5,287.84*	0.003*	267.75*	3.63281*	1.07475*	Initiate Powered Flight for Earth Return
5,731.29	0.500744*	4.282*	165.35*	8,390.95*	3.06*	267.47*	0.0*	0.0*	Powered Flight Burnout - Transearth Injection
6,031.29	1,245.371	21.535	162.231	3,452.78	-84.19	45.91	---	---	First Transearth Midcourse Correction
6,451.29	1,158.662	21.874	57.428	3,538.77	-80.91	55.79	---	---	Second Transearth Midcourse Correction
6,811.29	1,081.369	22.235	327.773	3,729.62	-80.03	57.43	---	---	Third Transearth Midcourse Correction
9,787.95	0.400	-8.332	100.541	36,178.11	-6.40	126.86	---	---	Earth Atmospheric Re-entry

Notes:

1) All quantities geocentric unless otherwise specified.

2) Quantities specified by * are selenographic.

Table 5.7-II. Spacecraft Weight History

	CM/SM
CM/SM Ignition for Transearth Injection	35,800
Propellant Flow	-9,468
Complete Transearth Injection	26,332
First Midcourse Propellant	-256
Second Midcourse Propellant	-256
Third Midcourse Propellant	-256
CM/SM Transearth Flight	25,564
CM at Re-entry	9,500

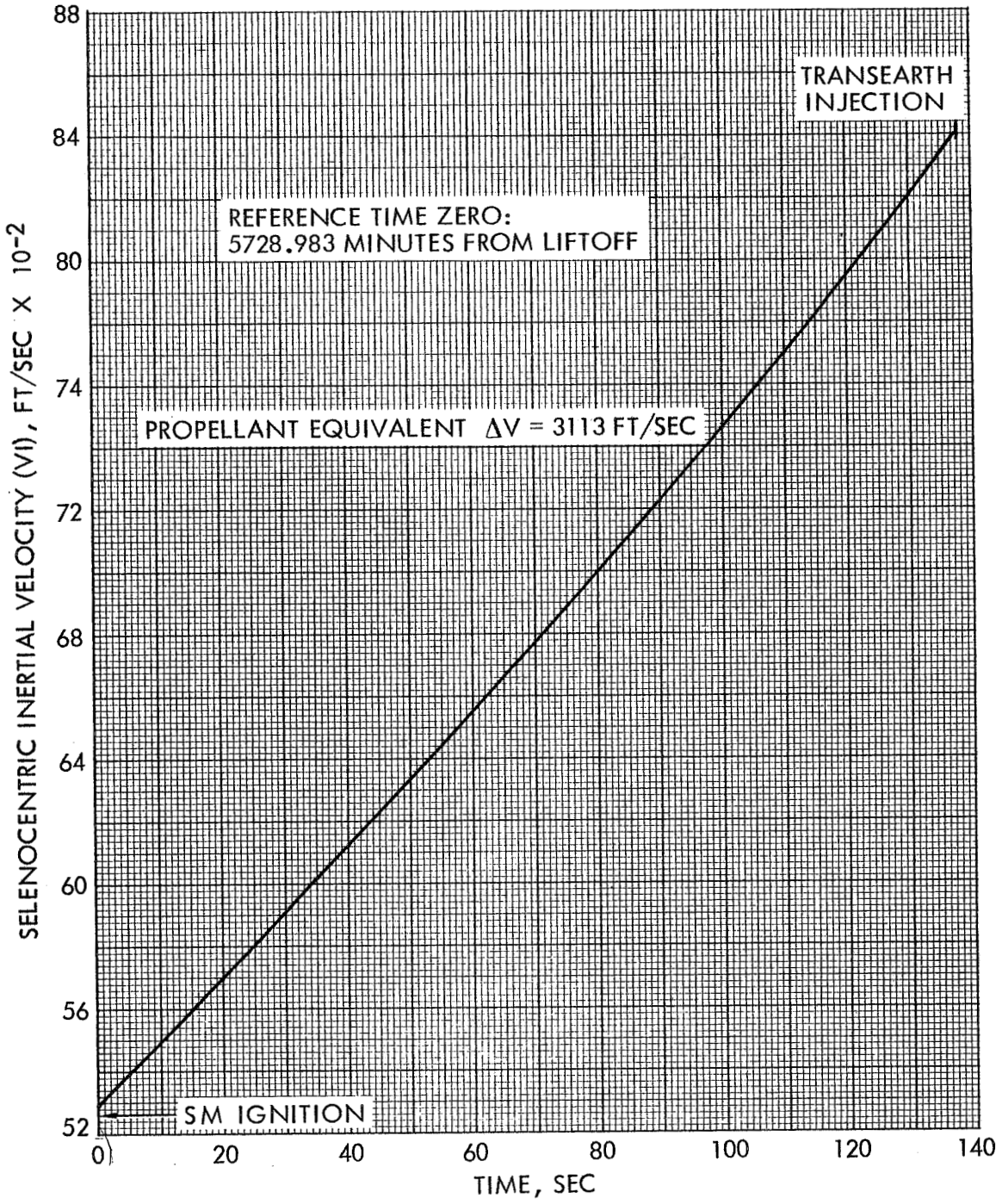

Figure 5.7-1a. Transearth Injection and Return – Inertial Velocity (VI)

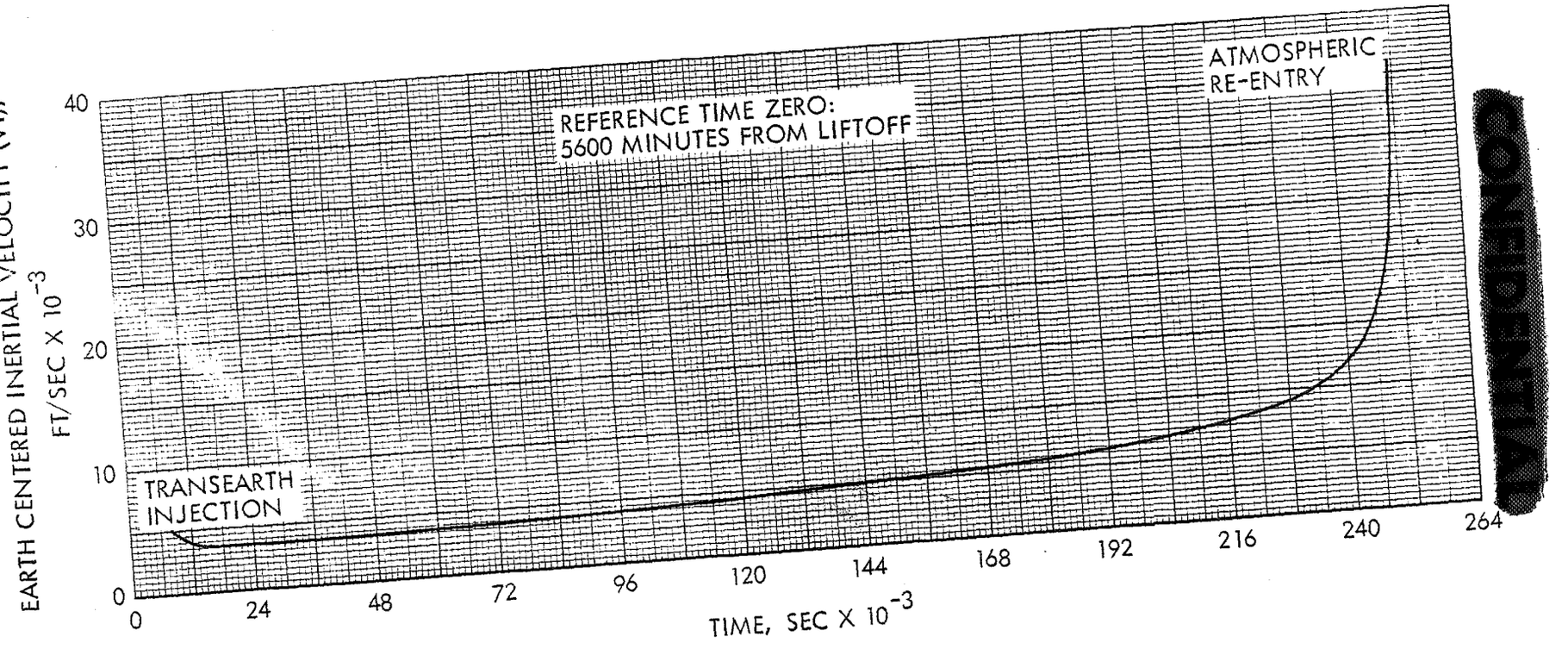

Figure 5.7-1b. Transearth Injection and Return - Inertial Velocity (VI)

CONFIDENTIAL

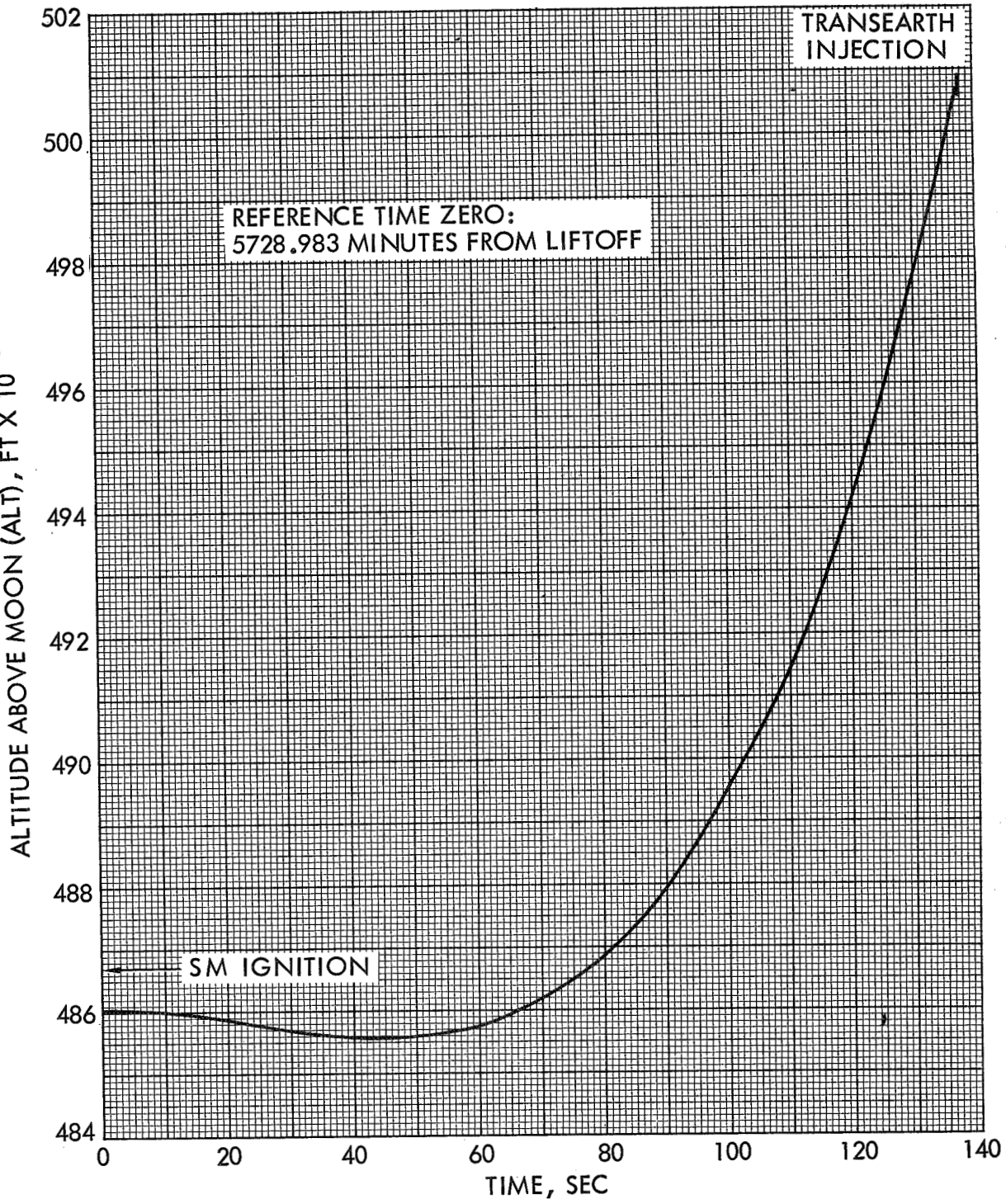

Figure 5.7-2. Transearth Injection and Return - Altitude (ALT)

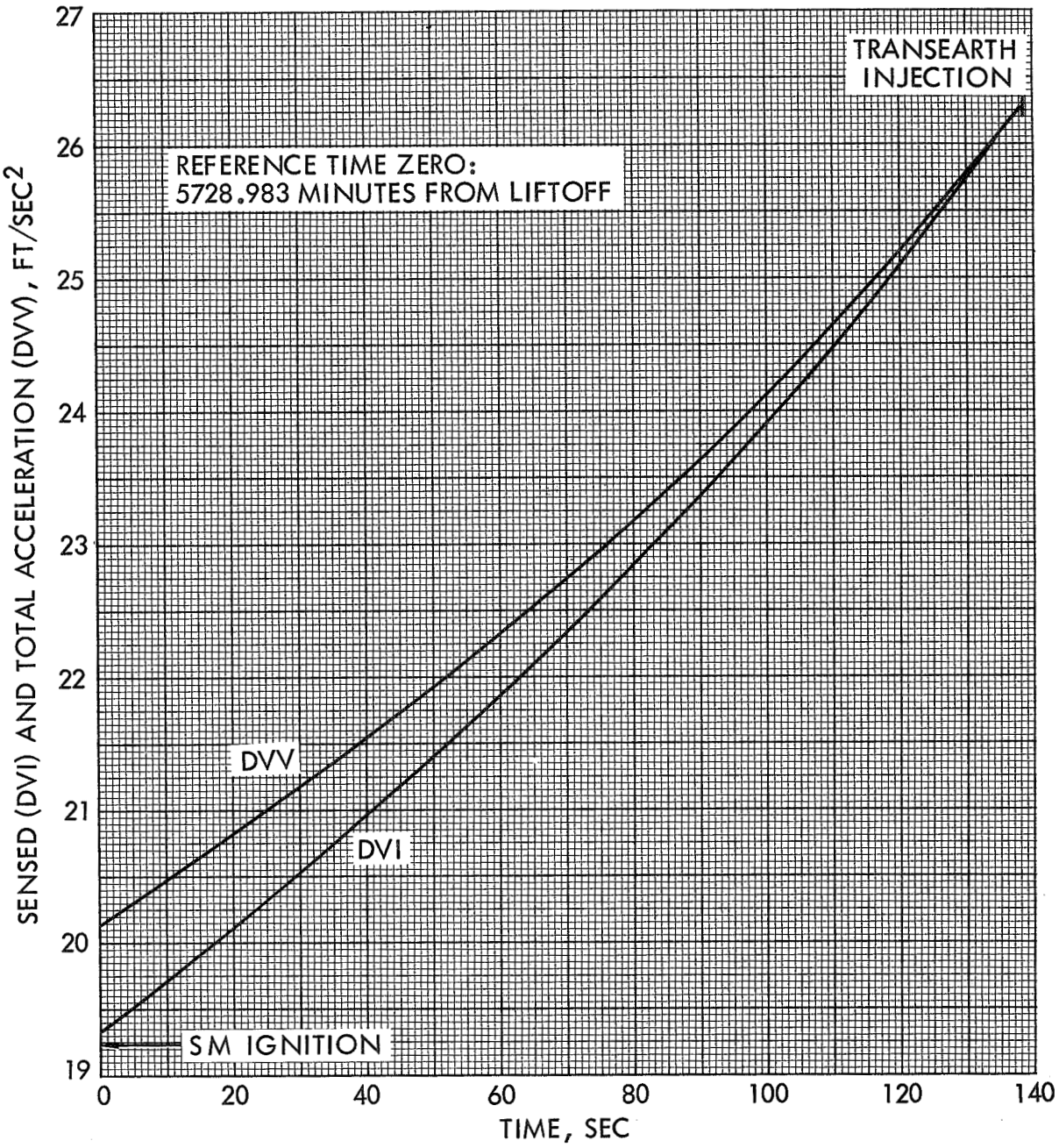

Figure 5.7-3. Transearth Injection and Return - Sensed (DVI) and Total (DVV) Acceleration

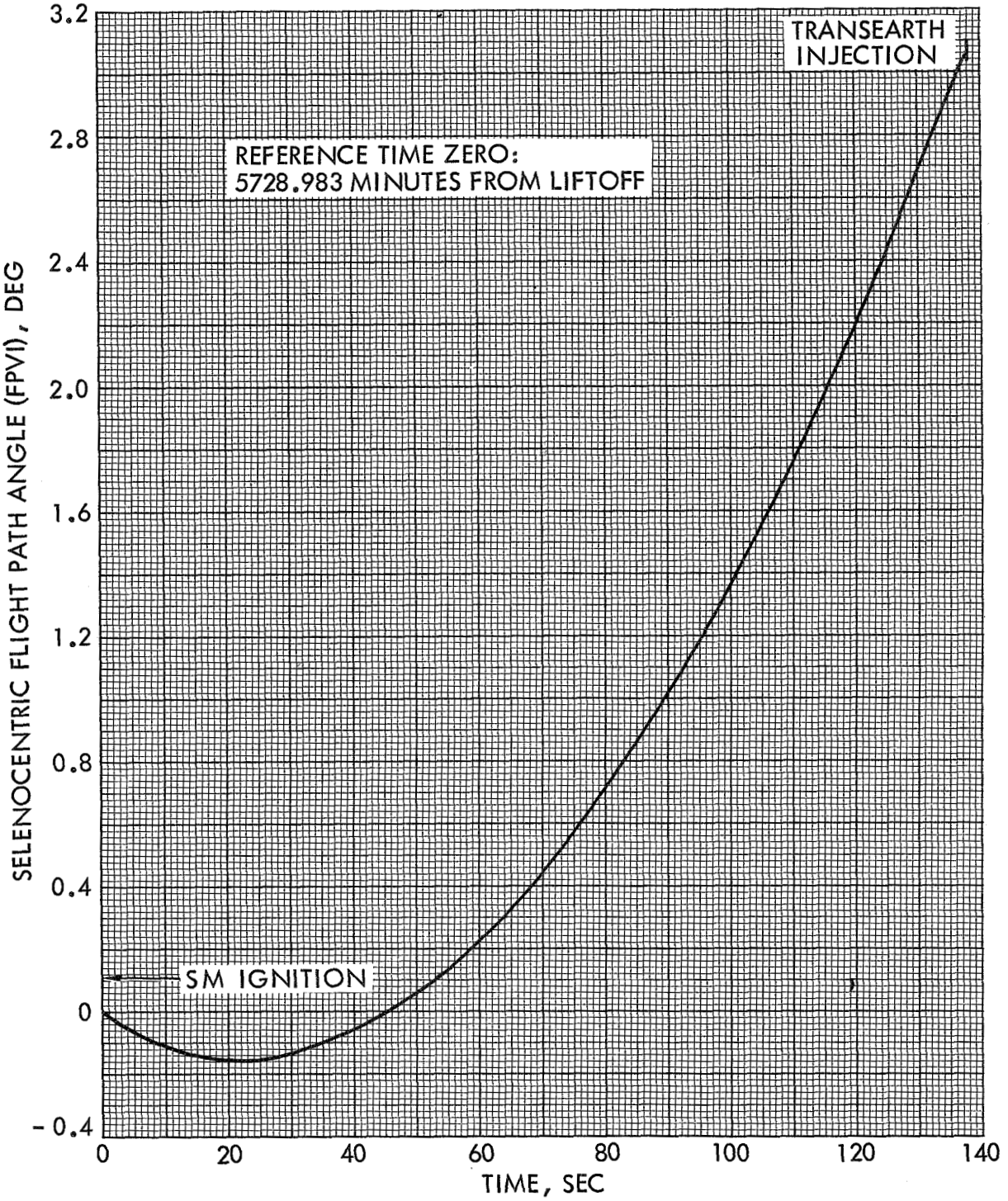

Figure 5.7-4. Transearth Injection and Return – Inertial Flight Path Angle (FPVI)

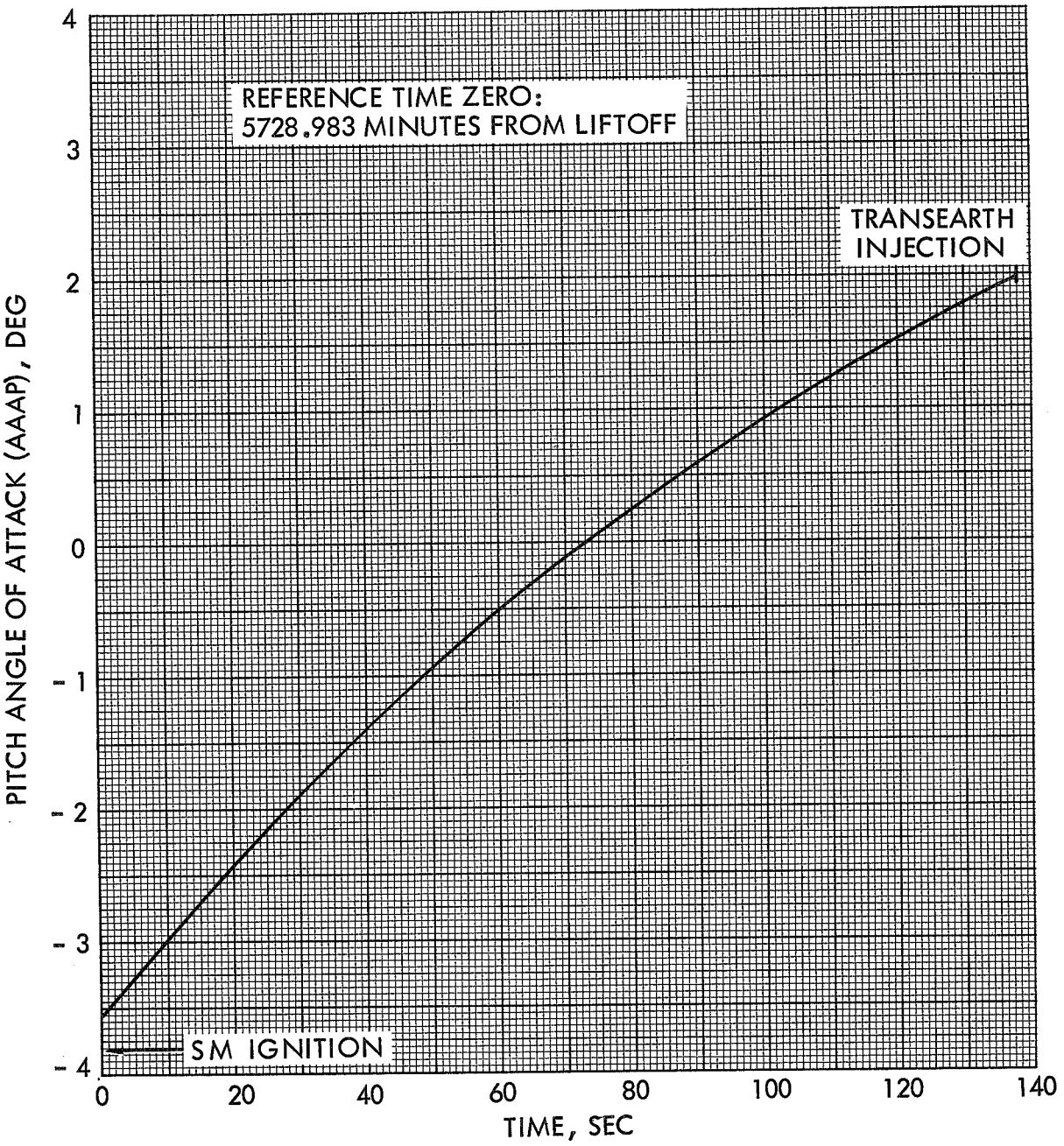

Figure 5.7-5. Transearth Injection and Return – Pitch Angle of Attack (AAAP)

CONFIDENTIAL

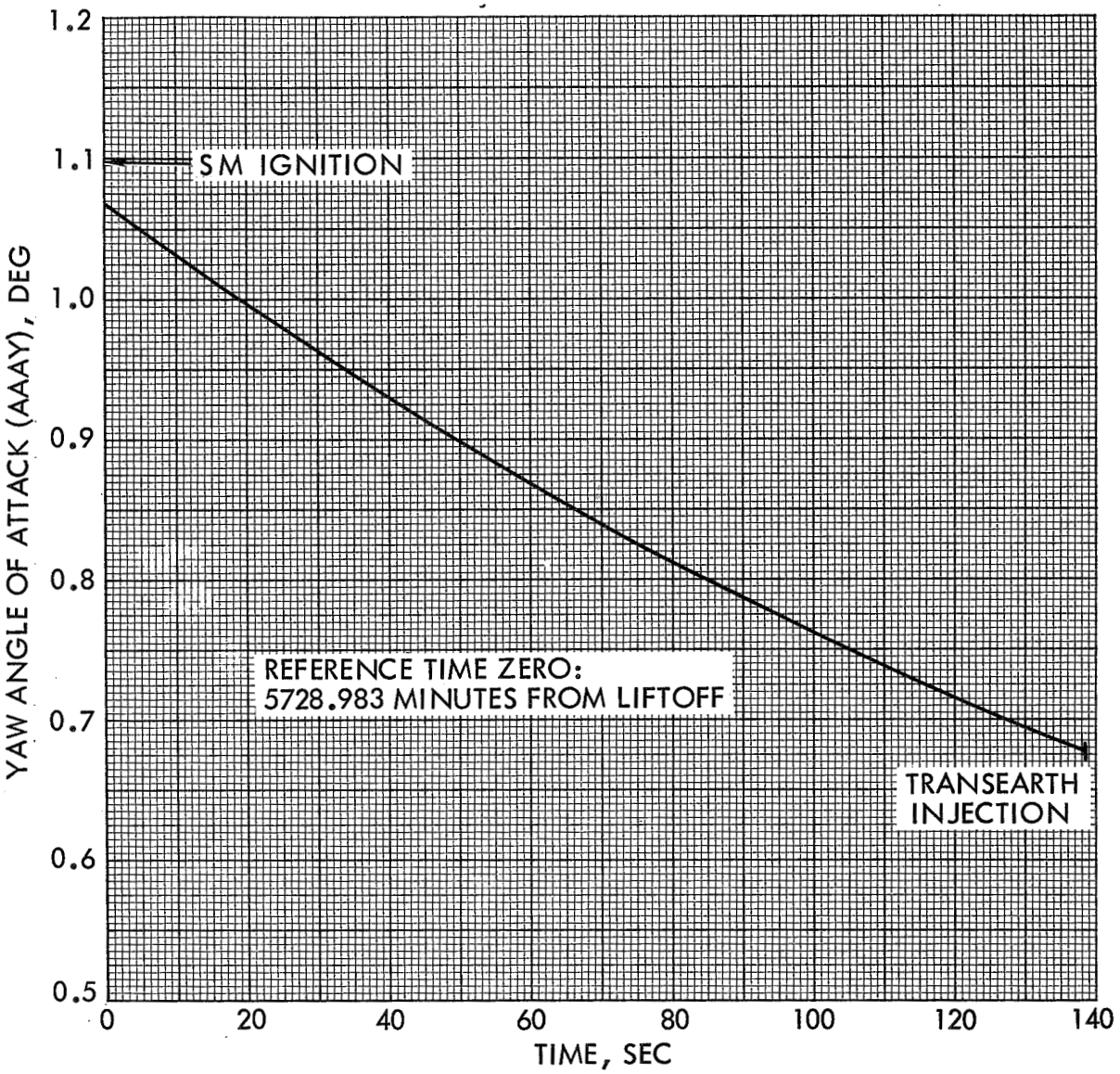

Figure 5.7-6. Transearth Injection and Return – Yaw Angle of Attack (AAAY)

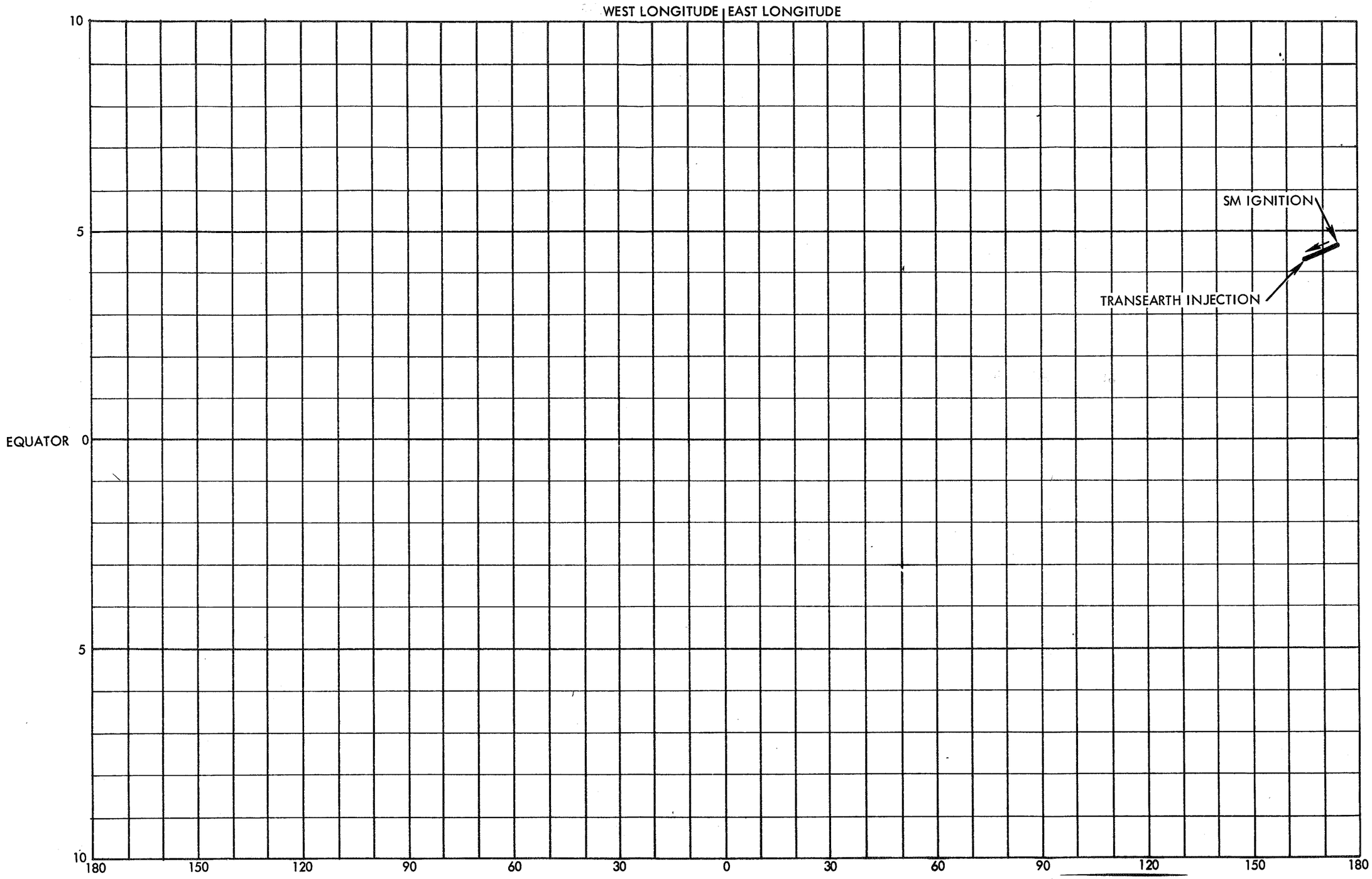

Figure 5.7-7. Transearth Injection and Return - Lunar Ground Track of Transearth Injection Powered Flight

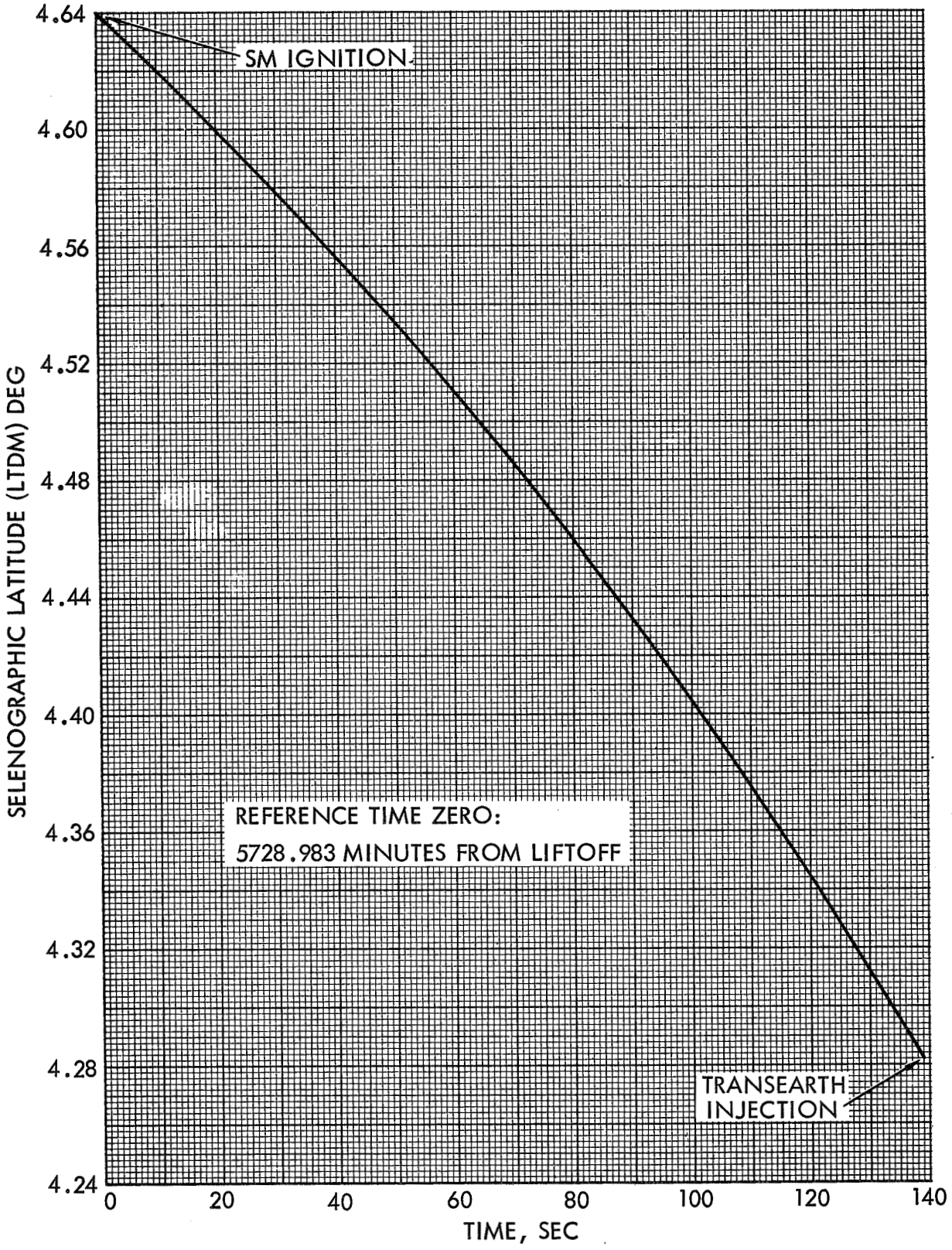

Figure 5.7-8a. Transearth Injection and Return - Selenographic Latitude

CONFIDENTIAL

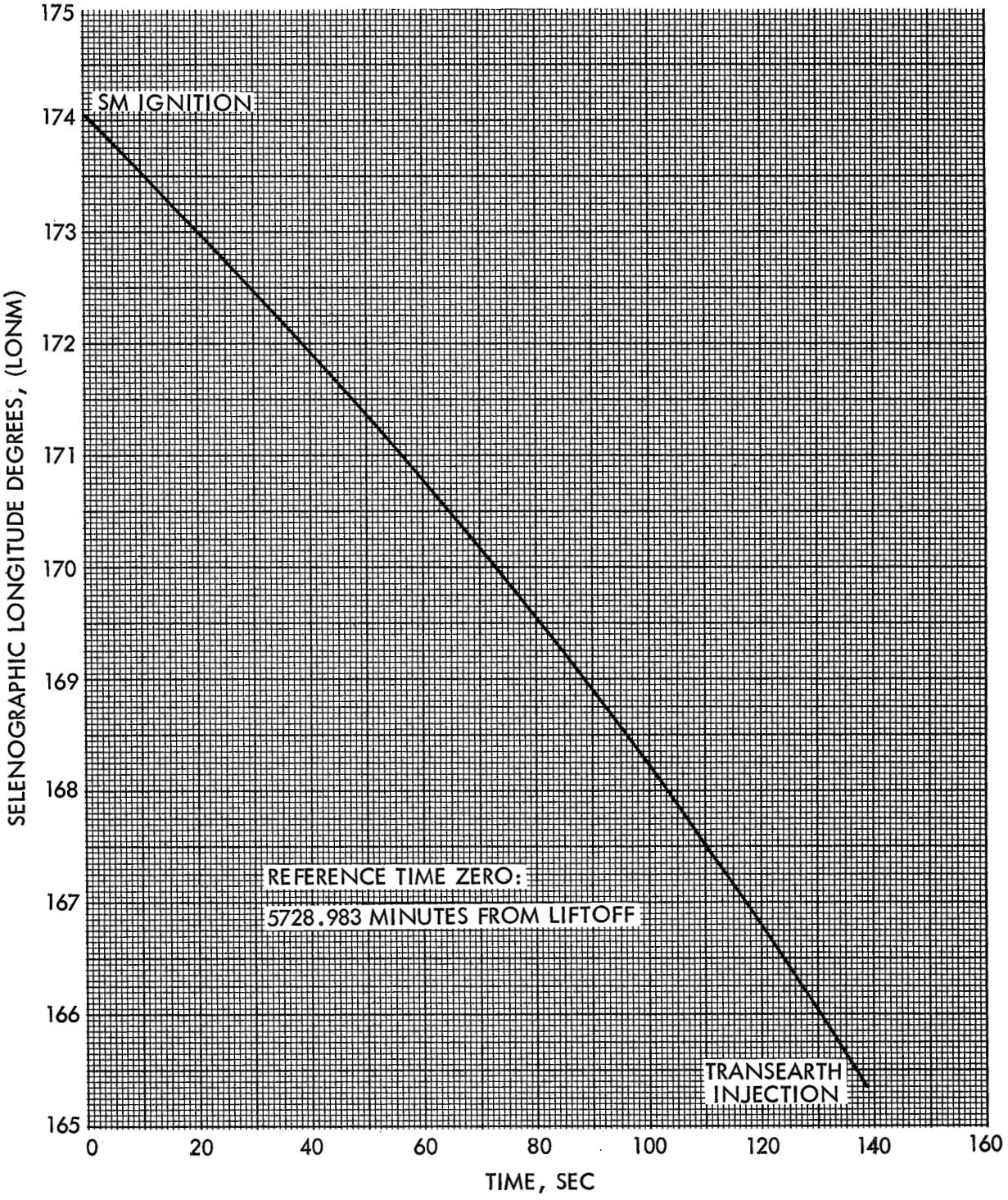

Figure 5.7-8b. Transearth Injection and Return - Selenographic Longitude

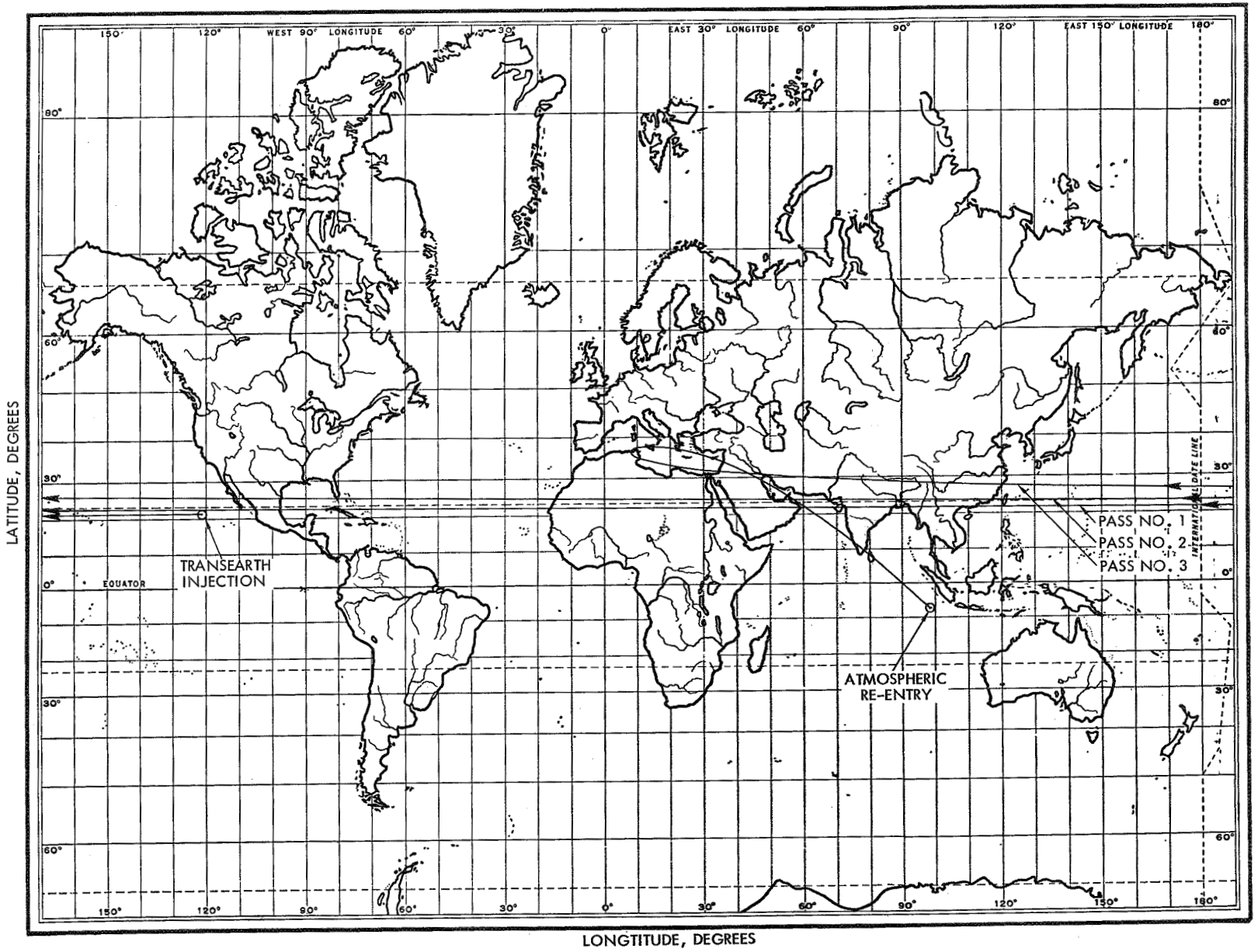

Figure 5.7-9. Transearth Injection and Return – Earth Ground Track

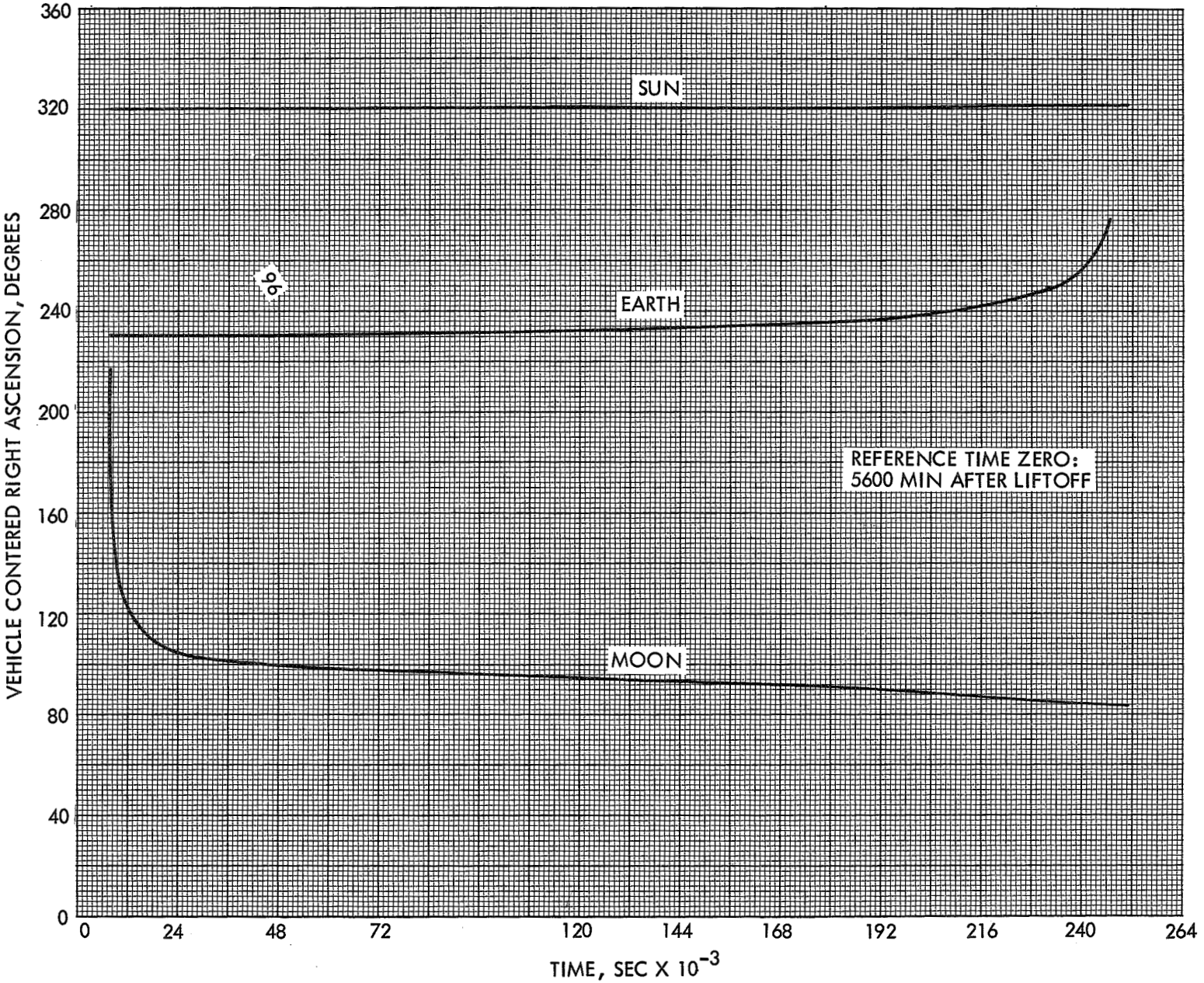

Figure 5.7-10. Transearth Injectionand Return - Vehicle Centered Right Ascension of Earth, Sun, and Moon

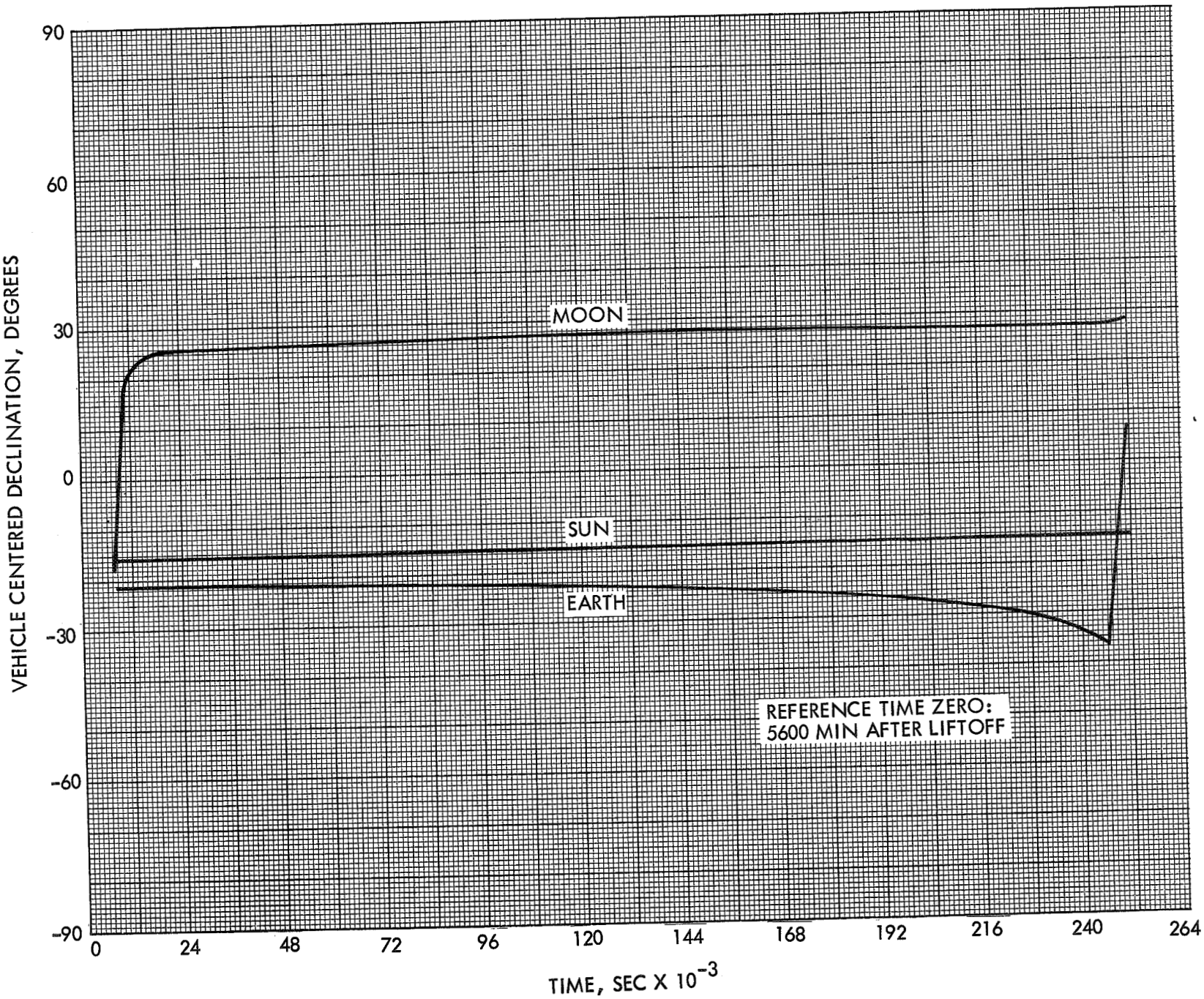

Figure 5.7-11. Transearth Injection and Return - Vehicle Centered Declination of Earth, Sun, and Moon

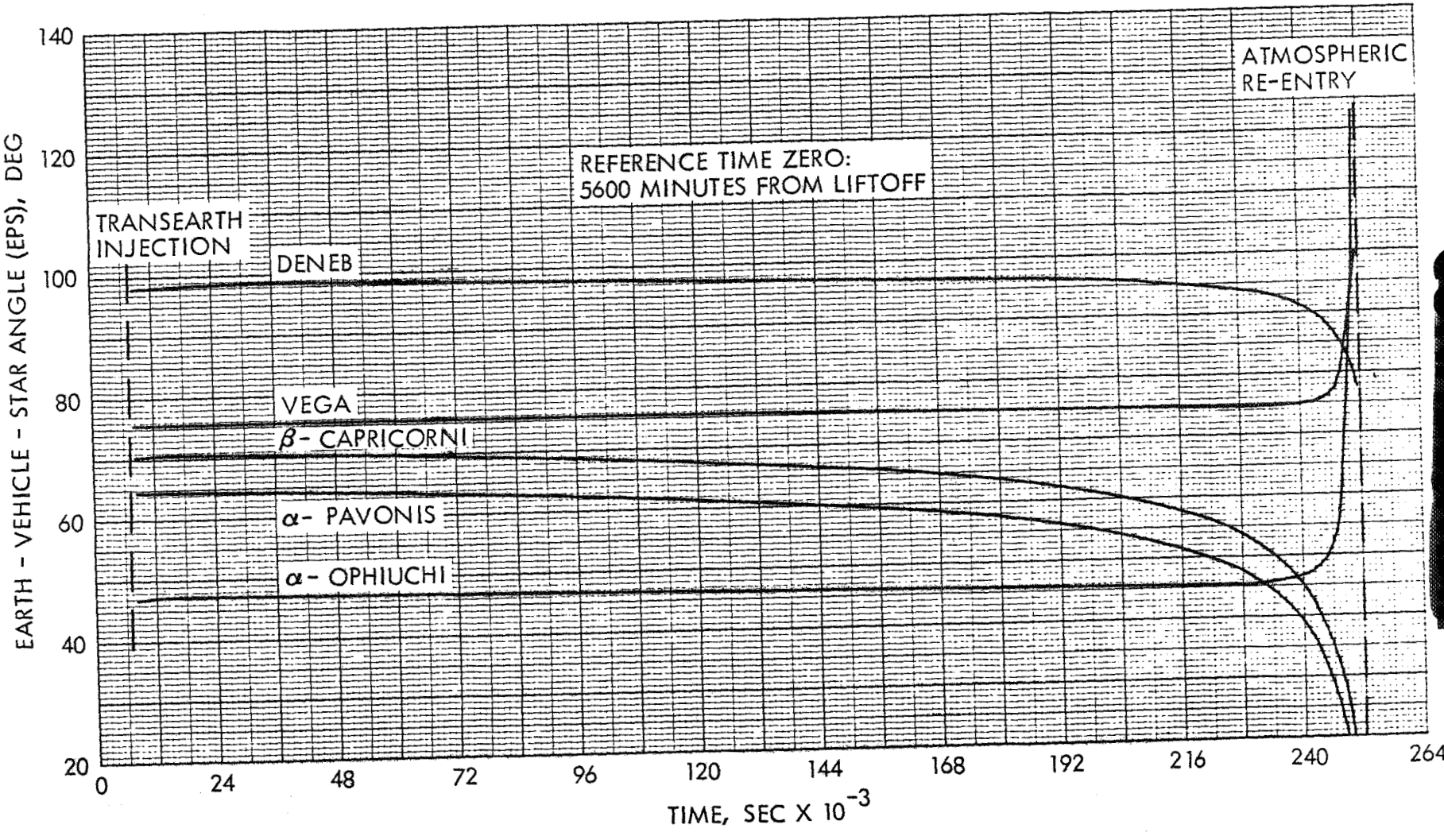

Figure 5.7-12. Transearth Injection and Return - Earth-Vehicle-Star Angles (EPS)

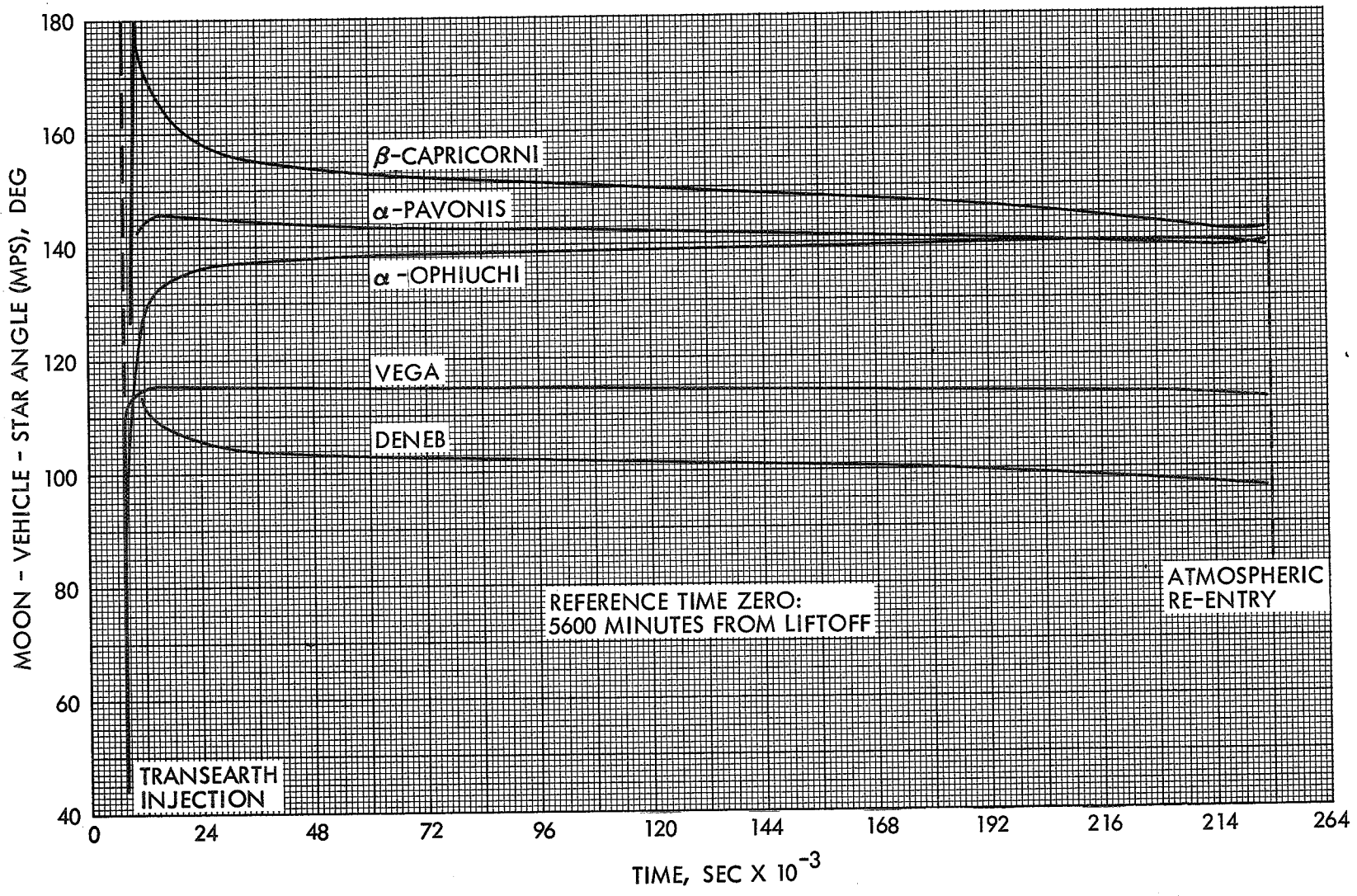

Figure 5.7-13. Transearth Injection and Return — Moon-Vehicle Star Angles (MPS)

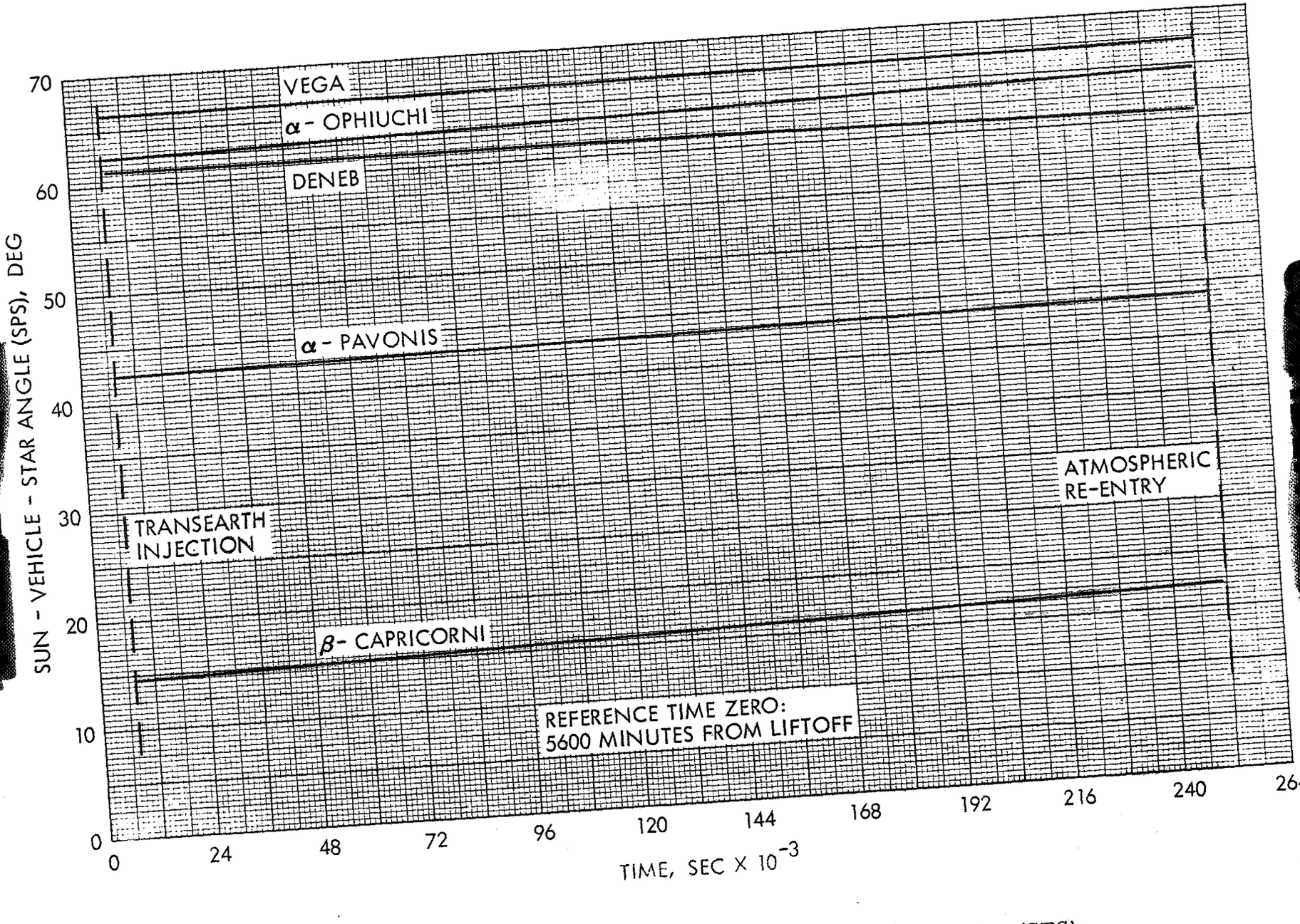

Figure 5.7-14. Transearth Injection and Return - Sun-Vehicle-Star Angles (SPS)

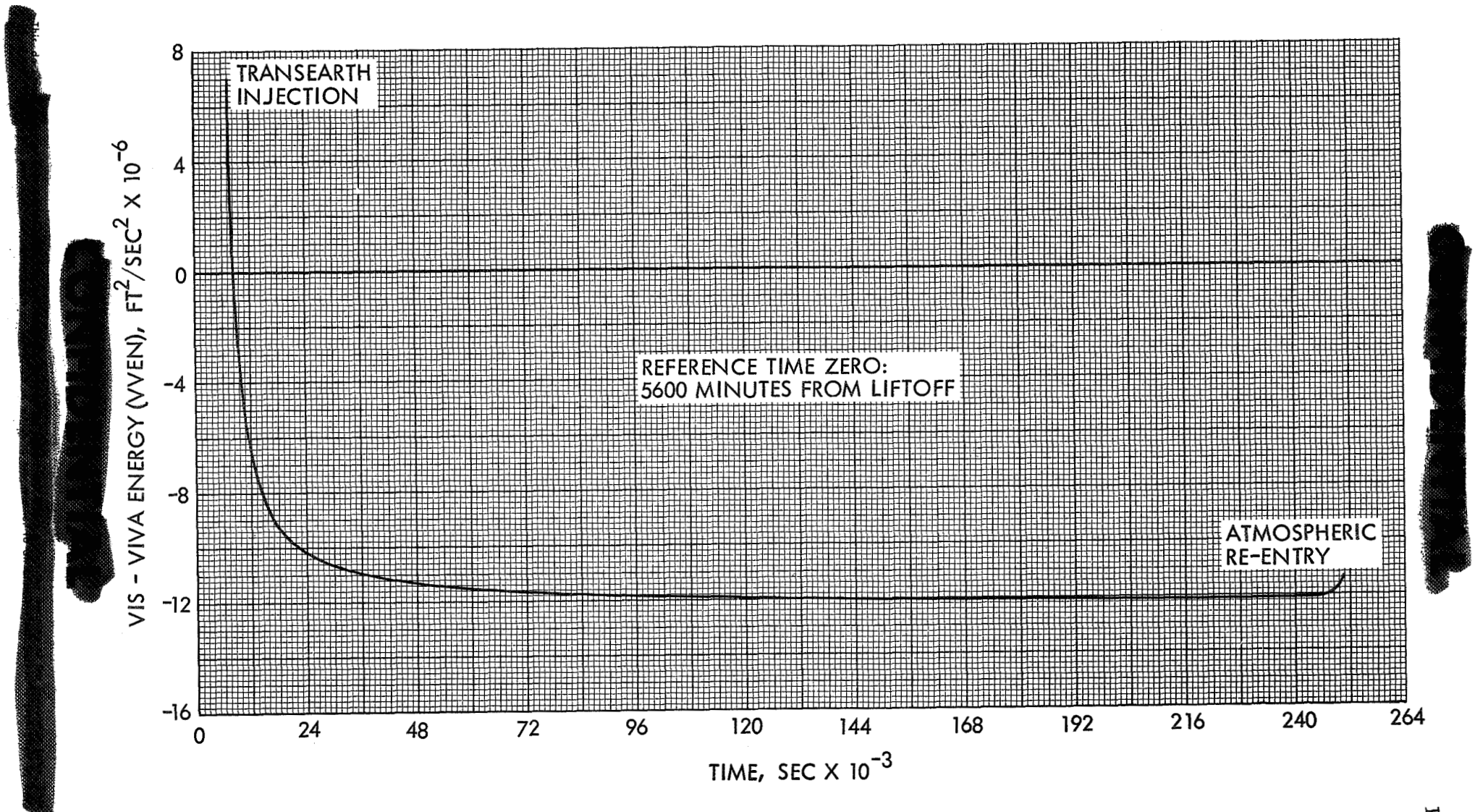

Figure 5.7-15. Transearth Injection and Return - Vis-viva Energy (VVEN)

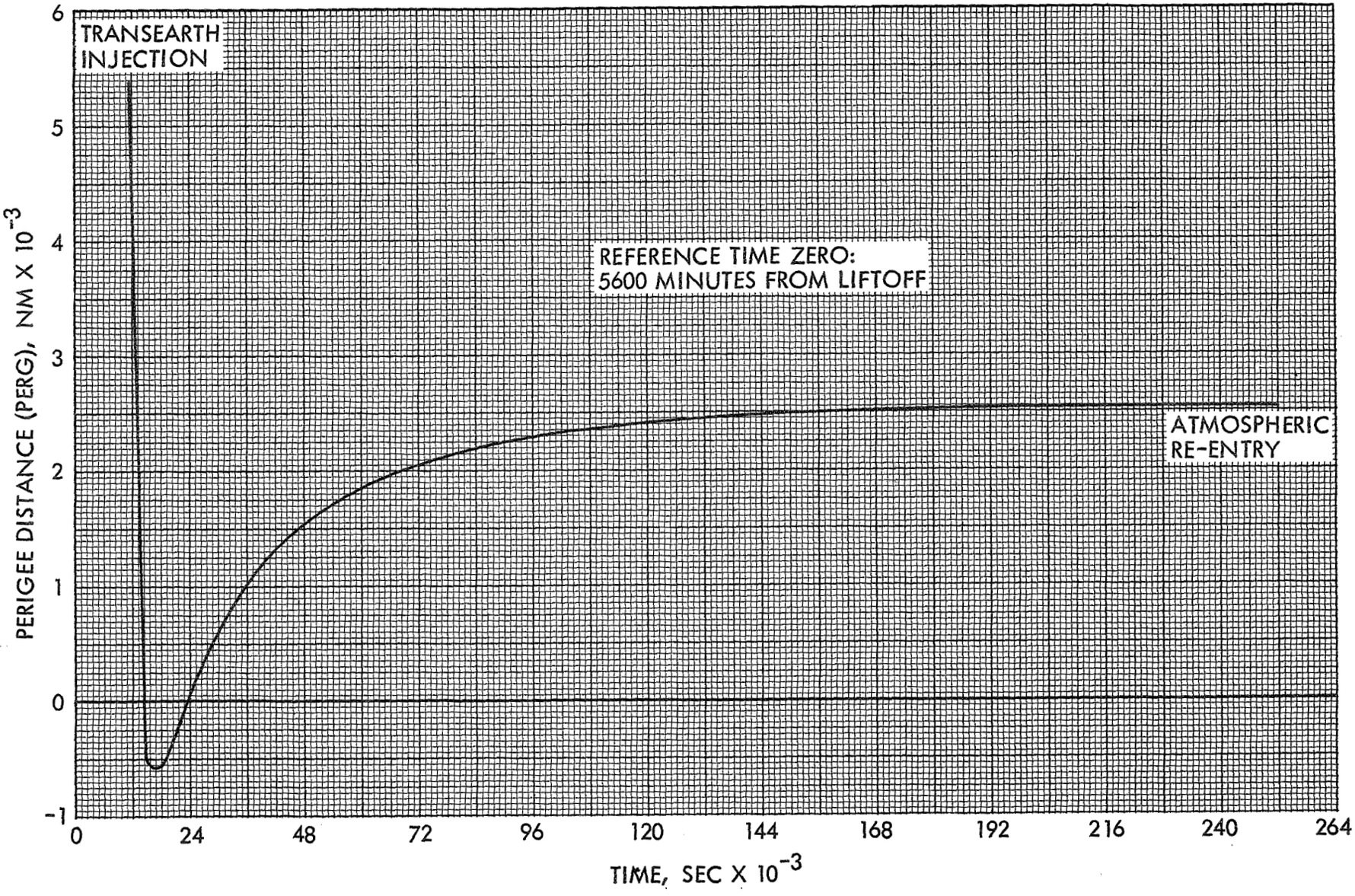

Figure 5.7-16. Transearth Injection and Return - Perigee Distance (PERG)

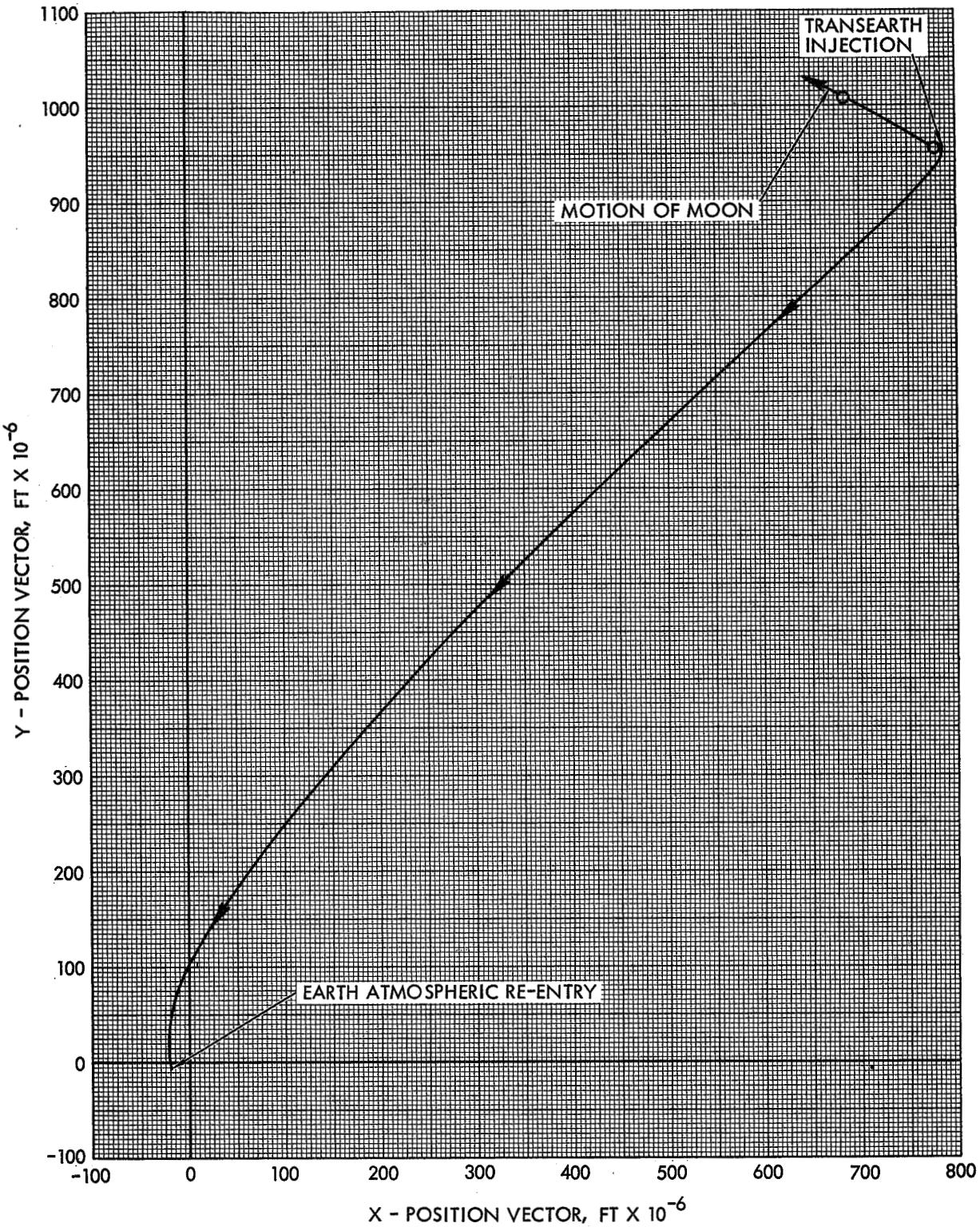

Figure 5.7-17. Transearth Injection and Return - Geocentric Position X versus Y

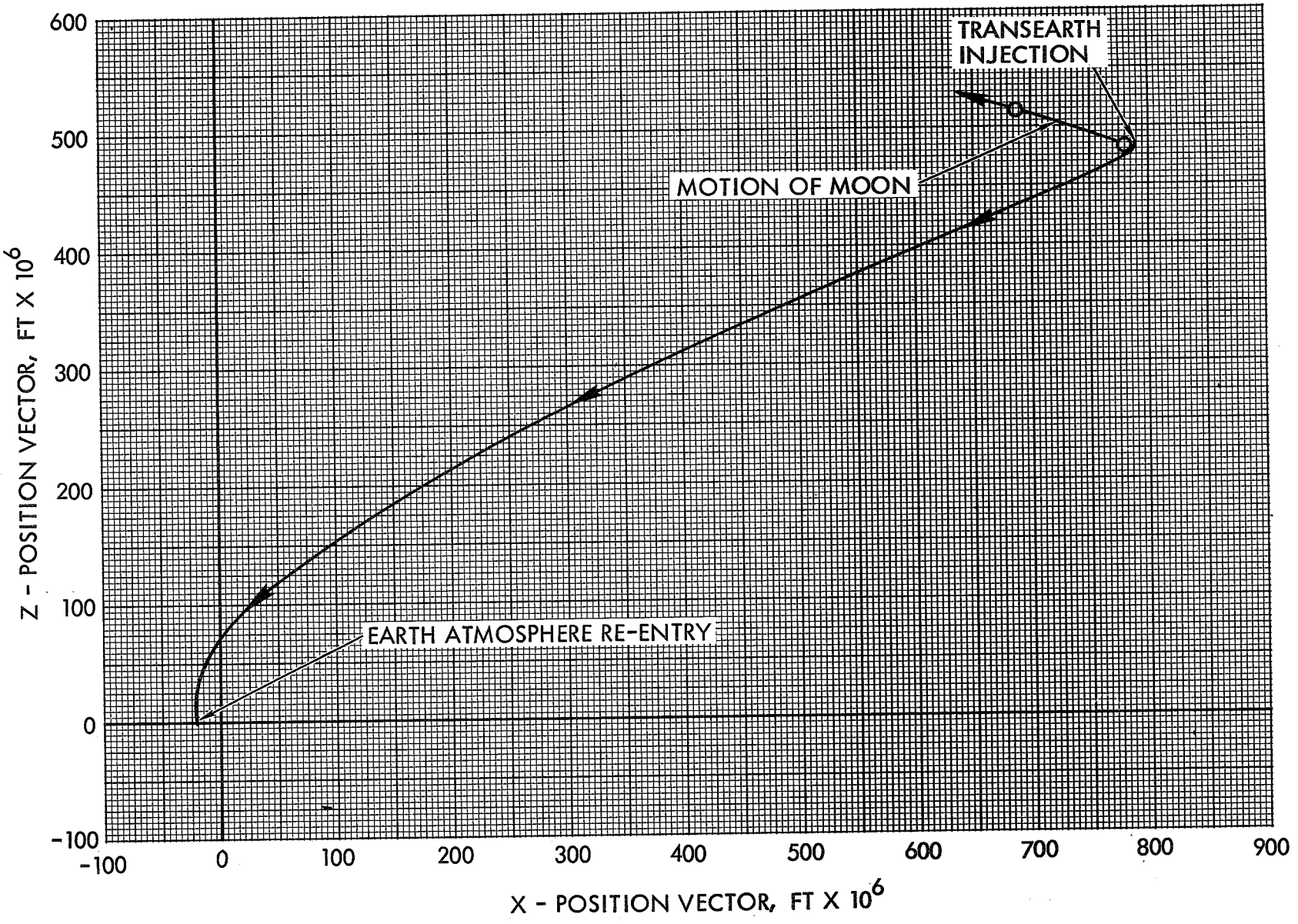

Figure 5.7-18. Transearth Injection and Return - Geocentric Position X versus Z

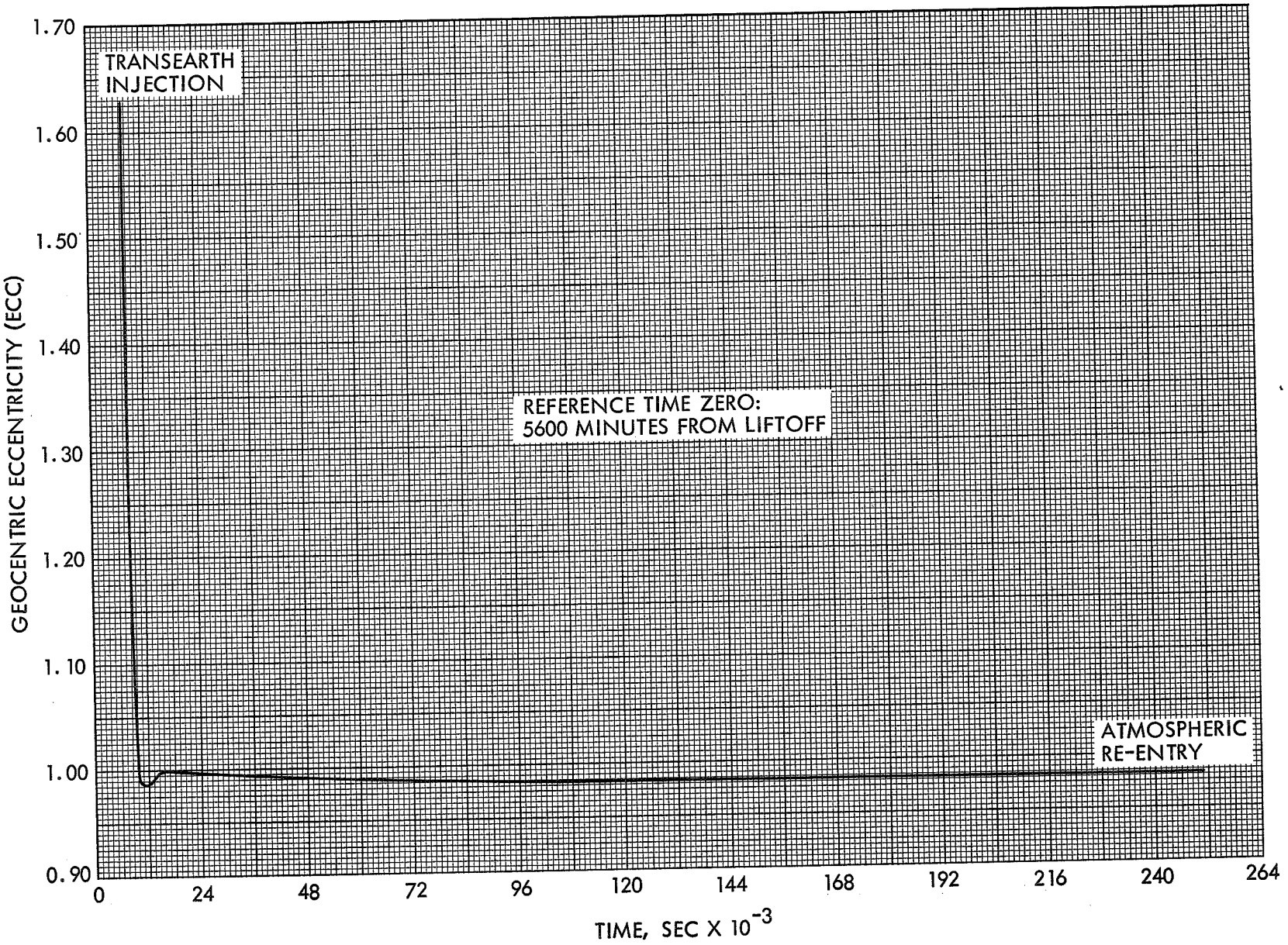

Figure 5.7-19. Transearth Injection and Return - Osculating Geocentric Eccentricity

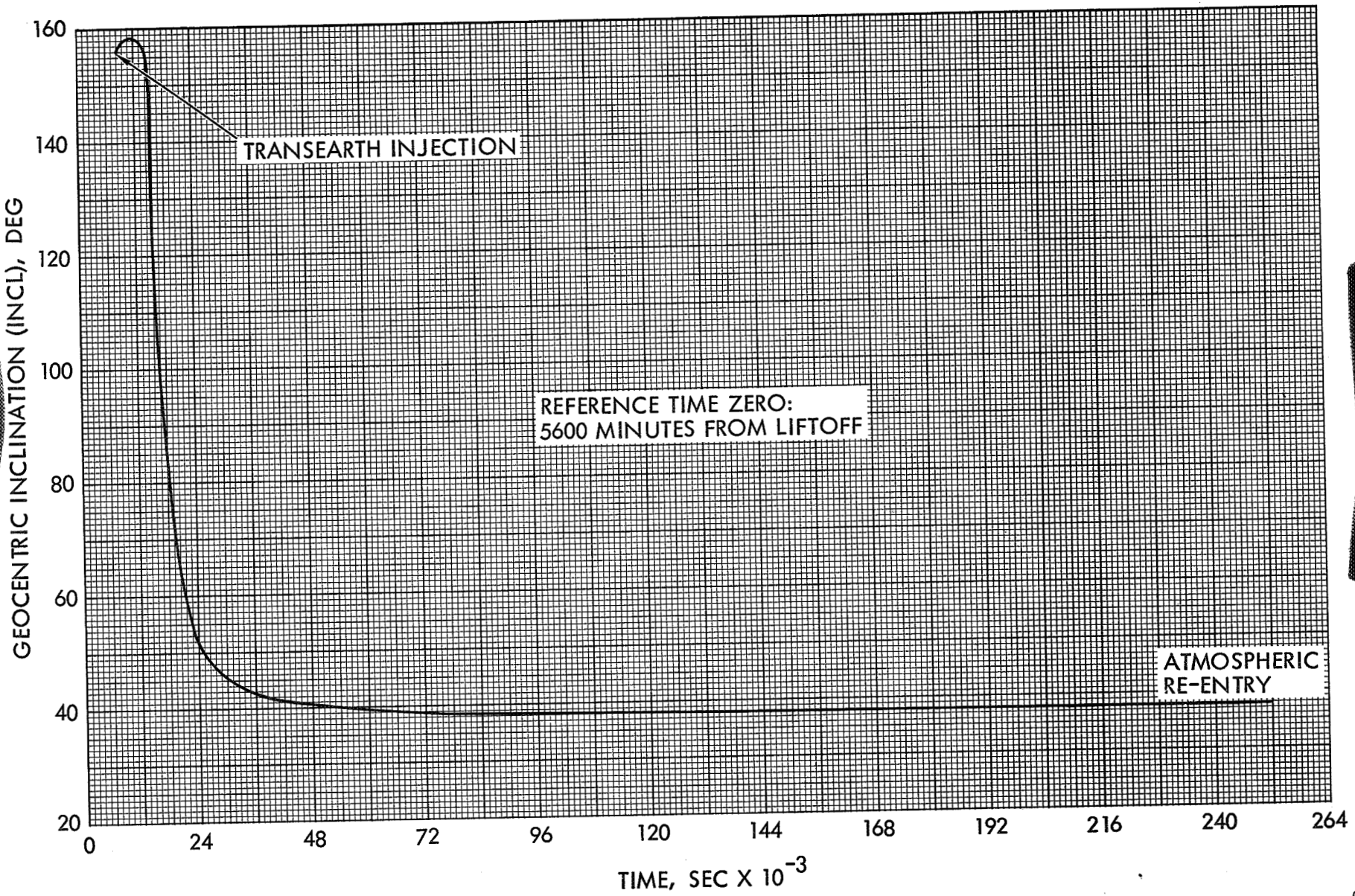

Figure 5.7-20. Transearth Injection and Return - Osculating Geocentric Inclination (INCL)

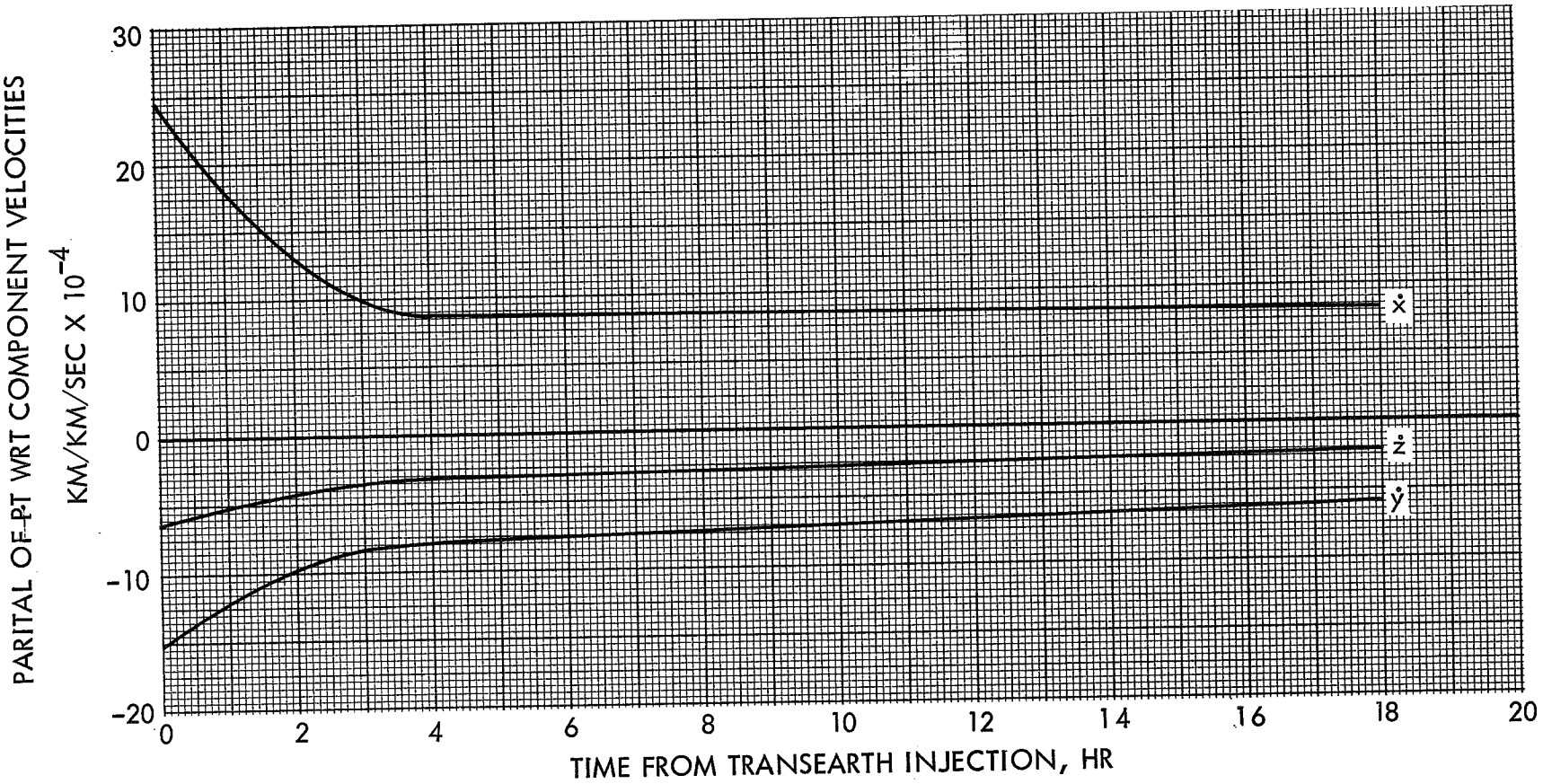

Figure 5.7-21a. Transearth Injection and Return - Midcourse Sensitivities

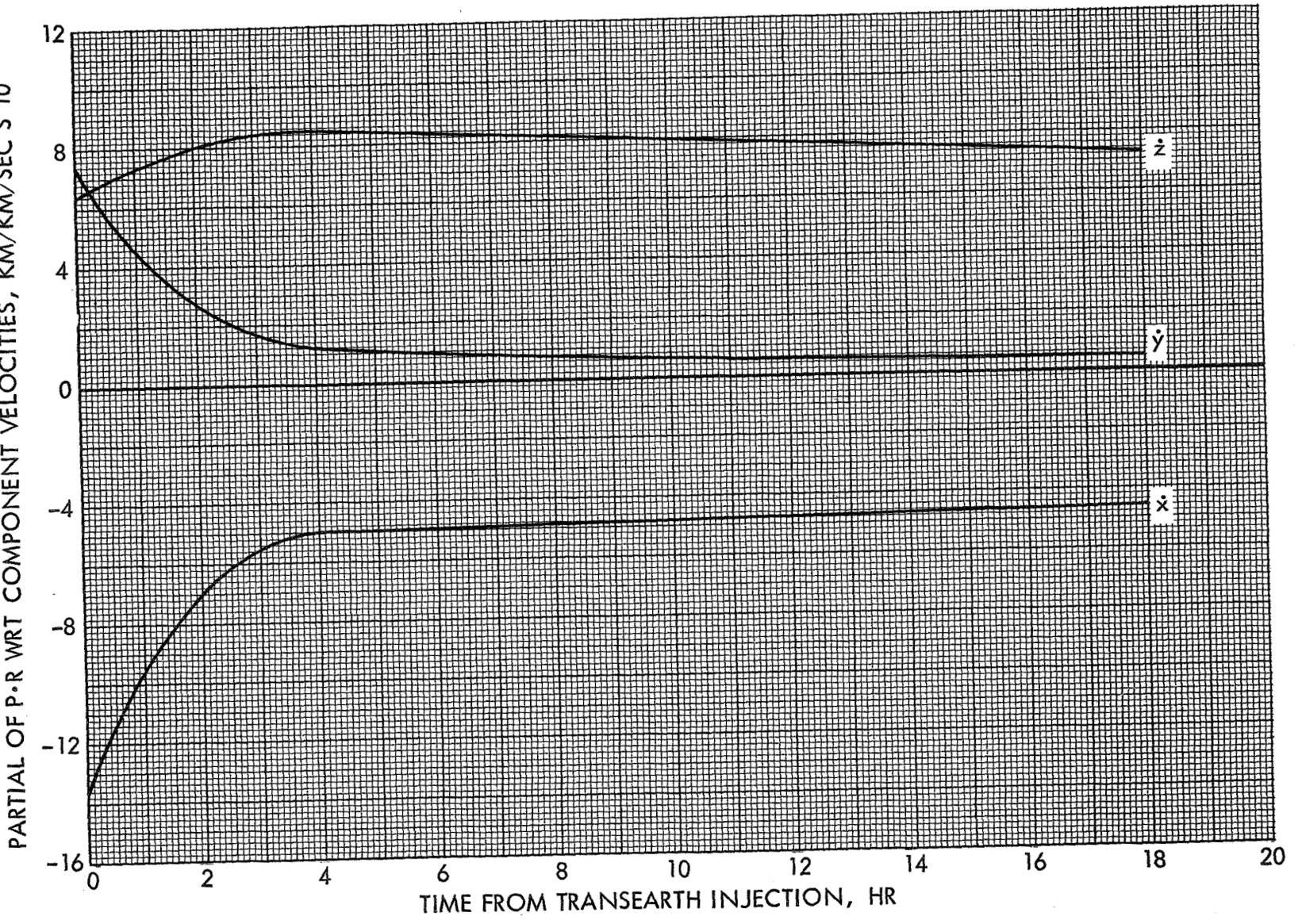

Figure 5.7-21b. Transearth Injection and Return - Midcourse Sensitivities

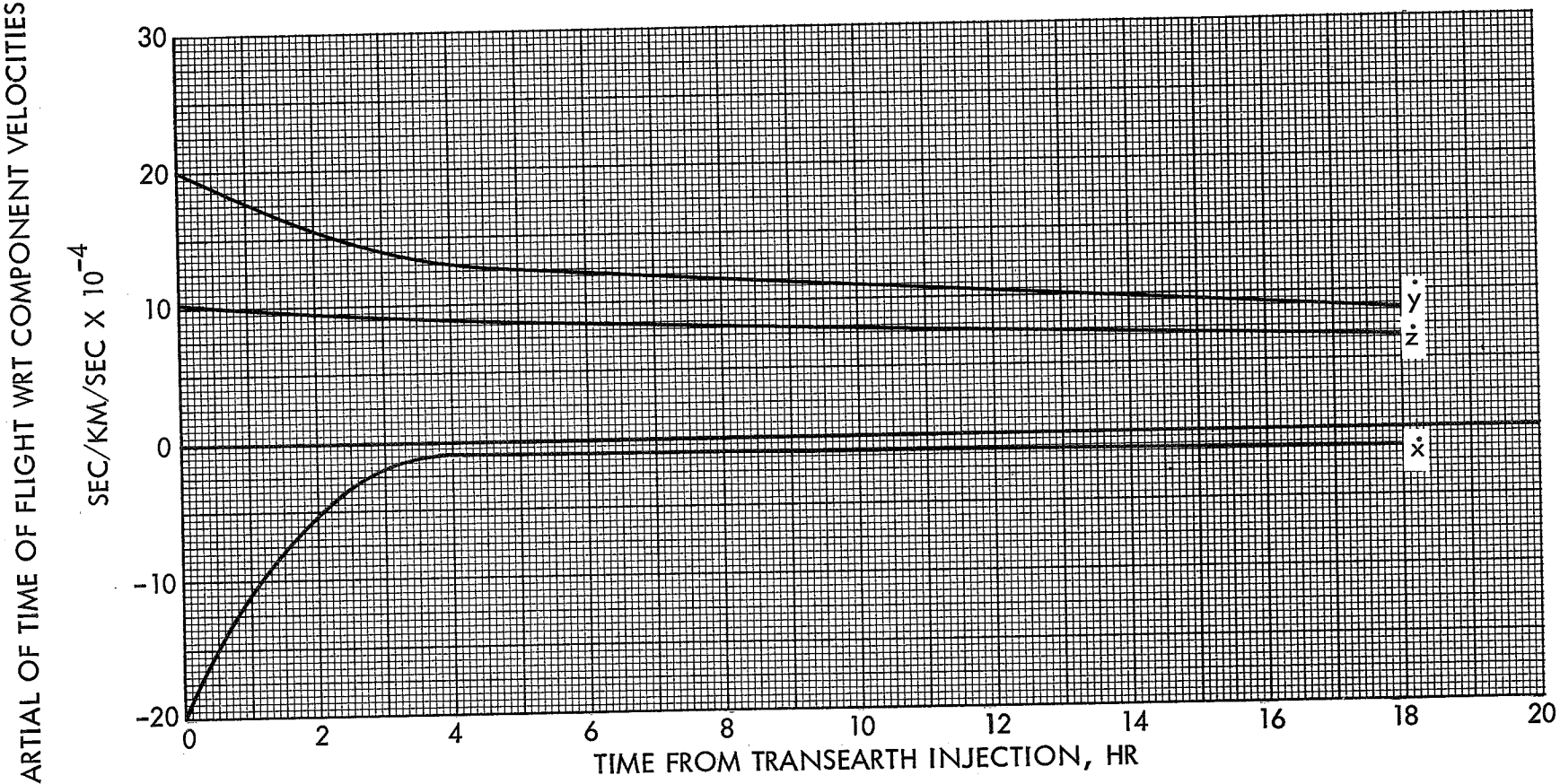

Figure 5.7-21c. Transearth and Return - Midcourse Sensitivities

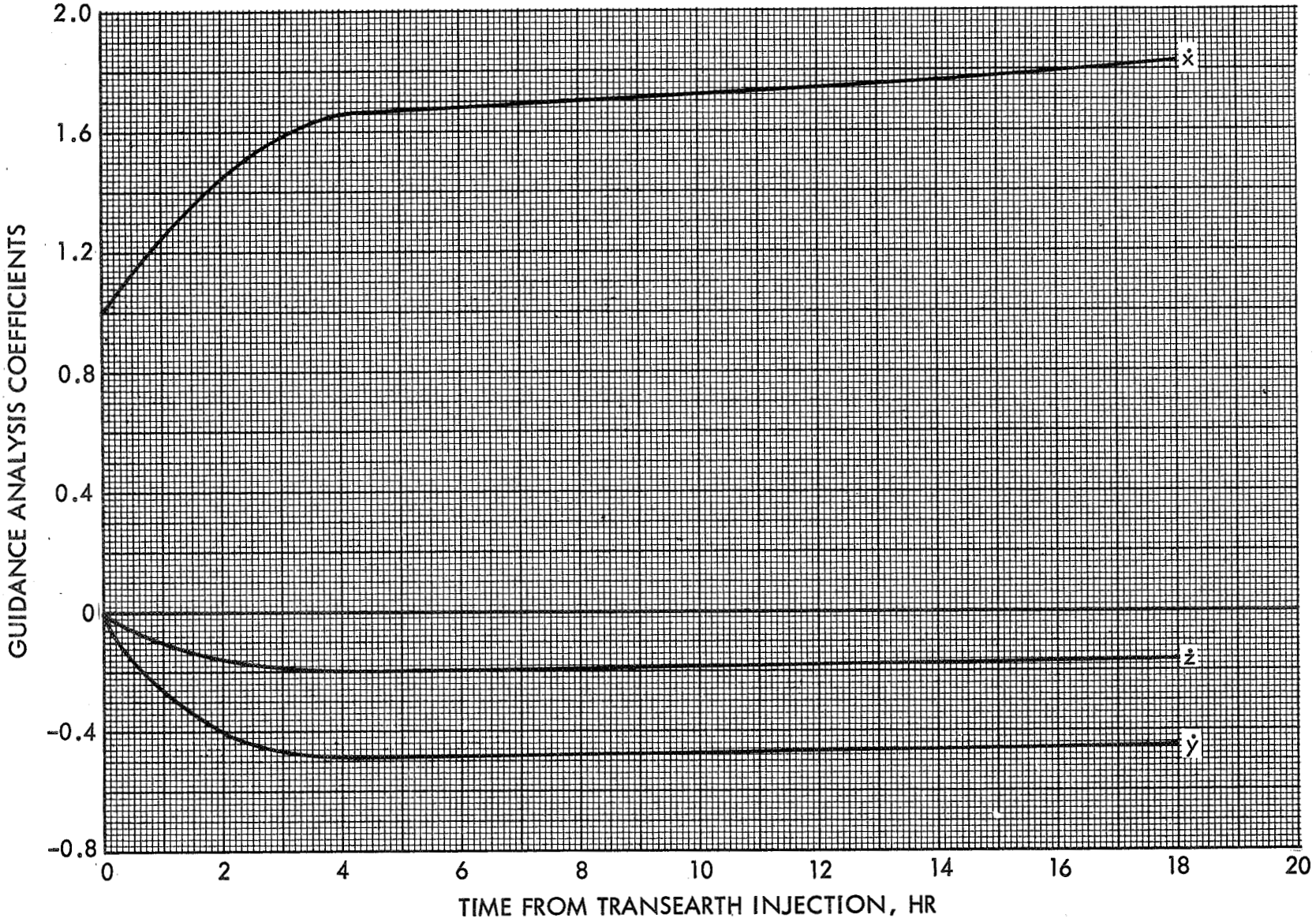

Figure 5.7-22a. Partials of the X Component of Midcourse Velocity with Respect to the Injection Velocity Components

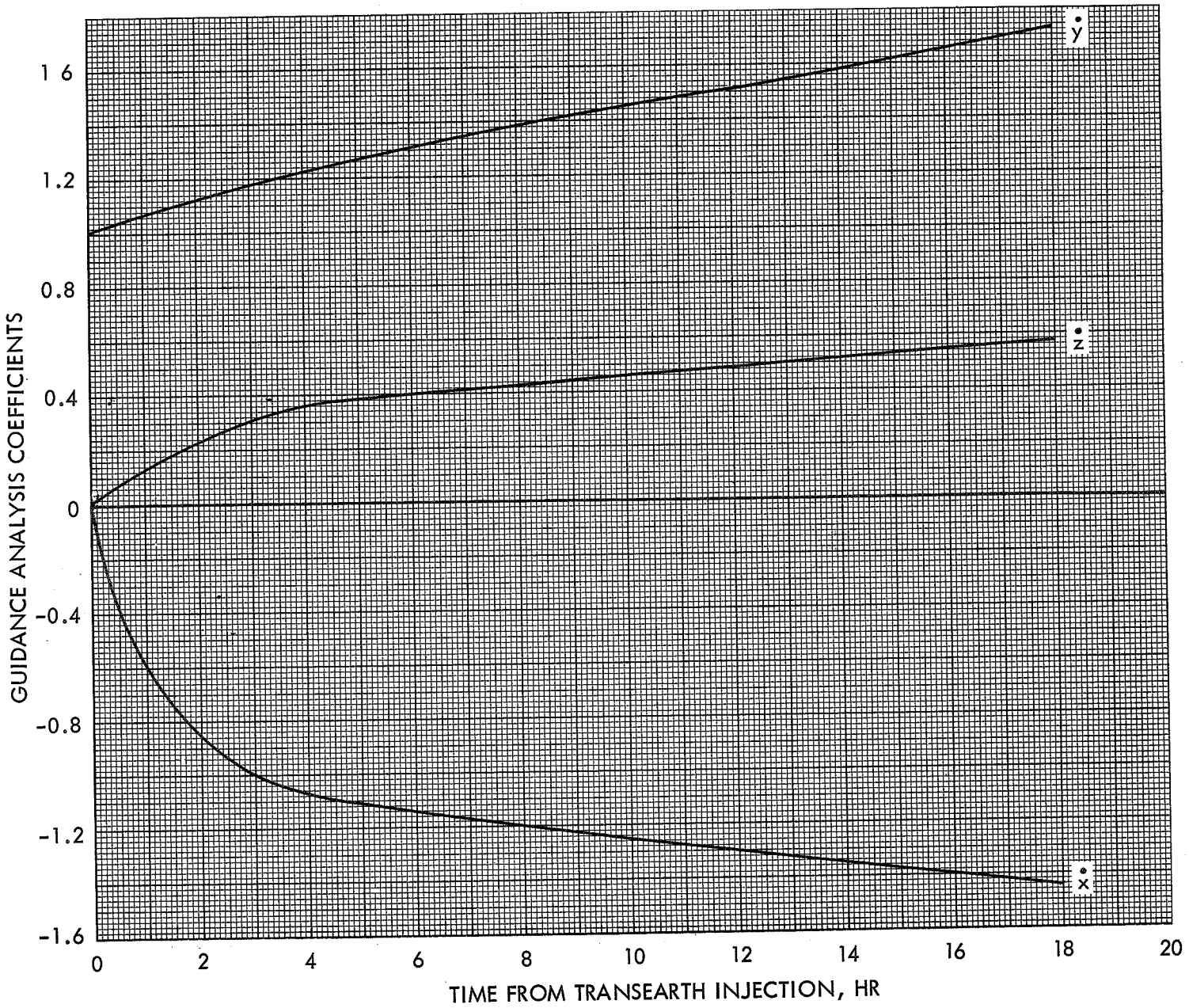

Figure 5.7-22b. Partials of the Y Component of Midcourse Velocity with Respect to the Injection Velocity Components

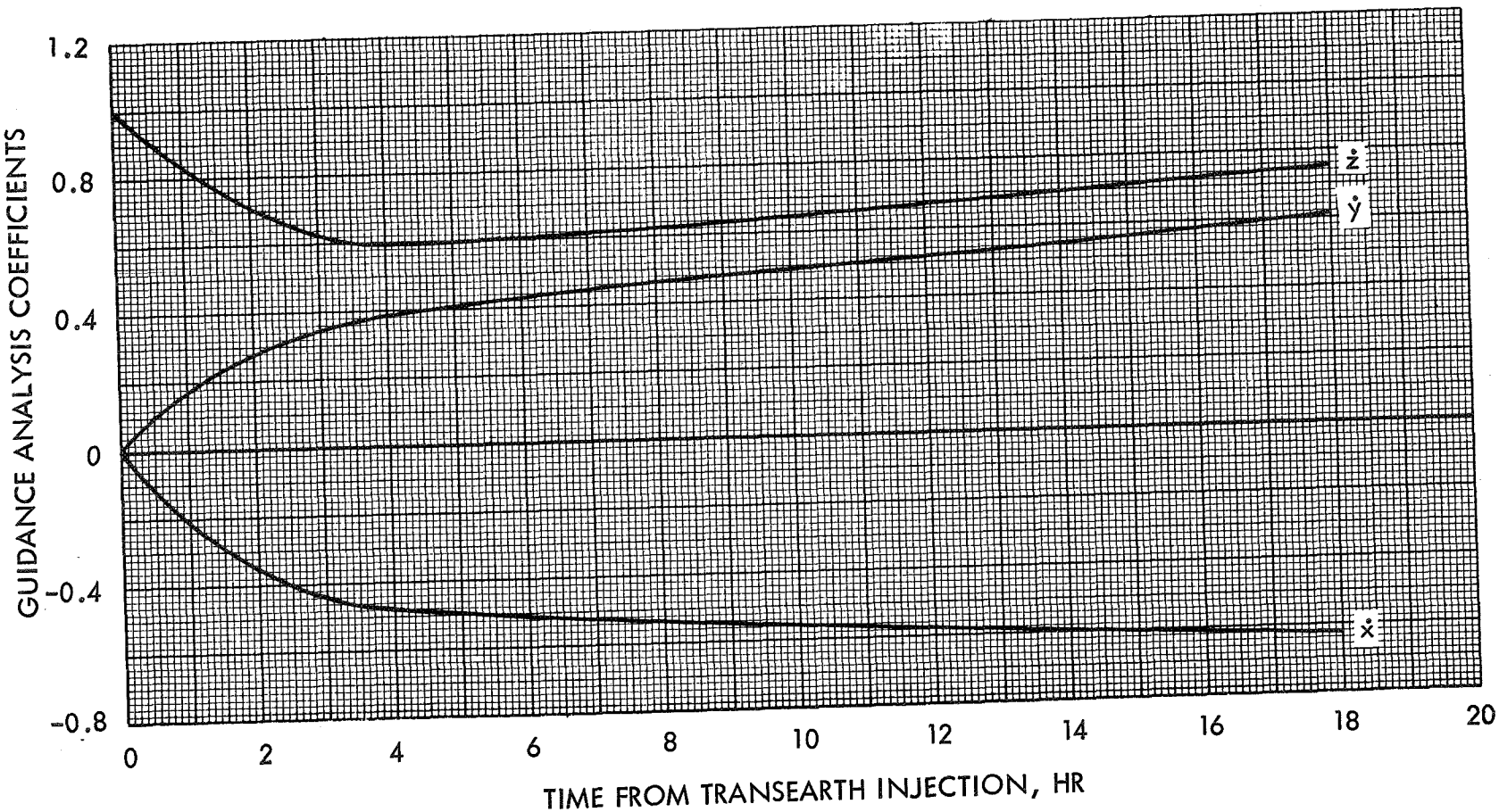

Figure 5.7-22c. Partials of the Z Component of Midcourse Velocity with Respect to the Injection Velocity Components

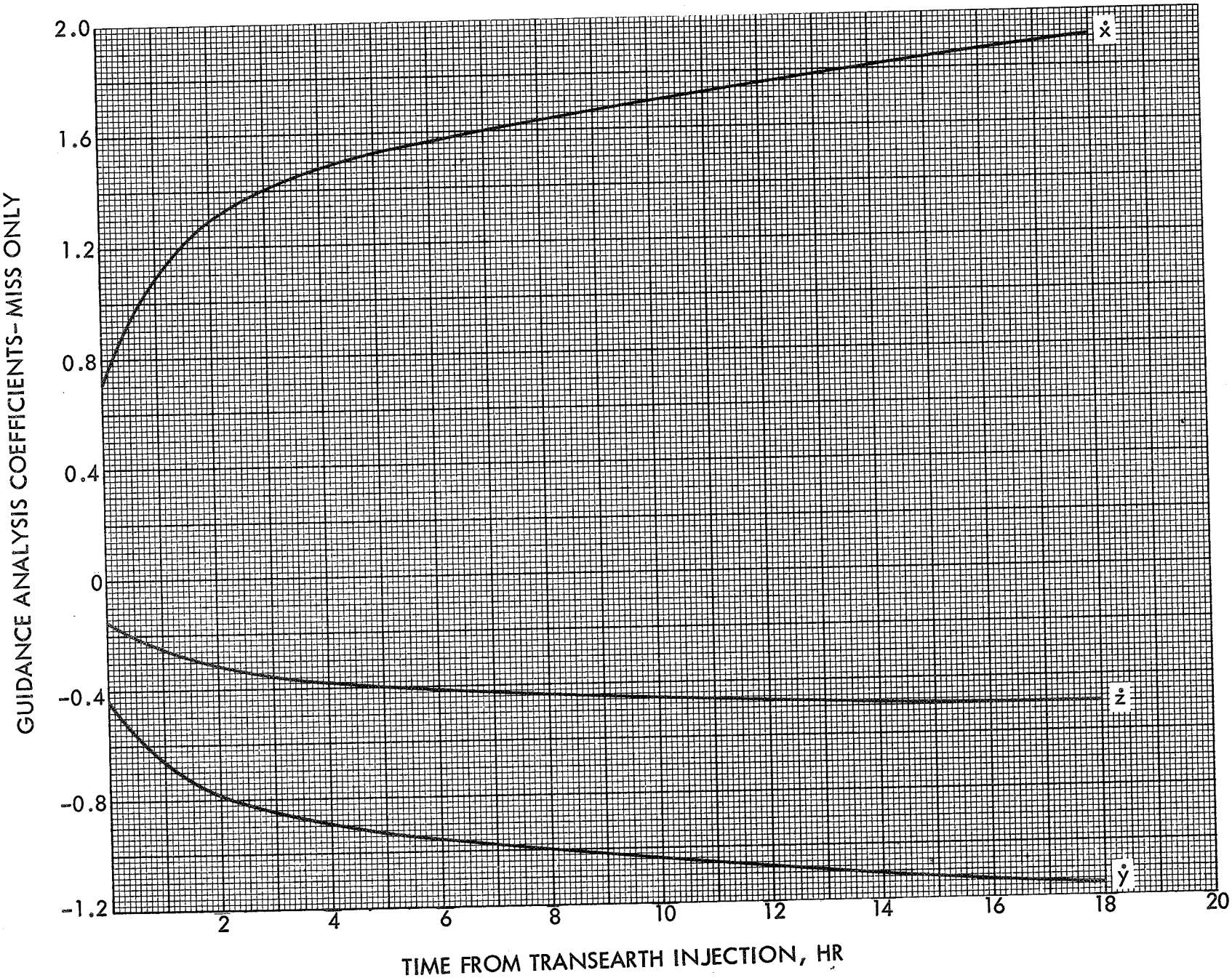

Figure 5.7-22d. Partials of the X Component of Midcourse Velocity with Respect to the Injection Velocity Components

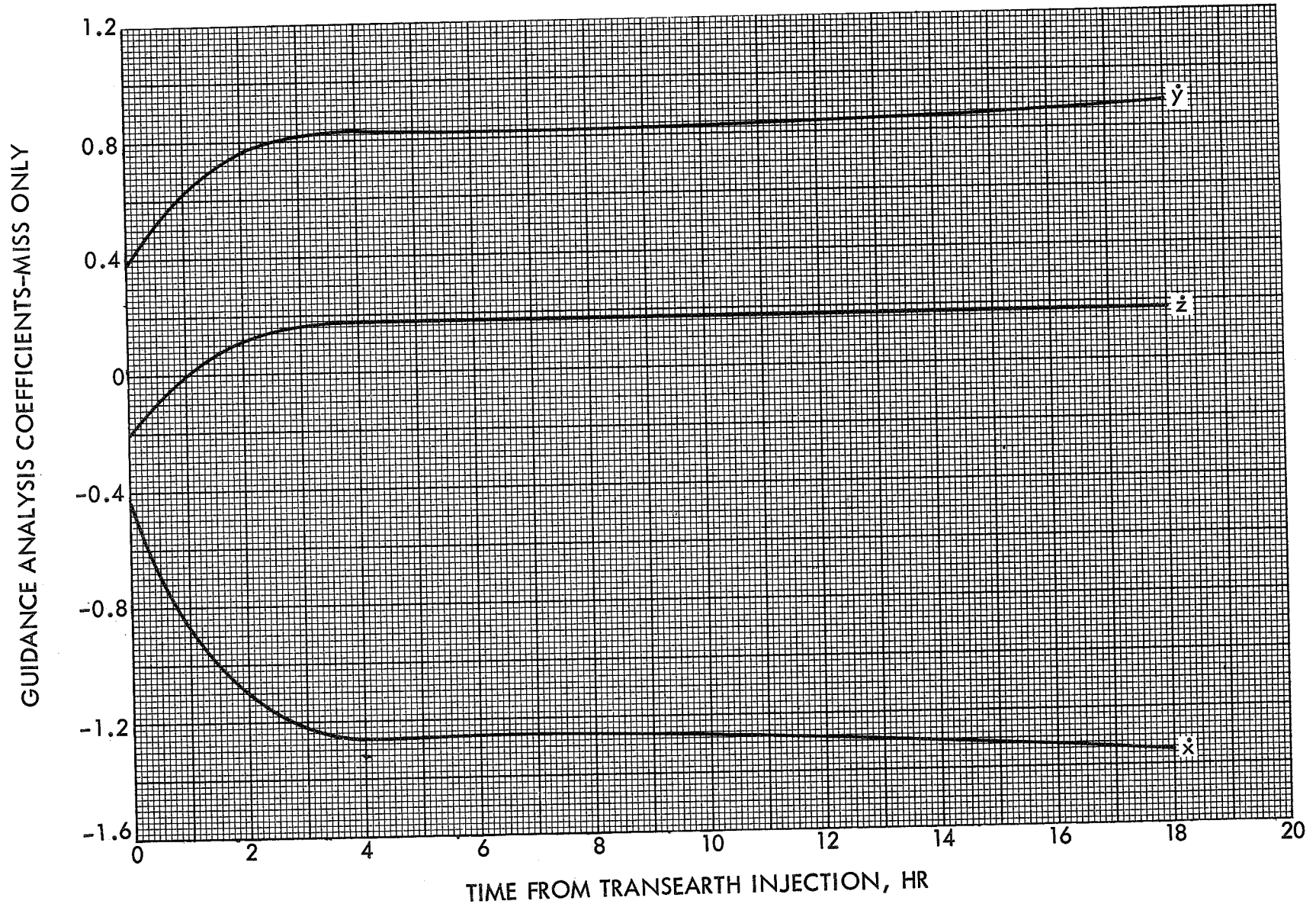

Figure 5.7-22e. Partials of the Y Component of Midcourse Velocity with Respect to the Injection Velocity Components

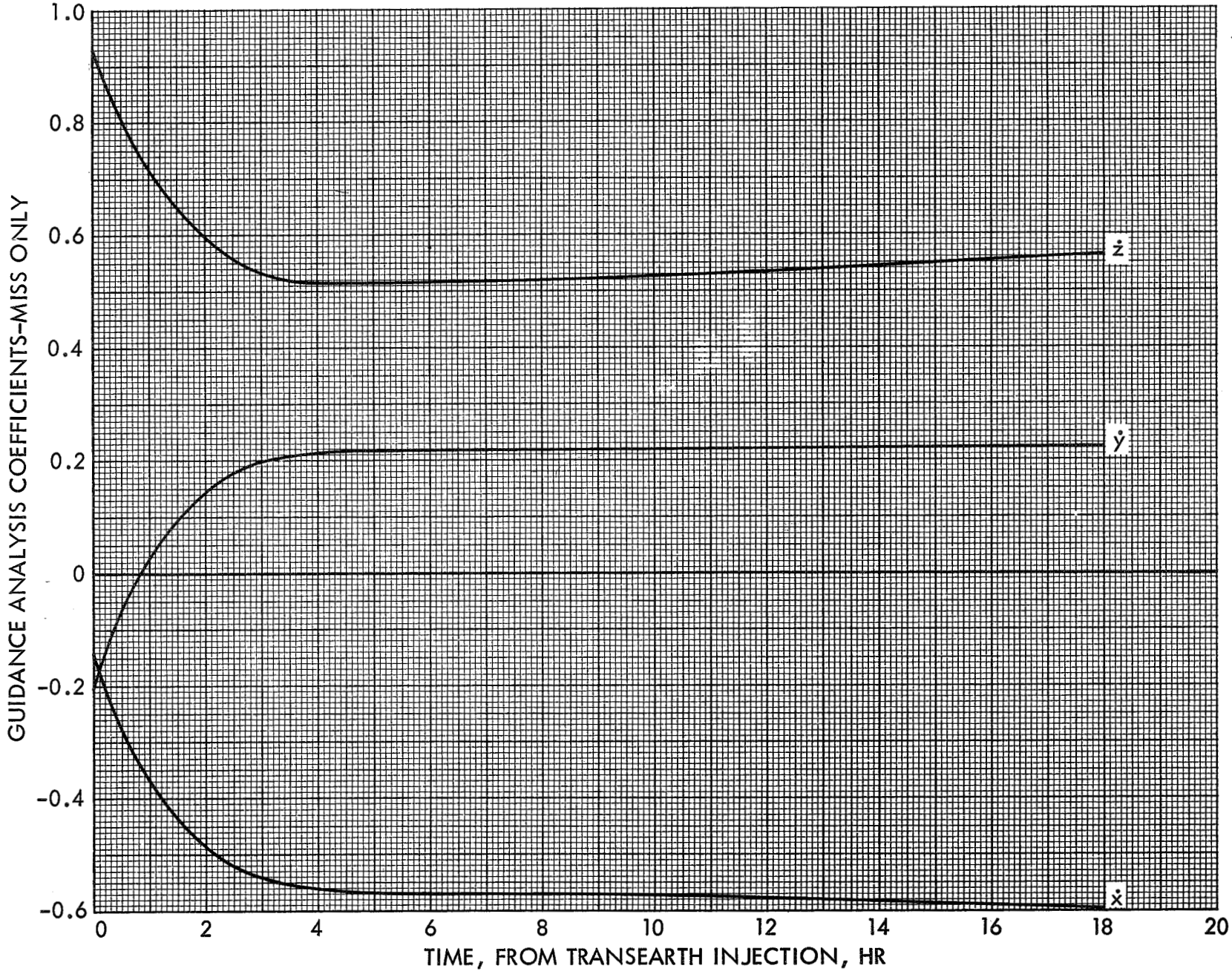

Figure 5.7-22f. Partials of the Z Component of Midcourse Velocity with Respect to the Injection Velocity Components

Table 5.8-I. Re-entry Phase - Discrete Events Summary

Time Since Liftoff (min)	Altitude (ft)	Longitude (deg E)	Latitude (deg N)	Velocity Relative to Air Mass (ft/sec)	Relative Flight Path Angle (deg)	Relative Azimuth (deg)	Sensed Acceleration (ft/sec^2)	Event
9787.95	400,000	100.541	-8.332	34966.98	96.62	128.38	0.00	Re-entry
9789.28	200,108	106.509	-12.910	31032.72	90.00	127.13	178.41	First advent of horizontal flight
9793.21	278,482	119.872	-21.896	22871.59	90.00	122.52	2.28	Second advent of horizontal flight
9797.67	130,032	134.328	-29.190	9390.53	96.69	112.11	235.54	Maximum acceleration

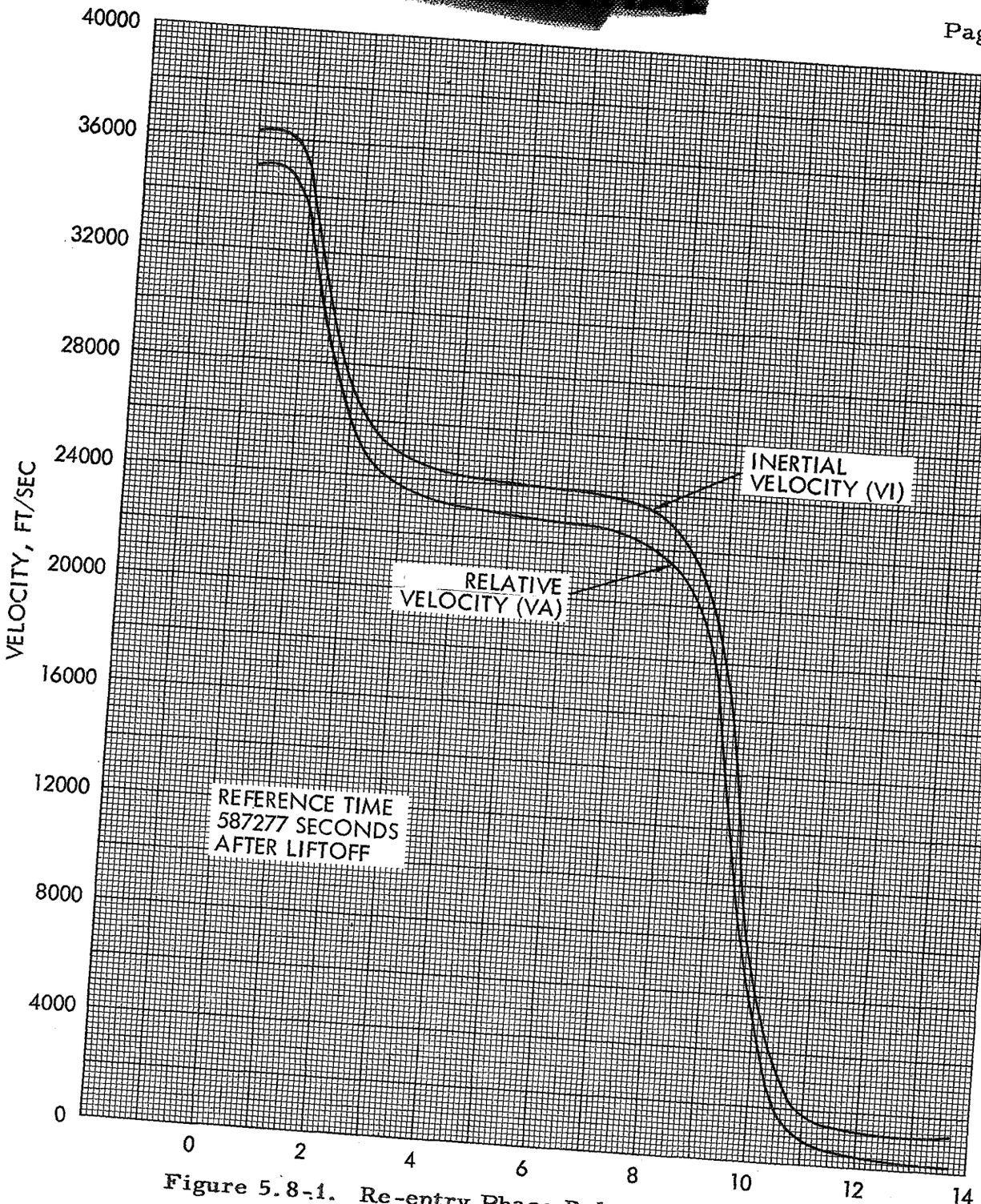

Figure 5.8-1. Re-entry Phase Relative (VA) and Inertial (VI) Velocity

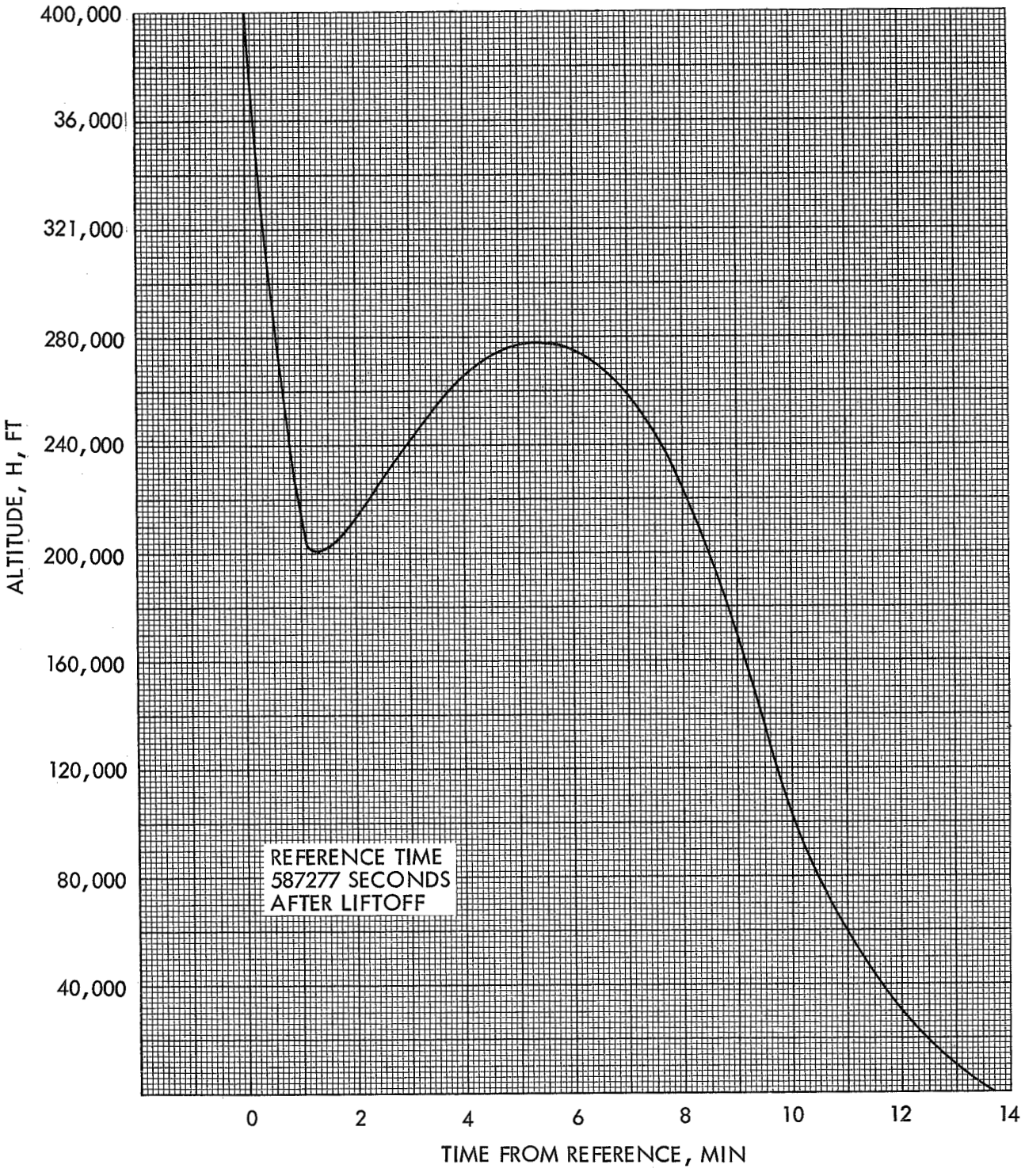

Figure 5.8-2. Re-entry Phase Altitude (H)

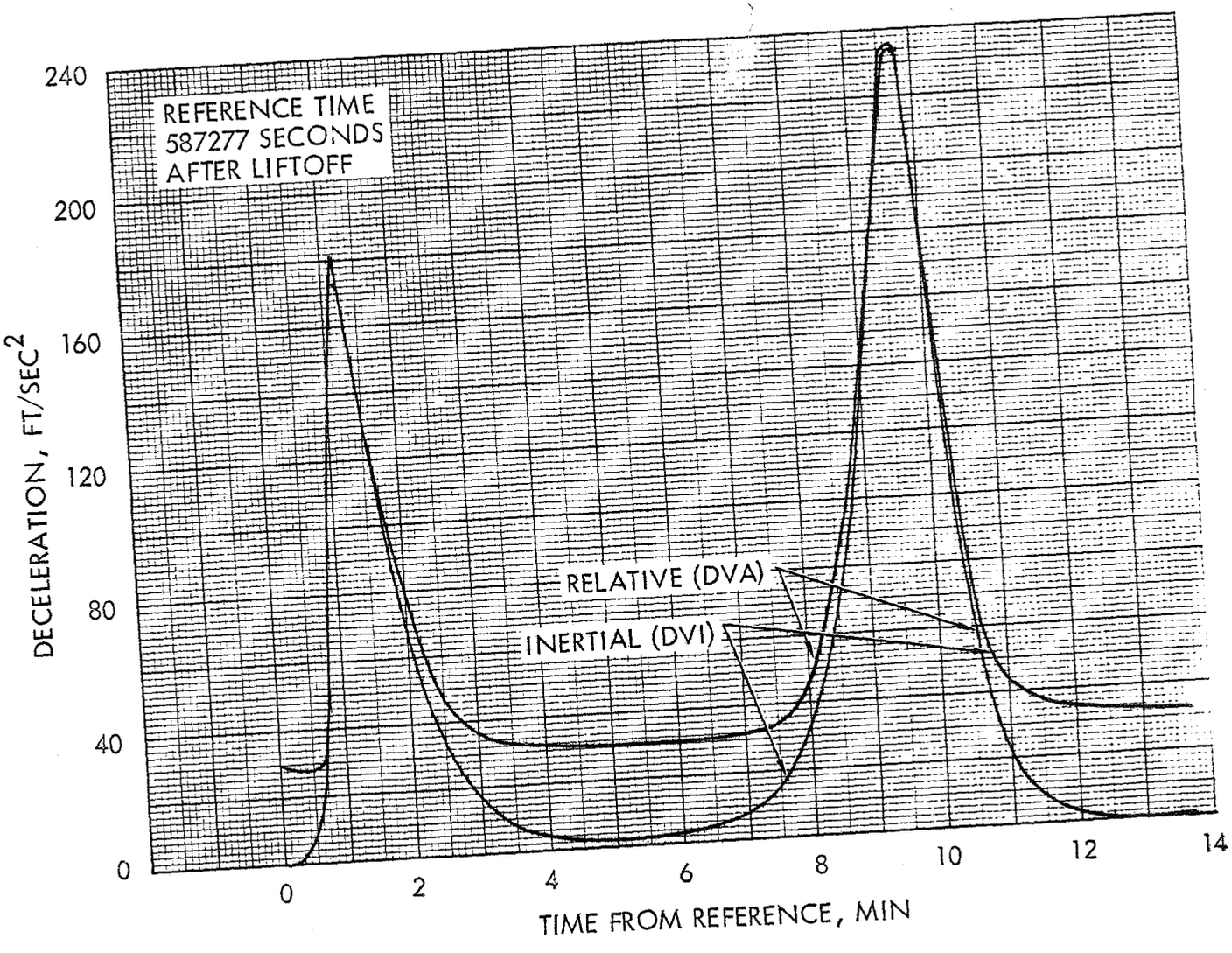

Figure 5.8-3. Re-entry Phase Relative (DVV) and Inertial (DVI) Deceleration

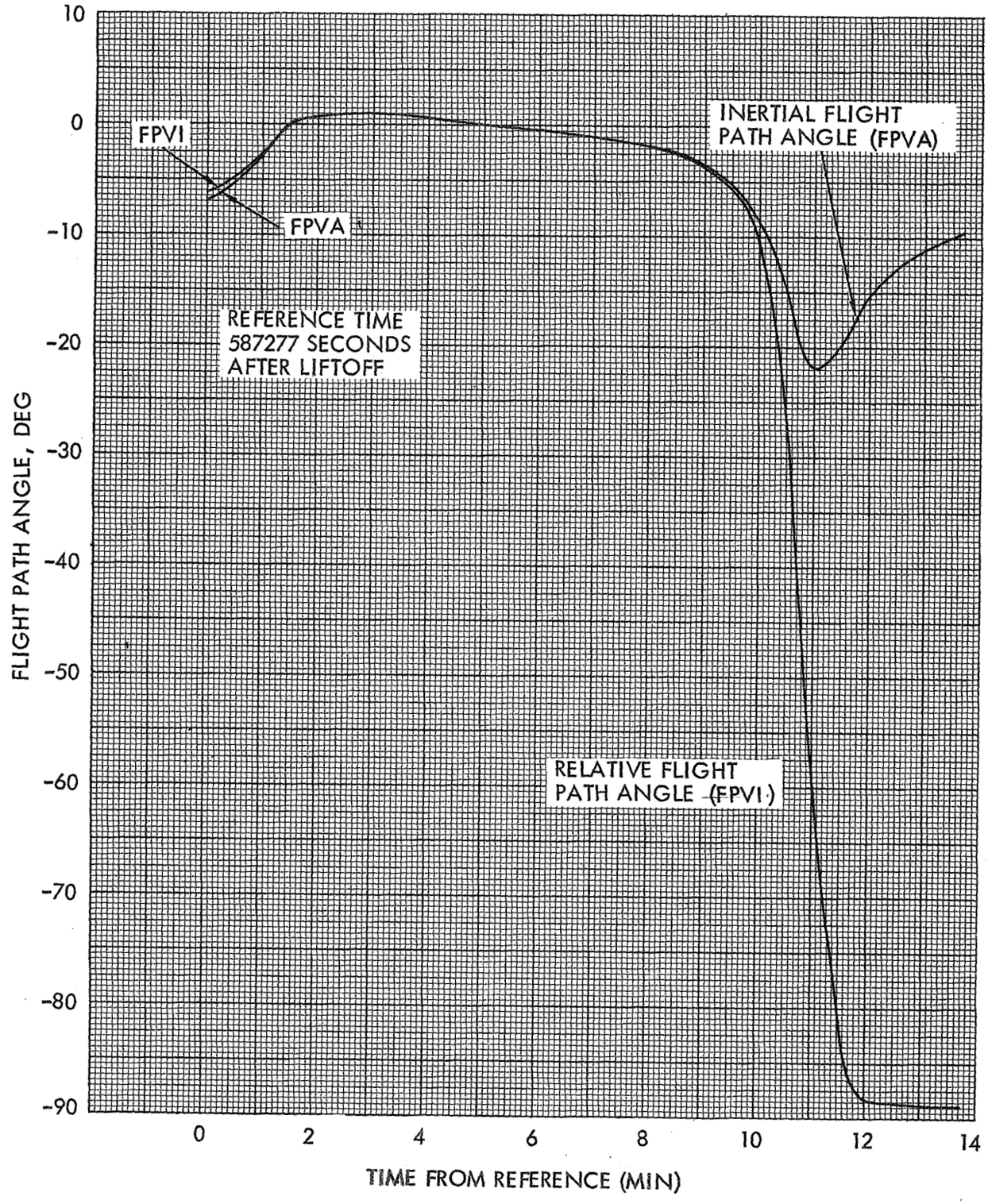

Figure 5.8-4. Re-entry Phase Relative (GMMA) and Inertial (GMMI) Flight Path Angle

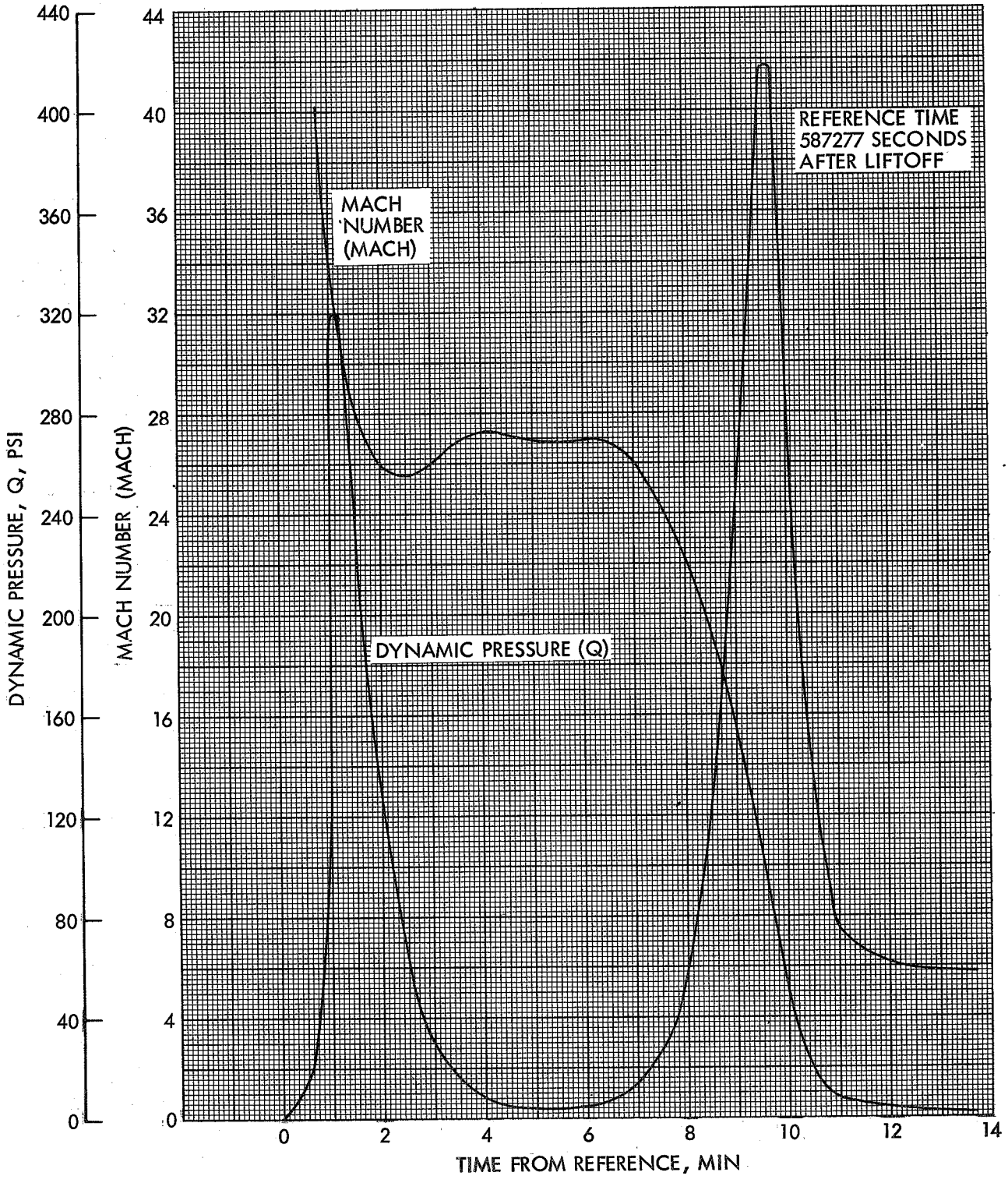

Figure 5.8-5. Re-entry Phase Dynamic Pressure (Q) and Mach Number (M)

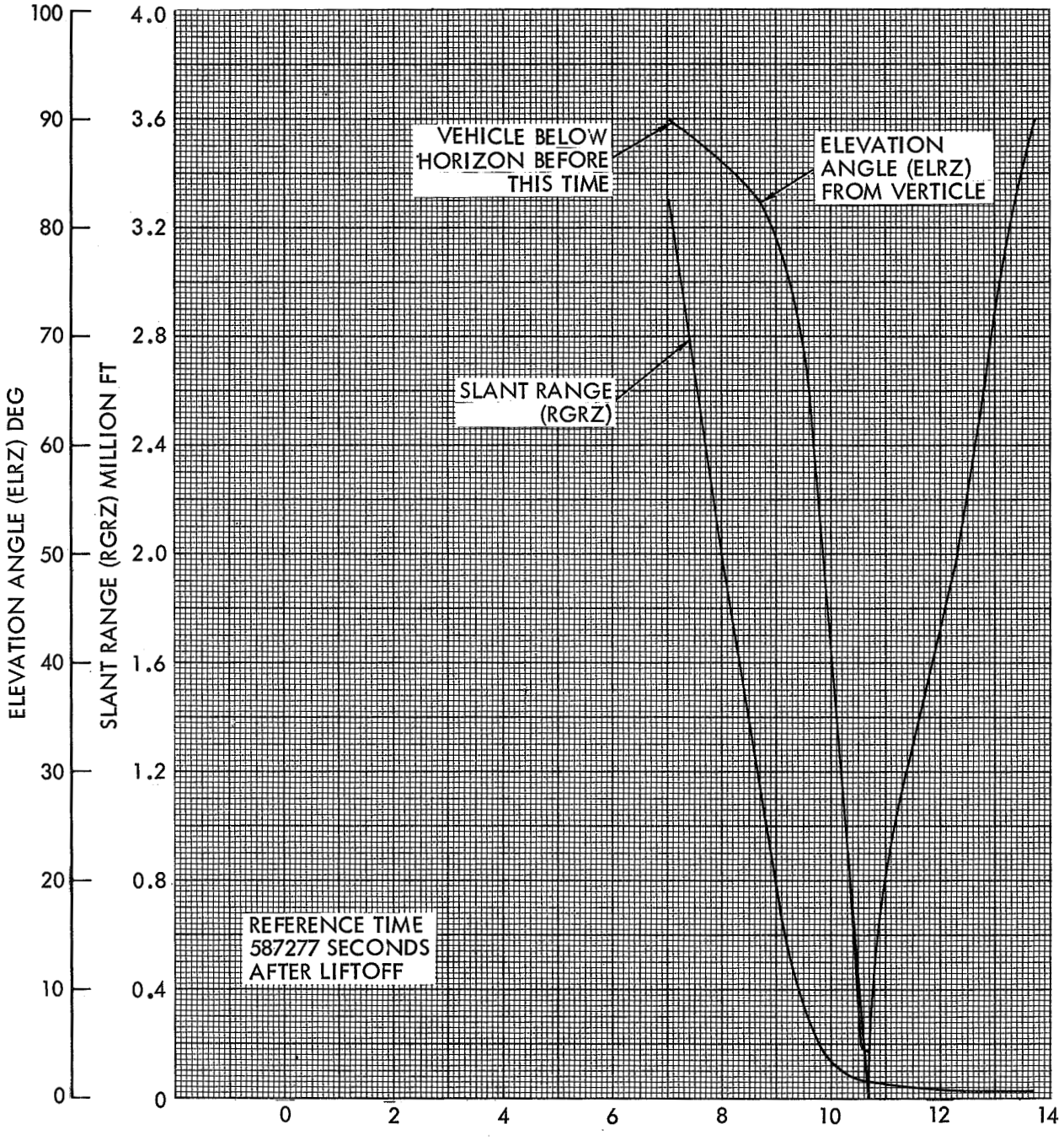

Figure 5.8-6. Re-entry Phase Slant Range (RGRZ) and Elevation Angle (ELZR) from Landing Site

6.0 Launch Windows and Vehicle Performance Studies

6.1 Introduction

In the days prior to computation of the reference trajectory, a thorough study was made to (1) analytically determine the kinds of free return trajectories available for choice, (2) determine the implications of free return on spacecraft performance required to land and depart from a specified lunar landing site, returning to a specified earth landing site, (3) weigh the alternatives and choose a reference trajectory, (4) optimize the Saturn V and spacecraft powered flight operations, (5) analyse the dynamics of re-entry from a near-parabolic approach trajectory.

The mission analysis work described in the subsections below, is addressed to these problems, and insofar as possible, definite results have been obtained covering all phases of an Apollo lunar orbit rendezvous mission. The analysis was bounded by a specification of a launch week (January 28 - February 3, 1968) and that the uncorrected translunar trajectory, after circumnavigating the moon, return to earth with acceptable re-entry conditions. Within this framework, most of the quantitative relationships among the geometrical and vehicle performance parameters have been obtained. Paragraph 6.2 deals with the earth launch conditions necessary to produce free return and derives a gross launch window duration. Paragraph 6.3 analyzes the lunar landing, LOR, and constrained return problems, taking as the point of departure, the hyperbolic lunar approach geometries produced by free return outbound trajectories. Particular attention is given to the problem of landing at a prescribed, non-equatorial site. Paragraph 6.4 describes all the vehicle and spacecraft powered flight optimization work which provided the basis for choosing a set of reference trajectory conditions acceptable to the system performance capability. Paragraph 6.5 combines the geometrical problems with powered flight performance to illustrate the effects on the launch windows available during the given launch week. Finally, paragraph 6.6 describes the parametric analysis of the re-entry problem. Of particular interest here is the method of treatment and the dynamical sensitivities derived therefrom.

6.2 Free Return Launch Opportunities

A free flight circumlunar trajectory is defined (for the purposes of this problem) to be one which requires no midcourse thrust from the time it leaves earth parking orbit until the time it returns to a specific re-entry condition at the earth. The number of such trajectories is restricted if launch is from a specific site through a limited range of launch azimuths, with fixed pericynthion distance and re-entry conditions. The general class of free return trajectories for the specified launch dates will provide all of the launch opportunities in the gross launch window. Return to earth in this case, is not restricted to any particular site.

The geometry of the problem is shown in Figure 6.2-1. The variables in the geometry are the lunar declination and distance shown in Figures 6.2-2 and 6.2-3, respectively. The constraints on earth departure are the launch azimuth, ranging from 72 to 108 degrees, the time in parking orbit of from 1.5 to 2.5 revolutions and the outward trip time (injection to pericynthion) of about 72 hours consistent with a free return, and an 80 nautical mile pericynthion altitude.

A launch opportunity occurs twice each day in the lunar month. The days eliminated from further consideration are those on which the landing site is in sunshine. The two daily launch opportunities correspond to short and long coast parking orbits. In the week of January 28 to February 3, 1962, the launch opportunity associated with type 5 trajectories, the short coast with 1.5 revolutions in the parking orbit, occurs late in the day. The type 6 long coast trajectories with two revolutions in the parking orbit, occur early in the day.

The type 6 trajectories, lying nearly in the lunar plane, are inclined at about 7 degrees for launch azimuths of 72 and 108 degrees and decrease to one-half a degree at 90 degrees while the type 5 trajectories are inclined from 40 to 60 degrees to the lunar plane throughout the entire launch period.

If the mission is analyzed by phases, the following results will completely describe the geometry, energies and times involved. In Figures 6.2-4 and 6.2-5 the liftoff time of day is given for the range of launch azimuths for each day of the specified week. These are for type 5 and 6 respectively.

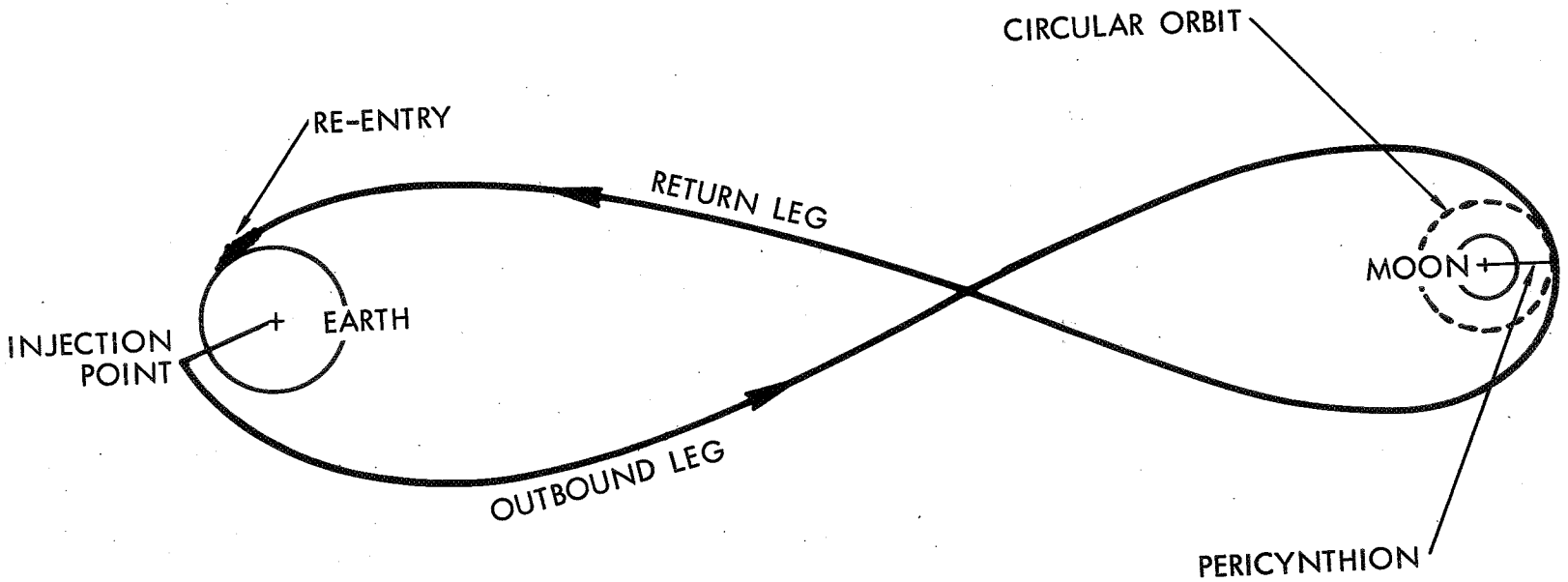

Figure 6.2-1. Geometry of the Free Return Trajectory

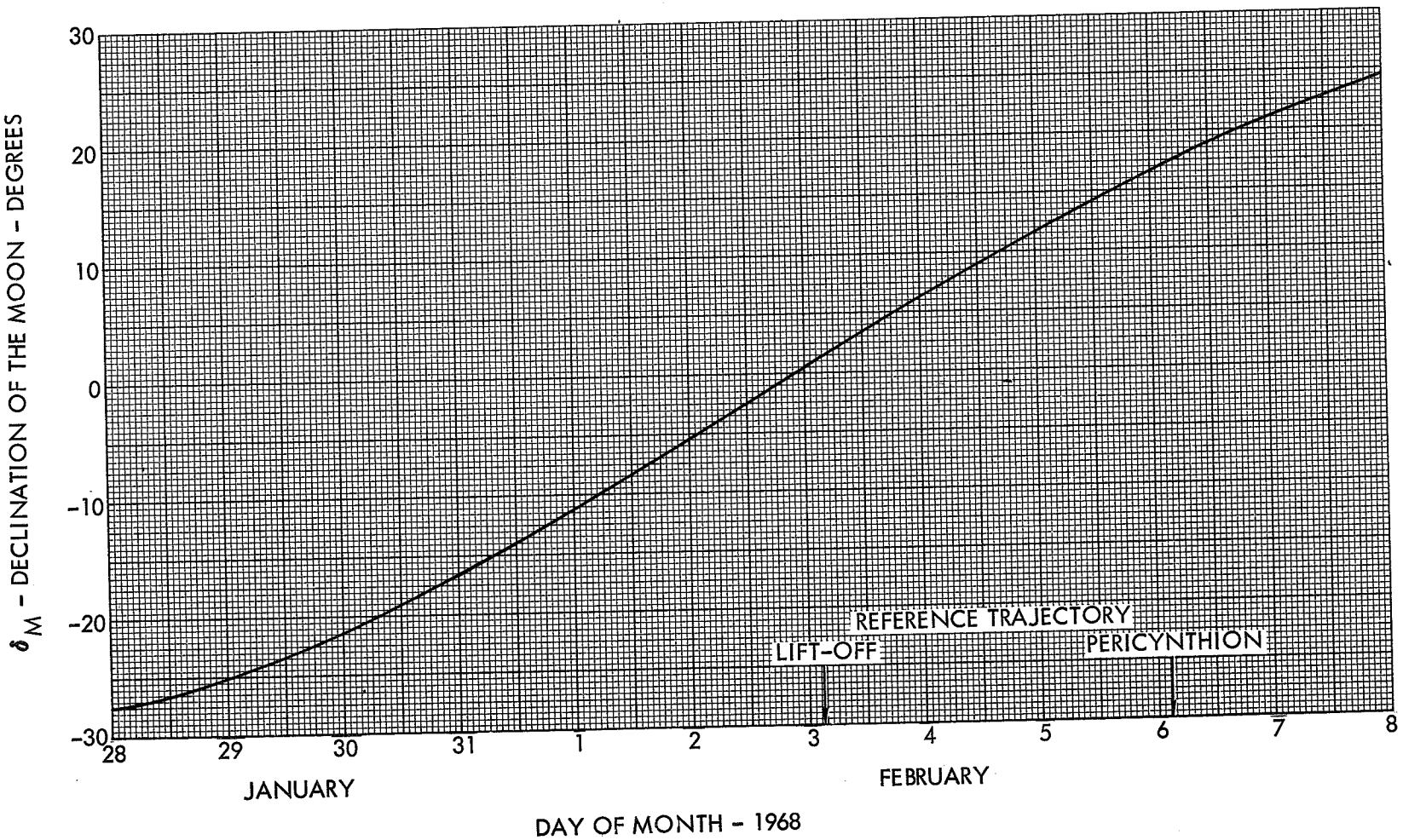

Figure 6.2-2. Lunar Declination During Issue 1 Analysis

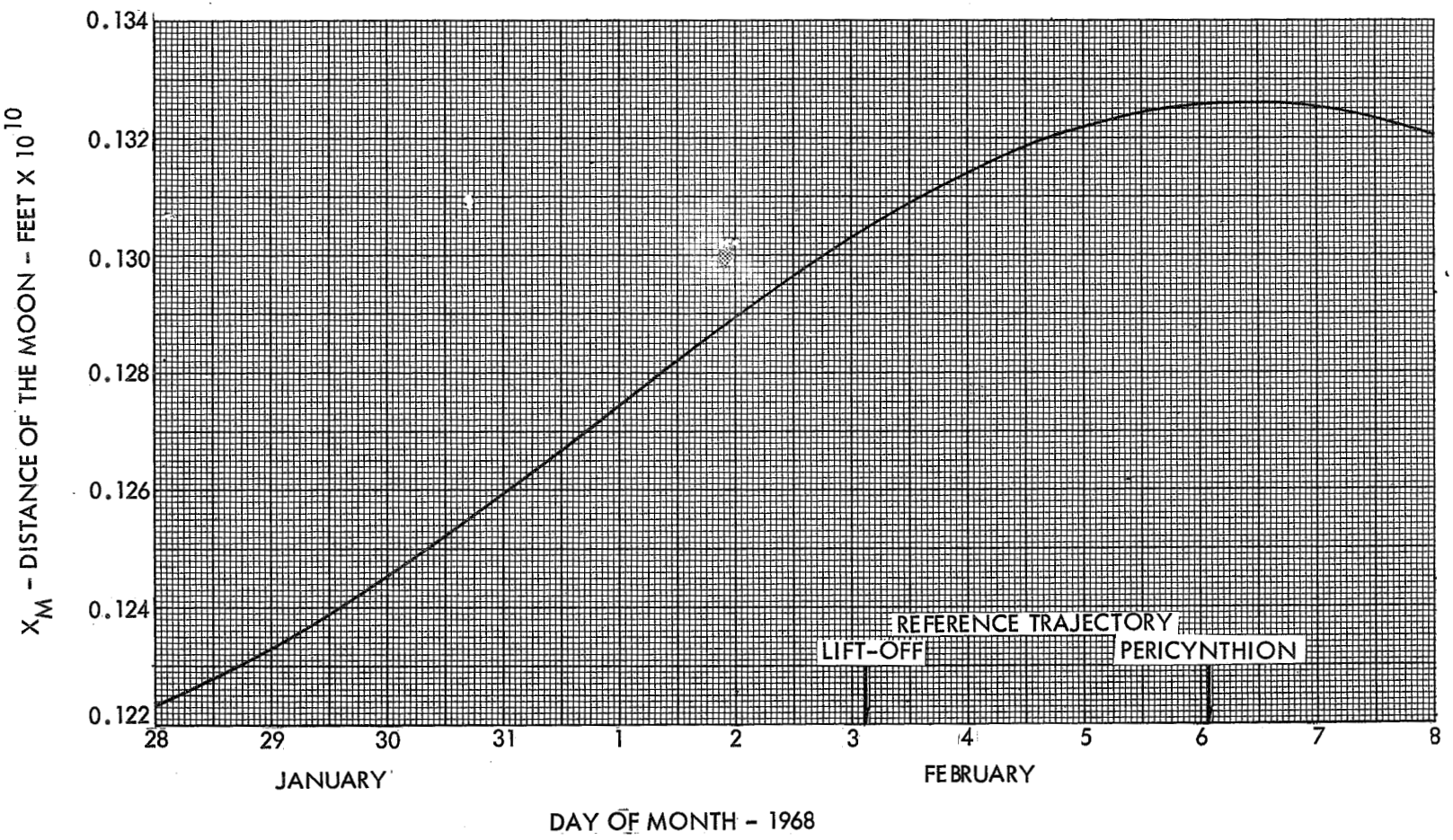

Figure 6.2-3. Lunar Distance During Issue 1 Analysis

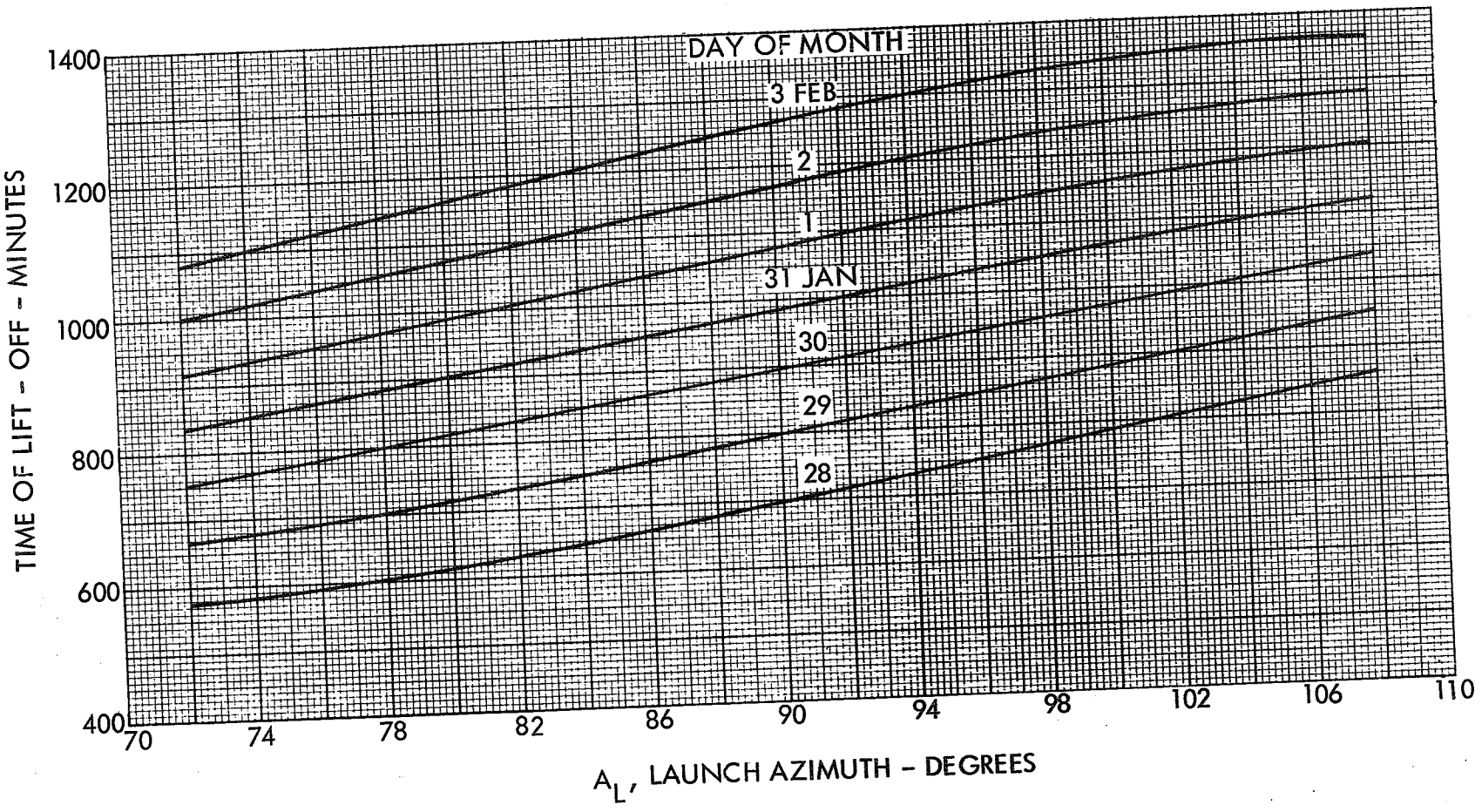

Figure 6.2-4. Liftoff Time versus Launch Azimuth for Short Coast, Type 5

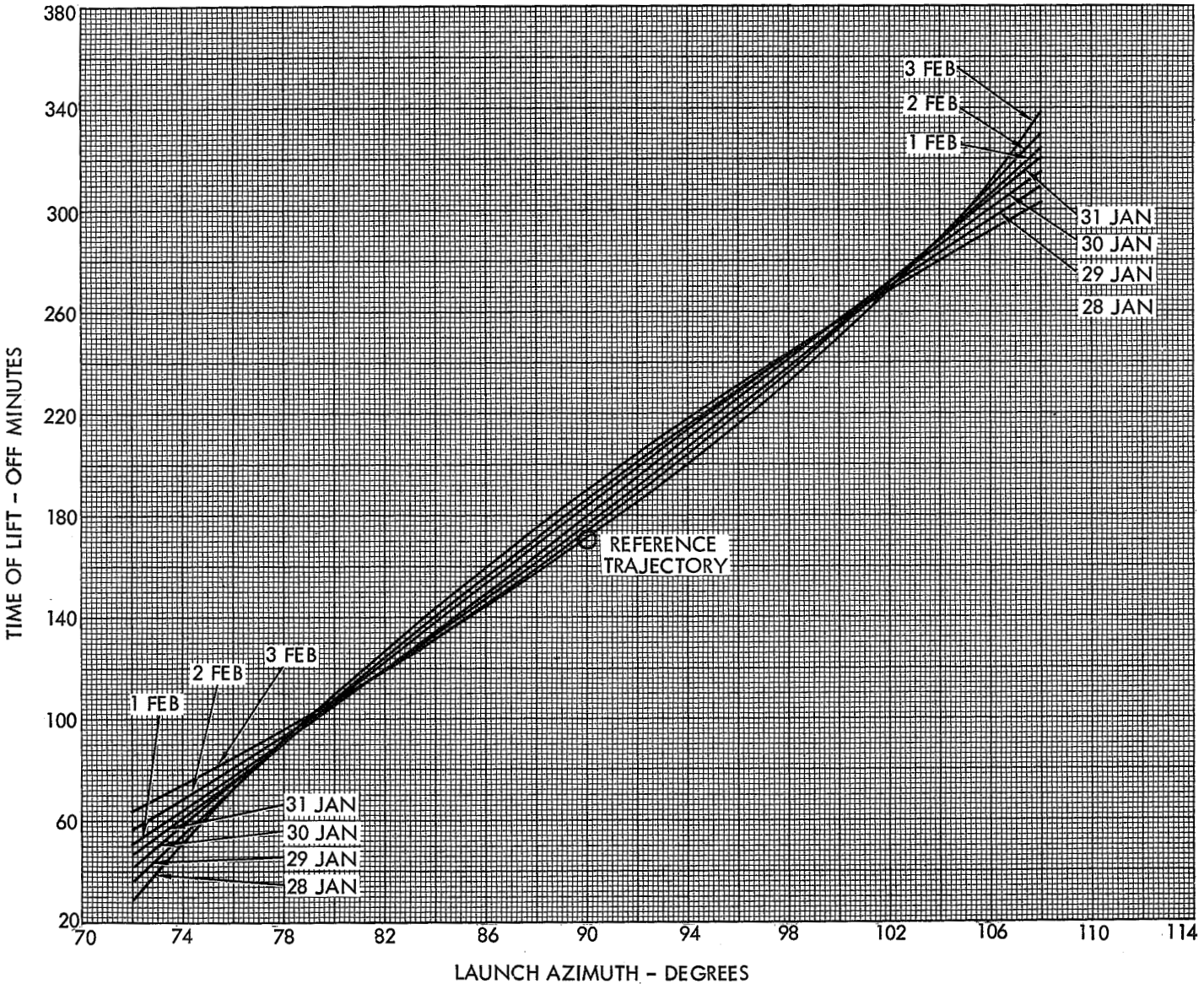

Figure 6.2-5. Liftoff Time versus Launch Azimuth for Long Coast, Type 6

The type 6 displays a peculiar characteristic in the liftoff time at an azimuth of 90 degrees. The liftoff time regresses on itself as the lunar month progresses. This is due to the in-plane launch and the geometrical coincidence of lunar inclination with the latitude of the launch site. The type 5 which provides the second window (occurring later) during each day has a smooth family of liftoff times.

In Figures 6.2-6 and 6.2-7 the injection time as a function of launch azimuth is plotted for type 5 and 6 trajectories. Here the same general trend is apparent in the figures and the difference in the time of injection minus the time of liftoff and the time of powered flight gives coast time, which can be translated into angular distance traveled by multiplying the time by 4.086 degrees per minute. These data were generated for a return inclination with respect to earth's equator of 35 degrees. There is a variance in both liftoff and injection time which is a function of the return inclination. This is small, varying about 2.5 minutes as the return inclination is varied from +90 to -90 for launch azimuths of 72 to 108 degrees. The variance drops to 1.5 minutes for launch azimuths of 90 degrees.

The return inclination, i_r, used here is inclined at 90 degrees or less to the earth's equator. That is, free return trajectories which return retrograde relative to the earth were not considered. The positive and negative signs affixed to this inclination refer to the mode of departure from the moon. Positive leaves the moon ascending with respect to equator and the negative is descending with respect to equator. Arrival at the earth is influenced by the declination of the moon at departure as to whether the approach is toward the ascending or descending node. When the moon has a positive declination, return is to the southern hemisphere. The approach to the landing site is northerly with a positive i_r and southerly with a negative i_r. When the moon is at negative declination return is to the northern hemisphere and the sign conventions hold for the approaches to the landing site.

The velocity required at injection is a function of the trip time, as shown on Figures 6.2-8 and 6.2-9. The trip time increases from day to day with a constant injection velocity because the lunar distance is increasing as previously shown in Figure 6.2-3. The outward trip time is also a function of

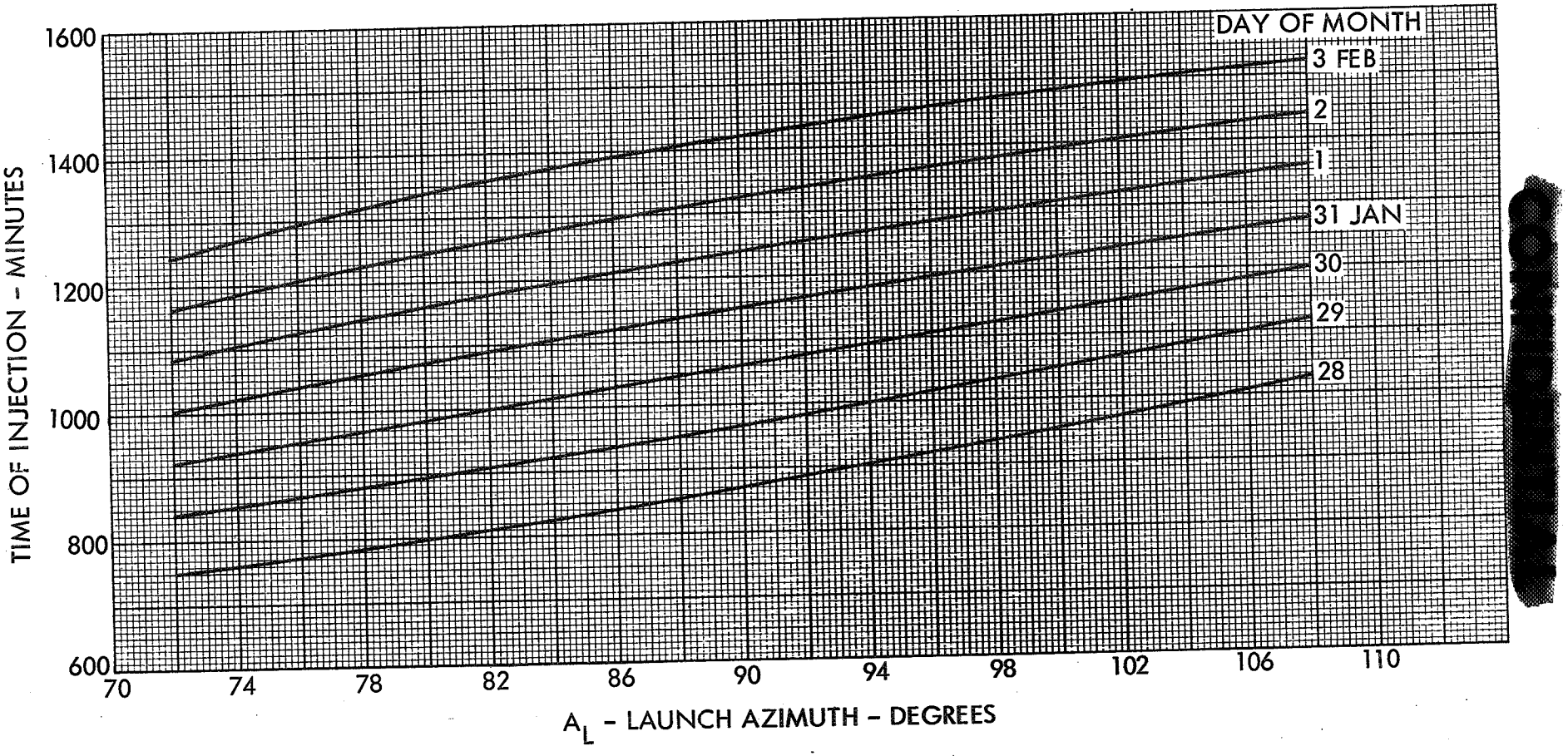

Figure 6.2-6. Injection Time versus Launch Azimuth for Short Coast, Type 5

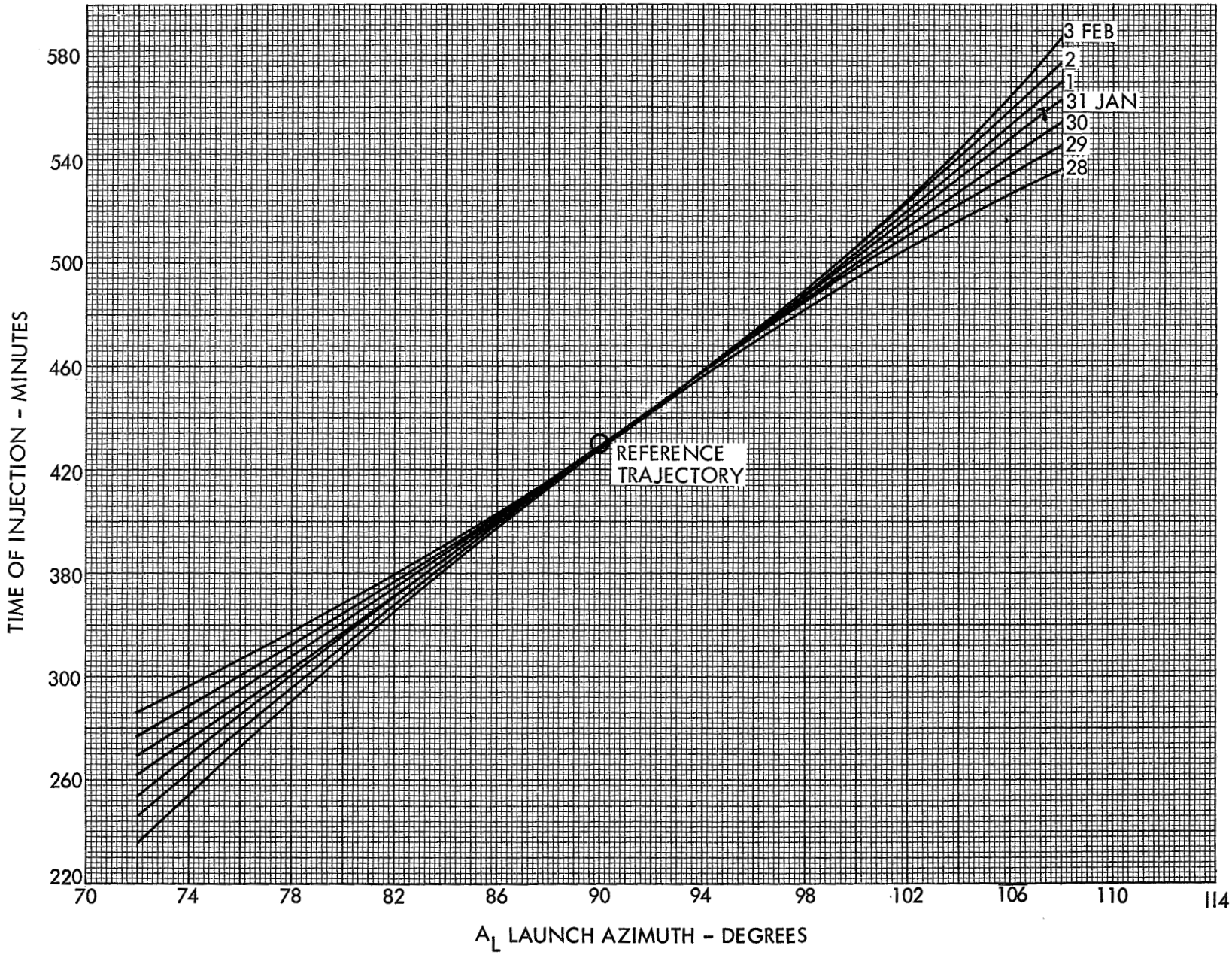

Figure 6.2-7. Injection Time versus Launch Azimuth for Long Coast, Type 6

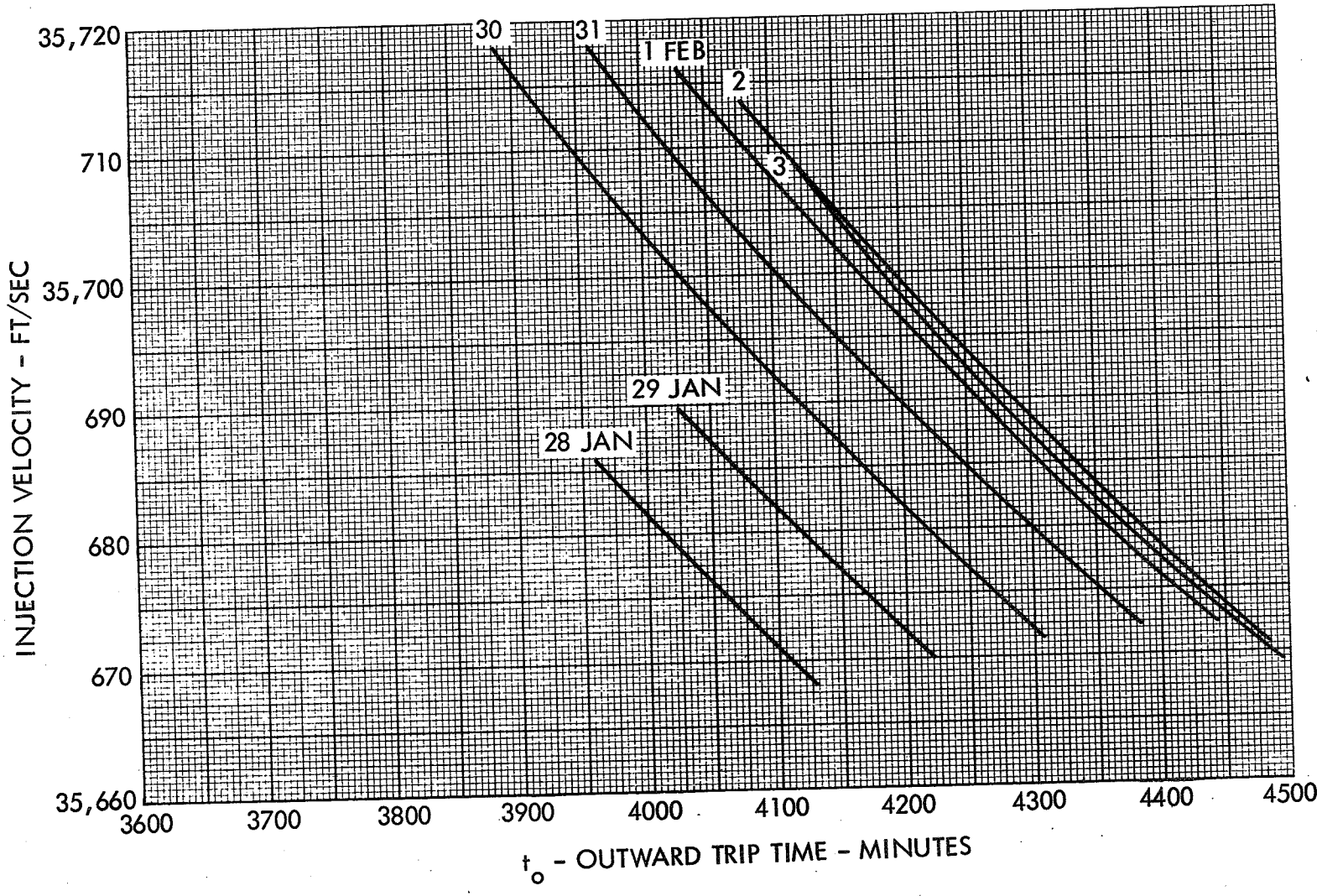

Figure 6.2-8. Injection Velocity versus Outward Trip Time for Short Coast, Type 5

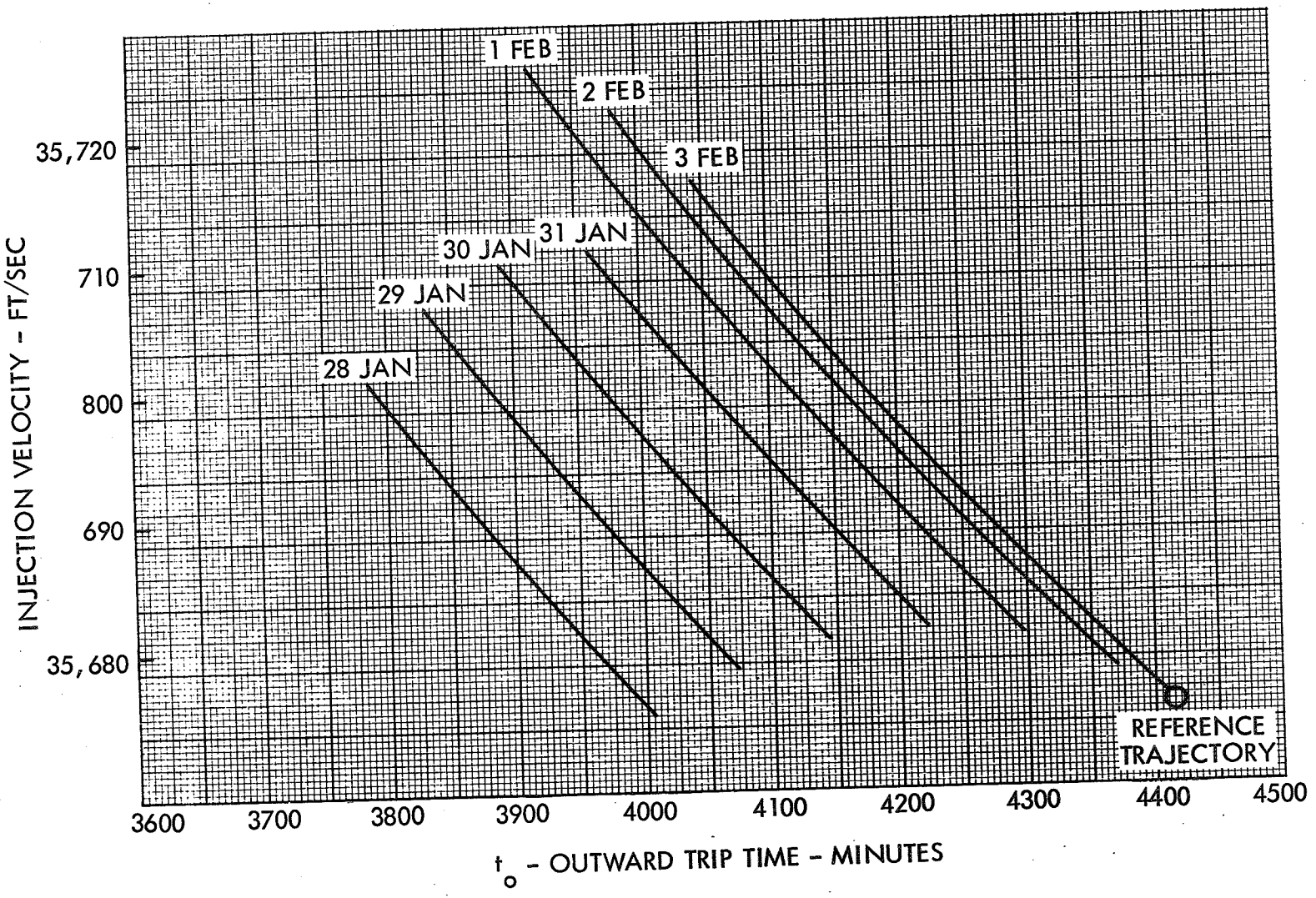

Figure 6.2-9. Injection Velocity versus Outward Trip Time for Long Coast, Type 6

the return inclination as Figures 6.2-10 and 6.2-11 indicate. These curves are true for the range of launch azimuths, the variance in trip time due to azimuth increases from 6 to 14 minutes through the launch window (being 14 the last 4 days). The curves were plotted for a 90 degree azimuth. At 72 degrees, trip time drops by one third of the variance, and at 108 degrees the time is greater by two thirds of the variance. For example (Figure 6.2-11) on the 29 January for a return inclination of -35 degrees read trip time, t_o, of 3938 minutes, the estimated variance is 9 minutes and at 72 degrees azimuth t_o would be 3935 minutes and at 108 degrees it would then be 3944 minutes. However, this difference may be ignored with no loss in application of the results.

The uncorrected moon phase conditions are displayed in the next six figures. The inclination to the lunar equator as a function of outward trip time is shown in Figures 6.2-12 and 6.2-13, for type 5 and 6 trajectories, respectively. These plots contain a single line for each day representing a constant azimuth of 90 degrees. In fact there is a band above this line about 1 degree higher which encompasses the launch azimuth range. The 108 degree azimuth provides this lower inclination and is the upper bound. If a launch azimuth of 90 degrees provides the highest inclination on a given day, using 90 degrees in the analysis will assure that all other azimuths will be expensive in terms of corrective velocity at the moon and in this way the length of the entire daily window is maintained. However, if the inclination desired has a higher value this is no longer true.

Similarly the longitude of the ascending node versus outward trip time is shown for a 90 degree azimuth for all days in the window. The combination of inclination and node location is significant when selecting a landing site or investigating a mission for a preselected site as will be shown in Section 6.3. Another important parameter is the latitude of the pericynthion where hyperbolic deboost will occur. This location affects the ability to move the node and/or change the orbit inclination during deboost.

Latitude of pericynthion is given in Figures 6.2-16 and 6.2-17 for an azimuth of 90 degrees. The longitude of pericynthion is always near 180 degrees increasing to a maximum of 190 degrees when the return inclination approached ±90 degrees.

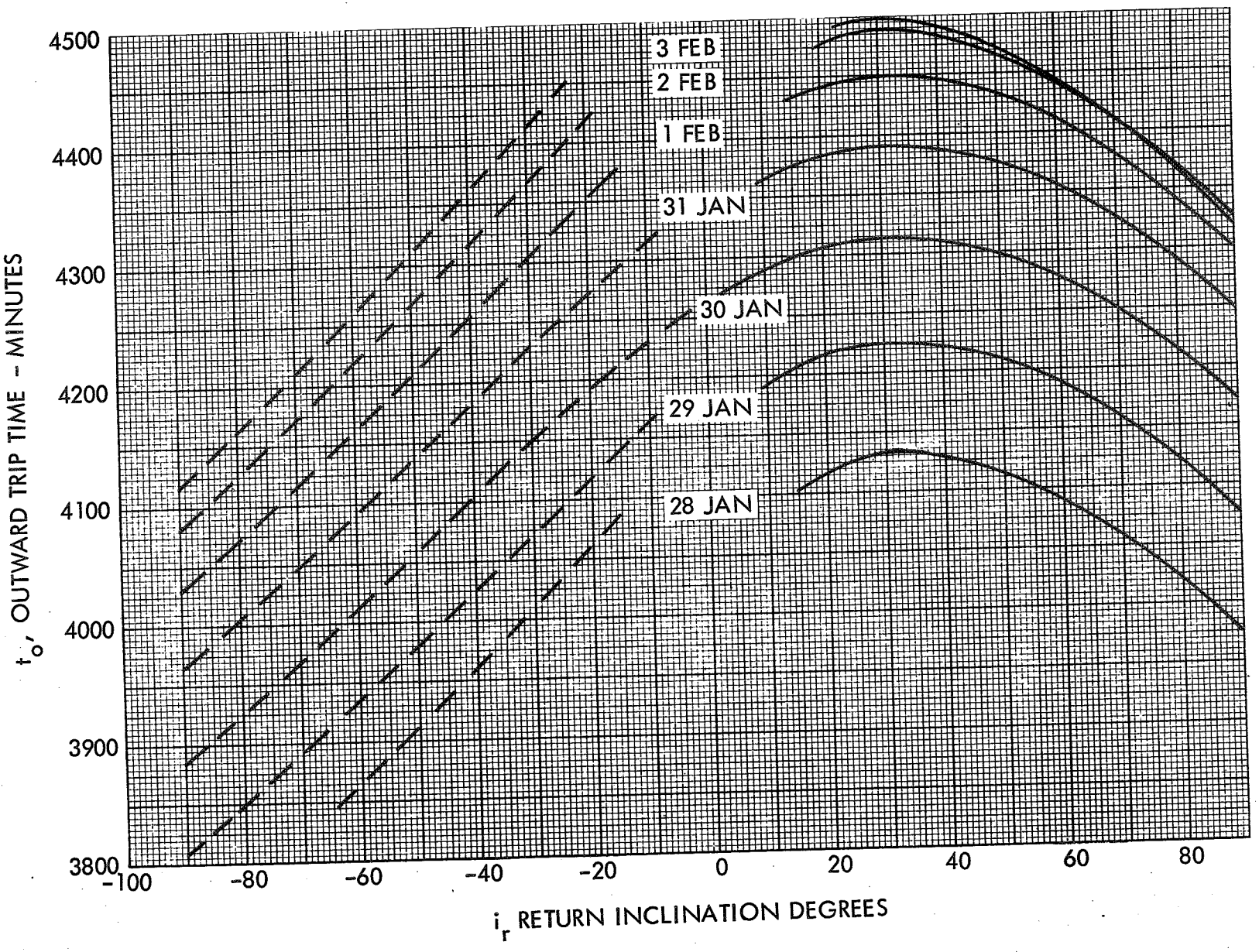

Figure 6.2-10. Outward Trip Time versus Return Inclination for Short Coast, Type 5

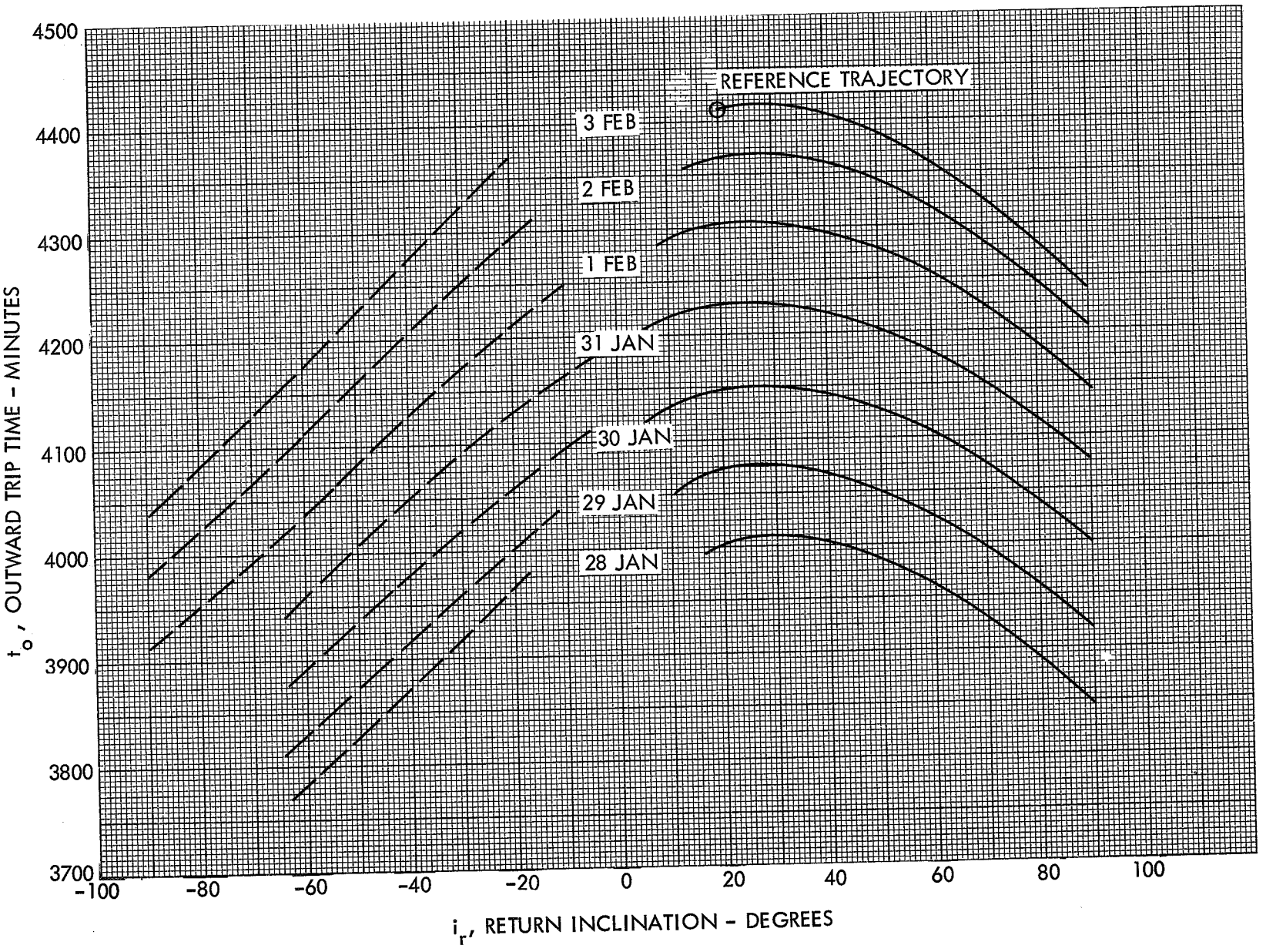

Figure 6.2-11. Outward Trip Time versus Return Inclination for Long Coast, Type 6

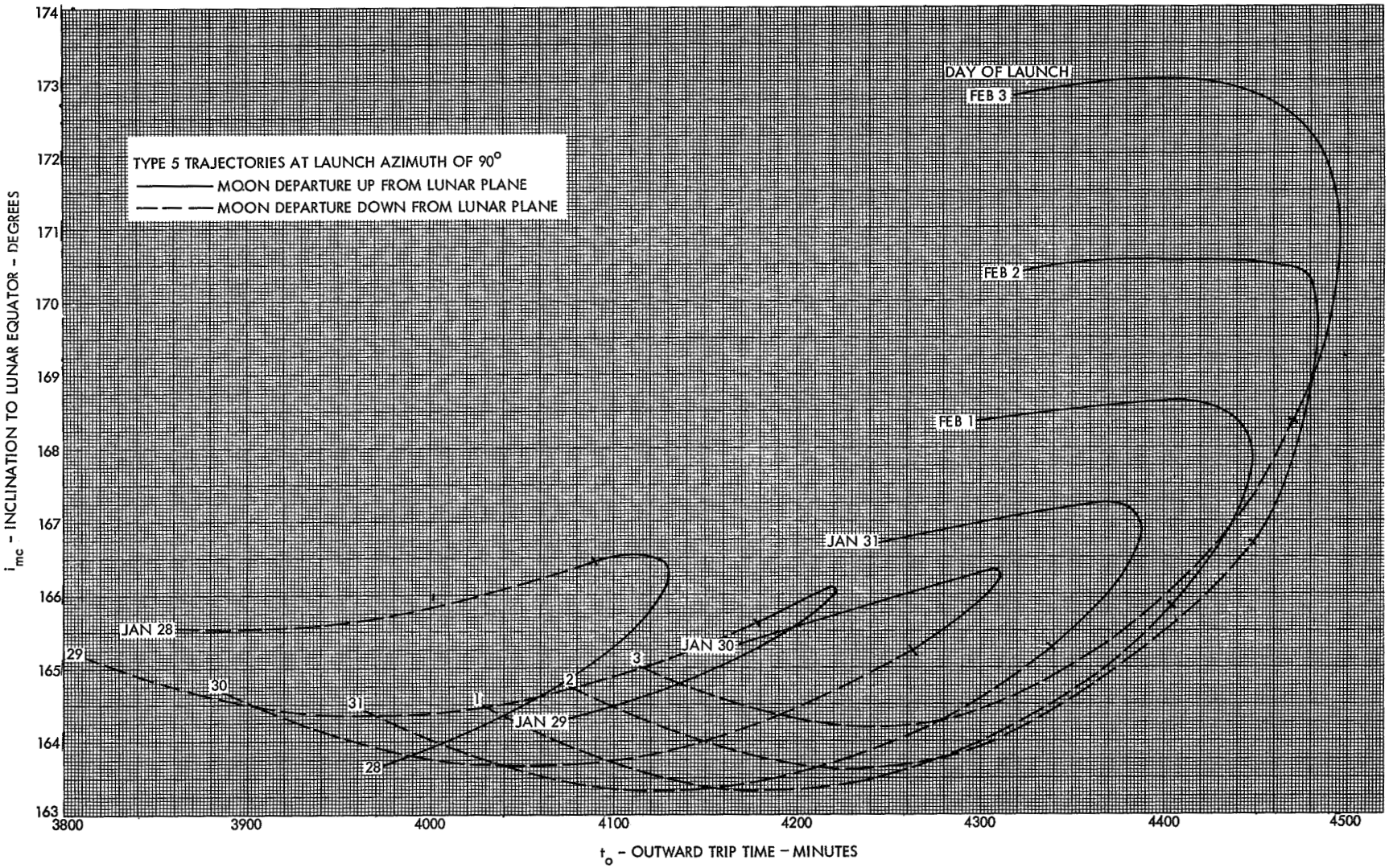

Figure 6.2-12. Lunar Phase Geometry – Inclination versus Trip Time, Short Coast

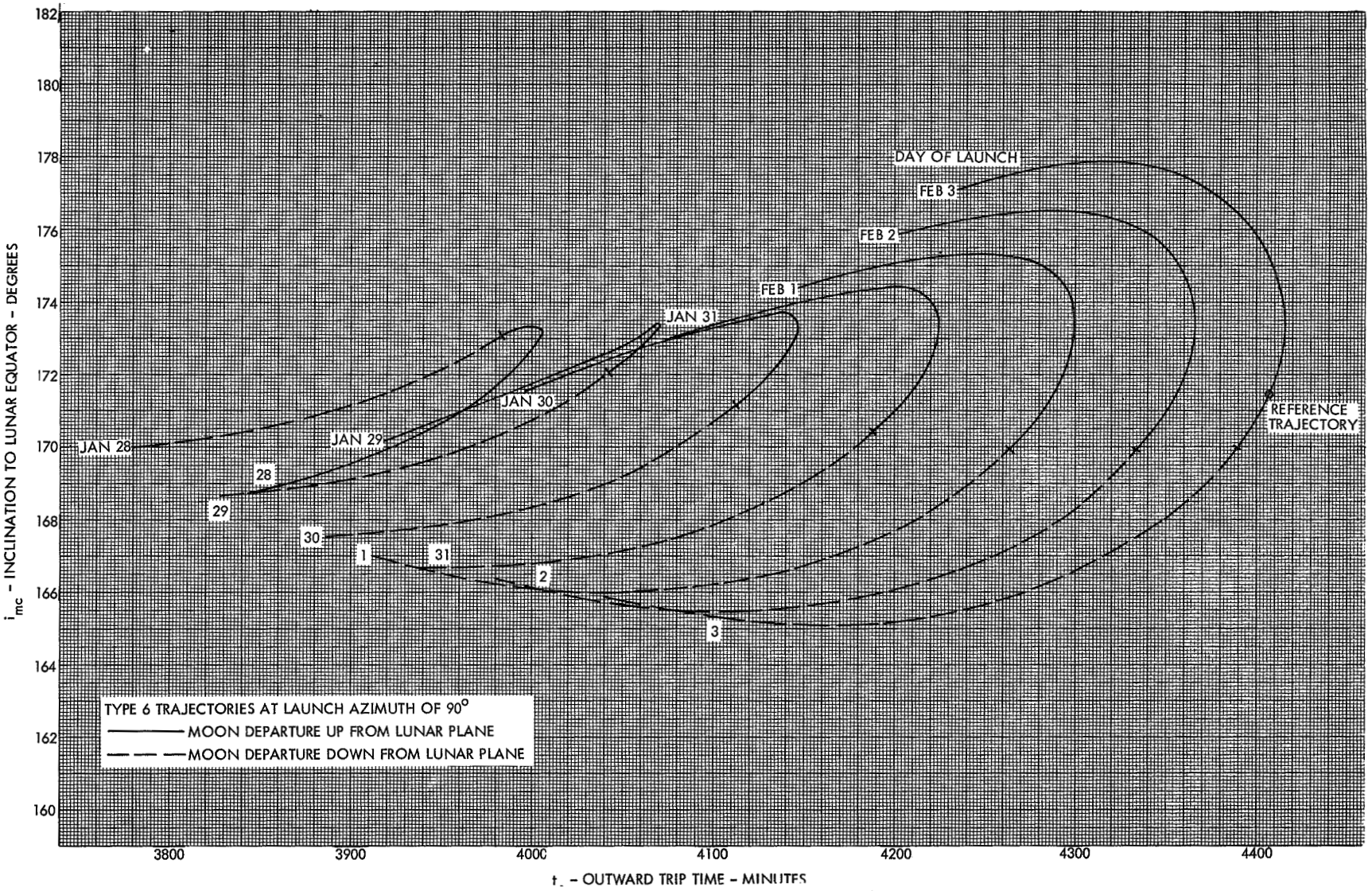

Figure 6.2-13. Lunar Phase Geometry – Inclination versus Trip Time, Long Coast

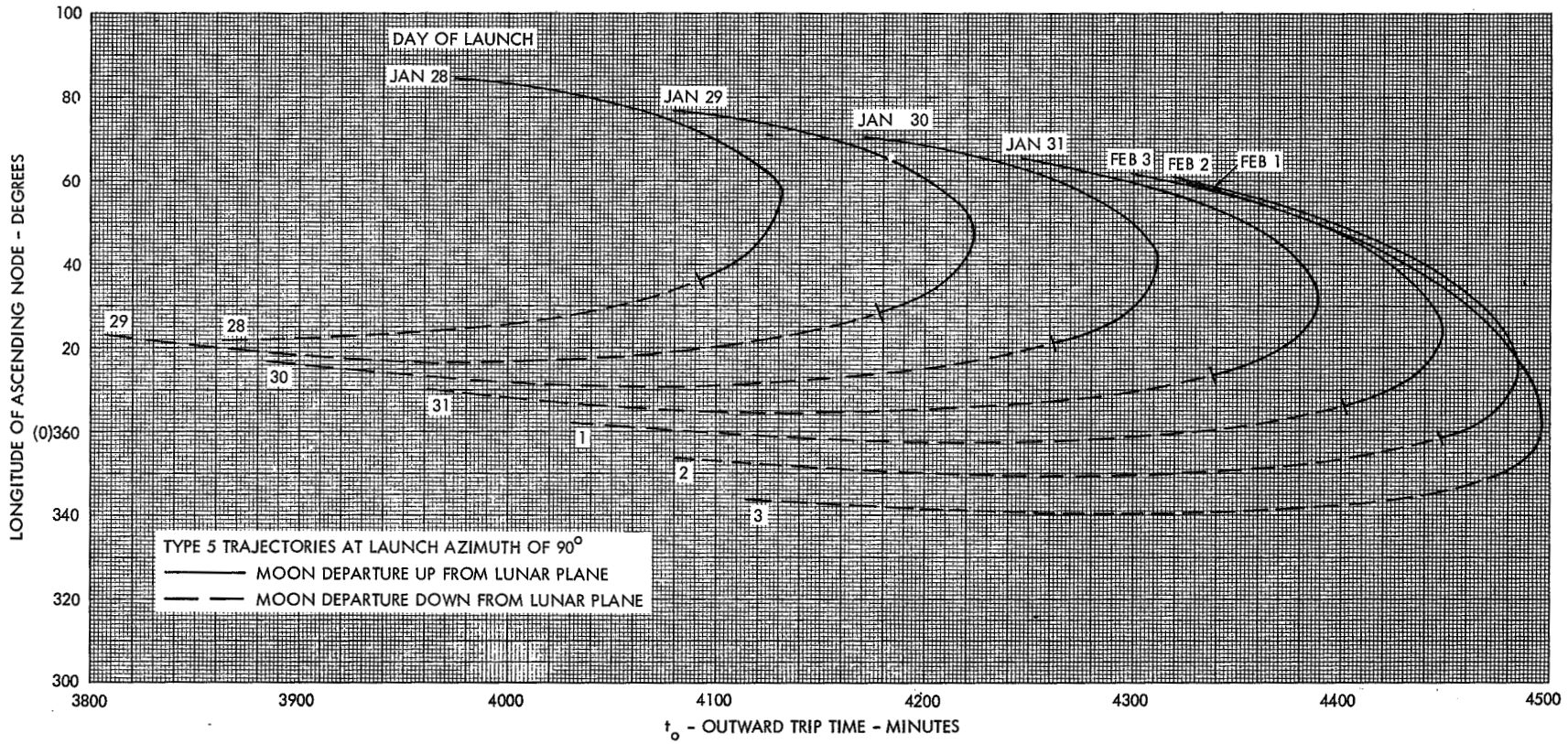

Figure 6.2-14. Lunar Phase Geometry – Longitude of Ascending Node versus Trip Time, Short Coast

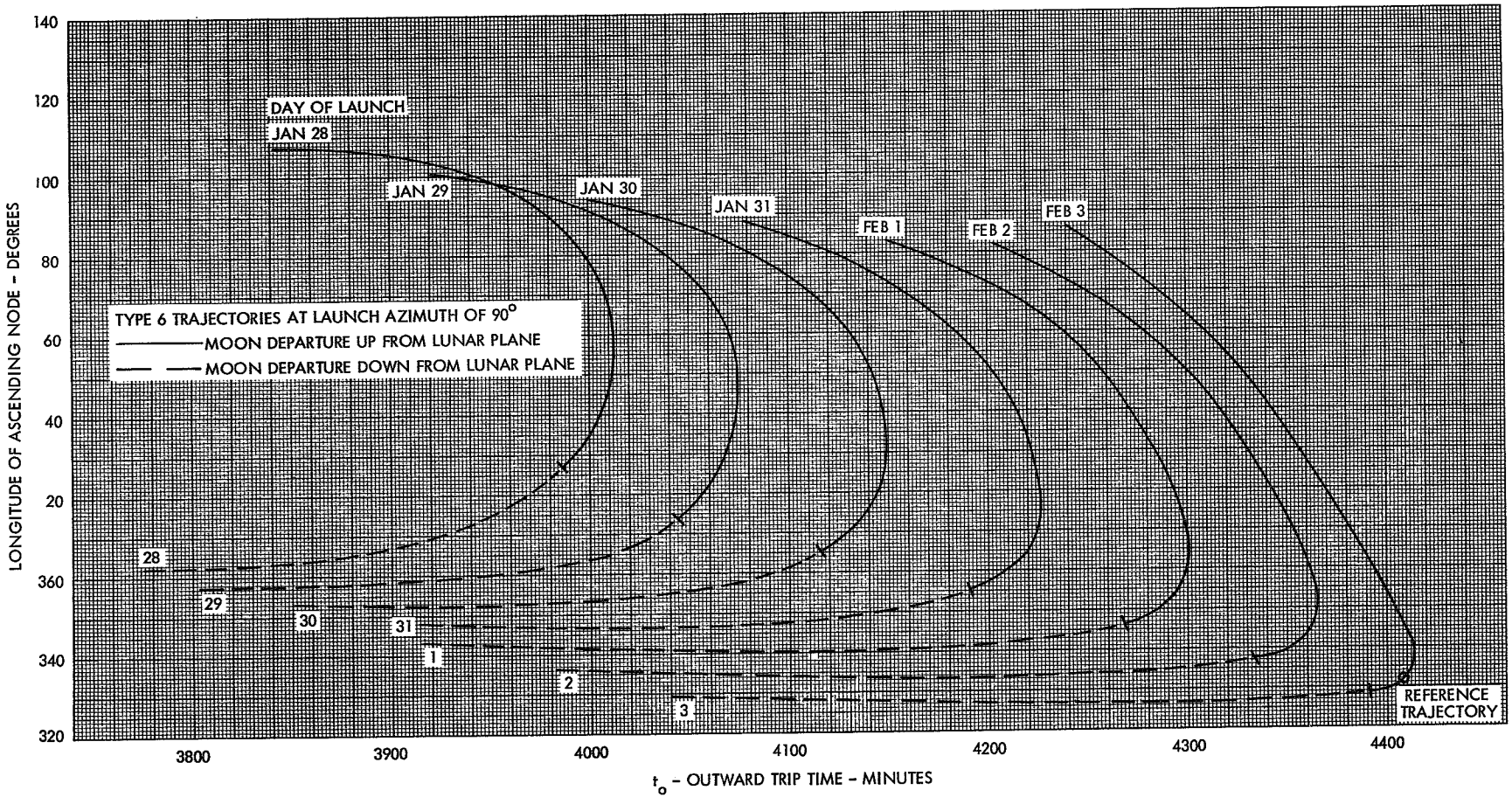

Figure 6.2-15. Lunar Phase Geometry – Longitude of Ascending Node versus Trip Time, Long Coast

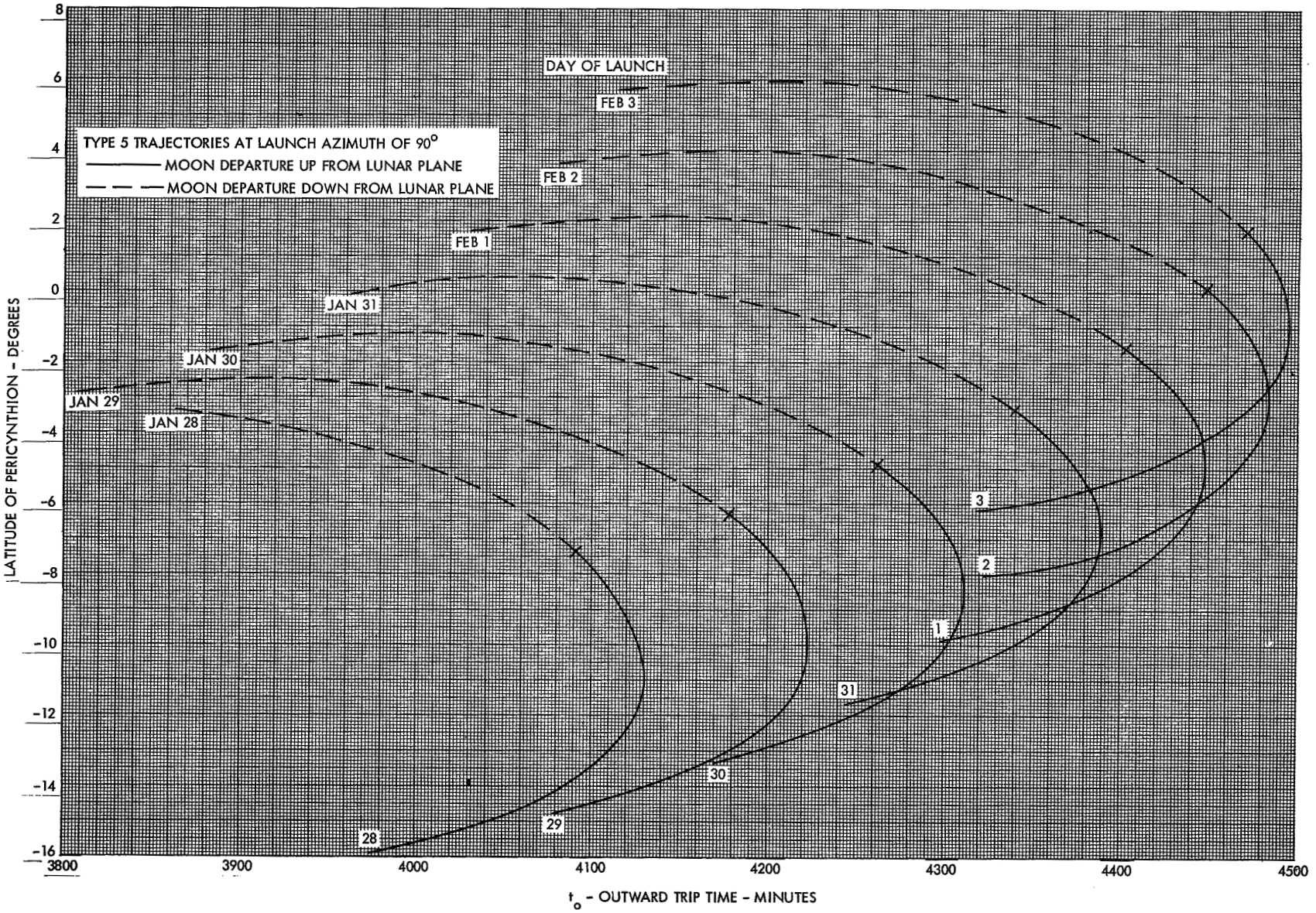

Figure 6.2 16. Lunar Phase Geometry – Latitude of Pericynthion versus Trip Time, Short Coast

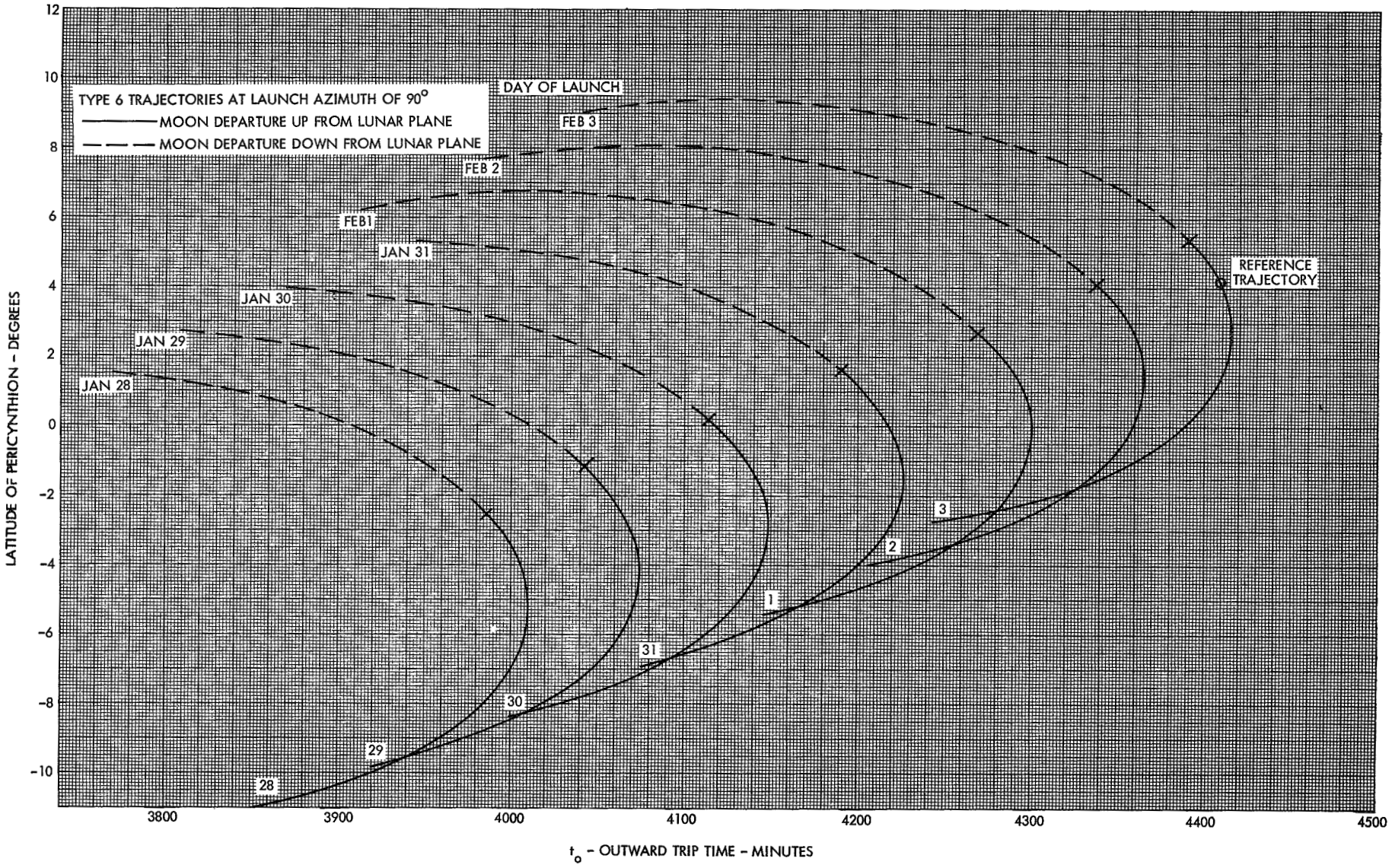

Figure 6.2-17. Lunar Phase Geometry – Latitude of Pericynthion versus Trip Time, Long Coast

The controlled return-parameters are the inclination (with respect to earth's equator), the re-entry altitude and flight path angle. The flight path angle at re-entry was held at 96.4 degrees and the re-entry altitude at 400,000 feet. These were not varied in this analysis and are important only for significant changes in re-entry angle. Small changes do not effect the injection or lunar geometry conditions. This has been determined in previous analysis.

The map of impact or touchdown points of the analytic free return trajectories is shown in Figure 6.2-18. It is interesting to note that all of them return to the approximate area of the Atlantic Missile Range. The points shown are for a re-entry maneuver angle of fifty degrees for the entire range of return inclinations. The markers are for specific return inclinations and the solid lines connect the points for each day. The discrepancies in these points occur at the high inclinations although the 28 and 31 of January have smooth curves. The positive return inclination (+90) begin at the end indicated by the arrow and progress to (-90). The sign on return inclination refers to the direction that the trajectory left the moon. The group of days form two distinct patterns. Days from the 28 to the 30 January return at high latitudes and drop to the south as return inclination is decreased. The moon during this time is at negative declination. The last four days, however, begin at low latitudes and move north as return inclination is decreased. The dashed boundary forms the locus of impact points whose inclination is 35 degrees or less.

The impact point for other azimuths moves roughly along the same latitude for a fixed return inclination on the same day. The longitude varies with launch azimuth as the liftoff times are different and the trip times about the same. Thus the earth moves under the impact point as the vehicle is pointed through the range of launch azimuths. The variance for days late in the period is about 63 degrees. For example, on February 3 the impact point for a return inclination of 35 degrees (at launch azimuth of 90 degrees) is -40 degrees West longitude and 30.5 degrees North latitude (see Figure 6.2-18). At a 72 degree azimuth the impact point is at same latitude and a longitude of 16.7 degrees West. As azimuth increases the longitude moves backward on the 30.5 degrees latitude line until the impact point of the 108 degrees launch azimuth is reached at 79.1 degrees West. Thus on a particular day the return inclinations that permit return to a suitable landing area could be found.

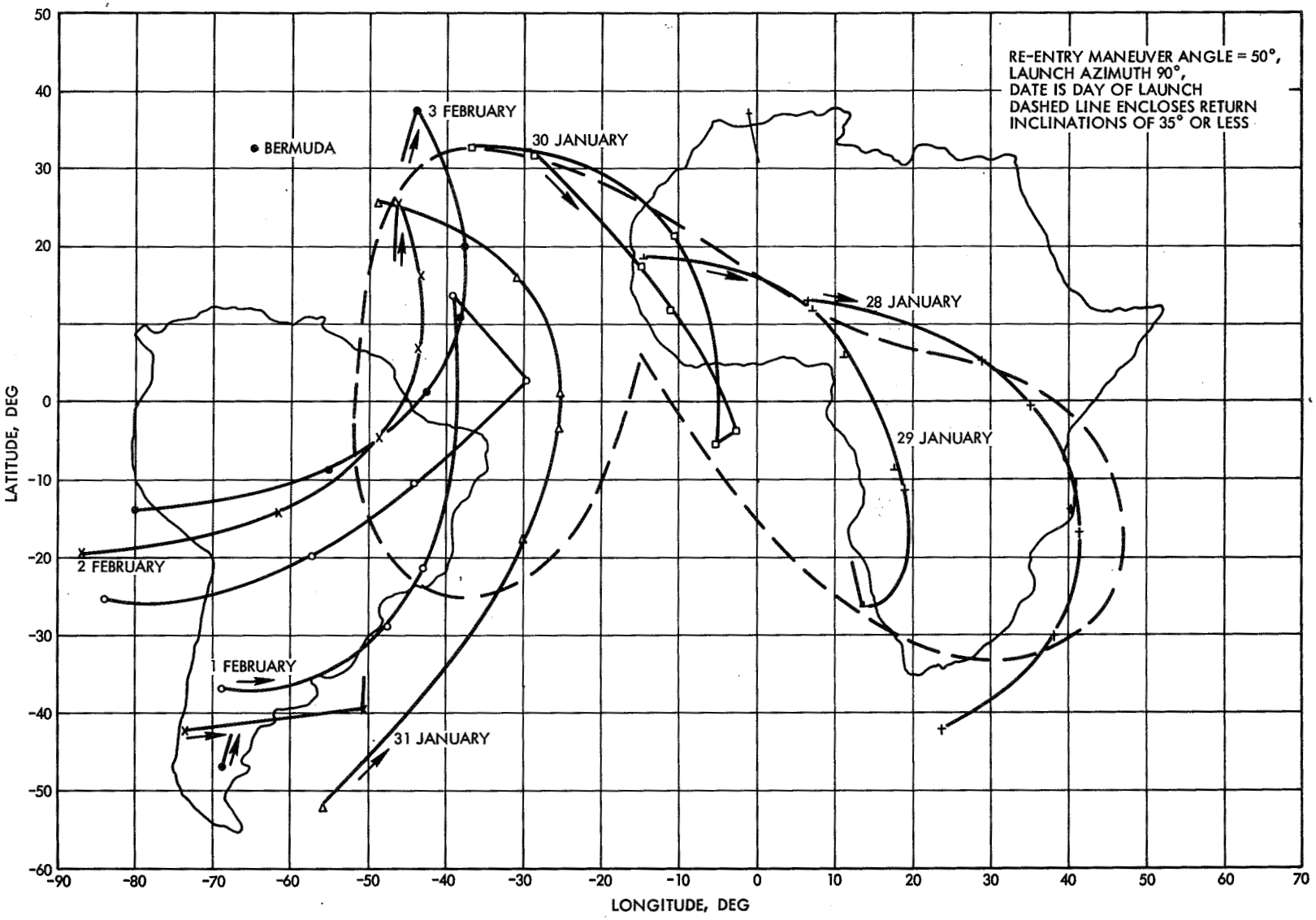

Figure 6.2-18. Map of Touchdown Point of Free Return Trajectories, Type 6

The gross launch window that is possible for all possible circumlunar free return trajectories is shown in Figure 6.2-19. This shows the length of the window during the two launch windows that occur each day.

The data presented in this parametric analysis has been generated by an analytic computer program. The gravitational model used in this program consists of enclosing the moon in a region within which only the moon's gravity is considered and outside of which only the earth's gravitational field is in effect. Thus, the motion will consist only of conic sections with no consideration of other perturbing forces. Three methods of comparison have been made in establishing the accuracy of this model when compared with an exact integration program.

1. Input the analytic injection conditions out of the parking orbit directly into the exact program.

2. Determine new injection conditions by performing a linear search within the exact program on the analytic impact parameter.

3. Determine new injection conditions by searching on the analytic values of distance of closest approach at the moon, return earth phase inclination and re-entry flight path angle.

In the first case, the integrated trajectory will compare very poorly with the analytic trajectory. This is expected, however, since the distance of closest approach at the moon may differ by as much as one earth radius which will result in a poor exit from the moon's sphere of action.

The second method attempts to correct this difference by searching on the impact parameter. The resulting exact trajectories will usually return to the earth with a perigee error of about 1000 nautical miles and have a pericynthion distance approximately 40 nautical miles too high.

The third method yields the most favorable comparison and this is the one which is of most interest here. Of these test cases which have been considered, most parameters have agreed quite well and, in fact, are as representative as data from the exact program. The liftoff times will be correct to within 10 minutes and the injection velocities to within 5 feet per second. Comparison of the moon phase geometry is excellent. The greatest discrepancy occurs in the pericynthion velocity in which case the exact value is about 50 feet per second greater than the analytic value.

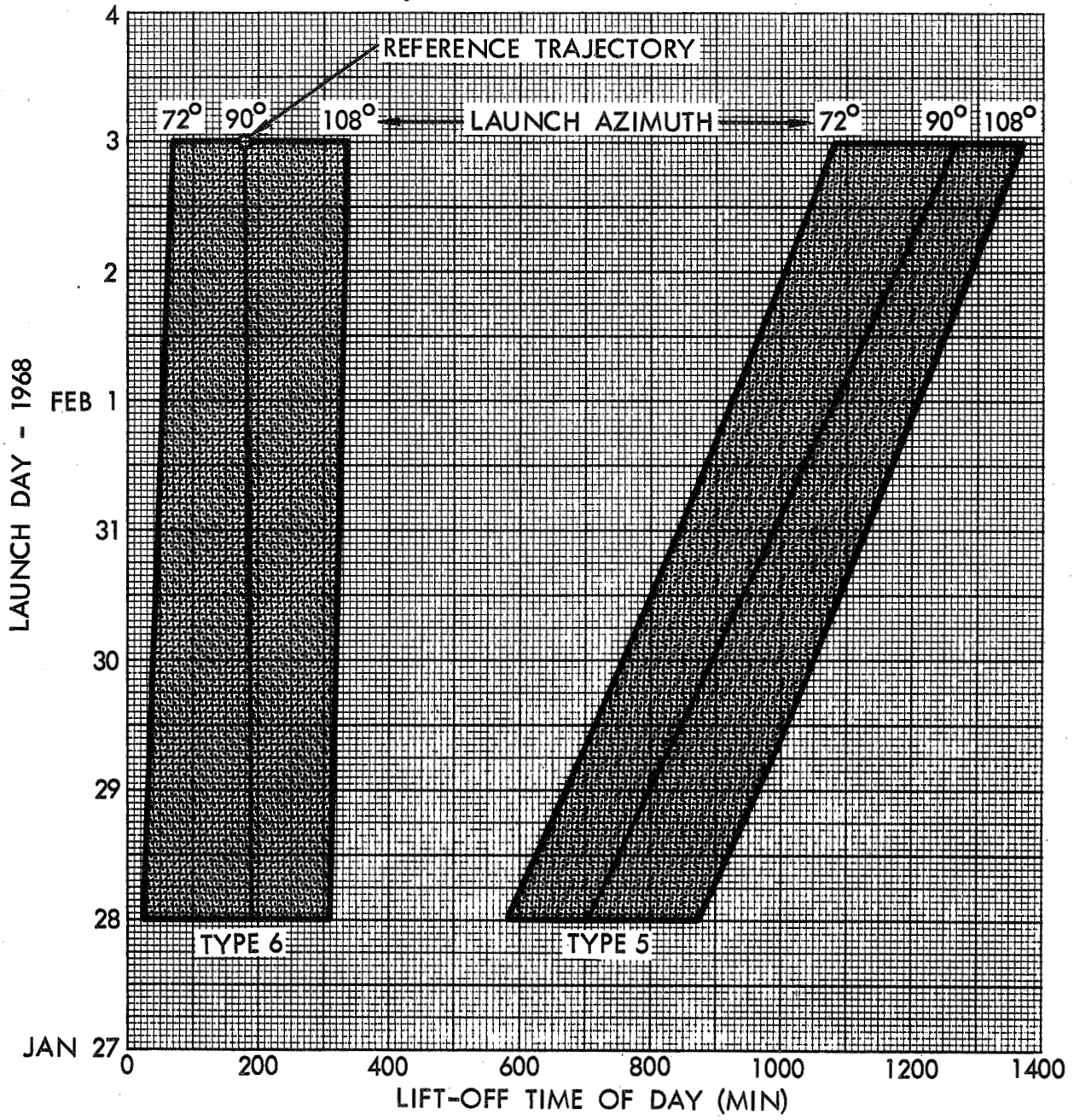

Figure 6.2-19. Free Return Launch Window

6.3 Lunar Landing, LOR, and Constrained Return Problem

The free return outbound leg to be committed to lunar landing can be selected as any one of the trajectories shown in Section 6.2 so long as mission and vehicle performance constraints are satisfied. The desirable conditions for the outbound leg are that it be within 10 degrees of the lunar plane, and have a return inclination with respect to the earth's equator of less than 40 degrees. These limits restrict the lunar phase geometry but do not restrict the launch window. Accordingly, because type 5 trajectories have a minimum inclination of greater than 40 degrees to the lunar plane, they would automatically be eliminated during the prescribed mission period.

If all possible launches of type 6 trajectories are considered for the moment, the map of lunar geometry can be drawn as was done in Figure 6.3-1. This shows the resultant inclination and node combinations during each day for the entire range of launch azimuths. The boundaries of the launch date bands are given by azimuths of 108 and 90 degrees, with 72 degrees falling between the two. The spacecraft is required to enter a circular orbit which will pass over the landing site permitting an in-plane LEM descent. The circular orbit which provides this geometry can have the combinations of node and inclination as plotted. The hyperbolic deboost problem is to change from some hyperbolic orbit node and inclination to some point on this line. The upper landing site curve applies to orbits approaching the landing site from the north and the lower curve to those from the south. Note that the only day which has an orbit which naturally passes over the site is 3 February at an azimuth of about 108 degrees. Selection of this outbound trajectory would require no plane change during hyperbolic deboost but the selenographic inclination is sufficiently high to warrant further considerations. The curves at the right hand side bend back on themselves as the same inclination is possible at two different trip times. (See Figures 6.2-12 and 6.2-13). Ideally with data of this nature it would be best to find a landing site or group of landing sites which would lie under these curves. That is, a selection of sites bearing the same inclination and node relationships that the trajectories provide. This would lessen the corrective velocity required to trim the orbit such that it passes over the site. In the case shown here it is necessary to modify the orbits to pass over the site.

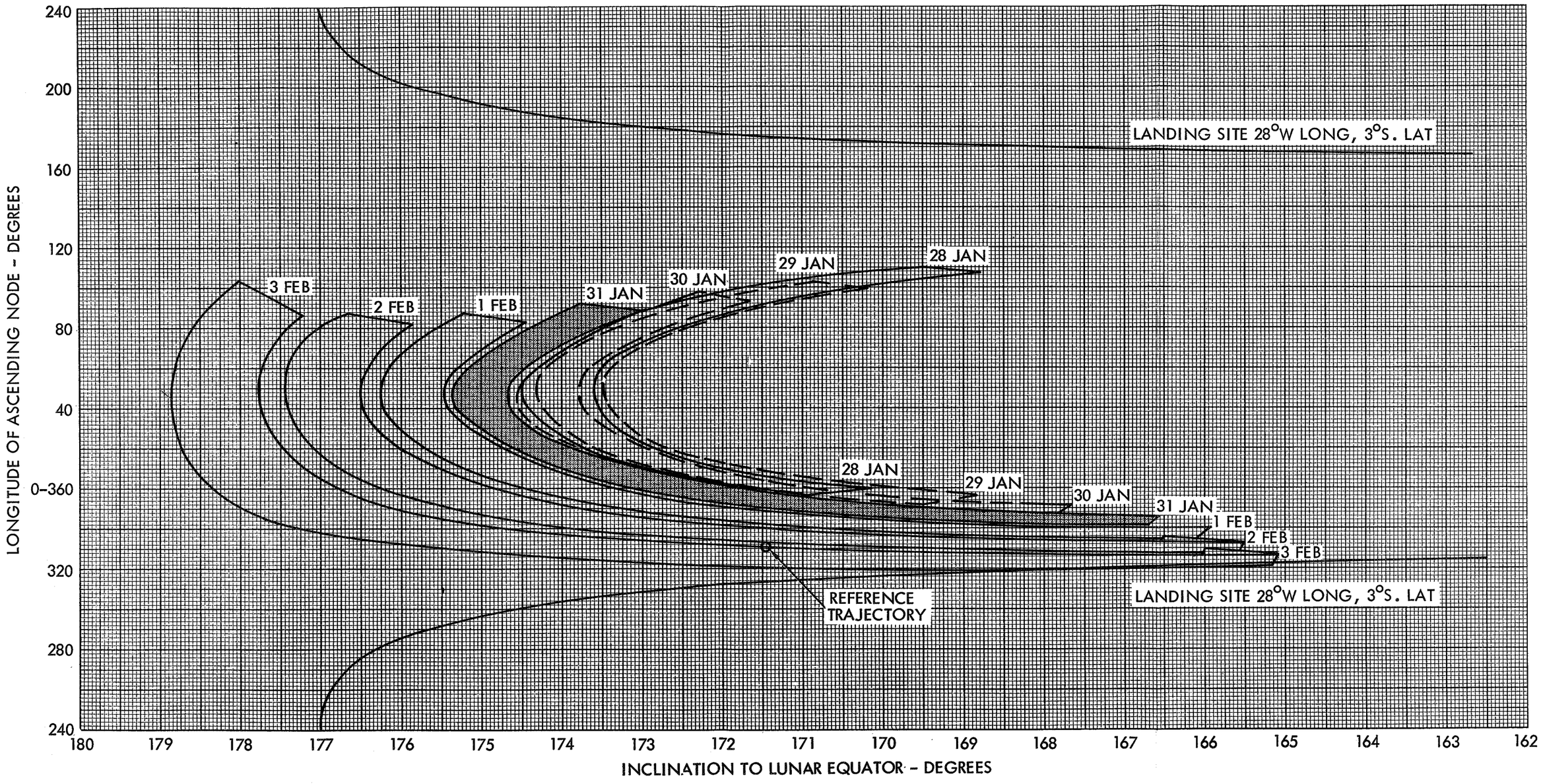

Figure 6.3-1. Map of Lunar Geometry of Gree Return Trajectories with Respect to Landing Site Requirements

The orbit selection is also complicated by the limitations of the LEM during its maneuvers. The descent must be in-plane and, inasmuch as the landing site does not lie on the lunar equator the CM/SM orbit must have an inclination equal to or greater than the latitude of the landing site. Thus, as stay time on the moon increases, the CM/SM orbit is moving away from the site requiring additional energy during the LEM ascent to execute a plane change. The effect on velocity required versus inclination is shown for various stay times in Figure 6.3-2. If for example, the additional LEM velocity increment limit is 300 feet per second the minimum orbit inclination that is permissable is 148 degrees with a stay time of only 8 hours - 4 revolutions of the CM/SM. If the stay time is increased to 24 hours (12 revolutions) the inclination must not be less than 170 degrees.

When there is a choice of return to either of two earth landing sites the selection is governed by the moon's declination at departure. For negative declinations of the moon, return will be to the site in the southern hemisphere, and to the northern hemisphere for positive lunar declinations. Thus for the first 3 days of the launch period return is to San Antonio, and for the last 4 days return is to Woomera. For 30 January departures, which leave the moon on 2 February when it is almost at zero declination, return can be made to either site.

There is a re-entry maneuver angle limitation inherent in return to a specified landing site. When the moon is at particular declinations the total in-plane angle required to reach a site may not be possible, that is there are limits as to where the moon can be. This was found to be true in the investigation of shorter maneuver angles in this analysis.

The analysis was restricted to orbits which pass over the specified lunar landing site. If the incoming hyperbola is corrected to such an orbit as it is deboosted into a circular orbit, the map of inclination and node becomes a single line identical to the landing site requirement in Figure 6.3-1. This is illustrated by Figures 6.3-3 and 6.3-4 for type 5 and 6 trajectories. The launch dates on the curve show the range of values that the inclination and node have been corrected to for that particular day. Dates on the outer perimeter refer to the outbound legs with a positive return inclination, and the inner dates

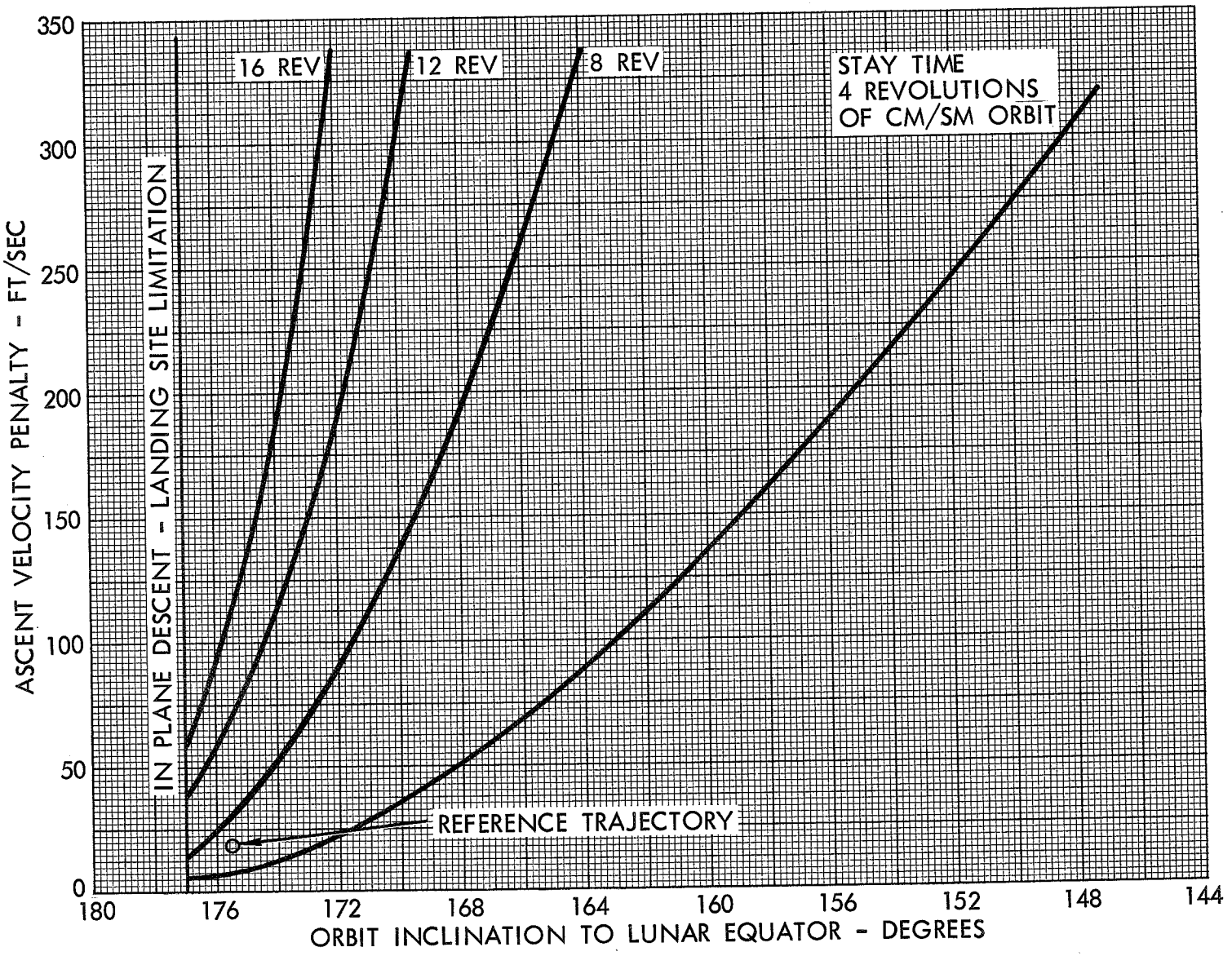

Figure 6.3-2. Ascent Limitations – Velocity Penalty versus Inclination for Various Stay Times

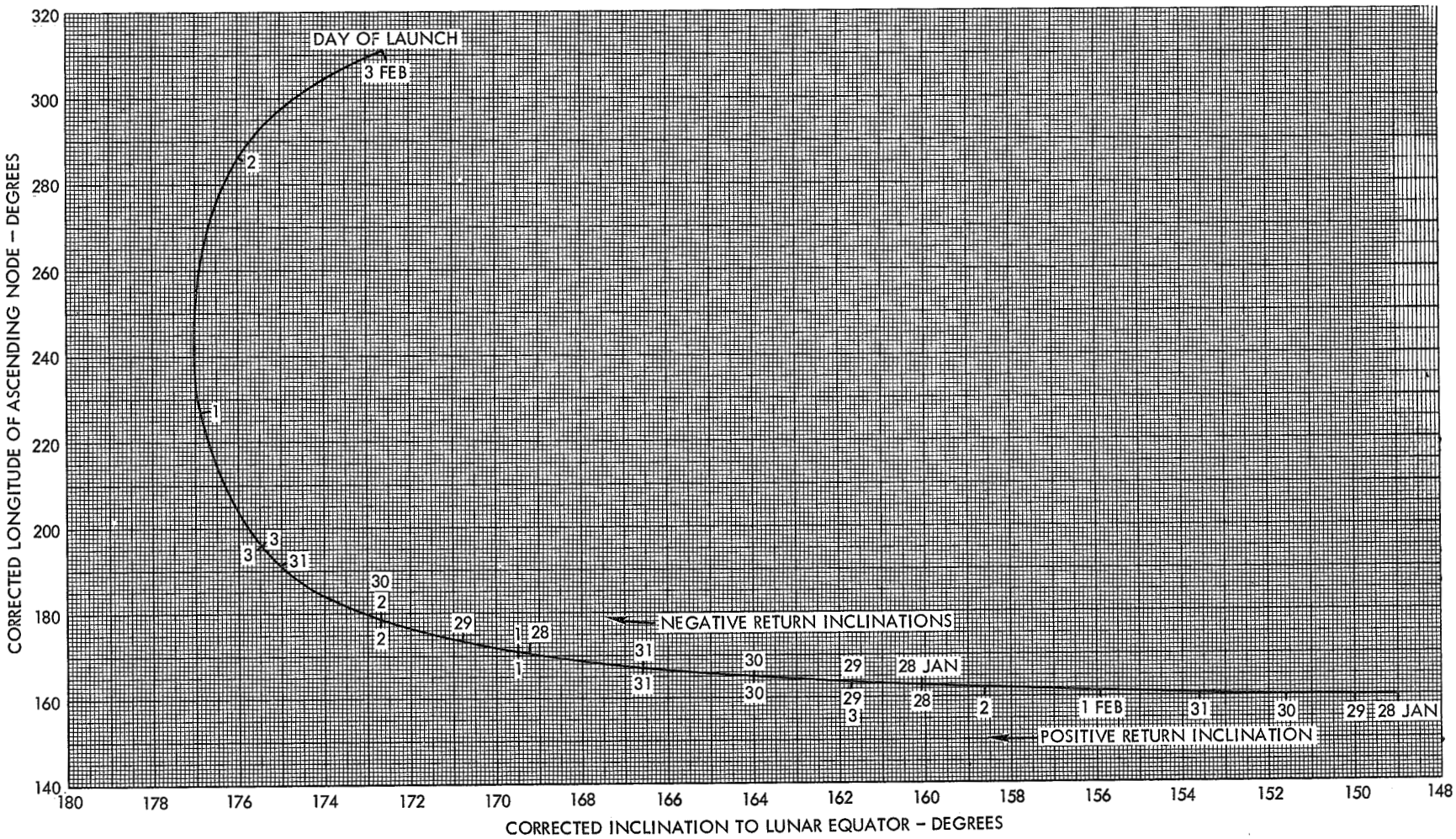

Figure 6.3-3. Corrected Moon Phase Conditions – Short Coast Trajectories, Type 5

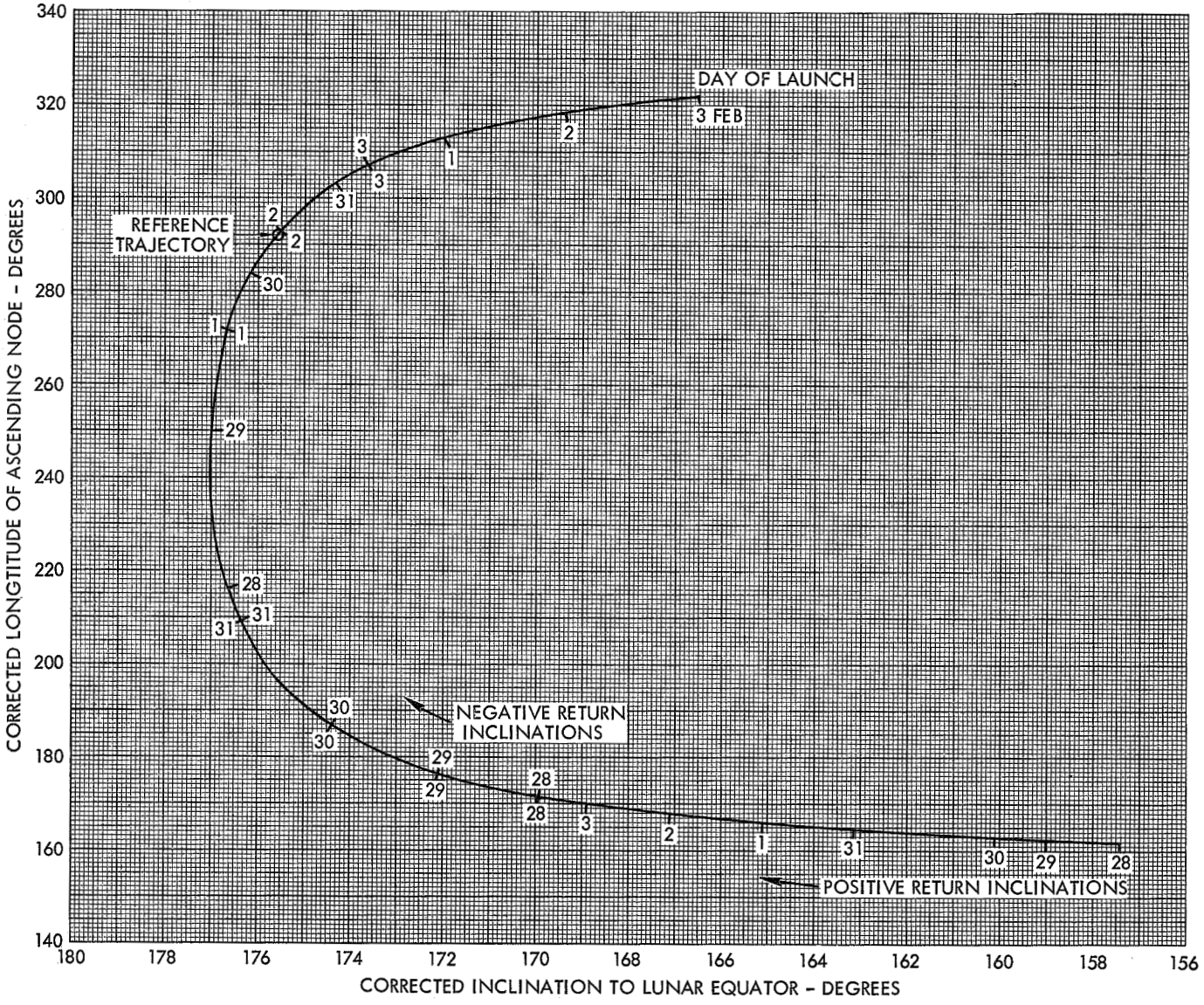

Figure 6.3-4. Corrected Moon Phase Conditions — Long Coast Trajectories, Type 6

to the negative inclinations. These corrected circular lunar orbits can be related to the free return outbound leg. The corrected inclination plotted against outward trip time will allow the injection conditions and uncorrected lunar geometry to be determined from Section 6.2. It has been shown (Figures 6.2-10 and 6.2-11) how the return inclination is related to trip time. Thus by knowing the launch day, the trip time and return inclination all other outbound parameters can be found.

The velocity required to deboost into the corrected circular orbit can be related to the outbound leg by the return inclination of the free return trajectory. Although deboost changes the free return trajectory that formed the outbound leg, the return inclination serves as a reference to the outbound portion, and bears no relation to the return leg beginning from the lunar orbit. The velocity required to deboost is shown in Figures 6.3-7 and 6.3-8 for a launch azimuth of 90 degrees. The minimum velocity required in the type 5 cases is greater than the maximum of type 6 for each day. The variance with azimuth is illustrated in Figures 6.3-9 and 6.3-10 showing a maximum decrease of 100 feet per second in the type 6, note that the 90 degree azimuth has the highest value. There is a maximum increase of 200 feet per second in the type 5 trajectories, now the 90 degree azimuth has the lowest value. These data for 3 February are representative of the last four days in the period.

The analytic optimizations during the hyperbolic deboost determine the combination of hyperbolic orbit energy and relative orbit inclination which minimizes propellant requirements for establishing the circular orbit inclination and node location necessary to pass over the landing site. These assume that the maneuvers are performed impulsively at pericynthion, which is adequate in determining the optimum values of total energy and relative inclination. The losses in the actual maneuvers are proportional to the magnitude of these analytic quantities and do not affect the exact optimization. The same general approach is used in determining the hyperbolic orbit at launch from the moon.

Return to earth from the corrected lunar orbit can now be analyzed. Six orbits about the moon after hyperbolic deboost were considered as the minimum. Movement of the line of nodes during this period is about 6.1 degrees. To provide a common basis for all seven days in the launch cycle, the return's

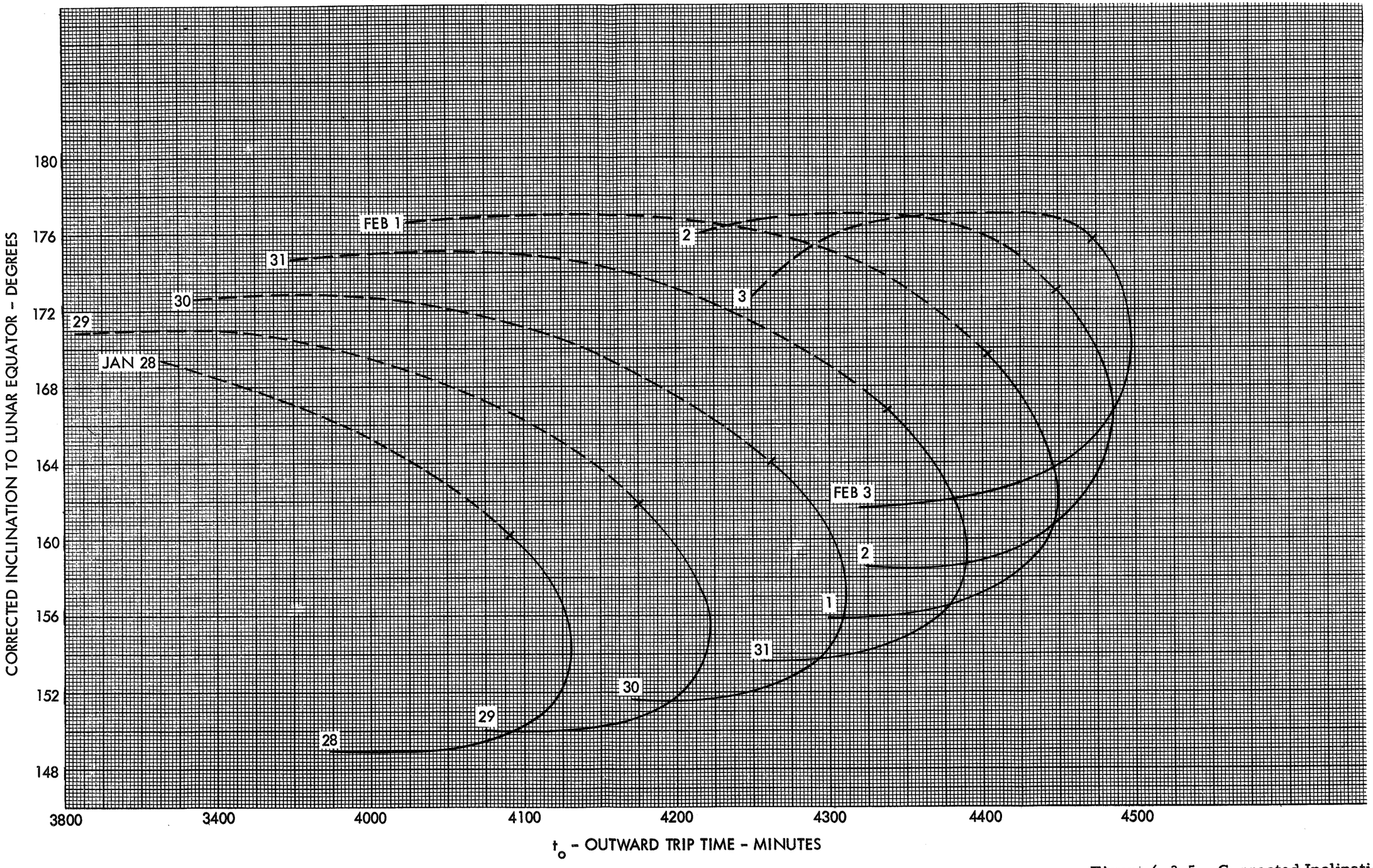

Figure 6.3-5. Corrected Inclination versus Outward Trip Time - Short Time Trajectories, Type 5

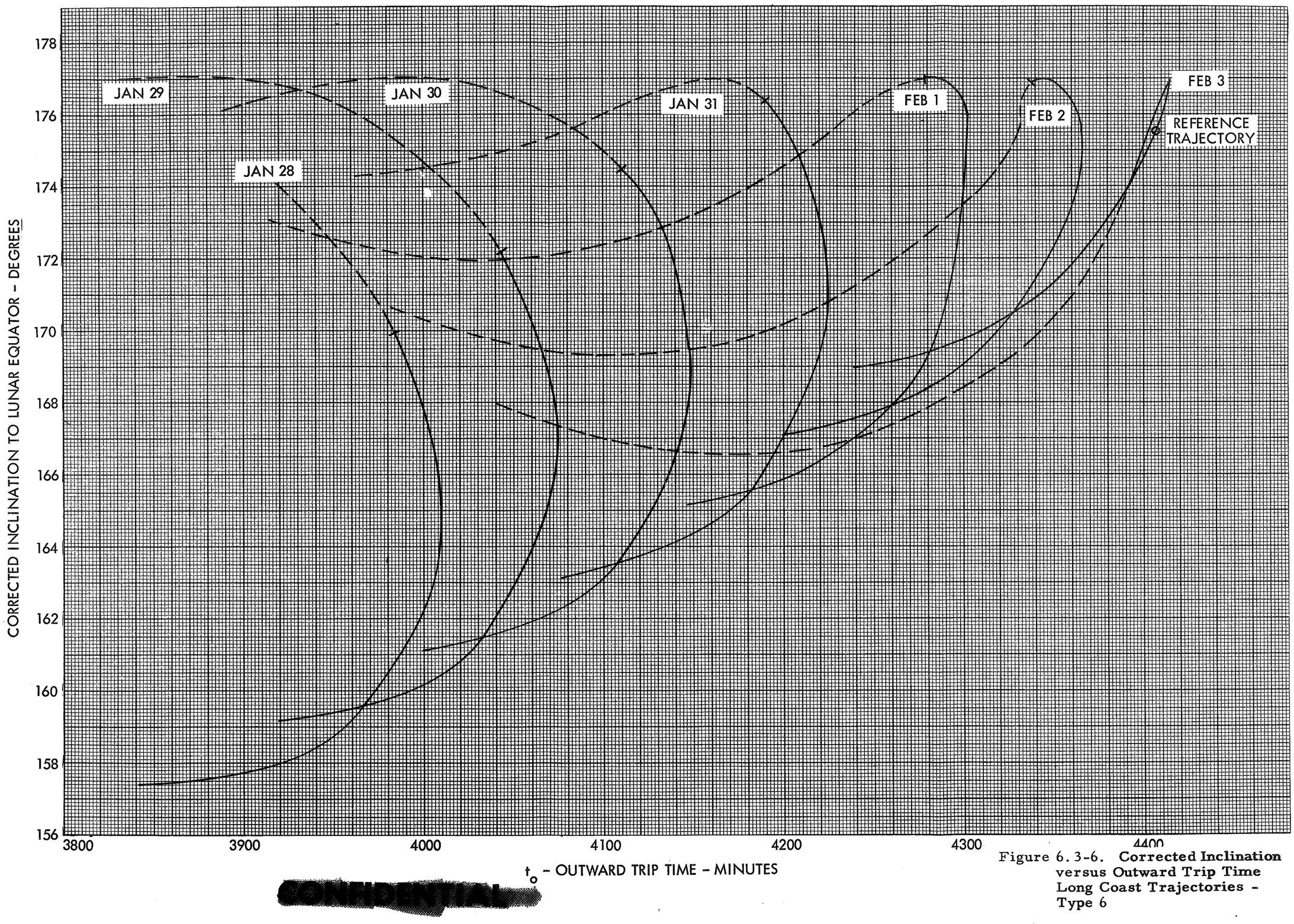

Figure 6.3-6. **Corrected Inclination versus Outward Trip Time Long Coast Trajectories - Type 6**

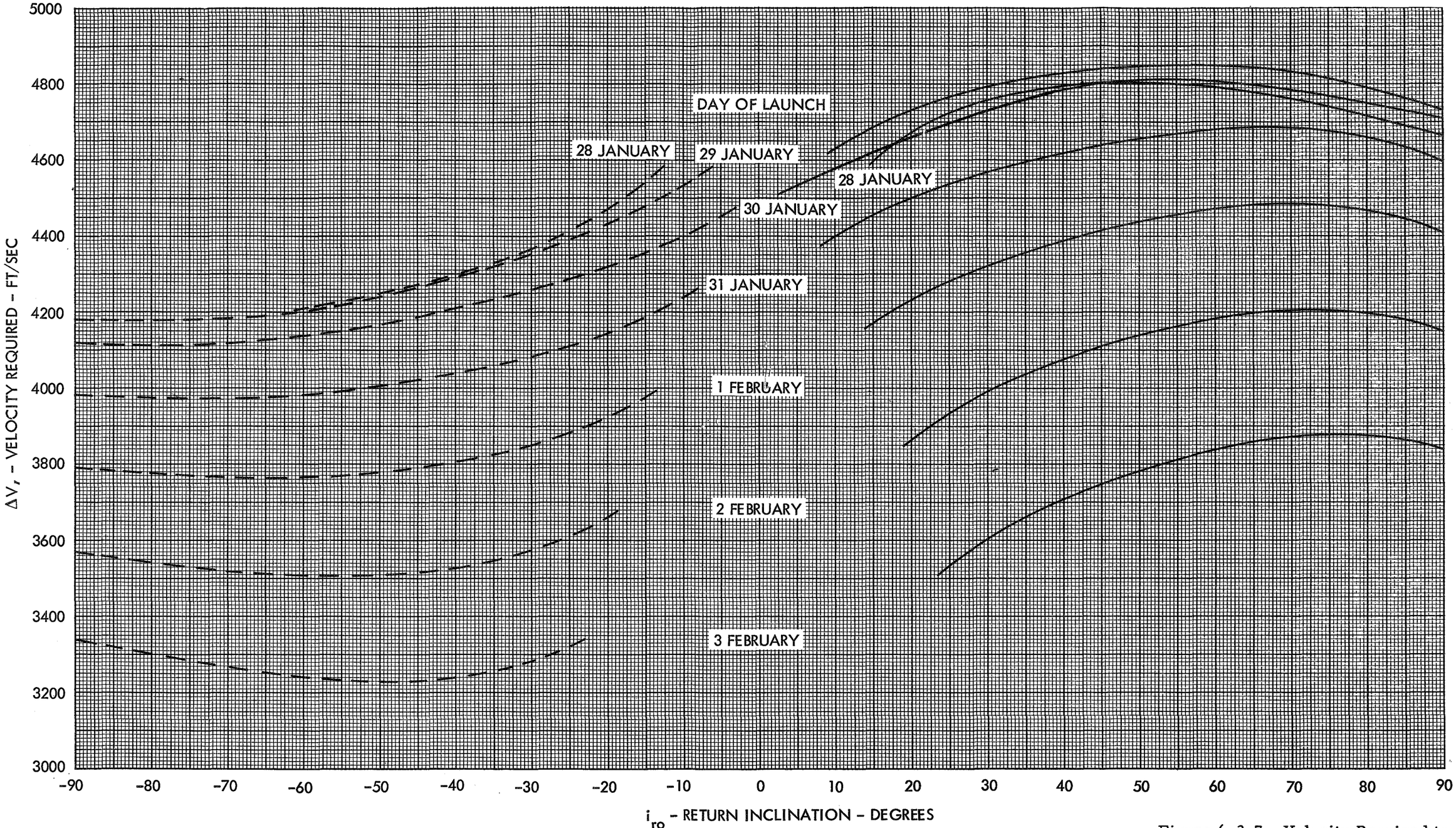

Figure 6.3-7. Velocity Required to Deboost into Corrected Orbit versus Return Inclination for Short Coast Trajectories (Type 5 at Launch Azimuth of 90°)

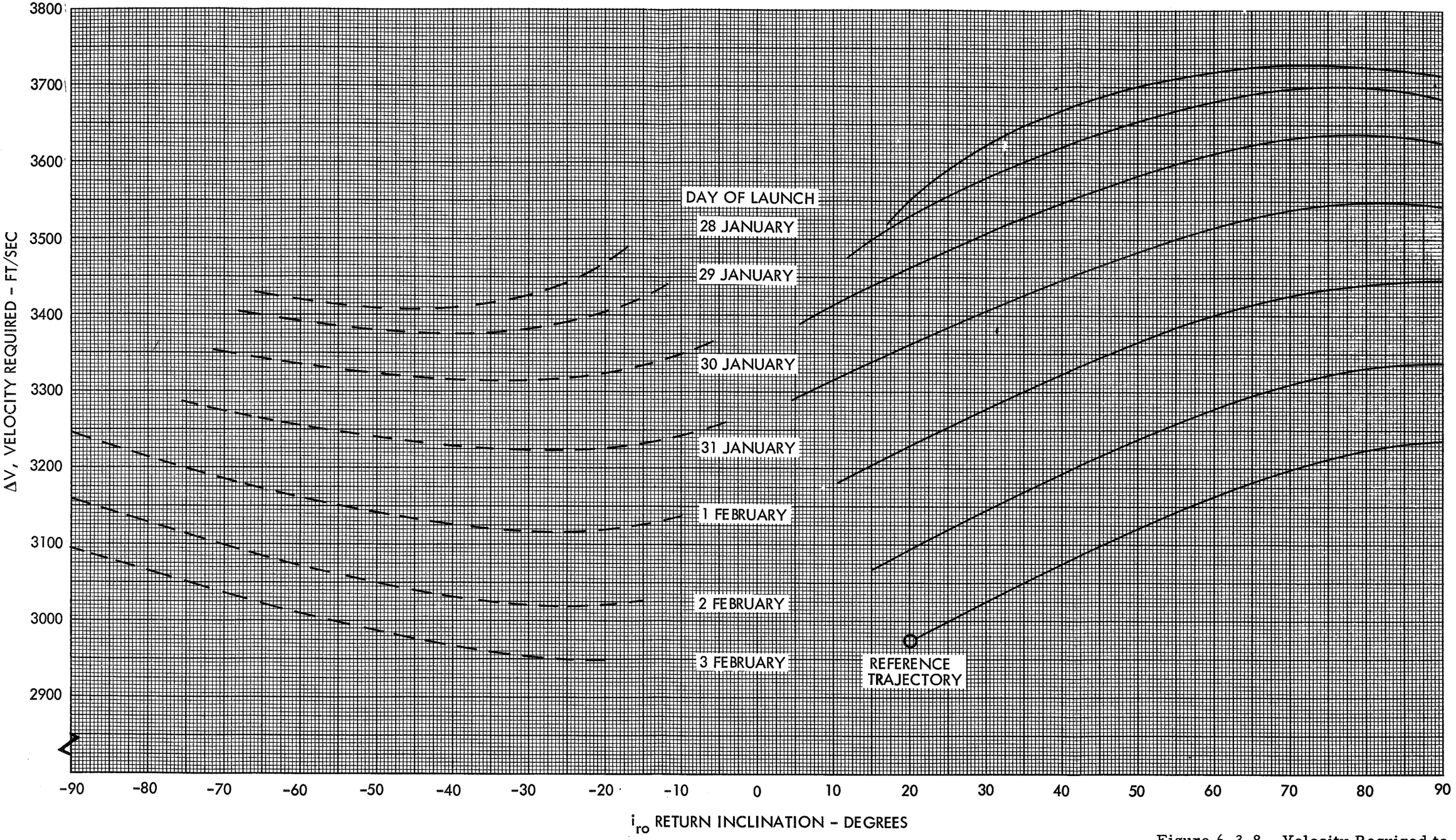

Figure 6.3-8. Velocity Required to Deboost into Corrected Orbit versus Return Inclination for Long Coast Trajectories (Type 6 at Launch Azimuth of 90°)

CONFIDENTIAL

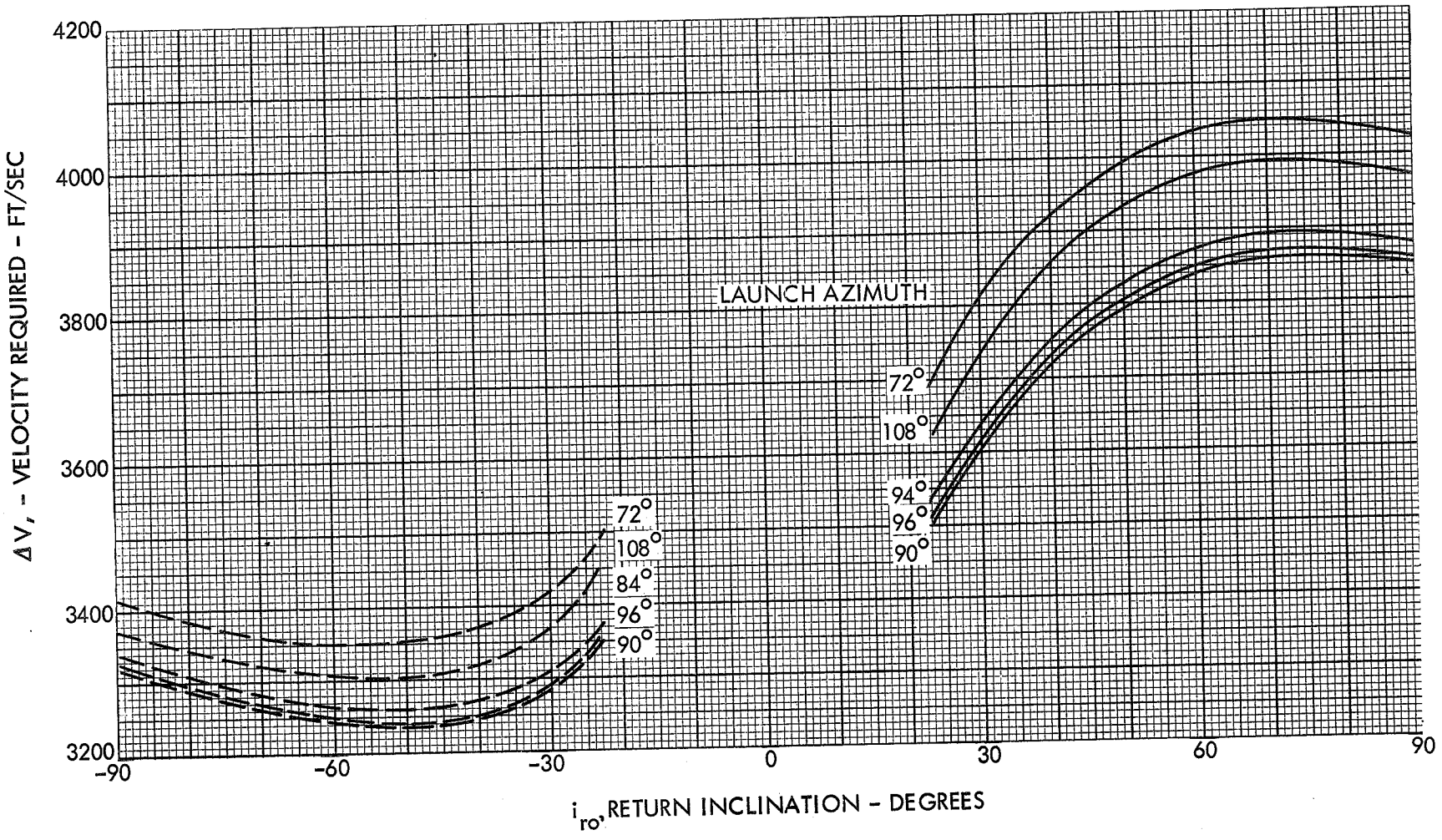

Figure 6.3-9. Effect of Launch Azimuth on Velocity Required
(Type 5, Long Coast Trajectories for 3 February 1968)

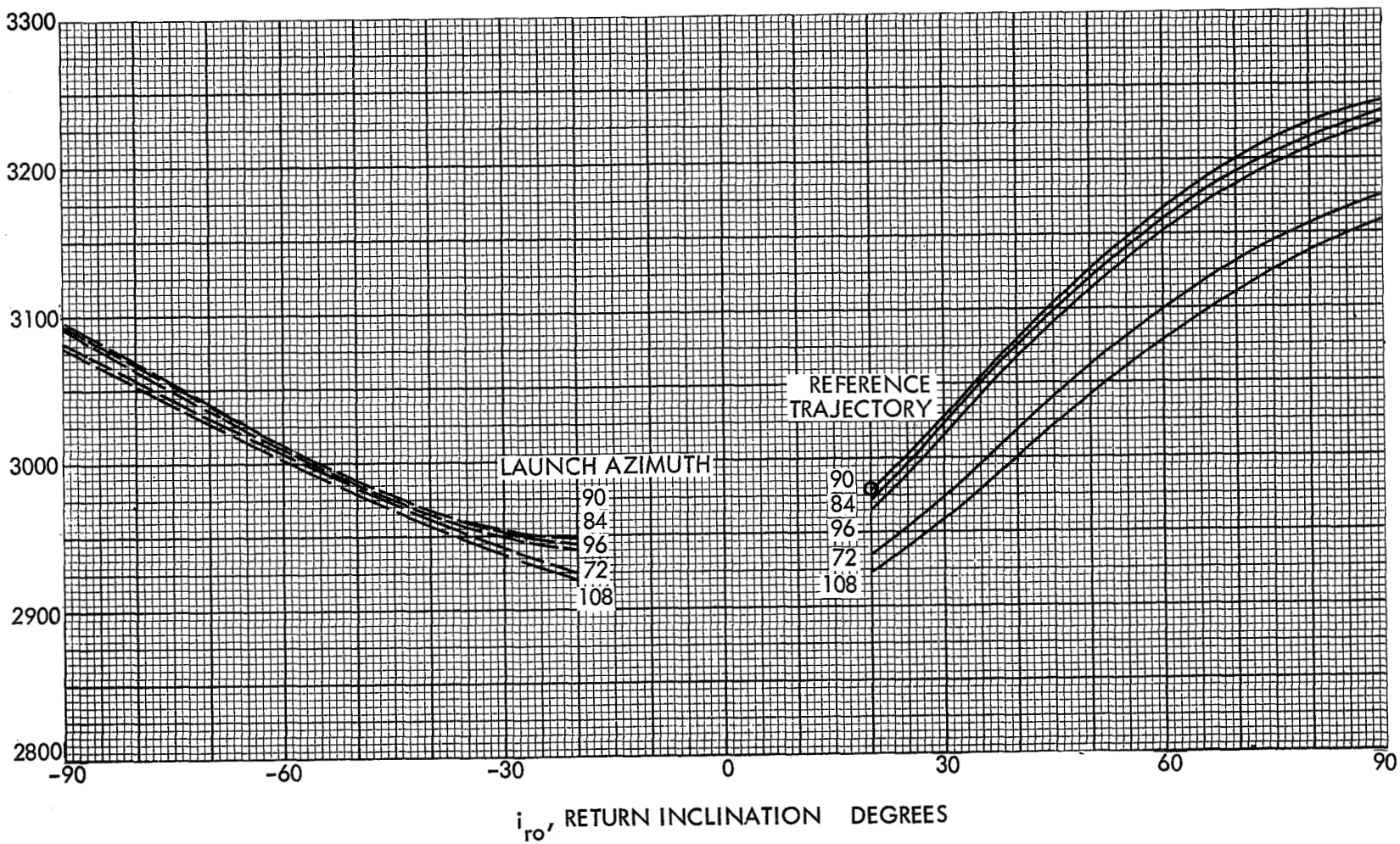

Figure 6.3-10. Effect of Launch Azimuth on Velocity Required
(Type 6, Long Coast Trajectories for 3 February 1968)

from the lunar orbits resulting from the smallest positive and the 35 degrees return inclinations of the free return outbound leg were investigated. These initial conditions coupled with an assumed maximum re-entry maneuver angle of 50 degrees give the velocity required for various return trip times as shown on Figures 6.3-11 and 6.3-12. The former returns to San Antonio whereas the latter returns to Woomera. The times for the points on each curve correspond to approximately 74, 70, 66 and 62 hours with the 74 hour time occurring at the lowest velocity. Other trip times are possible at about two hour intervals, which is half way between the data points. The vertical lines on each curve indicate the first time at which return could be initiated after the LEM completes its mission. In some cases the first time of injection eliminates some of the longer flight times. This is true for the San Antonio returns. And for the launches of the 30th of January this means no return to San Antonio is possible. But if more than 24 hours are spent in lunar orbit return could be made to Woomera. The four curves shown for each day correspond to the initial conditions at departure from the lunar orbit resulting from the free return outbound leg with the indicated return inclinations.

For the second and third of February lower re-entry maneuver angles are possible. In fact the maneuver angle can be reduced from 50 to 35 degrees, although for some free return starting conditions this reduction is sensitive. The additional velocity required for this 15 degree reduction is at most 200 feet per second at the moon.

It becomes apparent that there is a relatively small band of velocity required to return on a particular day when the moon is at a favorable declination. This band is not particularly influenced by the outbound free return leg (if return inclination is limited) as once the orbit is corrected to pass over the site every successive orbit will be similar. However, the changing declination and the distance of the moon will significantly affect the geometry of the return problem. This will change the total in-plane angle of the return and with limited re-entry maneuver angles it may be impossible to return to a specified site.

When return is possible, a map of the re-entry points is similar to those shown in Figures 6.3-13 and 6.3-14 for returns to San Antonio and

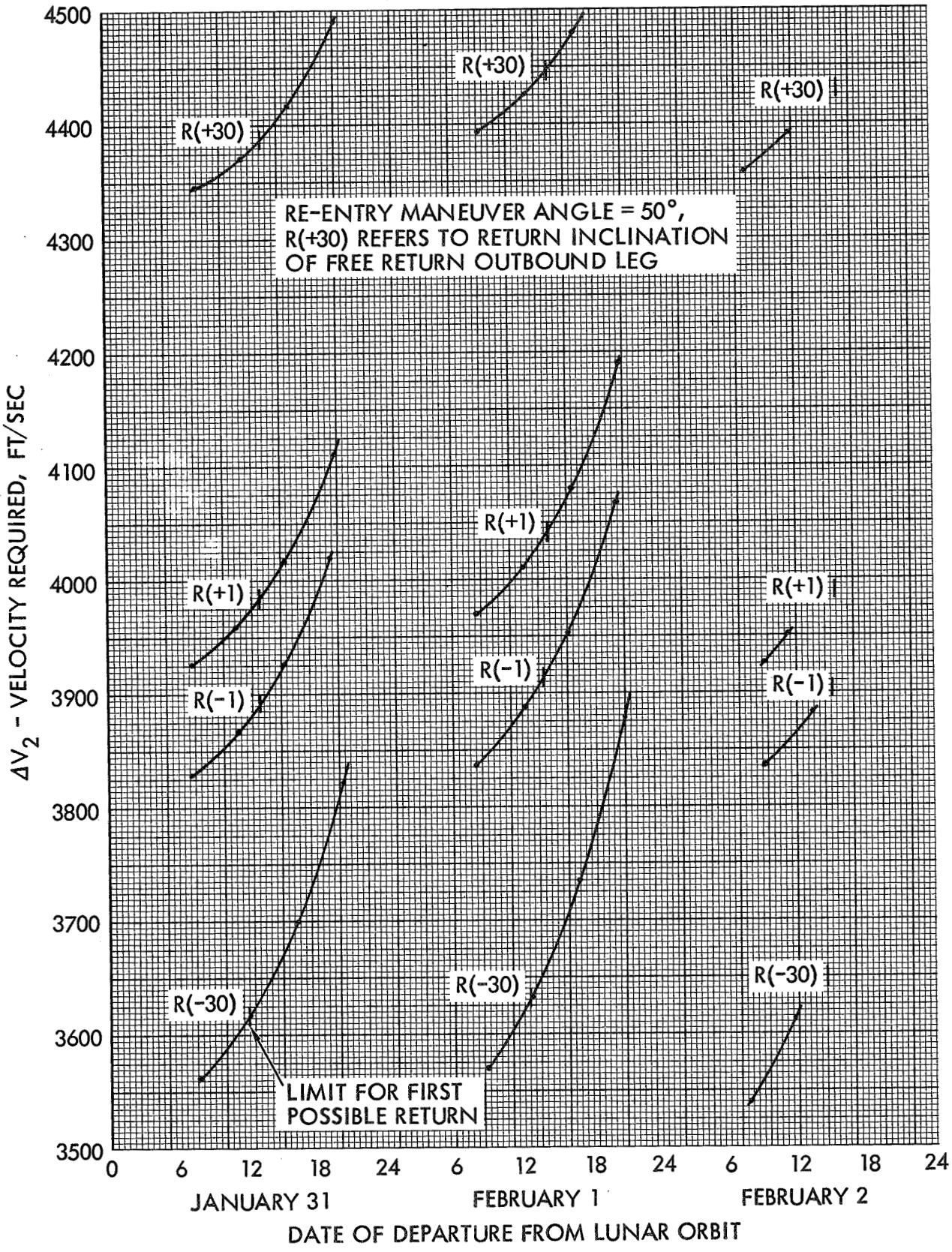

Figure 6.3-11. Velocity Required to Inject from Lunar Orbit and Return to San Antonio

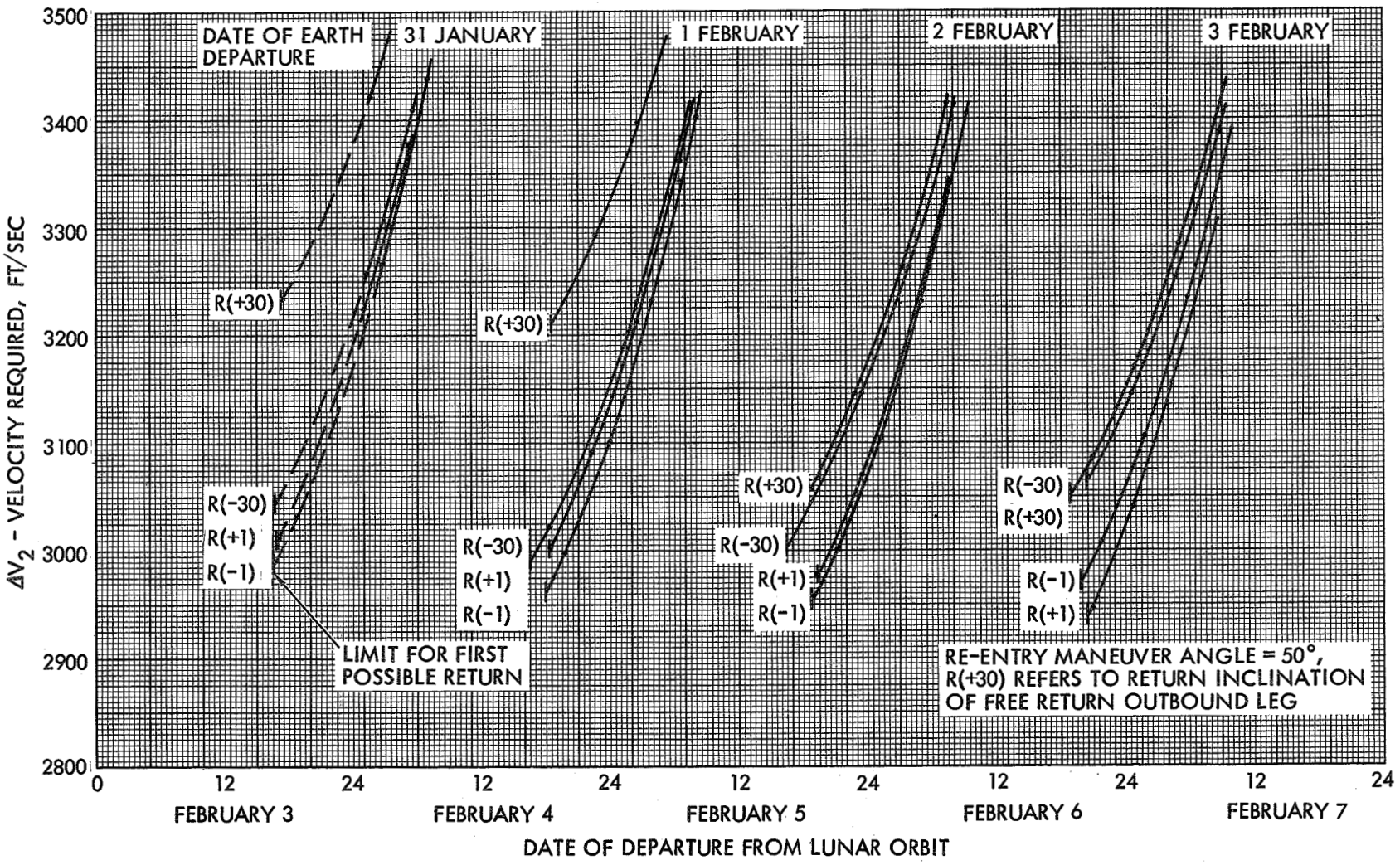

Figure 6.3-12. Velocity Required to Inject from Lunar Orbit and Return to Woomera

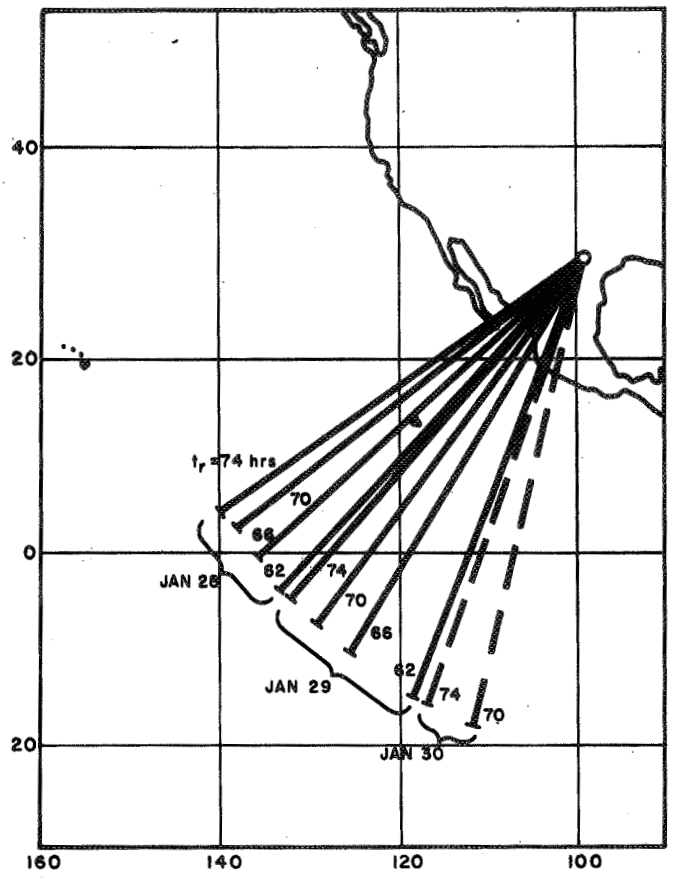

Figure 6.3-13. Dispersion of Earth Re-entry Points for Return to San Antonio -(Re-entry Maneuver Angle = 50^{o})

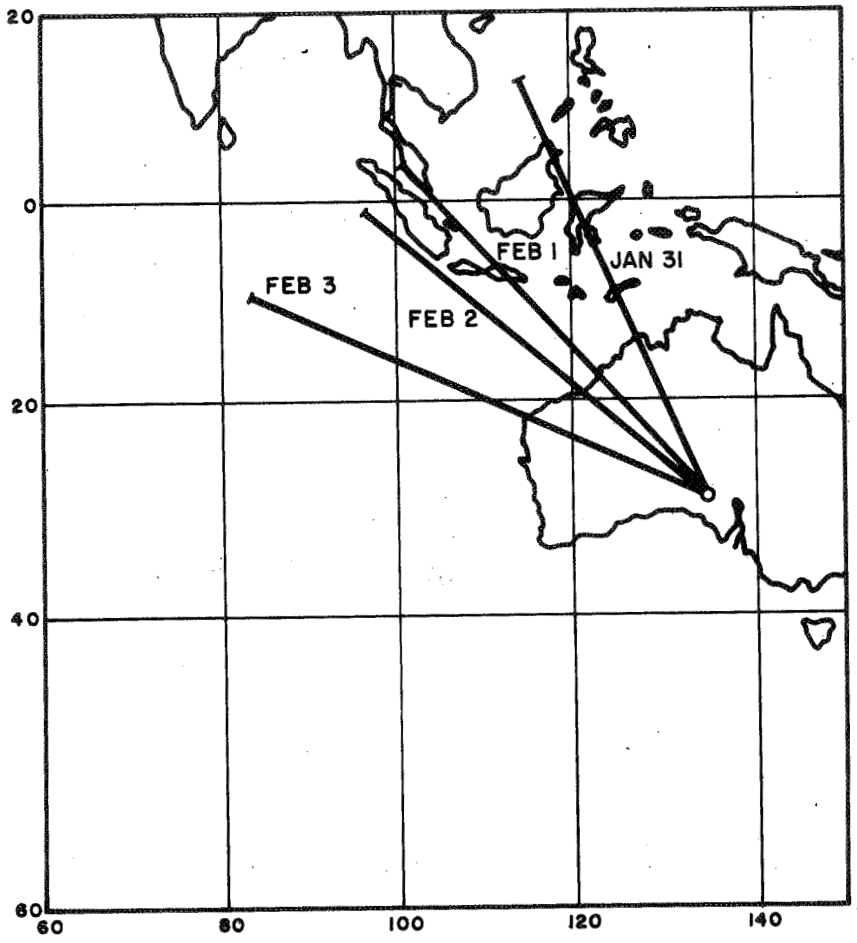

Figure 6.3-14. Dispersion of Earth Re-entry Points for Return to Woomera (Re-entry Maneuver Angle = 50°)

Woomera, respectively. Return to San Antonio is shown for each of the 3 days it is possible. For 28 and 29 January the 4 trip times are shown. The inclinations vary from 36 to 45 degrees on the 28th and from 46 to 65 degrees on the 29th. The dashed lines for the hypothetical return on the 30th are also shown, with a maximum inclination of 70 degrees. (In Figure 6.3-11, return on the 30th was shown to be impossible in view of the stay time requirements.)

In marked contrast to the previous rapidly changing inclination with trip time, the returns to Woomera on a given day practically lie atop one another. This means that within the trip time and the starting lunar orbit considered that the re-entry points will be within 35 miles of the nominal re-entry point.

The total velocity required of the service module in the vicinity of the moon is the sum of the hyperbolic deboost (and orbit correction) plus the return injection velocity. The trade-off in hyperbolic deboost velocity, ΔV_1, versus return injection velocity, ΔV_2, may be shown by plotting the latter versus the former. With a given propellant loading in the SM it is possible to compute the return injection velocity available for a given deboost velocity required. This will limit the possible returns that can be considered. However, the limit on the return velocity is high enough to warrant use of all possible returns considered thus far. At a ΔV_1 of 2900 feet per second, ΔV_2 is 5800 feet per second and at ΔV_1 of 3700 feet per second, ΔV_2 is 4300 feet per second. It can be seen on Figure 6.3-15 how far below these limits the requirements are, even if the trip time is reduced to 62 hours. The return conditions on the third of February were selected at the minimum of the velocities required.

The major portion of the data presented here has been generated by an analytic computer program which is based on the same model as the Analytic Circumlunar Program (see Section 6.2). Specifically, the lunar return program will accept the conic elements of the LOR orbit, the re-entry flight path and maneuver angles, and the latitude and longitude of the landing site and determine the time, position and velocity to launch out of a given orbit to minimize the transearth velocity required.

The accuracy of this program has been considerably improved over the pure gravitational model with the addition of an empirical correction. For

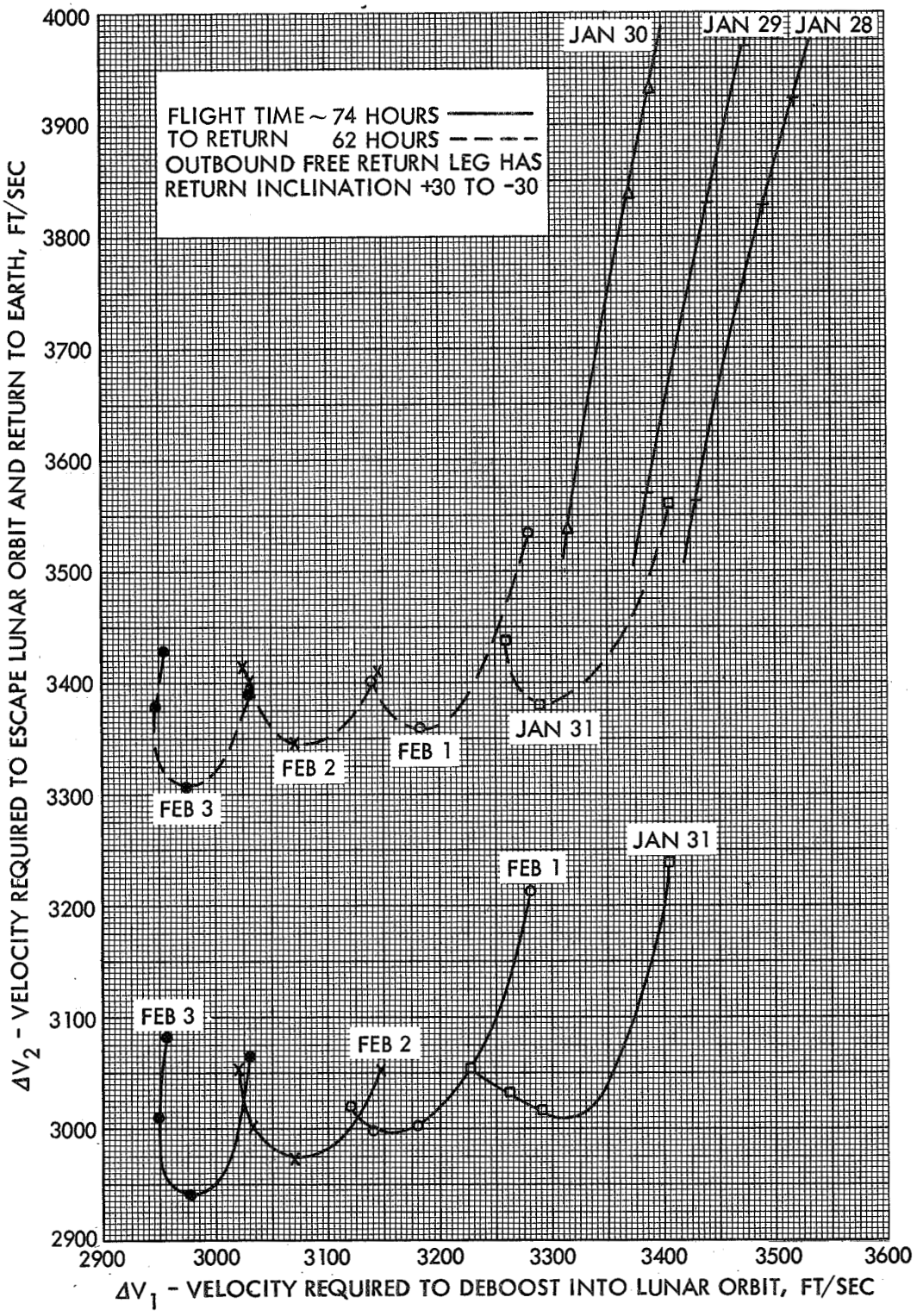

Figure 6.3-15. Total Service Module Velocity Required, Deboost and Return

example, if the injection from orbit conditions from the corrected model are placed in the integrating program, the resulting re-entry flight path angle, latitude and longitude at touchdown will be correct to within 5, 5 and 10 degrees, respectively, for a 70 hour flight time. Although there is not particularly good agreement in terminal conditions in an absolute sense, the corrections required are negligible due to sensitivity. Other less sensitive parameters at the moon and at the earth, including the time of flight also agree quite well. The injection time of the final targeted reference trajectory differed from the analytic value by about 1.5 minutes and the velocity differed by 3 feet per second.

6.4 Powered Flight Optimization

6.4.1 S-V Powered Flight Optimization

The optimization of the Saturn S-V vehicle was performed in two parts. The first part consisted of the liftoff to parking orbit injection portion and the second part consisted of the translunar injection phase. The philosophy used in each part of the optimization was to maximize injected weight.

The liftoff to parking orbit injection portion consists of three separate burn phases; the S-IC, S-II and S-IVB first burn. The optimization parameters used were:

1. Kick Angle at 12 seconds after liftoff - SIC
2. Pitch turning rate in S-II and S-IVB first burn phases (same pitch rate)
3. Body axis reorientation at the initiation of S-II phase.

The desired conditions at parking orbit injection were:

1. Altitude equal to 100 nautical miles
2. Flight path angle equal to 0 degrees
3. Maximum payload at circular velocity.

The procedure used in the optimization was to solve for the S-IC kick angle and S-II/S-IVB first burn pitch turning rate to produce the desired altitude and flight path angle, and to solve for the S-II body axis reorientation to produce the maximum payload.

itle
prohibited by law.

The translunar injection portion of the S-V trajectory consists of the S-IVB second burn. The optimizing parameters used were:

1. Reorientation of the vehicle body axis at S-IVB second burn ignition.
2. Pitch turning rate of S-IVB second burn phase.

The desired condition at translunar injection was maximum injected weight.

The procedure used was to determine the combination of pitch turning rate and reorientation angle which maximized injected weight for a representative injection energy cutoff.

6.4.2 Service Module Operations

General Optimization Philosophy

The problem of optimizing the service module powered flight maneuvers is one of selecting the set of independent variables which minimize propellant consumption and meet all mission constraints. The parameters which influence these maneuvers are divided into two classes, one being the powered flight maneuver variables and the other being those variables resulting from the initial and final orbital elements. The independent variables of the powered flight maneuvers are the initial pitch and yaw attitudes, the pitch and yaw rates, the maneuver initiation time and the maneuver cutoff or burning times. In the second class of parameters, the variables affecting the maneuver optimizations are the total energy of the hyperbolic orbit, the hyperbolic pericynthion altitude, and the relative inclination between the initial and final orbits. Of these, the hyperbolic orbit energy and relative inclination are not true optimization parameters, in that maneuver propellant requirements are proportional to the magnitude of these variables. The optimum sets of these parameters are determined by analytic optimizations, discussed in Section 6.3, consistent with all mission constraints. These parameters do, however, affect the optimum values of the remaining independent variables. The third parameter of this class, the hyperbolic orbit pericynthion altitude is a true optimization variable in that there is a definite tradeoff between maneuver losses and pericynthion altitude relative to the circular orbit altitude. The optimization procedure for each of the service module maneuvers is dependent on its initiation and burnout constraints and will, therefore, be discussed individually.

Hyperbolic Deboost Optimization

The deboost maneuver is initiated on a hyperbolic conic and is constrained to burnout in an 80 nautical mile circular orbit at some inclination relative to the hyperbolic orbit. The hyperbolic deboost maneuver for Issue 1 is shown as an example in Figure 6.4.2-1, projected onto the horizontal or yaw plane. The plane change requirement for this type of maneuver is defined as the relative inclination (dihedral angle) of the two orbits measured at their intersection or node. The hyperbolic conic is defined by two of its elements, pericynthion altitude and total energy. Maneuver initiation time is defined relative to the time of hyperbolic orbit pericynthion passage. For a given set of parameters, as defined above, initial pitch attitude, pitch rate and burning time are varied to achieve circular orbit conditions and initial yaw attitude is varied to achieve the desired relative inclination. In this context, the independent variables available for maneuver optimization are pericynthion altitude, initiation time and yaw rate. As previously mentioned the total energy and relative inclination will influence the optimum values of these parameters.

The first step of the optimization procedure was to determine the optimum value of initiation time for a co-planar deboost with a hyperbolic orbit pericynthion altitude of 80 nautical miles. Three values of total energy were used to demonstrate its effect on the initiation time and steering variables. The total energies were determined by specifying three values of pericynthion velocity representative of the range expected for free return orbits. Characteristic velocity, or ΔV, in excess of the impulsive deboost velocity, was used as a measure of propellant consumption. The impulsive deboost velocity is the difference between the hyperbolic pericynthion velocity and circular orbit velocity. The results of these studies are presented in Figure 6.2.4-2. It can be seen that the optimum initiation time varies slightly with pericynthion velocity. These results further indicate that propellant consumption is insensitive to initiation time in the optimum region. It is of interest to note also that the required pitch rate at the optimum initiation time is a function of pericynthion altitude.

The next step in the optimization procedure was to determine the effect of yaw rate on the propellant consumption for a required amount of plane change.

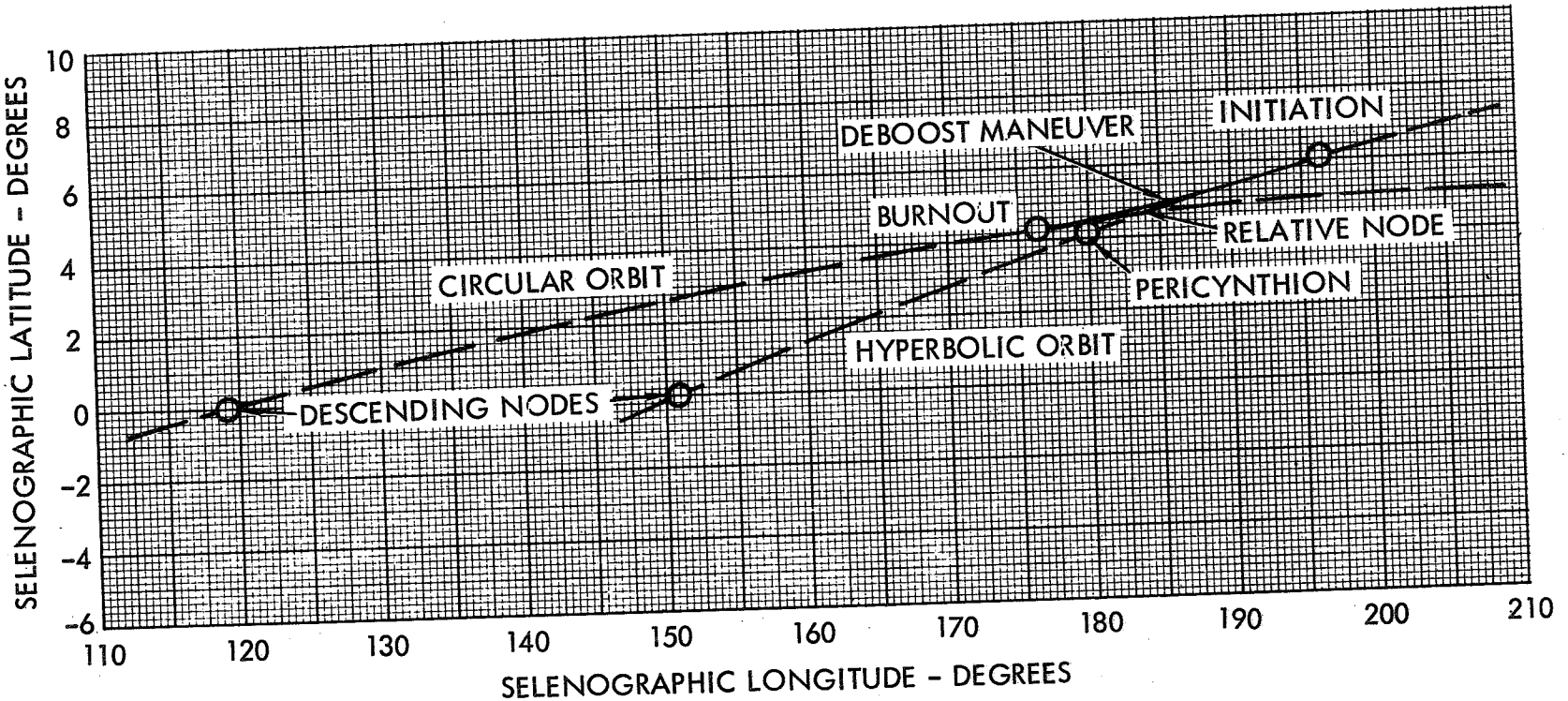

Figure 6.4.2-1. Hyperbolic Deboost Maneuver Geometry

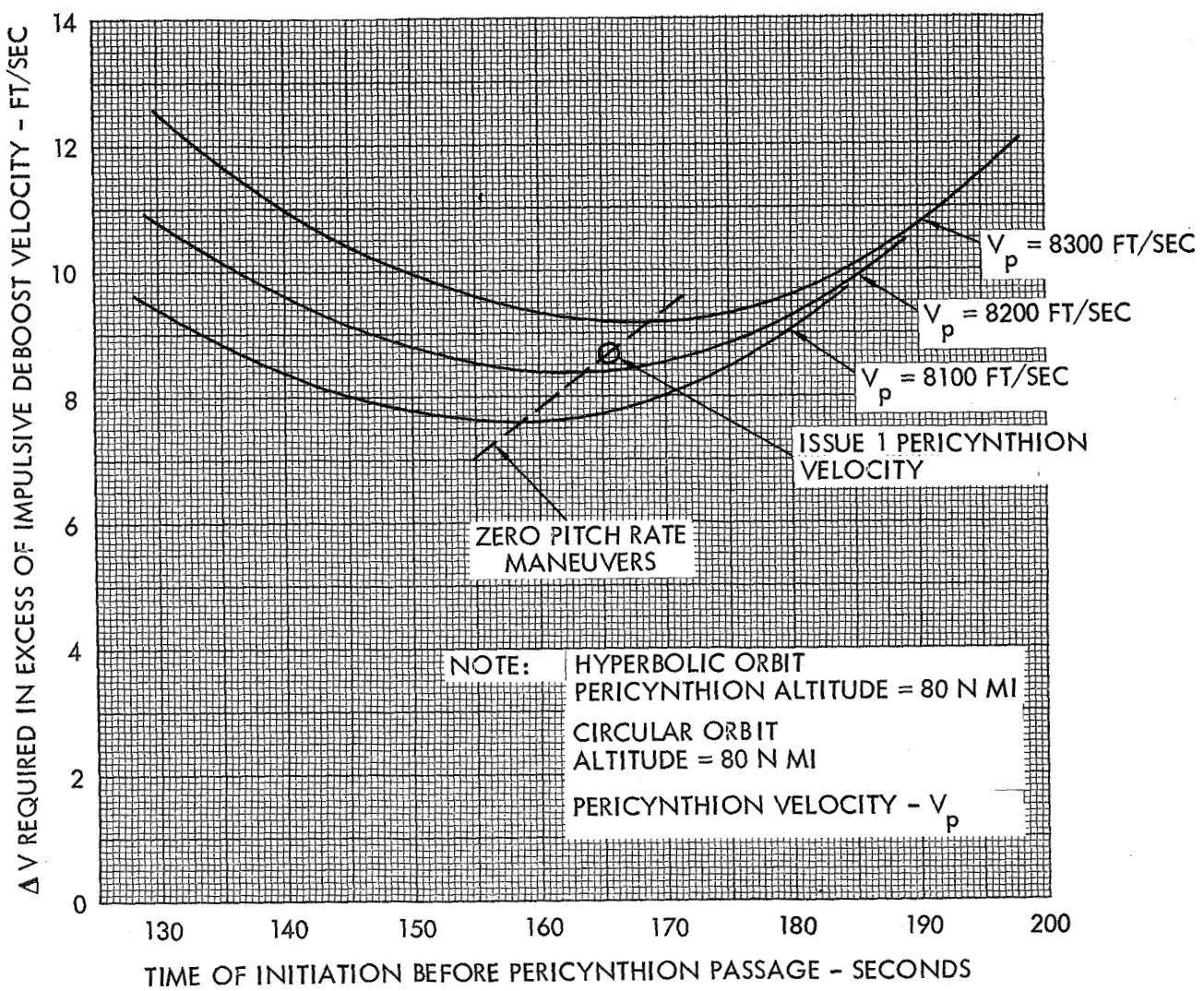

Figure 6.4.2-2. Coplanar Hyperbolic Deboost Optimization

Figure 6.4.2-3 presents this optimization for four values of plane change. It was found that constant yaw attitude (zero yaw rate) maneuvers were most efficient in producing plane change. It should be noted that yaw rate does control the location of the node of the initial and final orbits relative to the hyperbolic orbit pericynthion. It could, therefore, be useful as a selenographic nodal control parameter for the circular orbit and a second order optimization parameter in the selection of hyperbolic orbit total energy and relative inclination. Figure 6.4.2-4 presents characteristic velocity requirements (ΔV) as a function plane change magnitude for constant attitude yaw maneuvers. The pericynthion velocity of the hyperbolic orbit in this analysis was 8200 ft/sec at an altitude of 80 nautical miles. The effect of plane change on optimum initiation time is presented in Figure 6.4.2-5. In addition, yaw attitude has essentially no effect on pitch rate at the optimum initiation time.

The one remaining parameter to be optimized is the hyperbolic orbit pericynthion altitude. This analysis was started by optimizing initiation time for a co-planar deboost maneuver with a hyperbolic pericynthion altitude of 78 nautical miles. The energy of the hyperbolic orbit was held equal to that of an orbit with a pericynthion velocity of 8200 ft/sec at 80 nautical miles. Although this analysis was not completed at the time of writing, some preliminary results are compared in Figure 6.4.2-6. It can be seen that decreasing pericynthion altitude increases the characteristic velocity requirement. The pitch rate at the optimum initiation time for a pericynthion altitude of 78 nautical miles is increased in a negative sense to -0.03 degrees per second. Additional data indicate that the optimum pericynthion altitude will be slightly greater than 80 nautical miles and the pitch rate at the optimum initiation time will be very near zero.

The targeting of the free return trajectory for Issue 1 resulted in a hyperbolic orbit with a pericynthion altitude of 78.6 nautical miles and a pericynthion velocity of 8244 ft/sec. It was known that this value of pericynthion altitude was near optimum and was accepted on the basis that its relation to the true optimum could be defined. It was further concluded that a constant pitch and yaw attitude deboost maneuver would greatly simplify the lunar landing site targeting. The foregoing analysis indicated that a zero pitch rate maneuver would be very near optimum and this type of steering was thus adopted.

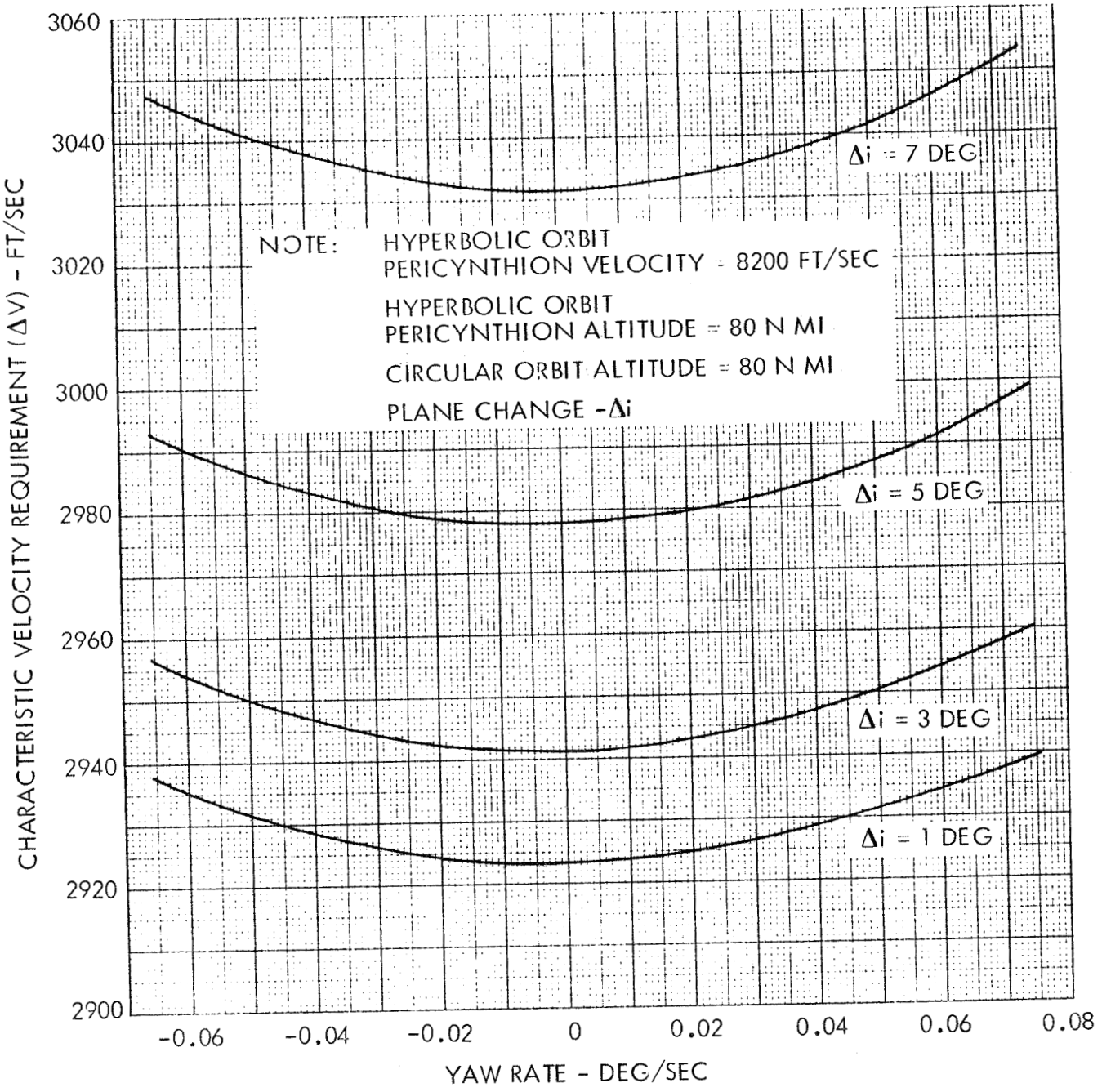

Figure 6.4.2-3. Yaw Maneuver Optimization

CONFIDENTIAL

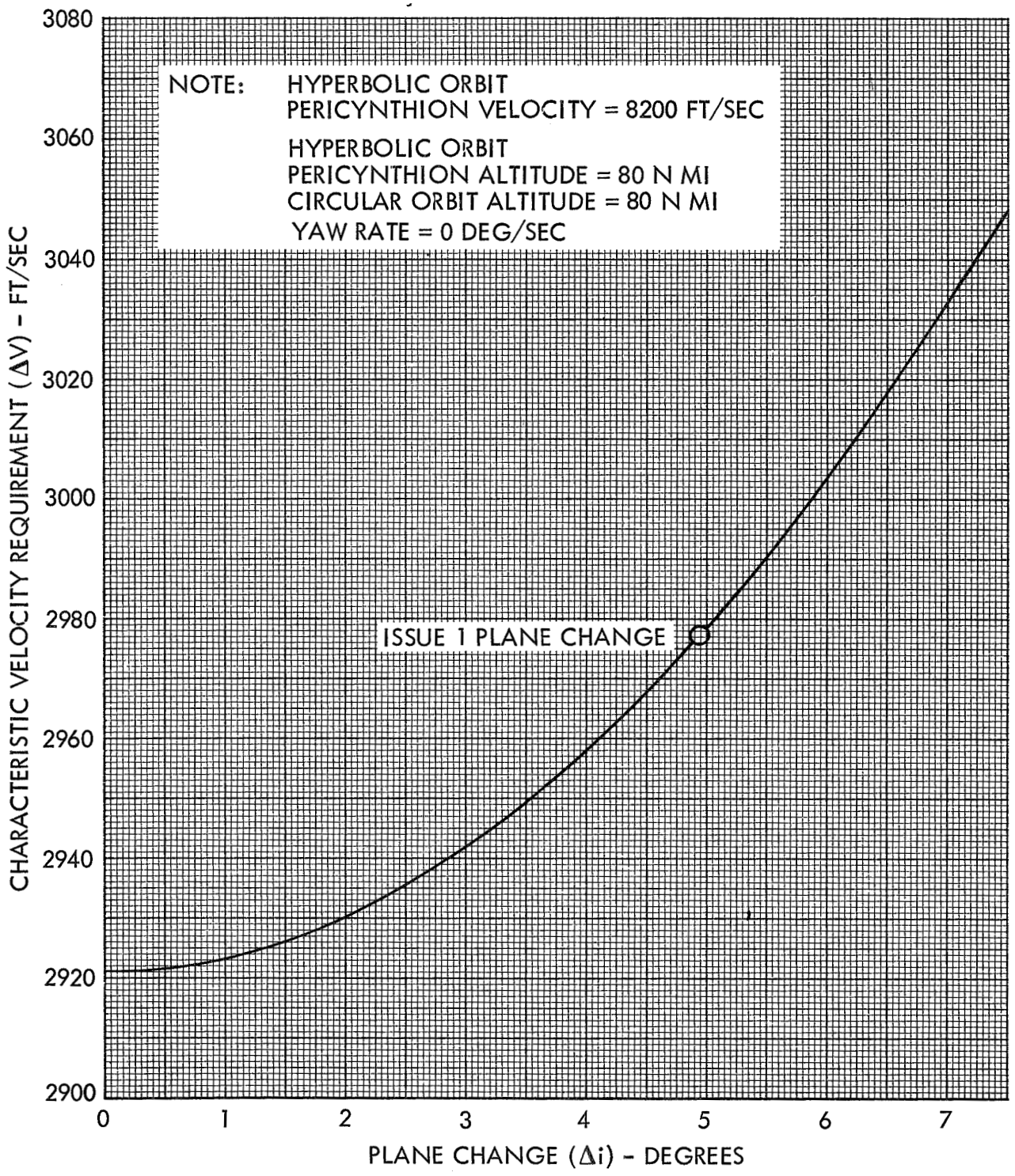

Figure 6.4.2-4. Plane Change Characteristic Velocity Requirements

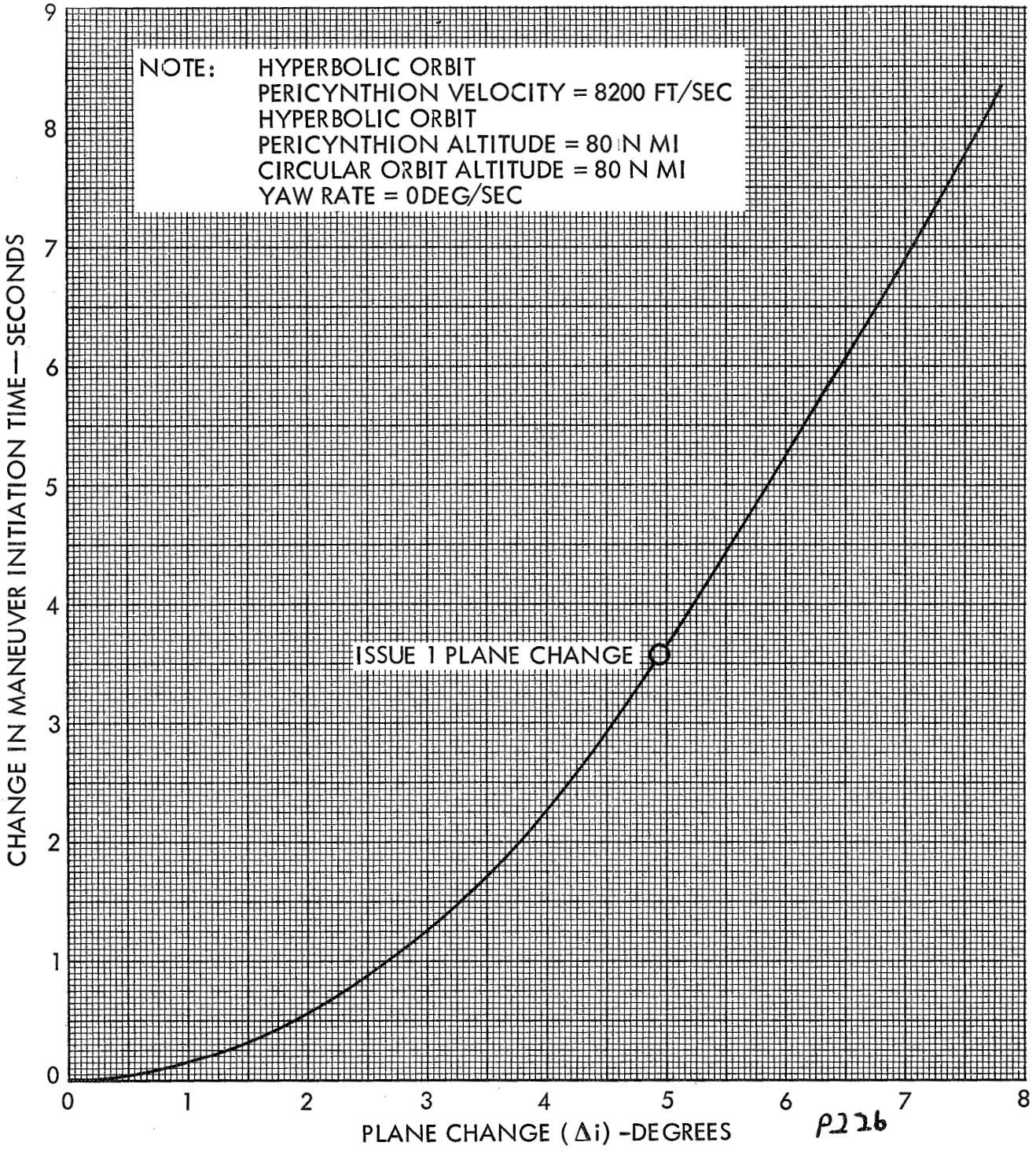

Figure 6.4.2-5. Effect of Plane Change on Maneuver Initiation Time

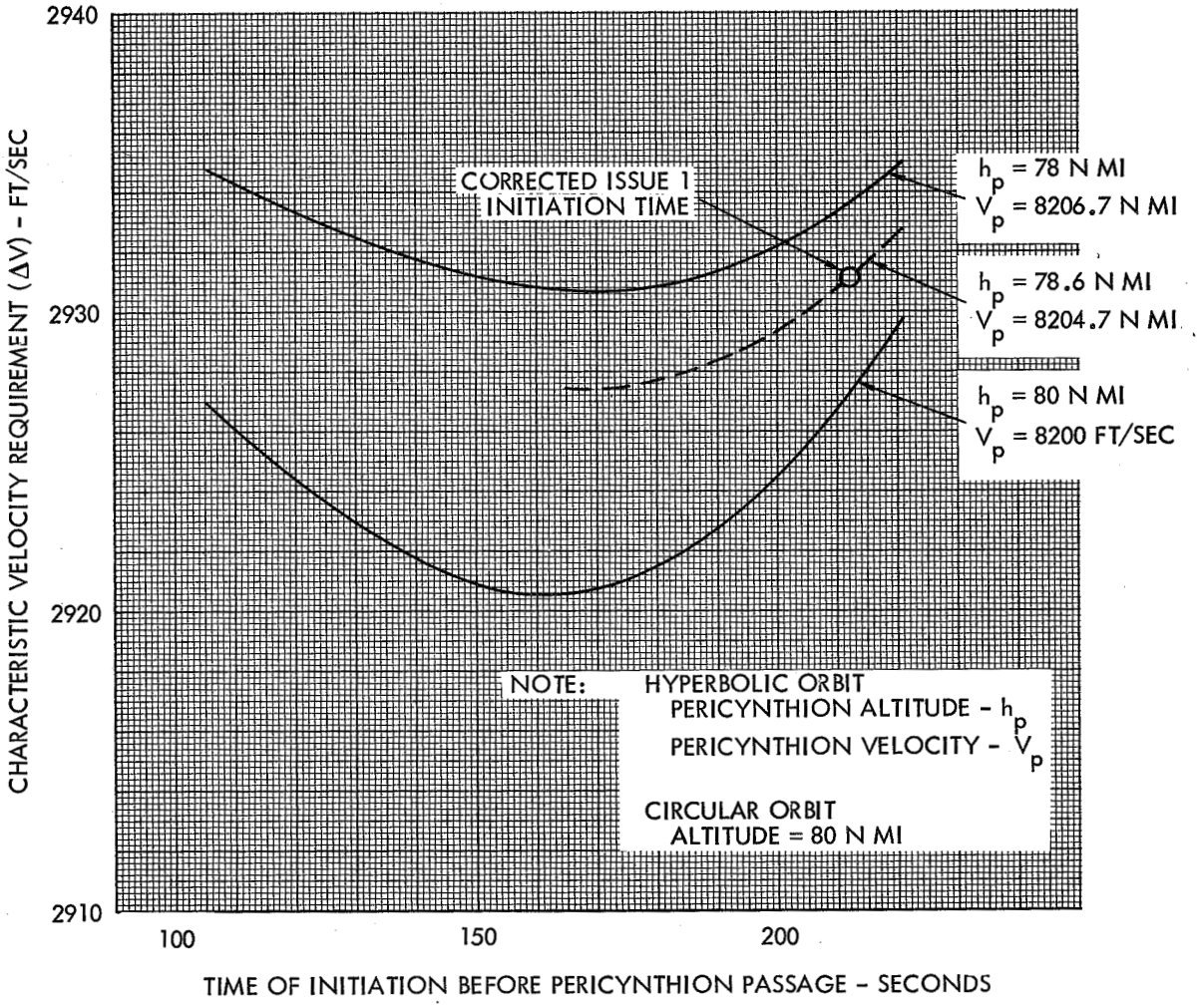

Figure 6.4.2-6. Pericynthion Altitude Optimization

The landing site targeting resulted in a hyperbolic deboost maneuver which produced a plane change of 4.95 degrees, was initiated 217.7 seconds before pericynthion passage and required a velocity increment of 3026 ft/sec. To compare this maneuver with the true optimum, the velocity requirements for a 78.6 nautical mile hyperbolic pericynthion altitude were interpolated on Figure 4.6.2-6 as a function of maneuver initiation time. This line then represents a co-planar deboost maneuver from a hyperbolic orbit with a pericynthion velocity of 8205 ft/sec. It is, therefore, necessary to correct the initiation time of Issue I to these conditions for a true comparison. The initiation time of the Issue I maneuver may be corrected to that of a co-planar maneuver with the aid of Figure 6.4.2-5. This figure indicates that the maneuver initiation time should be decreased by 3.6 seconds to be comparable with a co-planar deboost. The initiation time may further be corrected for the difference in pericynthion velocity with the aid of Figure 6.4.2-2. A two-second reduction in initiation time is indicated on the zero pitch rate line for a decrease in pericynthion velocity to 8205 ft/sec. The initiation time of Issue I, corrected to the conditions of Figure 6.4.2-6 is thus approximately 212 seconds. This point represents the zero pitch rate maneuver for a 78.6 nautical mile pericynthion altitude and indicates a characteristic velocity requirement of 2931 ft/sec. As a check, the velocity penalty for a plane change of 4.95 degrees and the pericynthion velocity difference added to this velocity requirement should equal the velocity requirement of Issue I. The velocity penalty for a 4.95 degree plane change is indicated to be 56 ft/sec on Figure 6.4.2-4 and the pericynthion velocity difference is 39 ft/sec between that of Issue I and Figure 6.4.2-6. The sum of these and 2931 ft/sec equal 3026 ft/sec and check quite well with the characteristic velocity requirement of Issue I. It can, therefore, be concluded from Figure 6.4.2-6 that the penalty incurred by the zero pitch rate assumption is of the order of 3 ft/sec. It is further indicated that increasing the pericynthion altitude to 80 nautical miles would decrease the characteristic velocity requirement by 7 ft/sec.

Transearth Injection Optimization

The transearth injection maneuver is initiated on the circular lunar orbit and constrained to burnout on a hyperbolic conic at some inclination relative to the circular orbit. The hyperbolic conic, initiation time, and the plane change

requirement are defined as they were in the hyperbolic deboost maneuver. The injection maneuver is performed by varying the initial pitch attitude and the burning time to achieve the desired hyperbolic conic and initial yaw attitude to achieve the desired relative inclination. The optimization variables available for this maneuver are, therefore, pitch rate, yaw rate, initiation time and pericynthion altitude

Time limitation did not permit the optimization of the transearth injection maneuver over a range of hyperbolic orbit energies and relative inclinations. The maneuver was optimized only for the one combination of these quantities required for Issue 1. Yaw rate was eliminated as an optimization variable on the basis of the results of the hyperbolic deboost study. The effect of varying pitch rate, to achieve a specified hyperbolic conic, is to control the burnout point on that conic and, therefore, the maneuver initiation time with respect to pericynthion passage. The hyperbolic deboost study indicates that at the optimum initiation time, pericynthion altitude having been optimized, the pitch rate is near zero. It was assumed that this relationship also exists in the transearth injection maneuver. The maneuver was, therefore, optimized, using zero pitch rate, by minimizing propellant consumption with respect to initial pitch attitude. Pericynthion altitude is controlled by initial pitch attitude and is optimized as a result. The zero pitch rate assumption insures that initiation time with respect to pericynthion passage is optimum, thus the maneuver is completely optimized. The results of this optimization are presented in Figure 6.4.2-7. It should be noted that the optimum value of initial pitch attitude, indicated here, is unique to the hyperbolic orbit energy and plane change requirement of Issue 1.

6.4.3 LEM Operations

Equiperiod Deboost

No optimization was performed on the basis that a constant thrust attitude maneuver is near optimum for the short duration of powered flight.

Descent Maneuver

Due to the complexity of the descent maneuver profile, time was not available to conduct optimization studies. One area which will be investigated

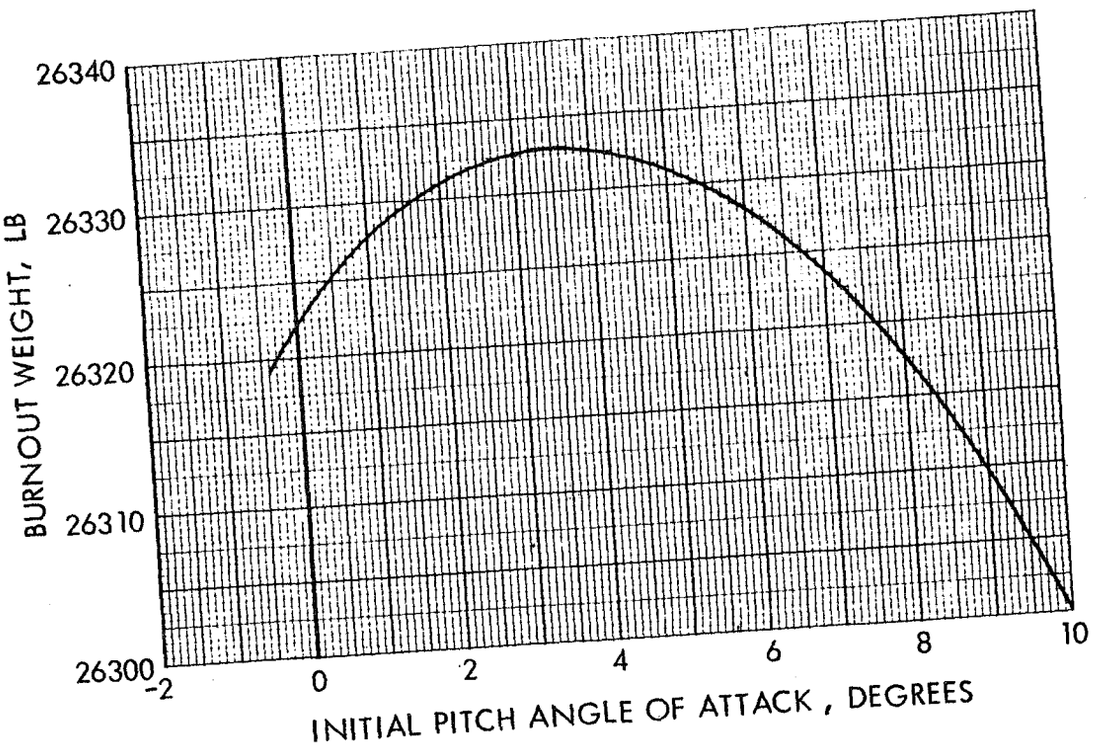

Figure 6.4.2-7. Transearth Injection Optimization

in the future, however, is the tradeoff between the velocity at the 10,000 foot transition and the total ΔV of the first two phases.

Ascent Maneuver

The ground rules of Issue 1 are such that a yaw maneuver must be performed during the ascent phase. Efforts were, therefore, directed towards the optimization of maneuvers with yaw using the basic co-planer ascent profile of Issue 0. The definitions of maneuver parameters with yaw are presented in Figure 6.4.3-1. Plane change is defined as the change produced in the azimuth of the velocity vector at burnout, measured with respect to a line through the launch site and the burnout point. The change in launch azimuth required to produce a plane change is also measured with respect to this line.

The plane change requirement introduces one addition constraint at the maneuver burnout. Two steering variables, initial yaw attitude and yaw rates, were introduced at the end of the high pitch rate phase, thus providing one parameter for optimization. It was found that the effect of initial yaw attitude or angle of attack was to produce a change in launch azimuth and essentially no plane change. This is due to the low magnitude of the velocity vector at the end of the high pitch rate phase. A parametric study was, therefore, conducted to define the maneuver characteristic velocity requirement (ΔV) as a function of plane change magnitude, using only yaw rate steering. These data are presented in Figure 6.4.3-2. In addition, launch azimuth change and powered flight maneuver angle are presented as a function of plane change magnitude in Figures 6.4.3-3 and 6.4.3-4, respectively. These data were used to determine the ΔV requirements as a function of lunar surface stay time as presented in Section 6.3. Having selected the stay time duration for Issue 1, these data were further useful in determining the required launch azimuth and launch time for the rendezvous search.

Rendezvous Maneuver

No optimization was performed here on the basis that a constant thrust attitude maneuver is near optimum for the short duration of powered flight.

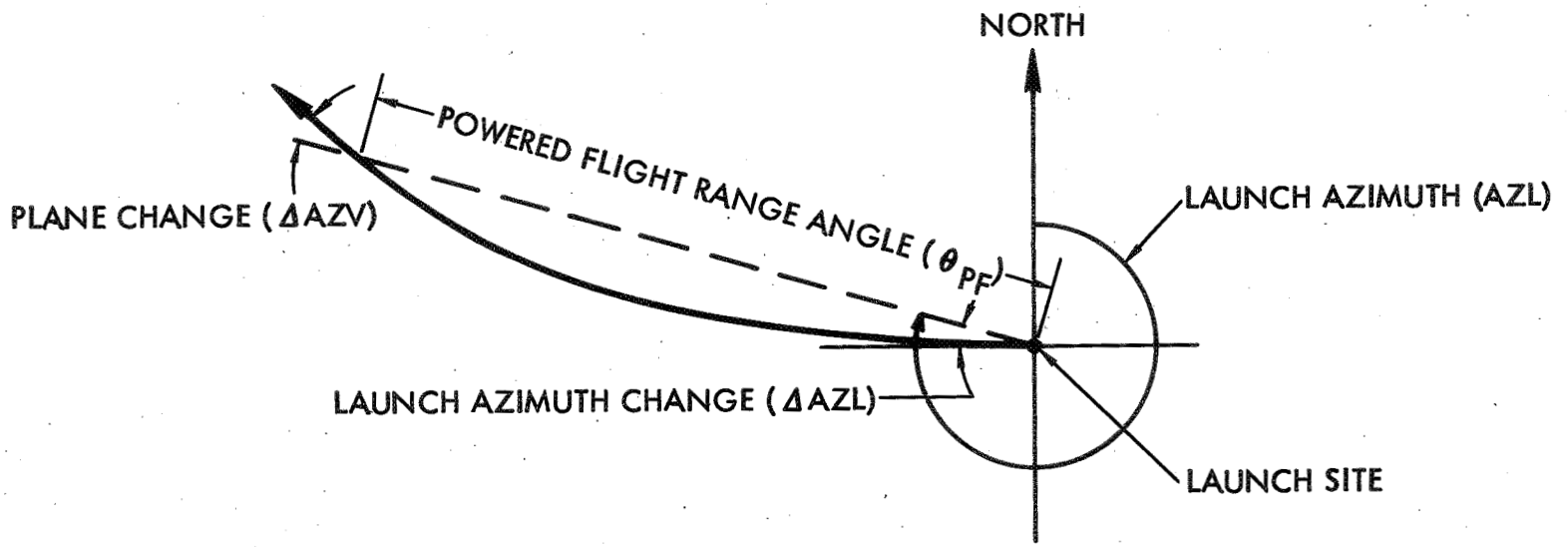

Figure 6.4.3-1. Ascent Maneuver Geometry

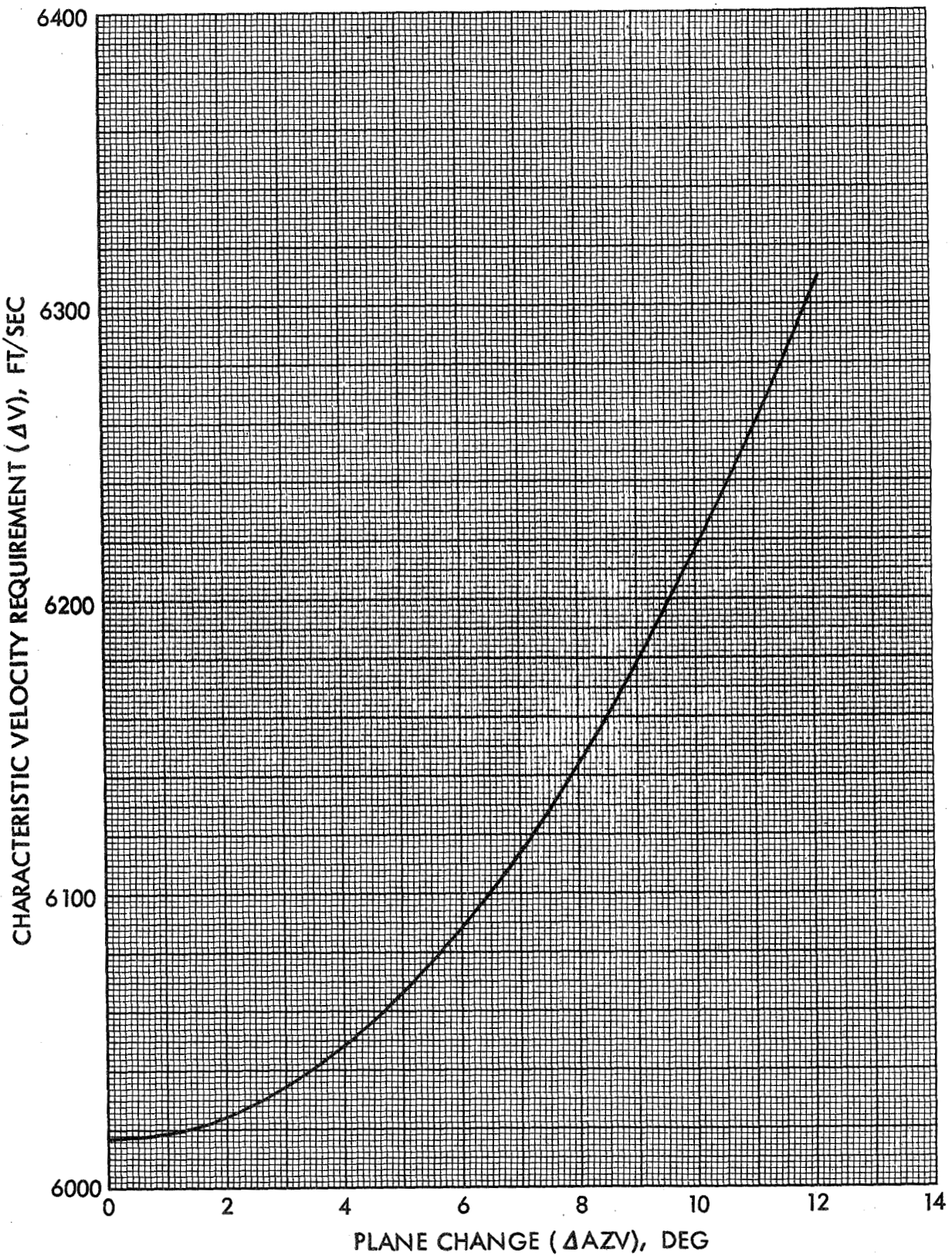

Figure 6.4.3-2. Ascent Phase Characteristic Velocity Requirements with Plane Change

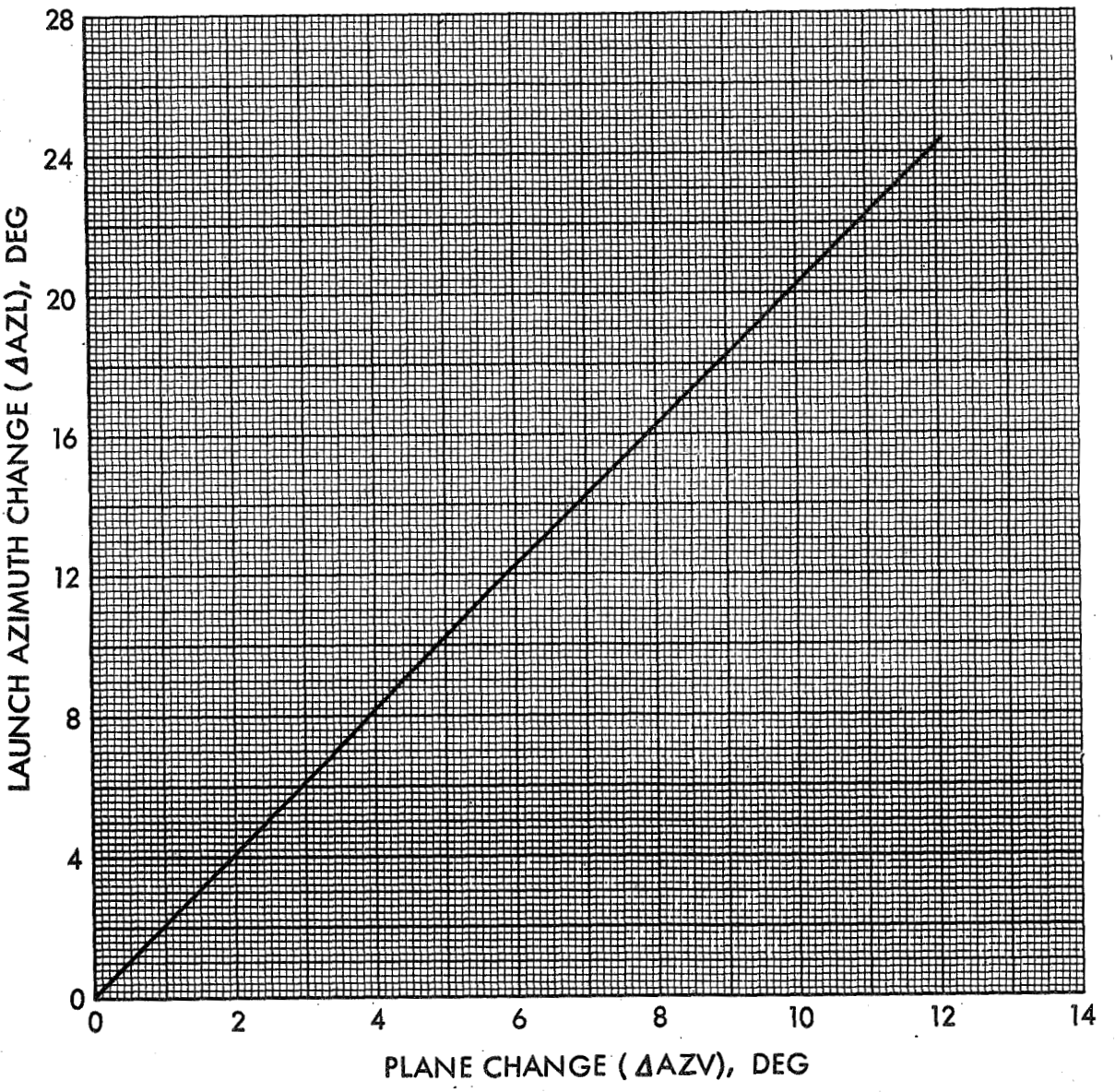

Figure 6.4.3-3. Effect of Plane Change on Launch Azimuth

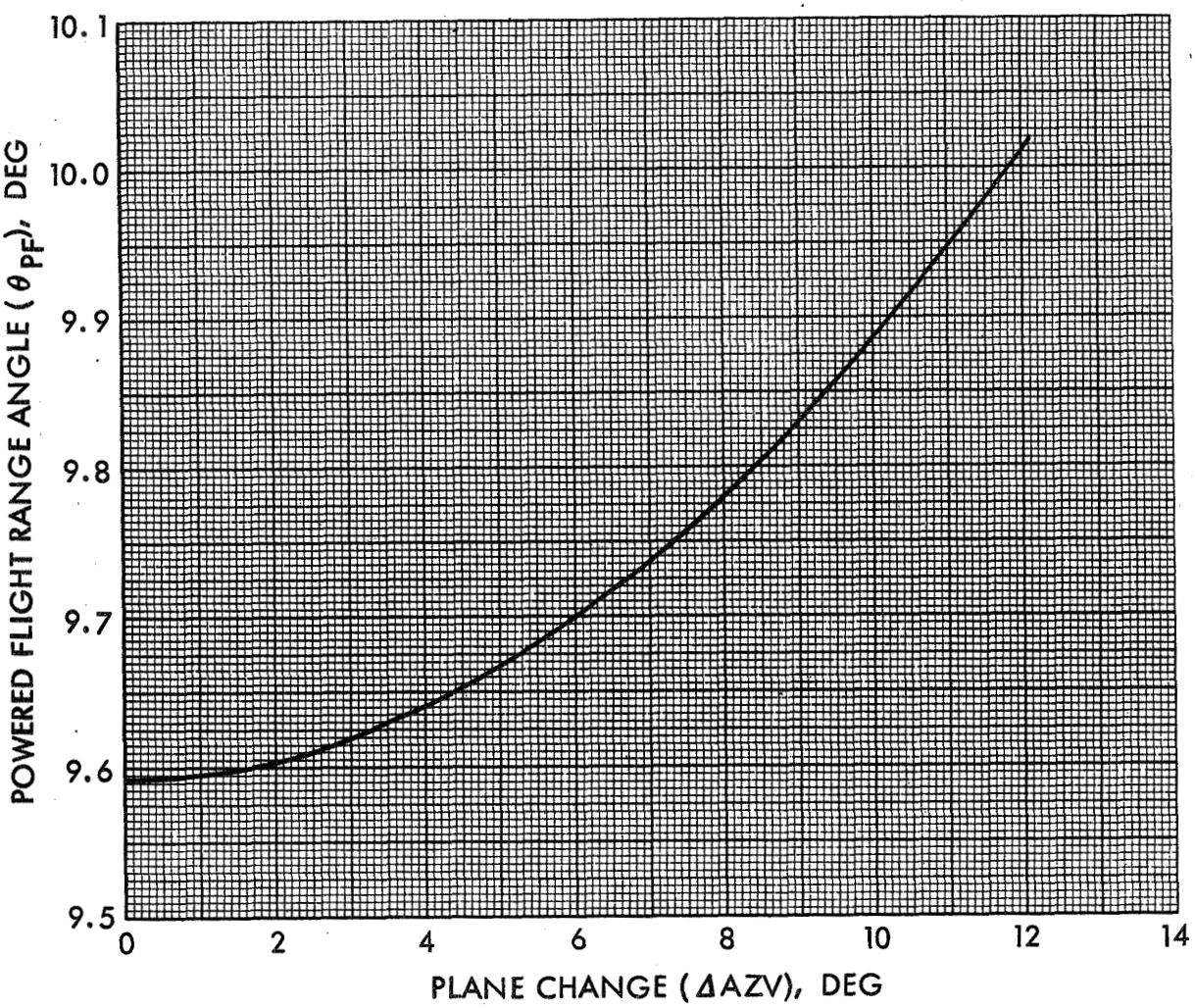

Figure 6.4.3-4. Effect of Plane Change on Powered Flight Range Angle

6.5 Launch Window Duration and Effects of Powered Flight Performance

The duration of the daily launch window is determined by the range of launch azimuths that are available from a given launch site. Further length is given the window by the amount of time spent in the parking orbit which is usually designated either short or long coast. It has been shown in Figure 6.2-19 how the length and location of the two daily windows shifts during the study period. The type 6 trajectory or long coast occurs early each day with a total length of 275 minutes as the azimuth sweeps from 72 to 108 degrees. The second daily window has a length of 290 minutes, for the short coast, type 5 trajectories. The period during each day remains the same, but the time liftoff moves ahead by six minutes a day for the long coast and 84 minutes for the short coast. None of the days during this period is restricted by the requirement that the lunar landing site be in earth shine and not in sunshine. There is a further small variation in launch time at each launch azimuth which depends on the return inclination selected for the free flight trajectory. However, this amounts to at most about two minutes on any given day.

The constraints on the trajectory are many although they have very little effect in decreasing the launch window. The most significant restraint on length of the launch opportunity is the launch azimuth which cannot be loosened at present. The selection of a pericynthion altitude with a free return trajectory restricts the trip time to that one which is consistent with these limits and consequently this limits the injection velocity required to its present nominal value.

Perhaps the first cutoff that can be made is to eliminate the short coast trajectories from further consideration. This is done on the basis of the outbound trajectories inclination to the lunar plane which ranges in value from 40 to 60 degrees, whereas, the suggested allowable limit is 10 degrees. It has been pointed out previously how these short coast trajectories also require more velocity at the moon than the long coast trajectories (compare Figures 6.3-7 and 6.3-8). Thus, effectively half of the daily window has been eliminated in one fell swoop.

A further limit to the return inclinations will be to prevent any difficult situations in recovery arising from inclinations approaching 90 degrees. The map indicating touchdown points for the free return trajectories was presented in Figure 6.2-18. Although all of the return inclinations returned the spacecraft to a reasonable latitude in this case, it probably would be wise to limit the return inclination to about 35 degrees. This assures a landing, in this case, in very favorable territory for a sea recovery, and none of the touchdown points are in "hostile" territory. Limiting return inclination does not shorten the window.

Targeting to a preselected fixed landing site at the moon will generally require a plane change during hyperbolic deboost to put the spacecraft into an orbit which passes over the landing site. This is required to allow the LEM to make an in-plane descent. The additional velocity required to execute this change does not exceed that available in the Service Module for this phase of the mission. The lunar geometry of the corrected orbit is such that none of the LEM ascent restrictions are exceeded. Compare the allowable inclination on Figure 6.3-2 with the actual corrected inclination of the orbit on Figure 6.3-4. Even the 90 degree return inclinations are within the allowable inclinations for minimum stay time and those with 40 degree return inclinations or less would apply for the 24 hour stay time. Thus, no limit exists because of lunar geometry of the LEM or SM capability.

In return requirements, the road becomes more difficult. It has been shown that the SM has the velocity capability to provide almost any return in Figure 6.3-15, which leaves two variables to constrict the problem. The first is the fixed landing site, which in itself is not too difficult as sites in both the northern and southern hemispheres are given to allow for positive and negative declinations of the moon. This would be sufficient if the re-entry maneuver angle were unlimited, and the spacecraft could always get back to one of the sites. But the geometry traps the return on one day, the 30th of January. Return is not possible to San Antonio with a 50 degree re-entry maneuver angle, and return is not possible to Woomera until more than 24 hours later. This is due to the moon being at almost zero declination at departure and with an in-plane angle of greater than 160 degrees in the return trajectory. It

is difficult to find an angle short enough or long enough to find either of the landing sites. Shorter re-entry maneuver angles are possible on other days at greater expenditure in return velocity.

Thus, in arriving at a final picture of the launch window for the period, only the short coast, type 5 trajectories were eliminated. That is, other than the problem of return on 30 January, all of the type 6 trajectories are practicable. This allows judicious selection of all of the parameters within the trajectory to assure that the ground rules are met.

6.6 Re-entry Studies

No re-entry guidance scheme was provided to STL for the Apollo mission, so a simple three-phase re-entry profile has been simulated for the first Apollo reference trajectories. An alternative scheme proposed by R. C. Wingrove of NASA/Ames was investigated and rejected. A combination of the two methods was also eliminated after a cursory study.

In all of the re-entry trajectory simulations, the sensible atmosphere is assumed to begin at 400,000 feet as defined by the 1959 ARDC model. The CM has a W/C_DA of 57 pounds per square foot at a maximum L/D of 0.4 at 33 degrees angle of attack. Lift modulation is achieved by rolling the CM, resulting in an effective L/D range between +0.4 and -0.4. Motion of the initial trajectory plane caused by rolling the lift vector is neglected. The only vehicle constraint considered is a 10 g acceleration limitation.

The three-phase re-entry profile consists of descent from re-entry with maximum lift until horizontal flight is reached. The second phase covers the ascent from this point until the flight path once again reaches the horizontal, and the third phase covers the final descent to impact. Lift is modulated during the final two phases to achieve the desired maneuver angle within the CM acceleration limits.

The study indicates that the re-entry maneuver angle is relatively independent of entry velocity and inclination, but very highly dependent upon re-entry flight path angle and latitude. A velocity range of ±100 feet per second or an inclination range from 0 to 36 degrees will cause a negligible effect on

maneuver angle, as is shown in Figures 6.6-1 and 6.6-2. The effect of entry flight path angle is shown in Figure 6.6-3 for an equatorial re-entry location. This figure will vary with the latitude of re-entry, as shown in Figure 6.6-4. The necessity to closely control re-entry flight path angle and roll angle (i.e., L/D) is evident from the graphs. For instance, for an L/D during the final two phases of +0.05, a change in the re-entry angle from 96.6 to 96.4 causes a 28 degree change in maneuver angle for an equatorial entry. This problem is particularly serious if computing machines are iterating on any of these parameters to achieve a specified landing site.

An alternate re-entry scheme as presented in Reference 6.6-1 was examined. In this method, L/D is not fixed in each phase but is varied according to the relationship $L/D = K\dot{H}$ where K is a fixed constant and $\dot{H}$ is the time derivative of altitude. Figure 6.6-5 shows example results of this method. The problem of severe entry flight path angle limitations is not relieved with this scheme. Selection of a proper L/D is replaced by selection of a proper K factor. Larger variation in maneuver angle with entry velocity, and therefore with inclination of the transearth orbit, was experienced with this scheme. In no case examined was the acceleration limit of 10 g's exceeded with this method, but the low maneuver angles at which the limit is exceeded with a three phase re-entry were never achieved. This can be seen by comparing Figures 6.6-3 and 6.6-5. Since this method seemed to offer no clear advantages over the three phase re-entry, it was rejected.

One additional step, that of combining the two re-entry schemes, was examined briefly. This combination gives the relationship

$$L/D = K_1 + K_2 \dot{H}$$

Reference 6.6-1. "A Study of Guidance to Reference Trajectories for Lifting Re-entry at Supercircular Velocity" NASA TR R-151, by Rodney C. Wingrove, 1963.

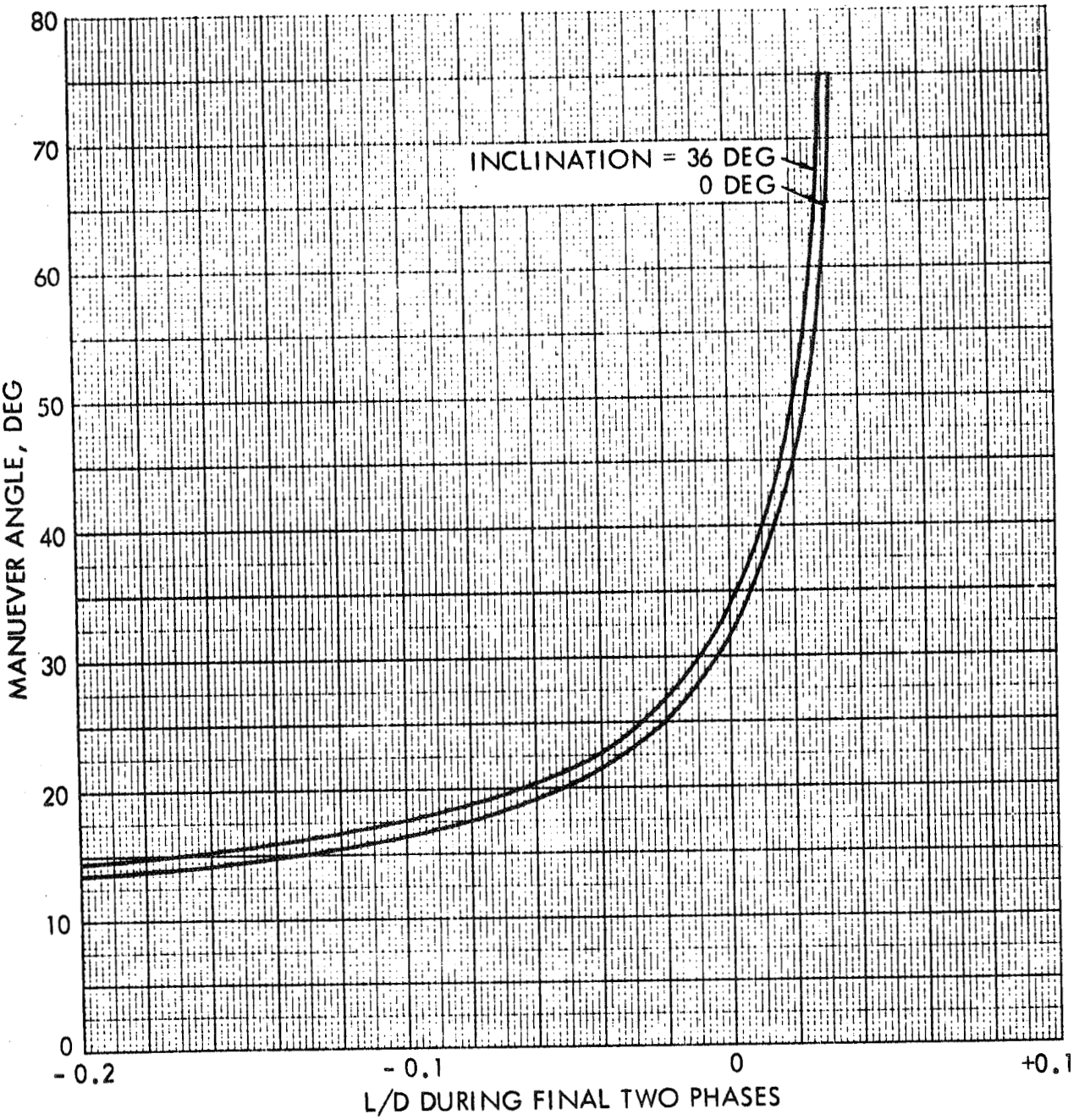

Figure 6.6-1. Maneuver Angle Variation with Inclination of Transearth Orbit for a Typical Case

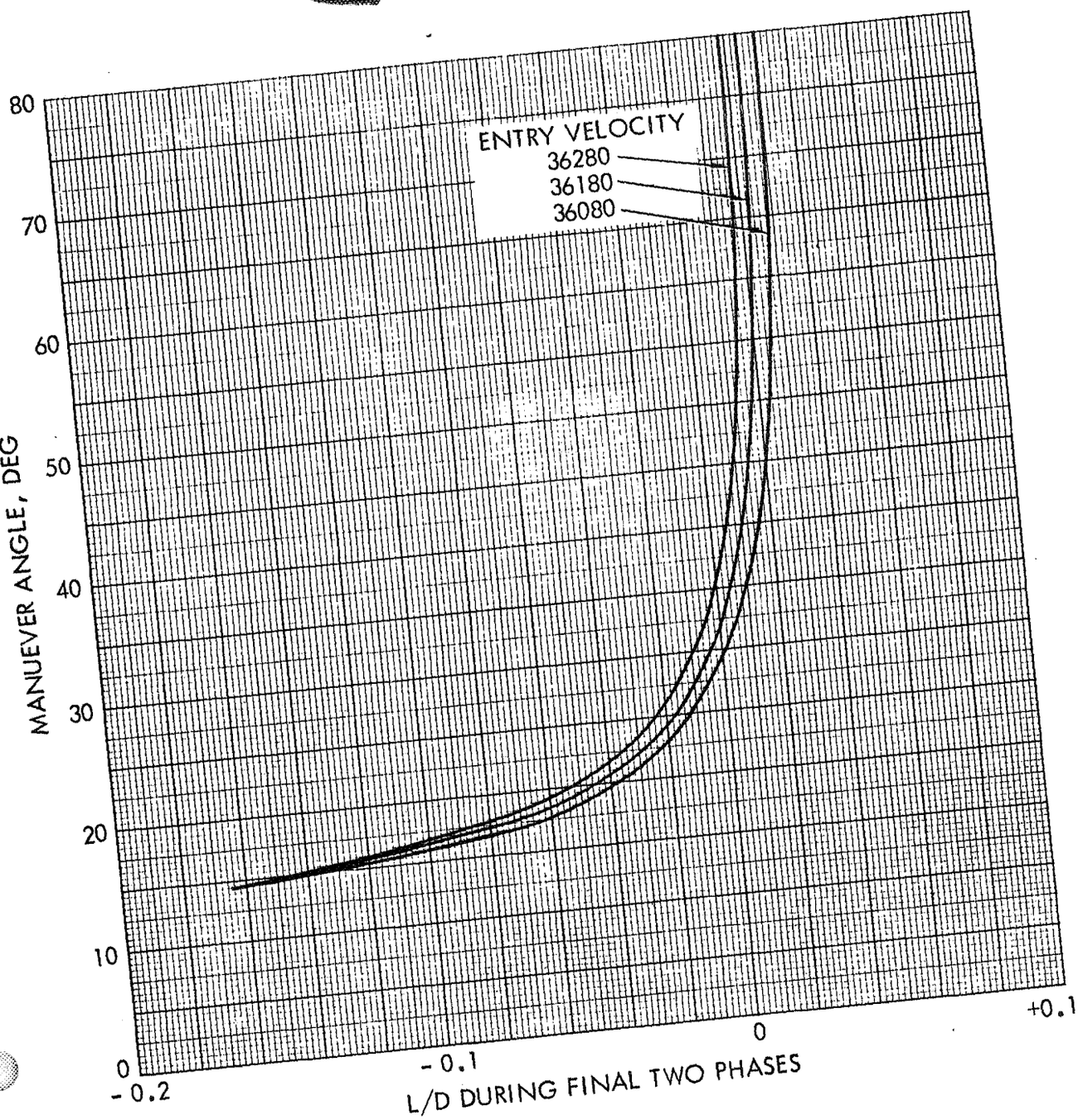

Figure 6.6-2. Maneuver Angle Variation with Entry Velocity for a Typical Case

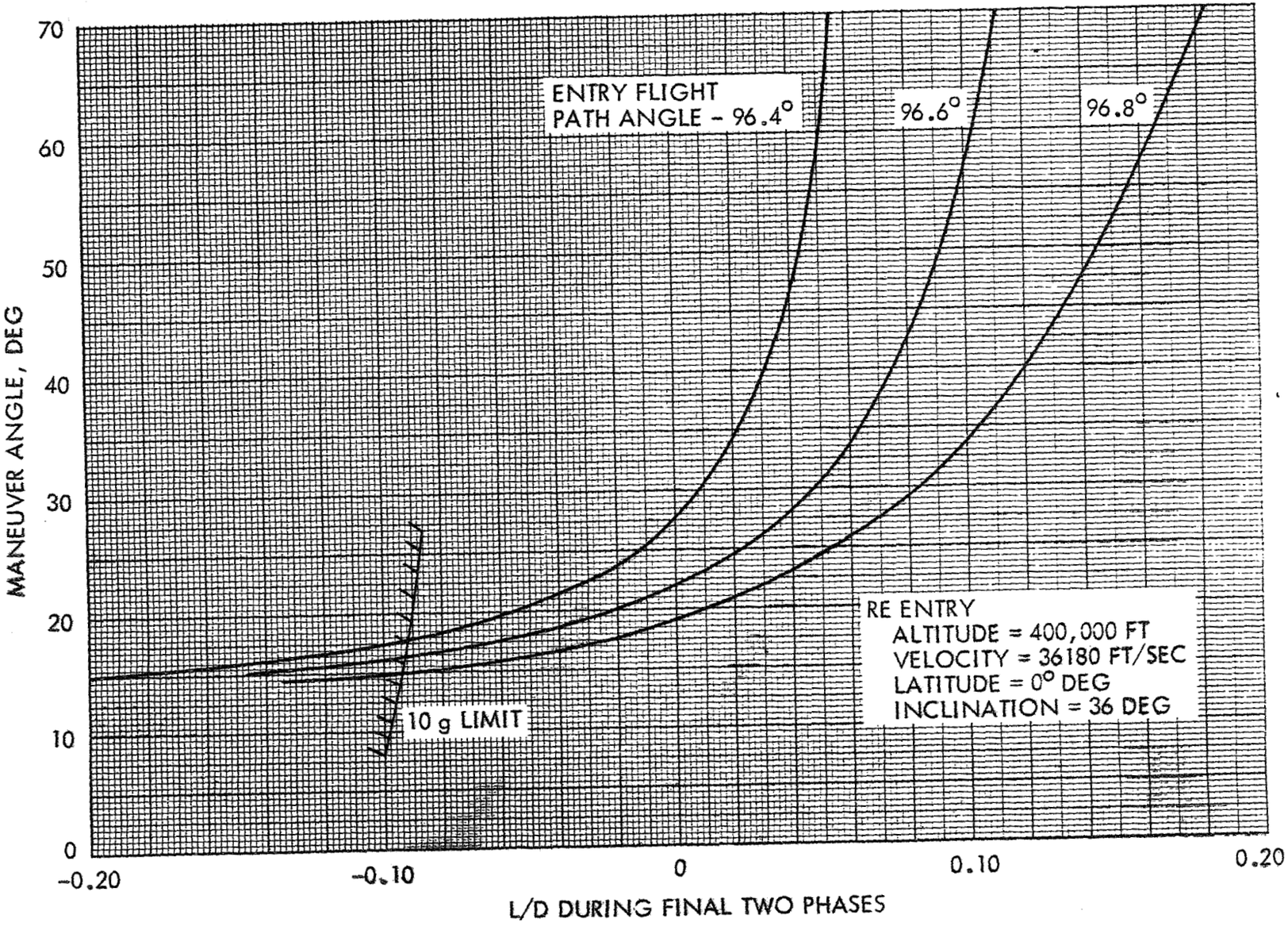

Figure 6.6-3. Variation of Re-entry Maneuver Angle with L/D and Entry Flight Path Angle

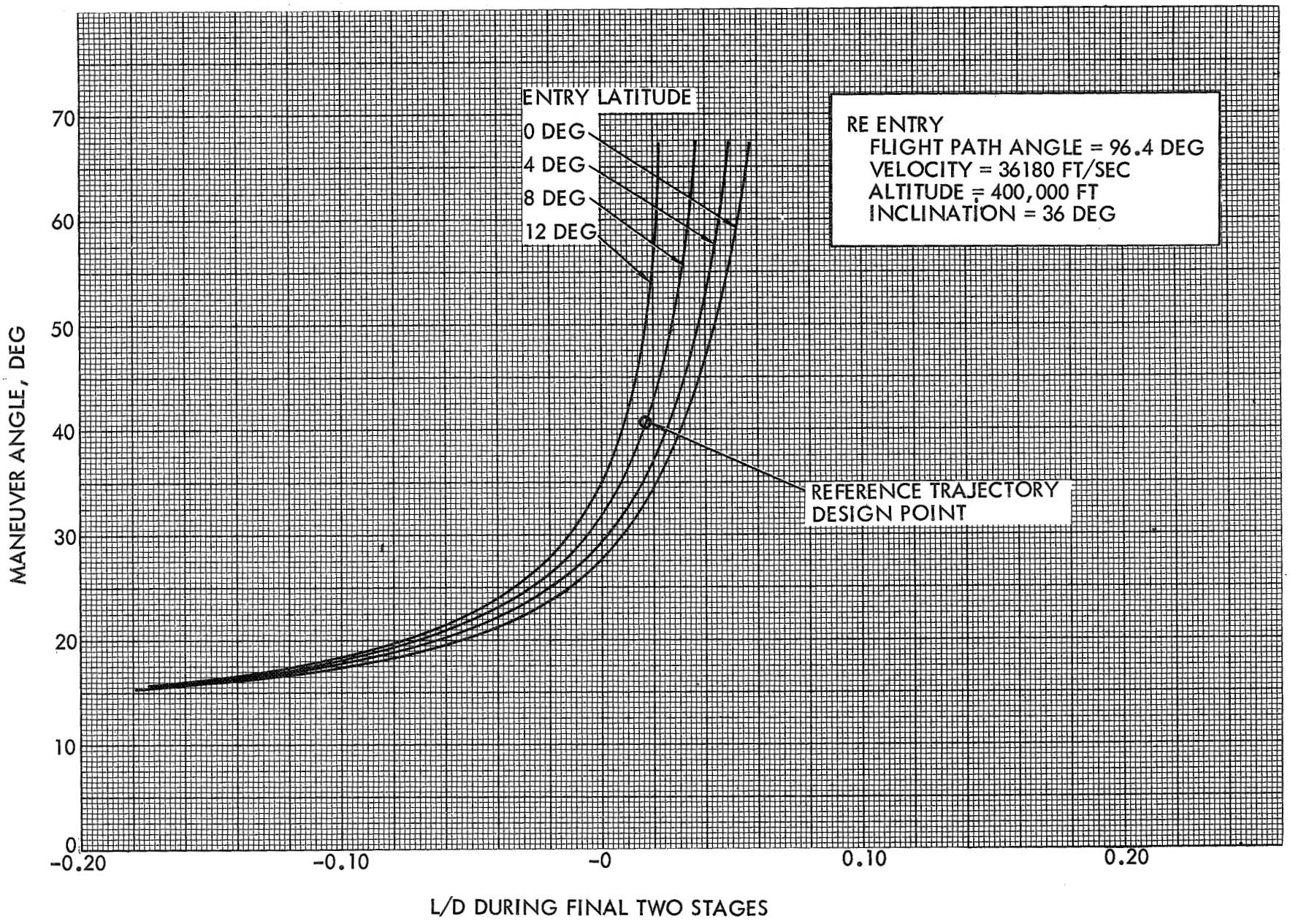

Figure 6.6 4. Effect of Re-entry Latitude on Maneuver Angle

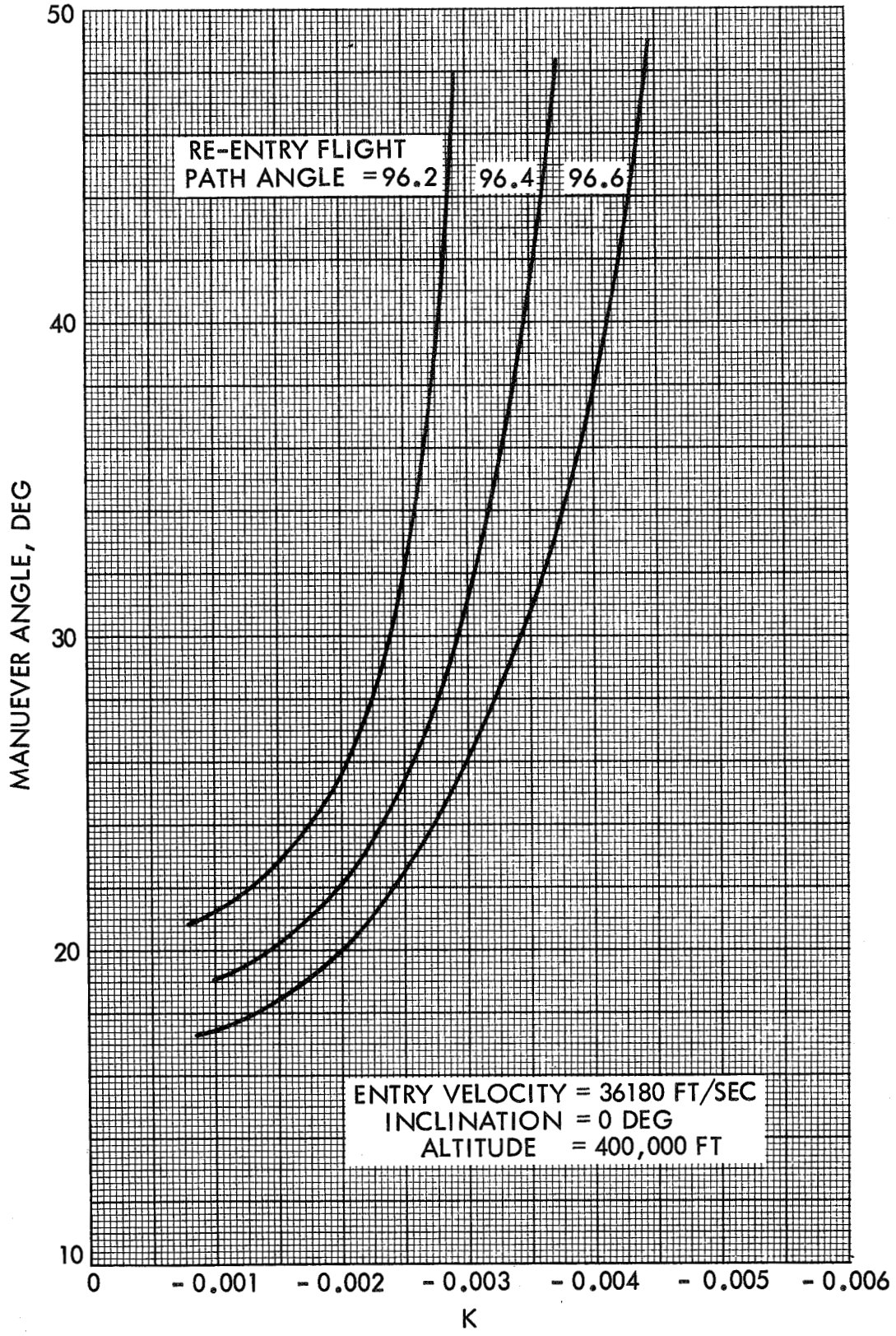

Figure 6.6-5. Variation of Maneuver Angle with Entry Flight Path Angle for Wingrove Method

When K_1 is zero, a pure Wingrove solution results; when K_2 is zero a three-phase re-entry is performed. This method was found to exhibit the worst qualities of each of the other methods. To make any significant change in maneuver angle over the three phase solution required values of K_2 which result in an L/D greater than 0.4. Also, the low decelerations experienced with the Wingrove method were not maintained with the combined method. The net effect is a very limited range of permissible values of K_1 and K_2.

It should be noted that these methods were examined for ease of use in a computer and simplicity. The problems of astronaut control, guidance system errors, on-board computers, etc., were neglected.

[redacted]

This doc[redacted]the national defe[redacted]

7.0 Range Safety Maps

7.1 Introduction

A map and other data have been developed to aid in the evaluation of the S-V range safety problem. The information presented below has been computed using the same S-V configuration data as used in the reference trajectory. The ascent flight profile has been optimally shaped for maximum burnout weight in the parking orbit using reference trajectory optimization variables.

7.2 Graphical Data

Figure 7.2-1 is developed for five launch azimuths: 72, 80, 90 (reference trajectory design point), 100, and 108 degrees. The figure illustrates the locus of instantaneous impact points determined by the ballistic trajectory that the vehicle would take at any instant if the thrust ceased. The impact points are computed including the effect of earth's rotation but without drag. Nominal impact points of the S-I and S-II stages are noted. Down range from S-II impact, loci are noted which correspond to impact points of the S-IVB stage if its thrust ceased at the indicated times in the powered flight trajectory.

Table 7.2-I gives the nominal impact point coordinates of the S-IC and S-II stages.

This [illegible] is furnished by the [illegible] organization of [illegible]

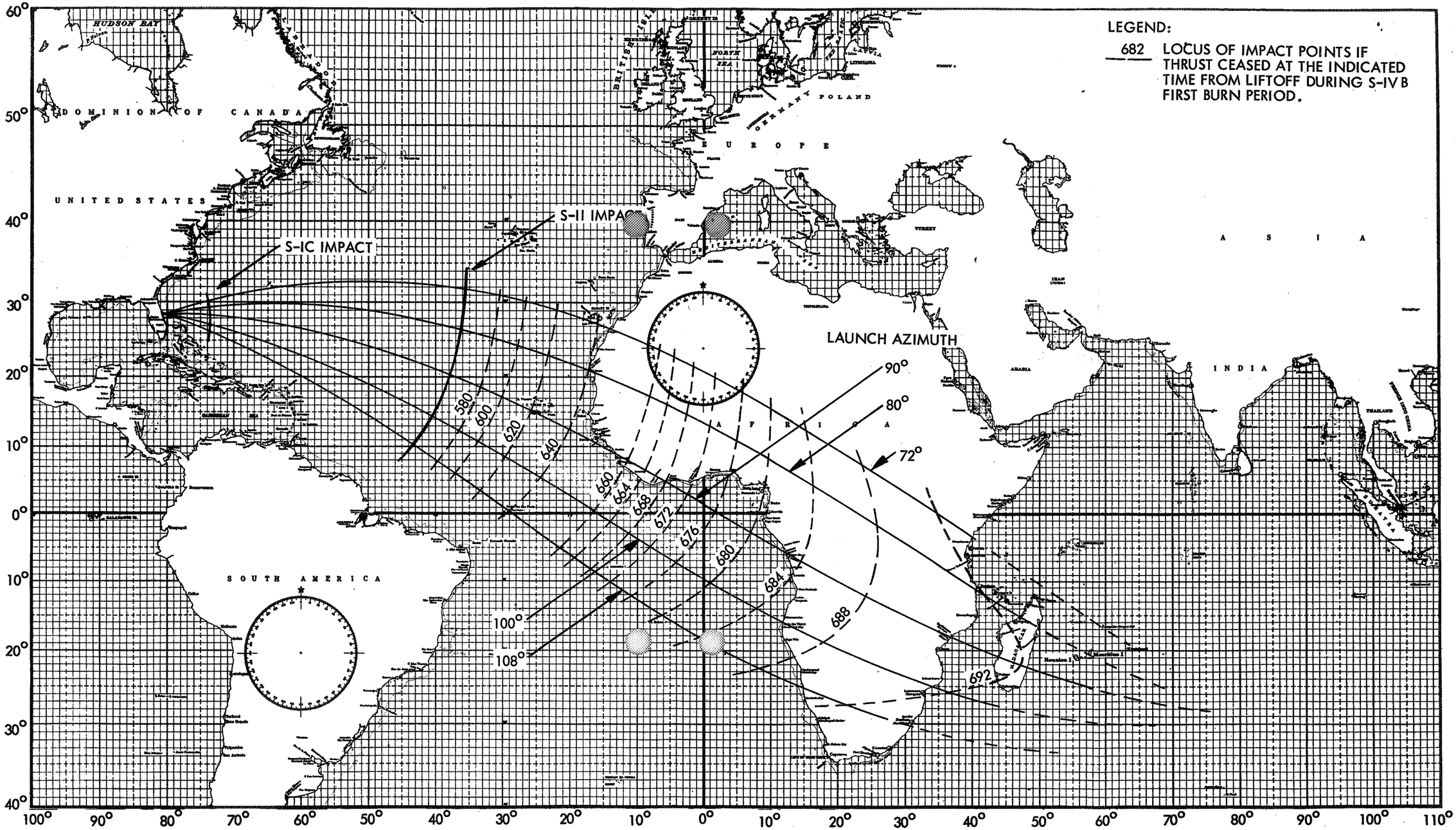

Figure 7.2-1. Earth Launch Phase - Instantaneous Impact Point Traces for Launch Azimuths of 72, 80, 90, 100, and 108 Degrees

Table 7.2-I. Nominal Stage Impact Coordinates

Stage	Azimuth (deg)	Latitude (deg N)	Longitude (deg E)
S-IC	72	30.261	-73.991
	80	29.427	-73.815
	90	28.367	-73.792
	100	27.317	-73.971
	108	26.511	-74.270
S-II	72	31.687	-35.547
	80	26.670	-36.266
	90	20.536	-38.032
	100	14.739	-40.745
	108	10.399	-43.434

8.0 Communication and Tracking Maps

8.1 Introduction

Maps and other data have been prepared in order to illustrate the amount of vehicle and spacecraft visibility available to the Mercury, AMR, and DSIF ground station networks during the earth parking orbit, translunar, circumlunar, and transearth trajectories. The maps and graphs are developed for the reference trajectory and are based on the ground station configuration and constraint data given in Section 3.2.3.

8.2 Graphical Data

Figures 8.2-1 through 8.2-3 show the relationship between ground station visibility circles and the vehicle ground track while in earth parking orbit. A visibility circle is the radial projection on the earth's surface of the intersection of the station visibility cone (constrained by minimum radar elevation angle) with a spherical surface whose altitude is everywhere equal to the orbit altitude (in this case, 100 nautical miles). Since this technique is applicable only to circular orbits, neither the powered flight trajectory to the parking orbit nor the translunar injection phase ground tracks have been shown on these figures.

Figures 8.2-4 through 8.2-6 give the station visibility durations of the Mercury, AMR, and DSIF networks, respectively, during the earth parking orbit phase.

Figures 8.2-7 and 8.2-8 give visibility durations for the three networks during the translunar flight. Mercury and AMR data are terminated shortly after injection because of slant range limitations.

Figure 8.2-9 gives DSIF sighting data for the circular lunar orbit of the Command Module.

Figures 8.2-10 and 8.2-11 give appropriate sighting data on the transearth trajectory phase.

Page intentionally left blank

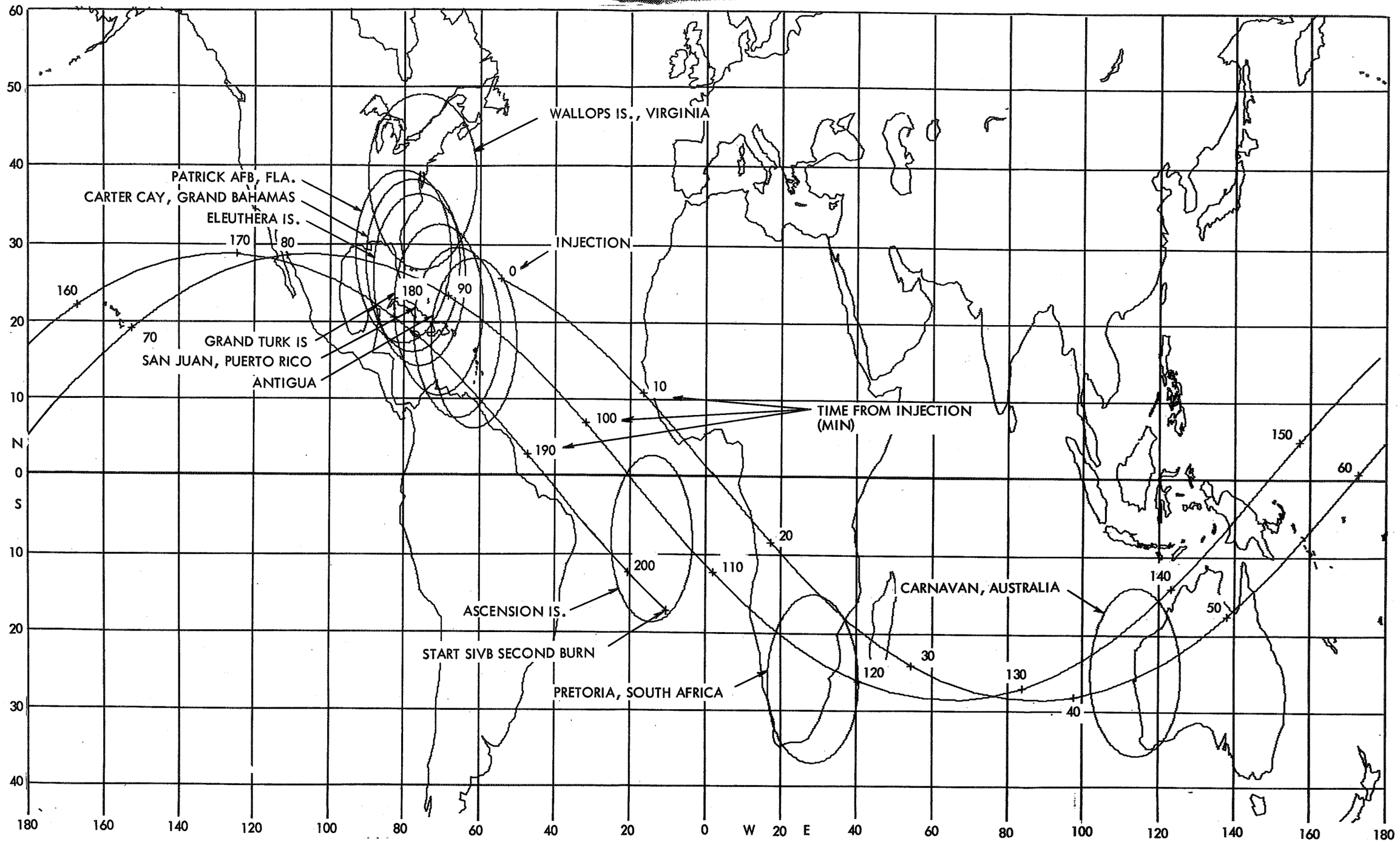

Figure 8.2-2. Earth Parking Orbit Phase - Reference Trajectory Ground Track Relative to A.M.R. Network Visibility Circles

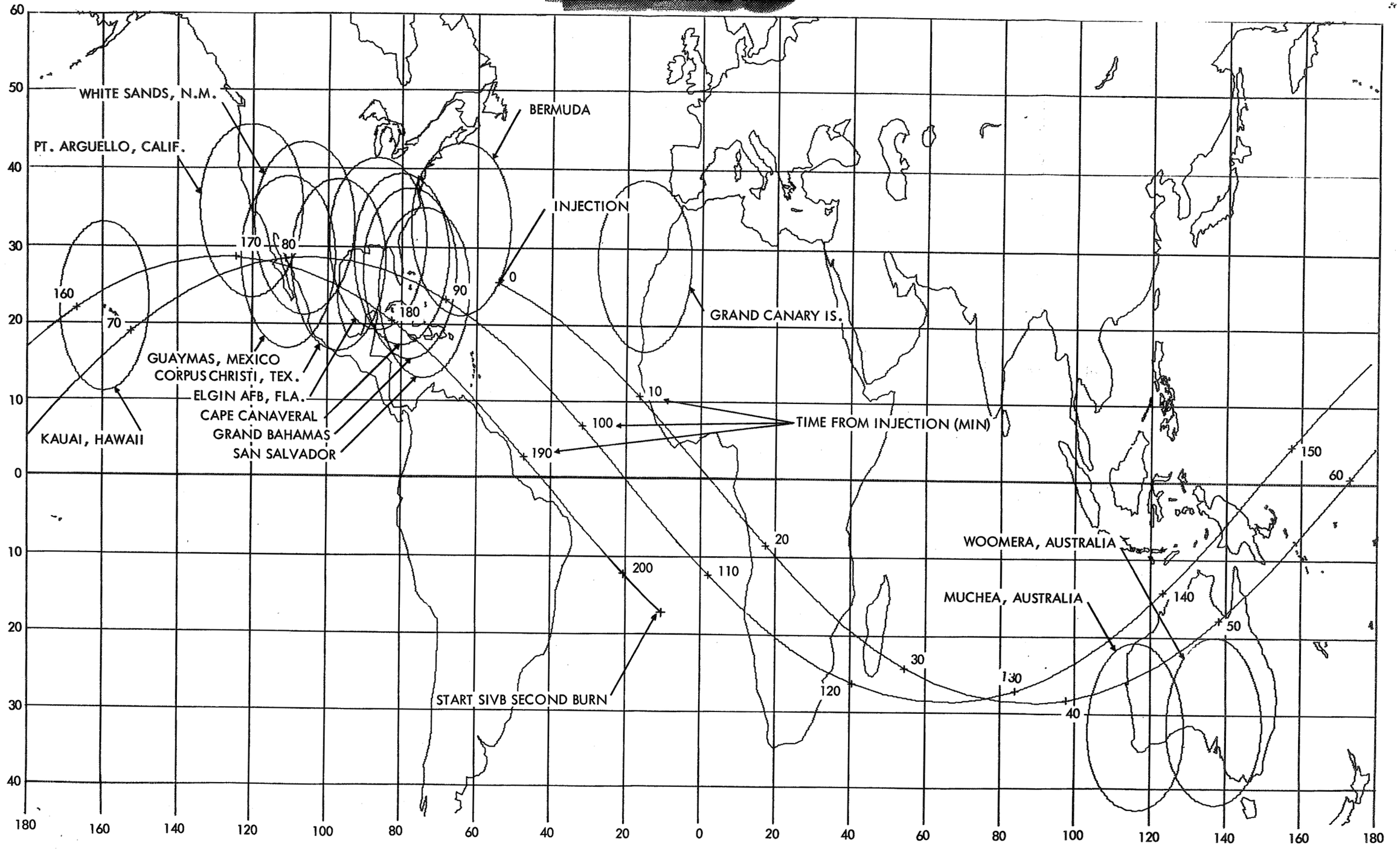

Figure 8.2-1. Earth Parking Orbit Phase - Reference Trajectory Ground Track Relative to Mercury Network Visibility Circles

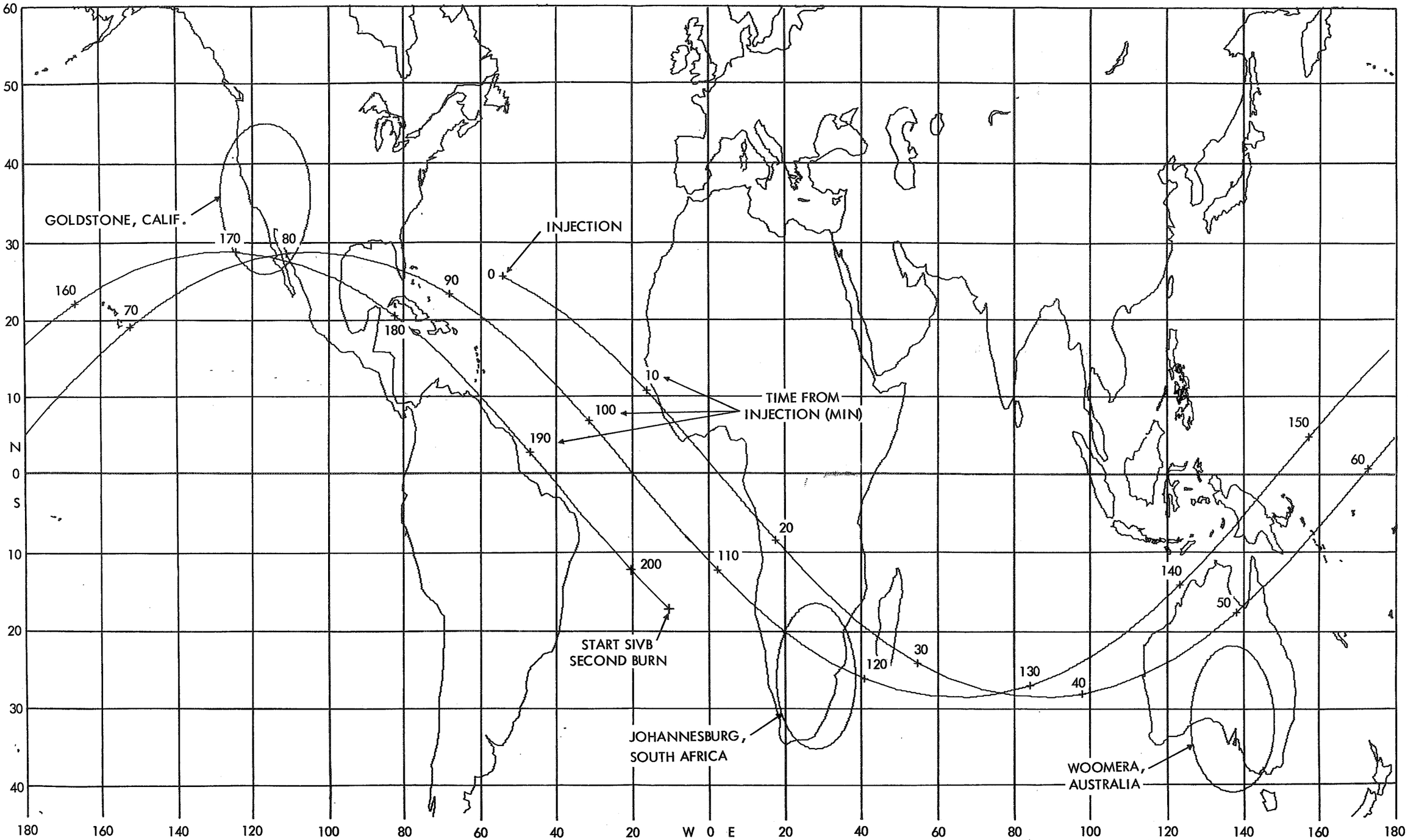

Figure 8.2-3. Earth Parking Orbit Phase - Reference Trajectory Ground Track Relative to DSIF Network Visibility Circles

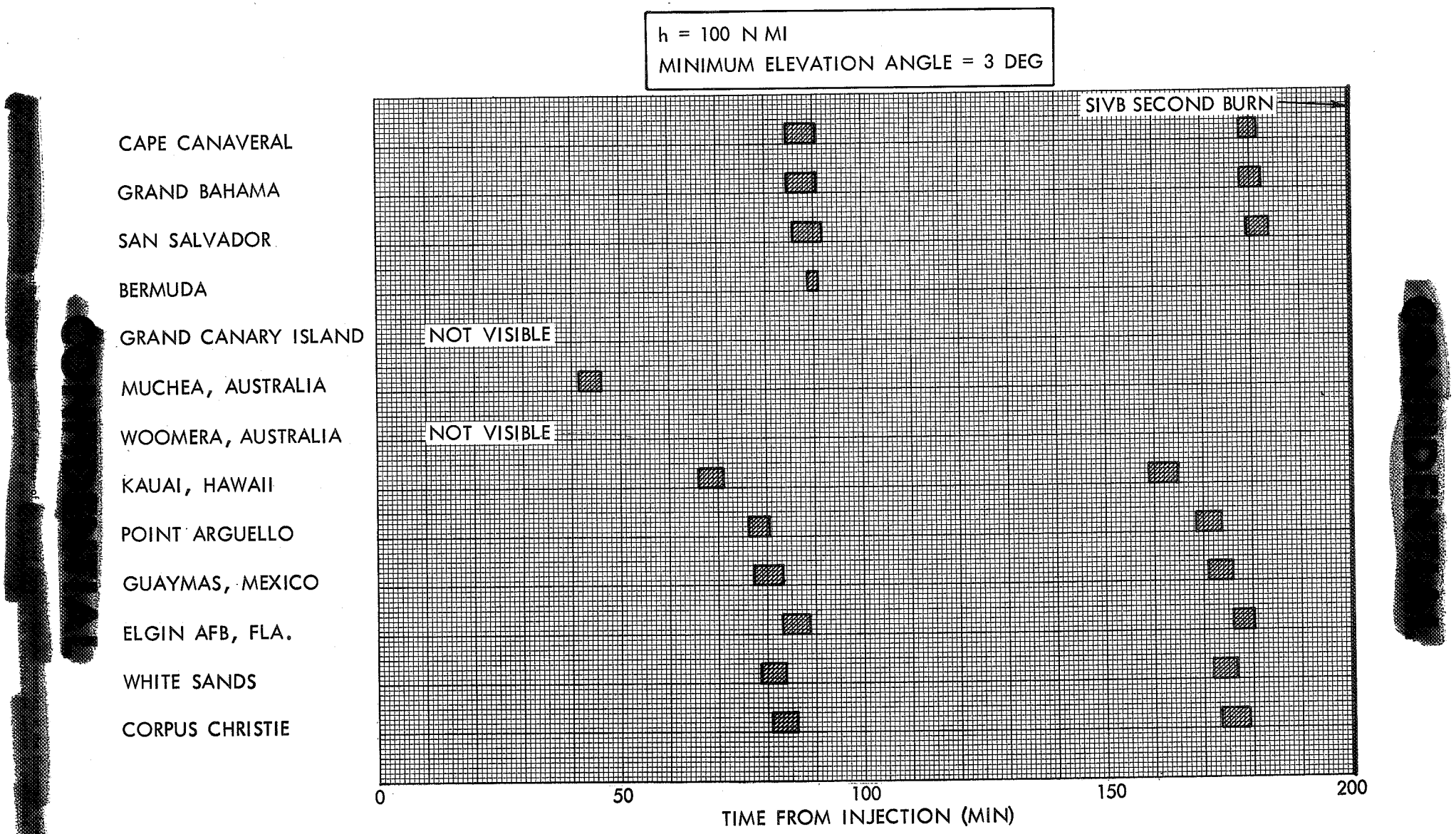

Figure 8.2-4. Earth Parking Orbit Phase – Mercury Network Visibility Durations

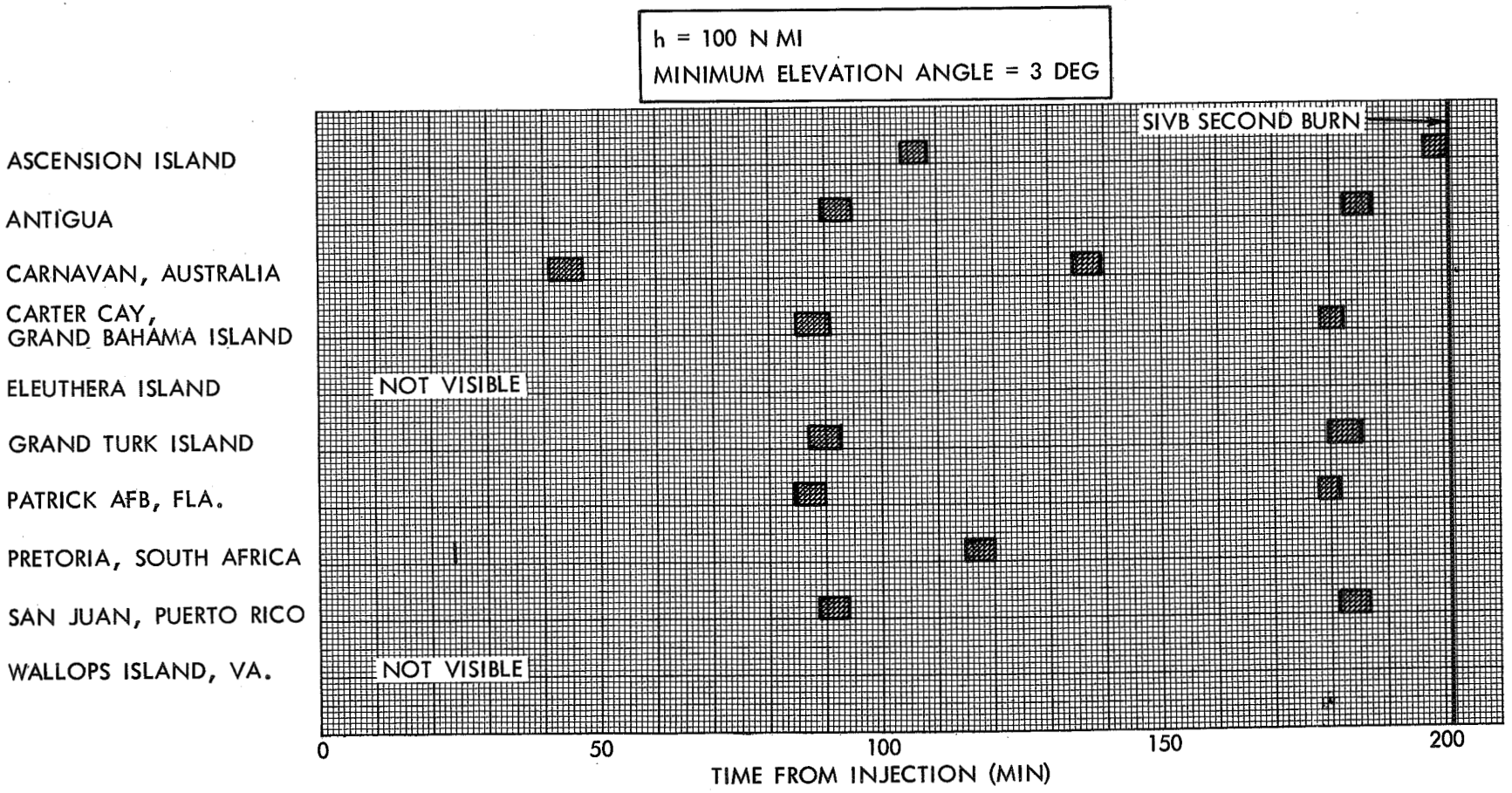

Figure 8.2-5. Earth Parking Orbit Phase – AMR Network Visibility Durations

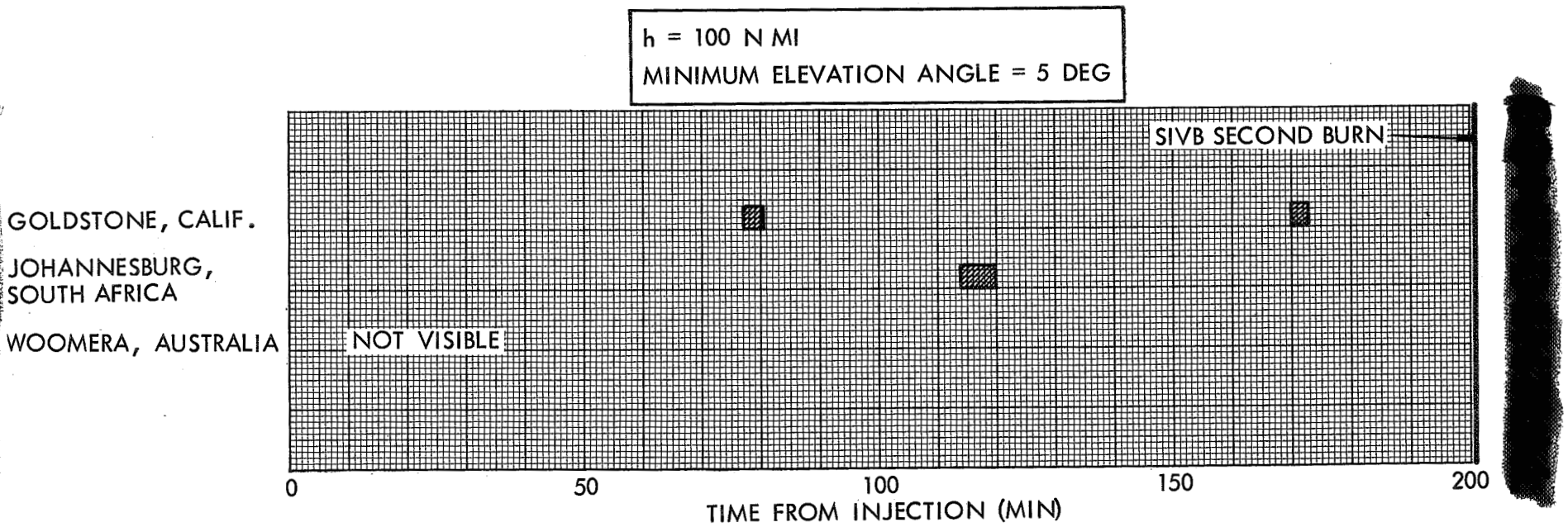

Figure 8.2-6. Earth Parking Orbit Phase – DSIF Network Visibility Durations

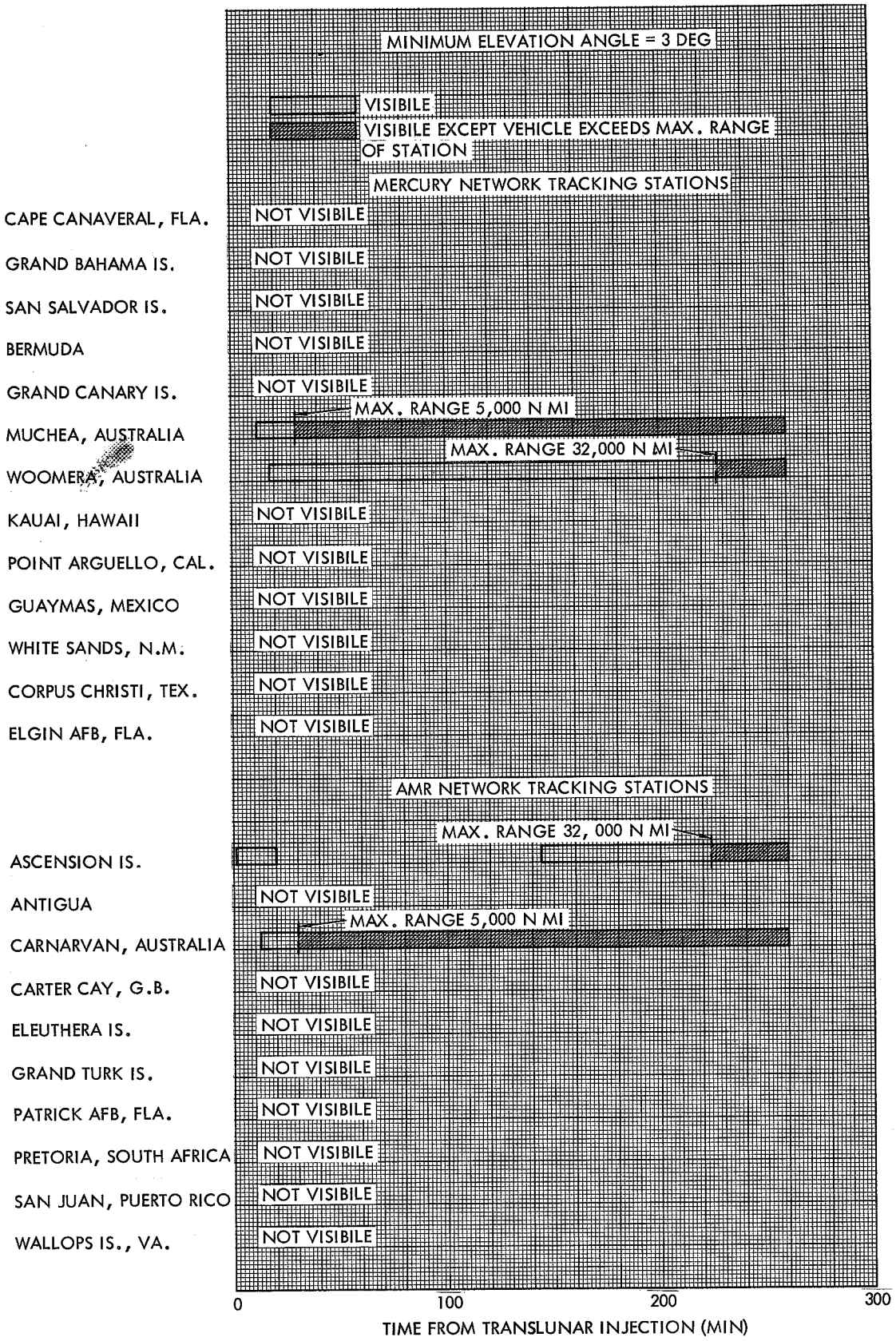

Figure 8.2-7. Translunar Flight – Mercury and AMR Network Visibility Durations

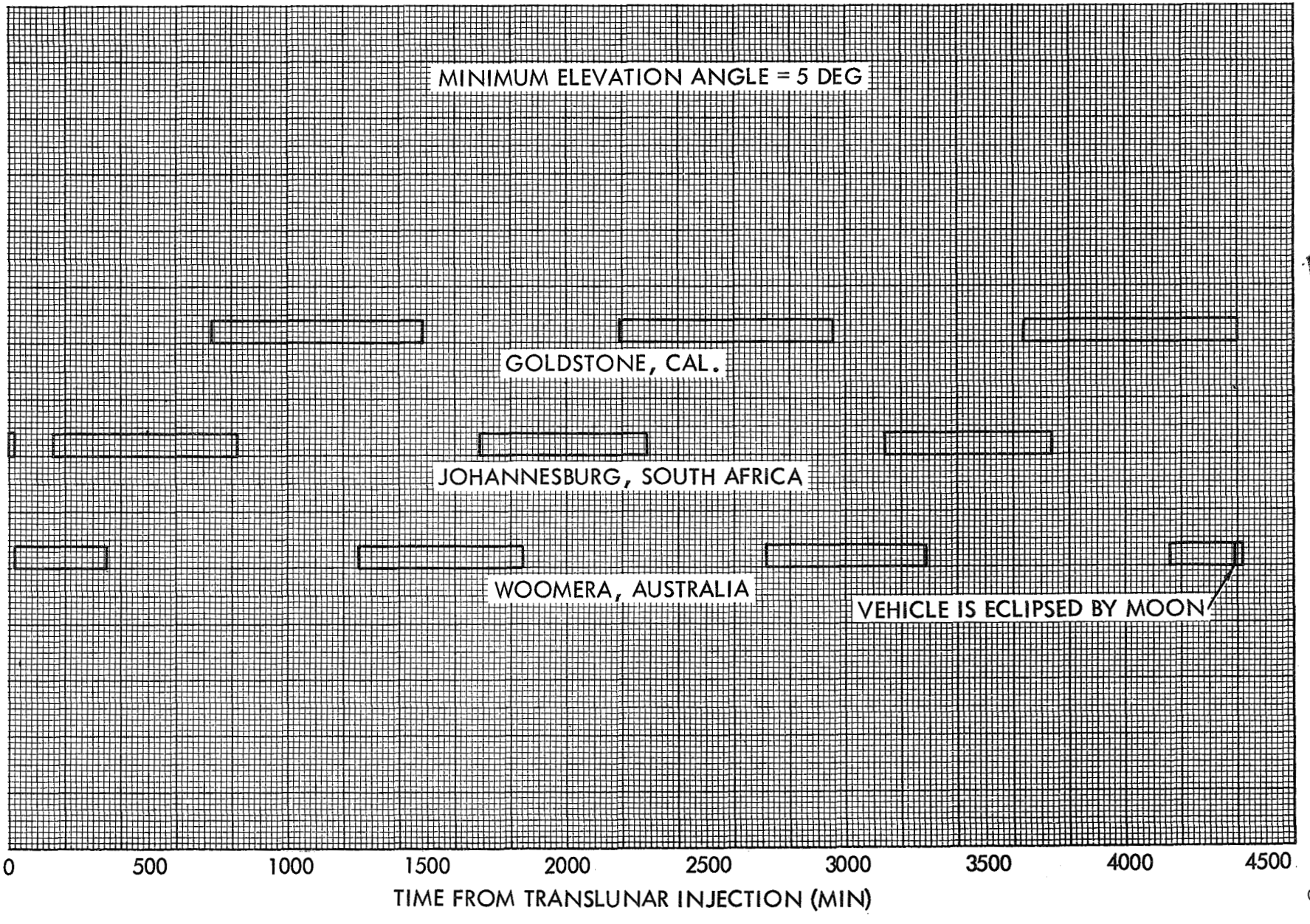

Figure 8.2-8. Translunar Flight - DSIF Network Visibility Durations

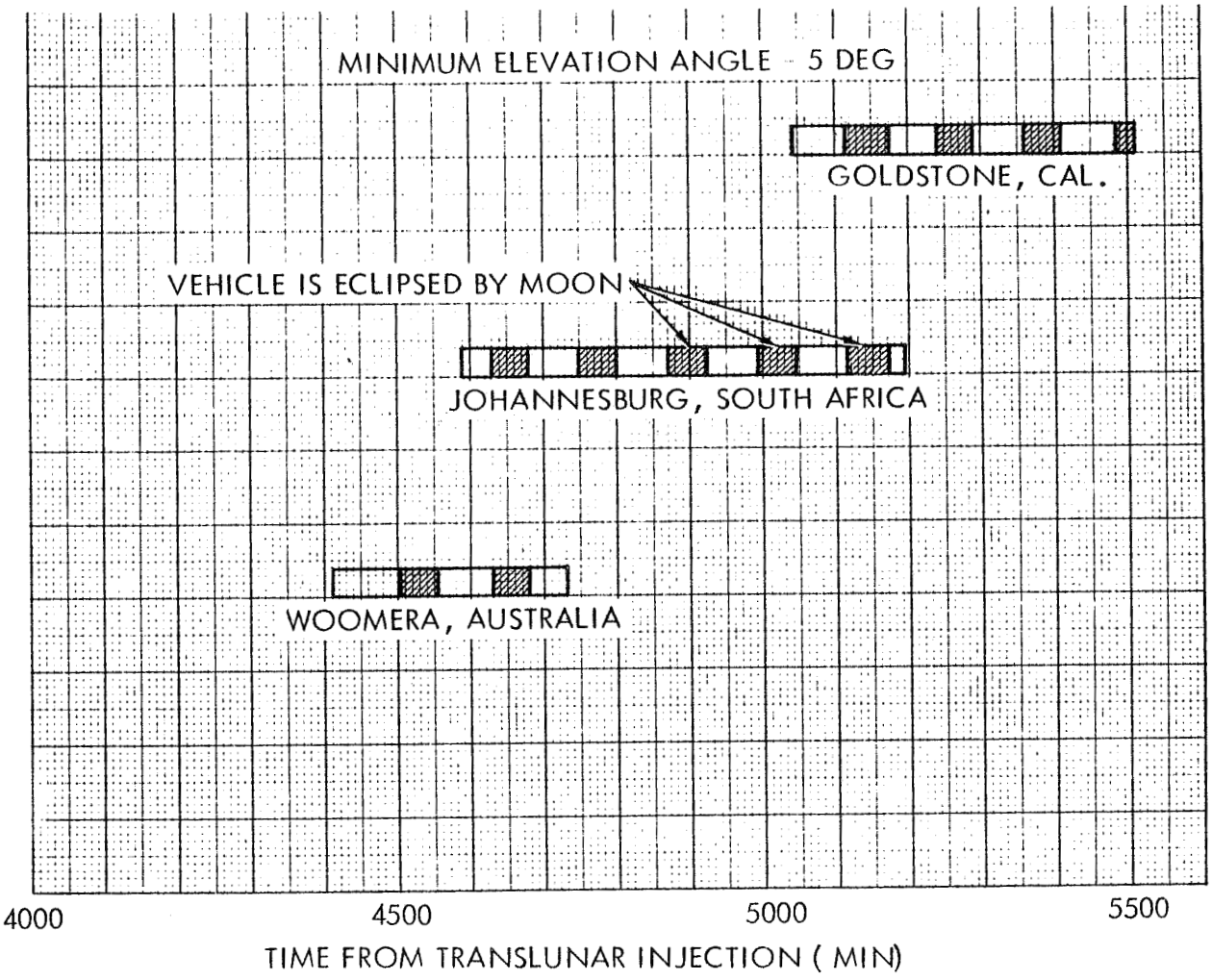

Figure 8.2-9. Circumlunar Flight - DSIF Network Visibility Durations

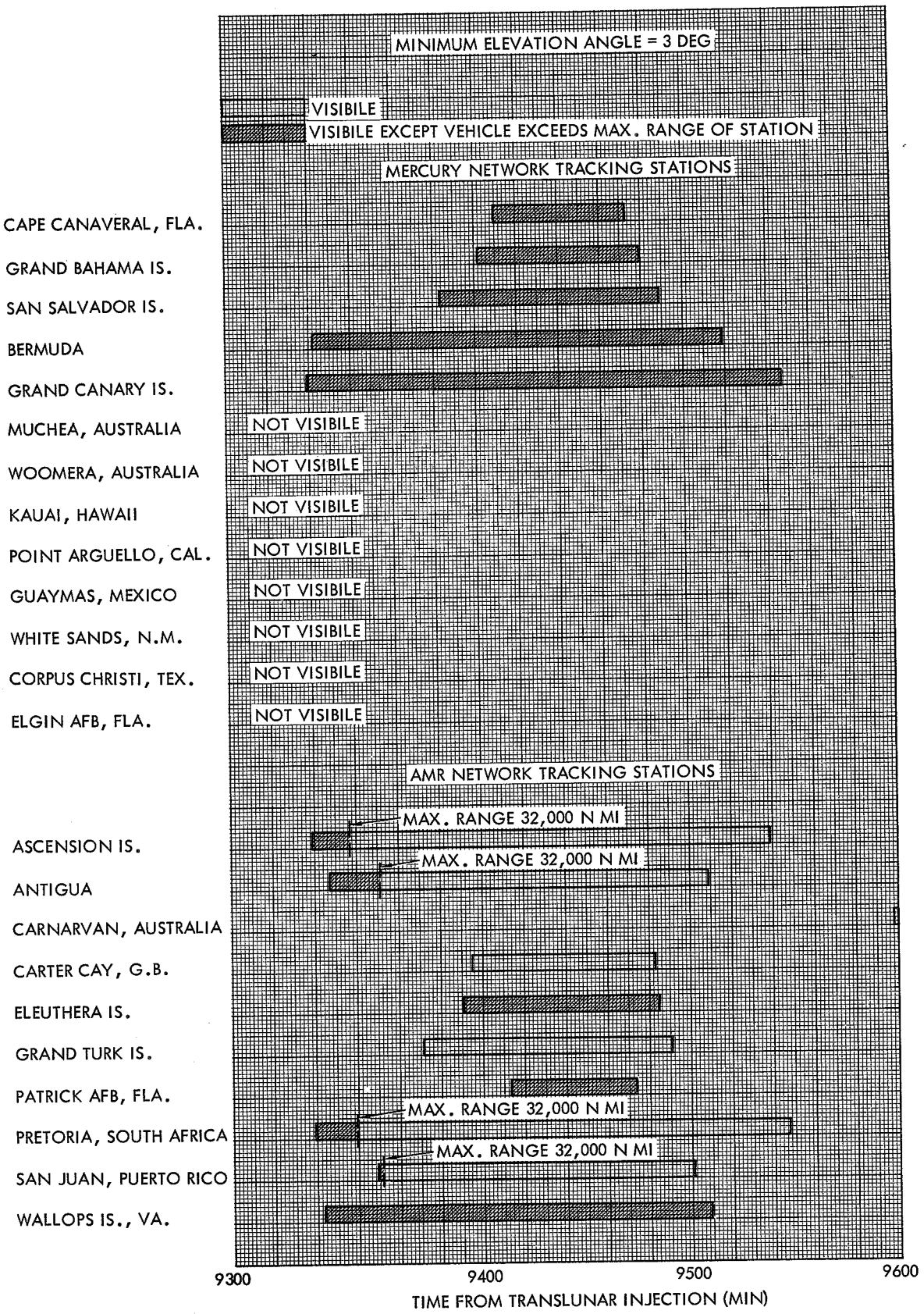

Figure 8.2-10. Transearth Flight – Mercury and AMR Network Visibility Durations

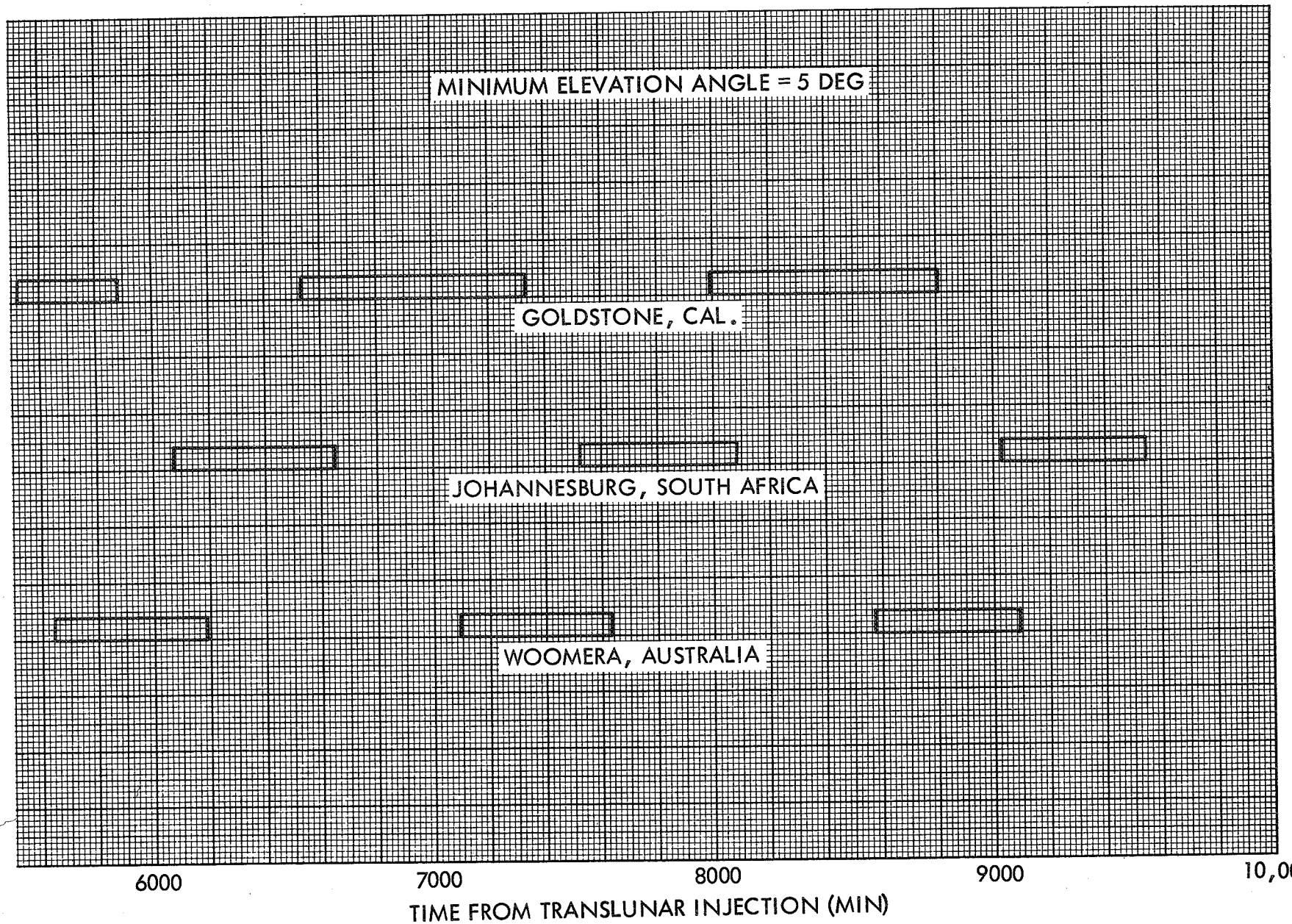

Figure 8.2-11. Transearth Flight – DSIF Network Visibility Durations

9.0 Earth and Lunar Landing Site Maps

9.1 Introduction

A display of the trajectory in the vicinity of the lunar and earth landing sites appears in this section.

9.2 Graphical Data

The lunar ground track of the complete LEM descent and ascent phases is shown in Figure 9.2-1. The re-entry ground track, terminating at Woomera, Australia, is shown in Figure 9.2-2.

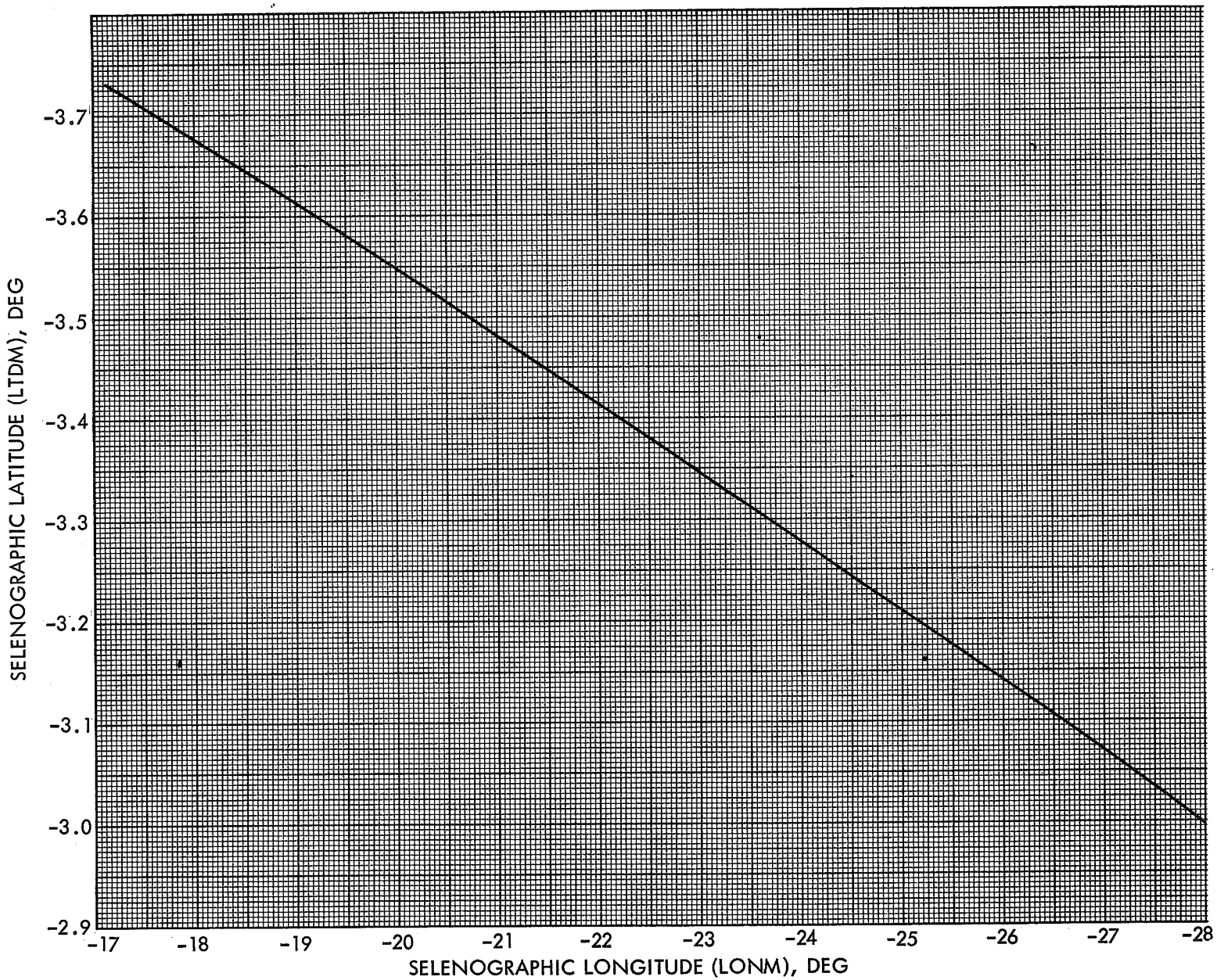

Figure 9.2-1a. Descent Phase - Selenographic Latitude (LTDM) versus Longitude (LONM)

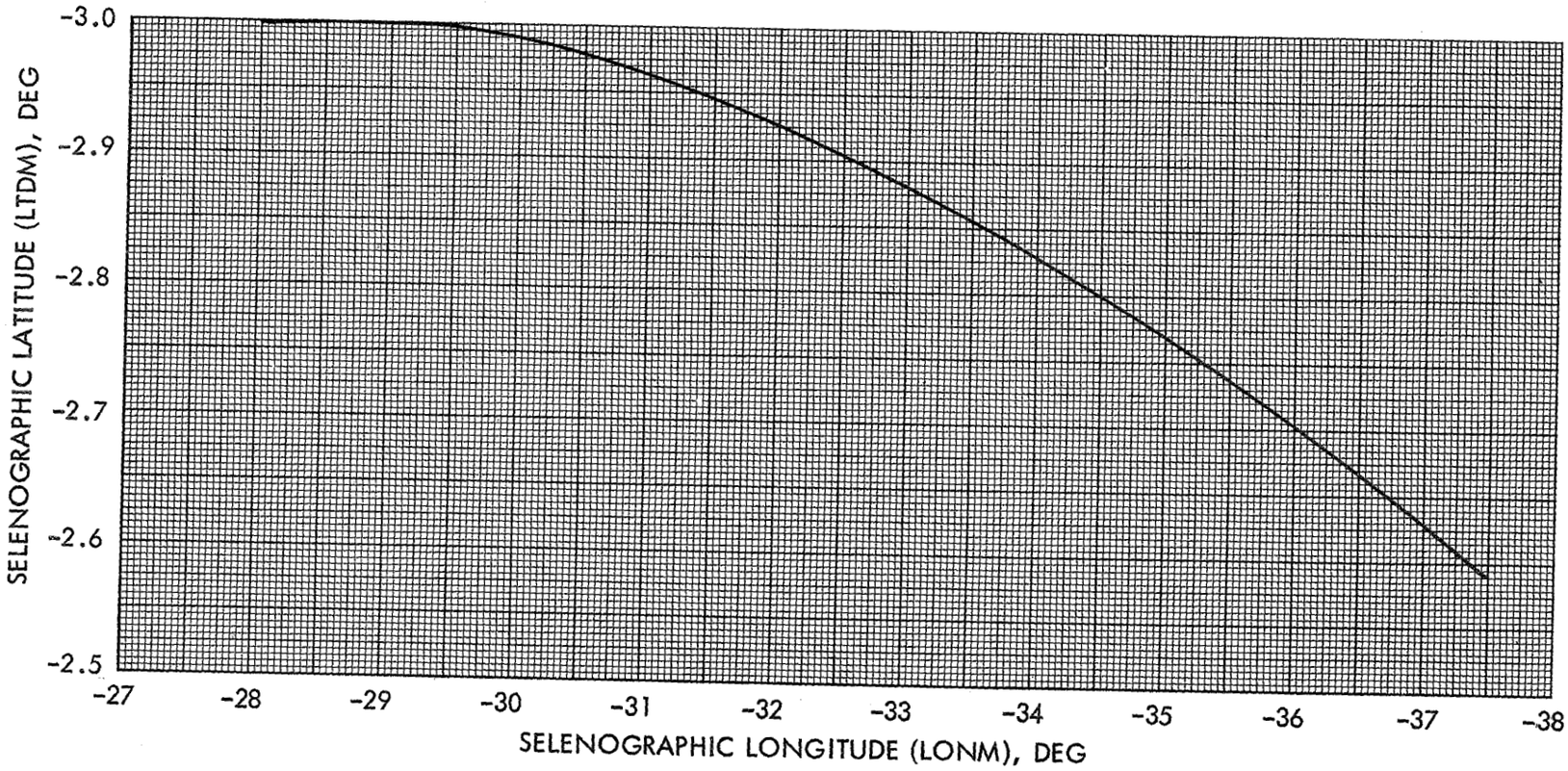

Figure 9.2-1b. Ascent Phase - Selenographic Latitude (LTDM) versus Longitude (LONM)

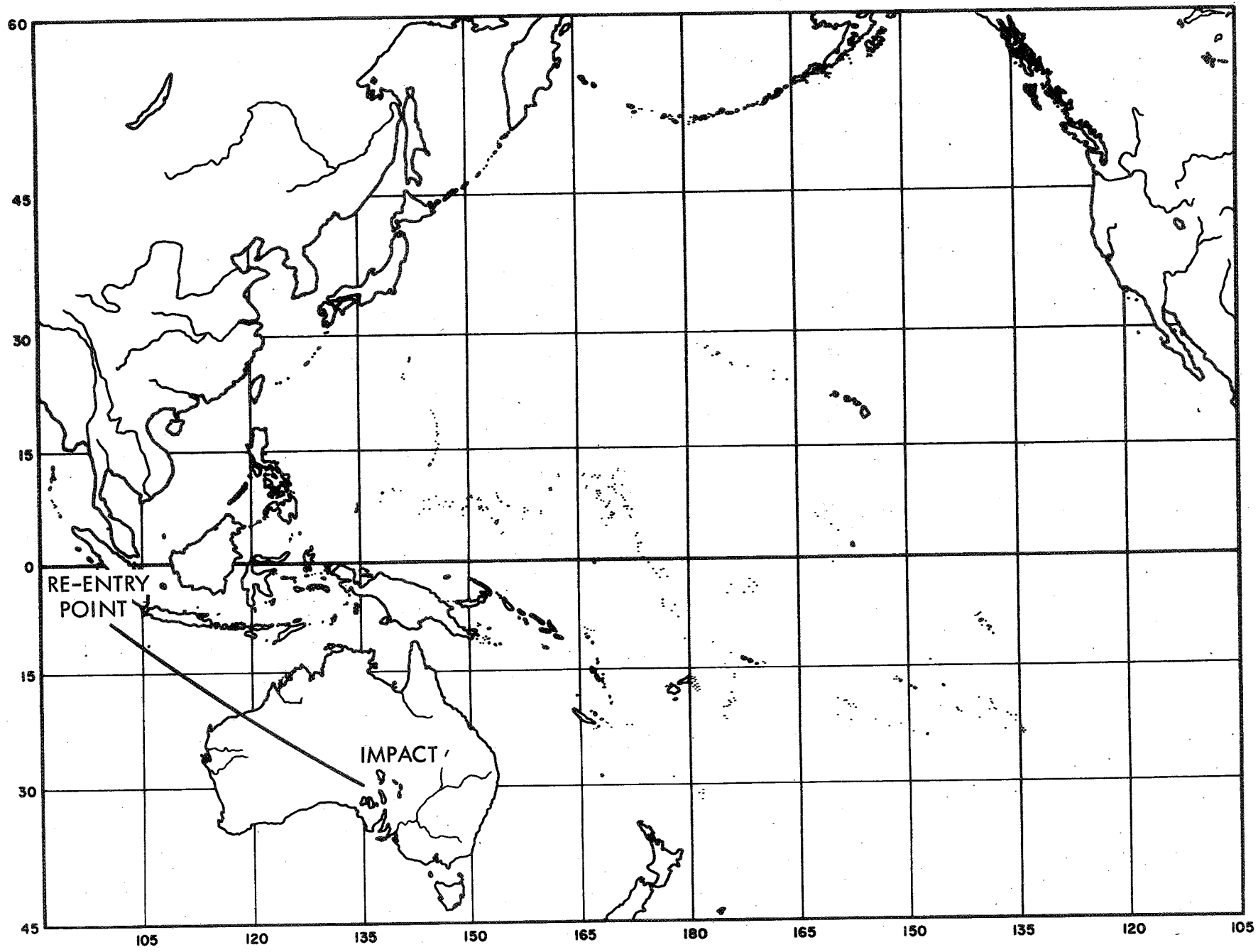

Figure 9.2-2. Re-entry Ground Track Relative to Woomera, Australia

10.0 Midcourse Sensitivities and Guidance Analysis Coefficients

10.1 Introduction

Presented in this section are the midcourse sensitivities and guidance analysis coefficients for the translunar and transearth phases of the reference trajectory.

These sensitivities have been computed at the following points on the translunar trajectory; namely, at injection, 4, 5, 6, 8, 10, 12, 14, 16, and 18 hours after injection. For this phase of the reference trajectory, the impact parameter (see definition in Volume 2) has been used in the calculation of the midcourse sensitivity coefficients.

The transearth sensitivities have been computed for the following times on this phase of the trajectory: at transearth injection, 4, 5, 6, 8, 10, 12, 14, 16, and 18 hours after injection. The midcourse sensitivity coefficients for this phase of the trajectory are computed in terms of the parameter of the orbit since the return leg is elliptical.

10.2 Tabular Data

The guidance analysis coefficients (miss plus time of flight) are the partials of midcourse velocity with respect to injection position and velocity. The guidance analysis coefficients (miss only) are also partials of midcourse velocity with respect to injection position and velocity but do not include any effects due to time of flight.

The midcourse sensitivity coefficients are the partials of $B \cdot T$, $B \cdot R$, T_f for the translunar phase and $P \cdot T$, $P \cdot R$, T_f for the transearth phase with respect to the position and velocity at the specified times of midcourse.

The units which have been used throughout for the generation of these coefficients are kilometers, seconds, and kilometers/second.

***** MIDCOURSE SUMMARY ***** TRANSLUNAR FLIGHT

MISS COMPONENTS

DB.T -.61035156-04(KM) DB.R -.59127808-04(KM) DTF -.29802322-07(DAYS)

TIME 1 3 FEBRUARY 6 HR 32 MIN 16 SEC TIME-START .00000000 00

GUIDANCE ANALYSIS COEFF.

	XO	YO	ZO	XDOTO	YDOTO	ZDOTO
MVX	-.63443738-03	-.35930939-03	-.35357583-03	.99999999 00	-.17733318-07	.61032800-08
MVY	-.35925639-03	-.47785432-03	.21422086-02	-.10047415-06	.99999992 00	-.30148931-07
MVZ	-.35359088-03	.21421334-02	-.32067373-02	.24296072-06	.59229775-07	.10000000 01

GUIDANCE ANALYSIS COEFF. -- MISS ONLY

	XO	YO	ZO	XDOTO	YDOTO	ZDOTO
MVX	-.34425785-03	-.42812742-03	-.59899849-03	.82239597 00	-.35516103 00	-.14114342 00
MVY	.22102589-03	-.61547211-03	.16514282-02	-.35516114 00	.28977186 00	-.28224951 00
MVZ	-.12298275-03	.20874431-02	-.34017768-02	-.14114317 00	-.28224941 00	.88783217 00

MIDCOURSE SENSITIVITIES

	X	Y	Z	XDOT	YDOT	ZDOT
M1	.29224309 03	.52786613 03	.27453740 03	-.73005879 06	.29009591 06	.18867767 06
M2	.28157032 00	-.34802941 02	.50508396 02	.61517857 04	.27283697 04	-.14606366 05
M3	.26107453 03	.69559550 03	.36711058 03	-.83553112 06	.46505048 06	.28831430 06

-.42143092 00 -.84275032 00 -.33491473 00

	DELTA V (KM/SEC)	DELTA VC (KM/SEC)
DVX	-.74990408-08	.39590376-09
DVY	-.17531351-07	-.17435511-08
DVZ	-.23850347-08	.38891447-08
MAGN	.19216458-07	.42804388-08

TIME 2 3 FEBRUARY 10 HR 32 MIN 16 SEC TIME-START .23999999 03

GUIDANCE ANALYSIS COEFF.

	XO	YO	ZO	XDOTO	YDOTO	ZDOTO
MVX	-.10696873-02	-.27968445-02	-.14923866-02	.33853055 01	-.18651782 01	-.11538758 01
MVY	-.29588419-03	-.16586740-03	.11568870-03	.37621874 00	.14210865 00	.17374625-01
MVZ	-.13082002-03	.22057965-03	-.22955486-03	.65639678-01	.11154774 00	.13886538 00

GUIDANCE ANALYSIS COEFF. -- MISS ONLY

	XO	YO	ZO	XDOTO	YDOTO	ZDOTO
MVX	-.44170607-03	-.79206117-03	-.42316012-03	.11023146 01	-.43886115 00	-.28275589 00
MVY	-.63149364-03	-.12372757-02	-.45573366-03	.15963083 01	-.62015219 00	-.44817446 00
MVZ	-.32946746-03	-.41358758-03	-.56778012-03	.78781146 00	-.33963495 00	-.13669342 00

MIDCOURSE SENSITIVITIES

	X	Y	Z	XDOT	YDOT	ZDOT
M1	-.90373454 01	-.15018681 01	-.45063086 00	-.18370356 06	-.26400556 06	-.13470911 06
M2	.12622422 00	-.11833497 01	.22605238 01	-.42975233 04	.81380167 05	-.15107527 06
M3	-.50405104 01	-.39091676 01	-.19357376 01	-.24787414 06	.68265488 04	.15696554 05

.84951194 00 -.45400123 00 -.26872361 00

	DELTA V (KM/SEC)	DELTA VC (KM/SEC)
DVX	.10064583-07	.10190859-09
DVY	-.53540758-08	-.29764247-10
DVZ	-.27790157-08	.37244769-09
MAGN	.11733920-07	.38728355-09

TIME 3 3 FEBRUARY 11 HR 32 MIN 16 SEC TIME-START .29999999 03

GUIDANCE ANALYSIS COEFF.

	XO	YO	ZO	XDOTO	YDOTO	ZDOTO
MVX	-.11642293-02	-.29988960-02	-.15977206-02	.36469272 01	-.19875282 01	-.12316085 01
MVY	-.34888204-03	-.30767379-03	.32366749-04	.54901149 00	.42893812-01	-.41973012-01
MVZ	-.15500318-03	.14361973-03	-.25504974-03	.14842263 00	.64658197-01	.10636433 00

GUIDANCE ANALYSIS COEFF. -- MISS ONLY

	XO	YO	ZO	XDOTO	YDOTO	ZDOTO
MVX	-.41888851-03	-.75108953-03	-.40137960-03	.10453607 01	-.41619441 00	-.26812610 00
MVY	-.69202401-03	-.13425249-02	-.51840794-03	.17467276 01	-.68052106 00	-.48554362 00
MVZ	-.36168234-03	-.47968546-03	-.58678896-03	.86982364 00	-.37106460 00	-.16080439 00

MIDCOURSE SENSITIVITIES

	X	Y	Z	XDOT	YDOT	ZDOT
M1	-.66396978 01	-.15262730 01	-.56033432 00	-.15585950 06	-.25852215 06	-.13285635 06
M2	.87919046-01	-.83834985 00	.16043534 01	-.46772570 04	.84975851 05	-.15794979 06
M3	-.34657866 01	-.29564626 01	-.14775073 01	-.23286376 06	.19073696 05	.21791899 05

.88084546 00 -.40552598 00 -.24425392 00

	DELTA V (KM/SEC)	DELTA VC (KM/SEC)
DVX	.10433027-07	.96737062-10
DVY	-.47689394-08	-.10290435-10
DVZ	-.25002554-08	.36594480-09
MAGN	.11740618-07	.37865492-09

TIME 4 3 FEBRUARY 12 HR 32 MIN 16 SEC TIME-START .35999999 03

GUIDANCE ANALYSIS COEFF.

	XO	YO	ZO	XDOTO	YDOTO	ZDOTO
MVX	-.12477168-02	-.31781089-02	-.16913084-02	.38786473 01	-.20963667 01	-.13006810 01
MVY	-.39812242-03	-.43268777-03	-.39160841-04	.70333384 00	-.41977218-01	-.93379941-01
MVZ	-.17782775-03	.77634182-04	-.27979077-03	.22247559 00	.24356441-01	.78991621-01

GUIDANCE ANALYSIS COEFF. -- MISS ONLY

	XO	YO	ZO	XDOTO	YDOTO	ZDOTO
MVX	-.39682681-03	-.71139554-03	-.38043381-03	.99027805 00	-.39428404 00	-.25394760 00
MVY	-.74245961-03	-.14309145-02	-.56964408-03	.18721958 01	-.73077406 00	-.51697081 00
MVZ	-.38875583-03	-.53384216-03	-.60474496-03	.93847669 00	-.39757474 00	-.18048430 00

MIDCOURSE SENSITIVITIES

	X	Y	Z	XDOT	YDOT	ZDOT
M1	-.51481405 01	-.14891711 01	-.59993743 00	-.13483175 06	-.25308606 06	-.13075573 06
M2	.63424585-01	-.60274869 00	.11561298 01	-.49467888 04	.87545586 05	-.16287245 06
M3	-.25927255 01	-.22958359 01	-.11506478 01	-.22209851 06	.28460239 05	.26491182 05

.90342864 00 -.36559845 00 -.22395194 00

	DELTA V (KM/SEC)	DELTA VC (KM/SEC)
DVX	.1076814-07	.91870066-10
DVY	-.43156980-08	.47764015-11
DVZ	-.22837526-08	.36280851-09
MAGN	.11823466-07	.37428991-09

TIME 5 3 FEBRUARY 14 HR 32 MIN 16 SEC TIME-START .47999999 03

GUIDANCE ANALYSIS COEFF.

	XO	YO	ZO	XDOTO	YDOTO	ZDOTO
MVX	-.13945898-02	-.34962385-02	-.18577669-02	.42887140 01	-.22905939 01	-.14237364 01
MVY	-.48802574-03	-.64959941-03	-.15983560-03	.97462544 00	-.18462754 00	-.18095623 00
MVZ	-.22003162-03	-.33335286-04	-.32664465-03	.35262495 00	-.43590147-01	.33861775-01

GUIDANCE ANALYSIS COEFF. -- MISS ONLY

	XO	YO	ZO	XDOTO	YDOTO	ZDOTO
MVX	-.35646859-03	-.63866599-03	-.34228200-03	.88949088 00	-.35421071 00	-.22796184 00
MVY	-.82470898-03	-.15763667-02	-.65133733-03	.20770607 01	-.81263489 00	-.56876957 00
MVZ	-.43327329-03	-.62031252-03	-.63794214-03	.10508632 01	-.44134483 00	-.21176365 00

MIDCOURSE SENSITIVITIES

	X	Y	Z	XDOT	YDOT	ZDOT
M1	-.34198418 01	-.13878088 01	-.61377214 00	-.10467740 06	-.24272926 06	-.12635876 06
M2	.34076998-01	-.30080892 00	.58194538 00	-.52867703 04	.90699692 05	-.16894153 06
M3	-.17228517 01	-.14572453 01	-.72565172 00	-.20701611 06	.41685019 05	.33107402 05

.93357007 00 -.30277523 00 -.19176570 00

	DELTA V (KM/SEC)	DELTA VC (KM/SEC)
DVX	.11391624-07	.83160589-10
DVY	-.36403994-08	.27158886-10
DVZ	-.19609162-08	.36196821-09
MAGN	.12118861-07	.37238994-09

TIME 6 3 FEBRUARY 16 HR 32 MIN 16 SEC TIME-START .59999998 03

GUIDANCE ANALYSIS COEFF.

	XO	YO	ZO	XDOTO	YDOTO	ZDOTO
MVX	-.15259366-02	-.37843189-02	-.20088052-02	.46584347 01	-.24676950 01	-.15357112 01
MVY	-.56989794-03	-.83817024-03	-.26184155-03	.12133903 01	-.30478217 00	-.25573998 00
MVZ	-.25880763-03	-.12660332-03	-.37058233-03	.46687534 00	-.10085480 00	-.32885516-02

GUIDANCE ANALYSIS COEFF. -- MISS ONLY

	XO	YO	ZO	XDOTO	YDOTO	ZDOTO
MVX	-.32135411-03	-.57530252-03	-.30920629-03	.80178273 00	-.31934990 00	-.20531736 00
MVY	-.89235607-03	-.16972010-02	-.71681205-03	.22457885 01	-.87987883 00	-.61187692 00
MVZ	-.47013156-03	-.68957182-03	-.66874866-03	.11434607 01	-.47774618 00	-.23668399 00

MIDCOURSE SENSITIVITIES

	X	Y	Z	XDOT	YDOT	ZDOT
M1	-.24652655 01	-.13003315 01	-.60409210 00	-.83787070 05	-.23306414 06	-.12196917 06
M2	.17238038-01	-.11527626 00	.22947570 00	-.54666437 04	.92149980 05	-.17177199 06
M3	-.13321239 01	-.95753541 00	-.46692611 00	-.19618619 06	.50239603 05	.37331660 05

.95240845 00 -.25495296 00 -.16708421 00

	DELTA V (KM/SEC)	DELTA VC (KM/SEC)
DVX	.11990958-07	.75722650-10
DVY	-.31460721-08	.43551440-10
DVZ	-.17251530-08	.36517665-09
MAGN	.12516269-07	.37547921-09

TIME 7 3 FEBRUARY 18 HR 32 MIN 16 SEC TIME-START .71999998 03

GUIDANCE ANALYSIS COEFF.

	XO	YO	ZO	XDOTO	YDOTO	ZDOTO
MVX	-.16491387-02	-.40576333-02	-.21523153-02	.50078129 01	-.26367377 01	-.16424073 01
MVY	-.64656455-03	-.10091526-02	-.35238388-03	.14317789 01	-.41118036 00	-.32266211 00
MVZ	-.29526844-03	-.20884487-03	-.41248894-03	.57096796 00	-.15147391 00	-.35512808-01

GUIDANCE ANALYSIS COEFF. -- MISS ONLY

	XO	YO	ZO	XDOTO	YDOTO	ZDOTO
MVX	-.29087614-03	-.52025307-03	-.28057255-03	.72564536 00	-.28909575 00	-.18564088 00
MVY	-.95200909-03	-.18046347-02	-.77329928-03	.23947479 01	-.93911543 00	-.65025809 00
MVZ	-.50273428-03	-.74915688-03	-.69838557-03	.12250414 01	-.51006108 00	-.25802447 00

MIDCOURSE SENSITIVITIES

	X	Y	Z	XDOT	YDOT	ZDOT
M1	-.18684828 01	-.12320751 01	-.59056339 00	-.68336415 05	-.22395786 06	-.11766799 06
M2	.63894514-02	.10182980-01	-.86238777-02	-.55490937 04	.92501651 05	-.17251635 06
M3	-.11323497 01	-.63147036 00	-.29569069 00	-.18738824 06	.55883978 05	.40038394 05

.96497900 00 -.21700338 00 -.14739432 00

	DELTA V (KM/SEC)	DELTA VC (KM/SEC)
DVX	.12588978-07	.69354521-10
DVY	-.27588617-08	.56537052-10
DVZ	-.15414705-08	.37082122-09
MAGN	.12979592-07	.38146411-09

TIME 8 3 FEBRUARY 20 HR 32 MIN 16 SEC TIME-START .83999998 03

GUIDANCE ANALYSIS COEFF.

	XO	YO	ZO	XDOTO	YDOTO	ZDOTO
MVX	-.17684499-02	-.43249670-02	-.22928469-02	.53483622 01	-.28029345 01	-.17471575 01
MVY	-.71994517-03	-.11688614-02	-.43549817-03	.16371339 01	-.50868813 00	-.38452445 00
MVZ	-.33022455-03	-.28379809-03	-.45311769-03	.66839344 00	-.19771637 00	-.64476684-01

GUIDANCE ANALYSIS COEFF. -- MISS ONLY

	XO	YO	ZO	XDOTO	YDOTO	ZDOTO
MVX	-.26427853-03	-.47217167-03	-.25564226-03	.65919366 00	-.26269628 00	-.16845250 00
MVY	-.10073018-02	-.19048987-02	-.82468534-03	.25329517 01	-.99397472 00	-.68611994 00
MVZ	-.53298107-03	-.80314012-03	-.72772506-03	.13004754 01	-.54013073 00	-.27728006 00

MIDCOURSE SENSITIVITIES

	X	Y	Z	XDOT	YDOT	ZDOT
M1	-.14644023 01	-.11789425 01	-.57759193 00	-.56422625 05	-.21528591 06	-.11346353 06
M2	-.11324965-02	.10047224 00	-.17981448 00	-.55666229 04	.92086890 05	-.17180670 06
M3	-.10219008 01	-.40492566 00	-.17546541 00	-.17966869 06	.59569270 05	.41710858 05

.97373881 00 -.18602287 00 -.13125625 00

	DELTA V (KM/SEC)	DELTA VC (KM/SEC)
DVX	.13198672-07	.63865690-10
DVY	-.24418403-08	.67430505-10
DVZ	-.13922955-08	.37822599-09
MAGN	.13494666-07	.38946194-09

TIME 9 3 FEBRUARY 22 HR 32 MIN 16 SEC TIME-START .95999998 03

GUIDANCE ANALYSIS COEFF.

	XO	YO	ZO	XDOTO	YDOTO	ZDOTO
MVX	-.18866411-02	-.45920733-02	-.24333873-02	.56876098 01	-.29697121 01	-.18521495 01
MVY	-.79140574-03	-.13213787-02	-.51370173-03	.18343019 01	-.60032427 00	-.44309301 00
MVZ	-.36427760-03	-.35380063-03	-.49306785-03	.76147334 00	-.24100426 00	-.91199276-01

GUIDANCE ANALYSIS COEFF. -- MISS ONLY

	XO	YO	ZO	XDOTO	YDOTO	ZDOTO
MVX	-.24091689-03	-.42990474-03	-.23379532-03	.60081989 00	-.23951112 00	-.15334055 00
MVY	-.10604631-02	-.20018463-02	-.87331022-03	.26659346 01	-.10466813 01	-.72082912 00
MVZ	-.56204919-03	-.85398086-03	-.75739939-03	.13727681 01	-.56910067 00	-.29535022 00

MIDCOURSE SENSITIVITIES

	X	Y	Z	XDOT	YDOT	ZDOT
M1	-.11749529 01	-.11369427 01	-.56612130 00	-.46975275 05	-.20695442 06	-.10934705 06
M2	-.66269657-02	.16835465 00	-.30841352 00	-.55376618 04	.91108225 05	-.17002847 06
M3	-.95759772 00	-.24017678 00	-.87305485-01	-.17256369 06	.61861962 05	.42641456 05

.98002951 00 -.16022378 00 -.11777308 00

	DELTA V (KM/SEC)	DELTA VC (KM/SEC)
DVX	.13828886-07	.59103166-10
DVY	-.21742177-08	.76986556-10
DVZ	-.12676760-08	.38708008-09
MAGN	.14056042-07	.39906278-09

TIME 10 4 FEBRUARY HR 32 MIN 16 SEC TIME-START .10800000 04

GUIDANCE ANALYSIS COEFF.

	XO	YO	ZO	XDOTO	YDOTO	ZDOTO
MVX	-.20058816-02	-.48635634-02	-.25763388-02	.60315379 01	-.31398545 01	-.19591535 01
MVY	-.86203227-03	-.14696947-02	-.58877049-03	.20269000 01	-.68821081 00	-.49963042 00
MVZ	-.39791438-03	-.42048445-03	-.53285020-03	.85192674 00	-.28233371 00	-.11637629 00

GUIDANCE ANALYSIS COEFF. -- MISS ONLY

	XO	YO	ZO	XDOTO	YDOTO	ZDOTO
MVX	-.22023351-03	-.39245040-03	-.21450001-03	.54913190 00	-.21898629 00	-.13994725 00
MVY	-.11130112-02	-.20981250-02	-.92073504-03	.27974710 01	-.10987488 01	-.75532609 00
MVZ	-.59074937-03	-.90332708-03	-.78790893-03	.14439805 01	-.59776291 00	-.31283527 00

MIDCOURSE SENSITIVITIES

	X	Y	Z	XDOT	YDOT	ZDOT
M1	-.95909986 00	-.11031852 01	-.55621976 00	-.39327593 05	-.19889413 06	-.10530764 06
M2	-.10801129-01	.22106868 00	-.40820510 00	-.54740320 04	.89698743 05	-.16743431 06
M3	-.91919544 00	-.11621662 00	-.20511922-01	-.16581643 06	.63125023 05	.43018814 05

.98465200 00 -.13839622 00 -.10633414 00

	DELTA V (KM/SEC)	DELTA VC (KM/SEC)
DVX	.14487789-07	.54941940-10
DVY	-.19429053-08	.85680879-10
DVZ	-.11613807-08	.39724552-09
MAGN	.14663551-07	.41007784-09

***** MIDCOURSE SUMMARY ***** TRANSEARTH INJECTION AND RETURN

MISS COMPONENTS

DP.T .48828125-03(KM) DP.R .00000000 00(KM) DTF .29802322-07(DAYS)

TIME 1 7 FEBRUARY 2 HR 25 MIN 41 SEC TIME-START .00000000 00

GUIDANCE ANALYSIS COEFF.

	XO	YO	ZO	XDOTO	YDOTO	ZDOTO
MVX	.66013385-03	.31380505-04	.89108484-04	.99999998 00	-.15373093-07	.43528175-08
MVY	.31274144-04	-.53865858-03	.25160644-03	.10375712-06	.99999998 00	.12074227-07
MVZ	.89317516-04	.25175366-03	-.90526232-03	-.12920095-06	-.70130695-07	.99999995 00

GUIDANCE ANALYSIS COEFF. -- MISS ONLY

	XO	YO	ZO	XDOTO	YDOTO	ZDOTO
MVX	.43403414-03	.22028076-03	.83415601-04	.69771127 00	-.43588616 00	-.14461594 00
MVY	-.29475100-03	-.26627379-03	.24339752-03	-.43588611 00	.37147374 00	-.20852904 00
MVZ	-.18849297-04	.34212404-03	-.90798595-03	-.14461605 00	-.20852909 00	.93081543 00

MIDCOURSE SENSITIVITIES

	X	Y	Z	XDOT	YDOT	ZDOT
M1	.15336813 03	.73160470 02	.41501694 02	.24805995 06	-.15099777 06	-.63395382 05
M2	-.81522631 02	-.27120905 02	-.52319879 02	-.13568091 06	.72651969 05	.64632380 05
M3	-.11453315 03	-.88511512 02	-.60974546 02	-.19710429 06	.20141138 06	.10393372 06

-.54980814 00 -.79279655 00 -.26302973 00

	DELTA V (KM/SEC)	DELTA VC (KM/SEC)
DVX	.21621936-07	.16737680-08
DVY	.25054077-07	-.37102088-08
DVZ	.17227524-07	.76842650-08
MAGN	.37309549-07	.86956929-08

TIME 2 7 FEBRUARY 6 HR 25 MIN 41 SEC TIME-START .24000000 03

GUIDANCE ANALYSIS COEFF.

	XO	YO	ZO	XDOTO	YDOTO	ZDOTO
MVX	.10656733-02	.26353198-03	.19672104-03	.16623659 01	-.47980664 00	-.18703148 00
MVY	-.63668795-03	-.60324025-03	-.11218169-03	-.10711119 01	.12253016 01	.35904542 00
MVZ	-.25159467-03	-.72302017-04	-.48236905-03	-.47938898 00	.38303982 00	.59212305 00

GUIDANCE ANALYSIS COEFF. -- MISS ONLY

	XO	YO	ZO	XDOTO	YDOTO	ZDOTO
MVX	.90764959-03	.43215483-03	.24771233-03	.14683118 01	-.89309314 00	-.37732848 00
MVY	-.79228129-03	-.43721079-03	-.61974635-04	-.12621814 01	.81837134 00	.17167515 00
MVZ	-.31548508-03	-.41262553-05	-.46175280-03	-.55784679 00	.21594430 00	.51518423 00

MIDCOURSE SENSITIVITIES

	X	Y	Z	XDOT	YDOT	ZDOT
M1	.62699949-01	-.90756361 00	-.45280733 00	.89747656 05	-.78330106 05	-.31219321 05
M2	-.15870865-01	.58288669 00	.19473591 00	-.48102382 05	.13677032 05	.85666388 05
M3	-.68656410-01	.16768287 01	.81406347 00	-.61099929 04	.13291043 06	.93004441 05

-.68471589 00 -.67418506 00 -.27683687 00

	DELTA V (KM/SEC)	DELTA VC (KM/SEC)
DVX	.20700368-07	.28716844-08
DVY	.13724751-07	-.38297306-08
DVZ	.94322075-08	.22239083-08
MAGN	.26567660-07	.52781793-08

CONFIDENTIAL

Reproduced by IBM

TIME 3 7 FEBRUARY 7 HR 25 MIN 41 SEC TIME-START .30000000 03

GUIDANCE ANALYSIS COEFF.

	XO	YO	ZO	XDOTO	YDOTO	ZDOTO
MVX	.10687950-02	.26435907-03	.19708586-03	.16672040 01	-.48120808 00	-.18734777 00
MVY	-.66059822-03	-.62289323-03	-.12351424-03	-.11121953 01	.12690349 01	.37967508 00
MVZ	-.26257896-03	-.82278423-04	-.48716476-03	-.49835035 00	.40489918 00	.60162975 00

GUIDANCE ANALYSIS COEFF. -- MISS ONLY

	XO	YO	ZO	XDOTO	YDOTO	ZDOTO
MVX	.93981283-03	.44696193-03	.25779296-03	.15205072 01	-.92441290 00	-.39203121 00
MVY	-.79186186-03	-.43706041-03	-.61733333-04	-.12614869 01	.81799053 00	.17137112 00
MVZ	-.31706716-03	-.51382814-05	-.46151919-03	-.56032203 00	.21766837 00	.51516171 00

MIDCOURSE SENSITIVITIES

	X	Y	Z	XDOT	YDOT	ZDOT
M1	.87441244-01	-.66982578 00	-.32662097 00	.89478090 05	-.75536109 05	-.29840086 05
M2	-.25091336-01	.40268834 00	.20837653 00	-.48029961 05	.11936329 05	.84939526 05
M3	.57537060-01	.13267159 01	.67777611 00	-.61195123 04	.12756671 06	.90343501 05
		-.67204187 00	-.68392917 00	-.28390247 00		

	DELTA V (KM/SEC)	DELTA VC (KM/SEC)
DVX	.20764416-07	.29622702-08
DVY	.14287544-07	-.38294916-08
DVZ	.97336690-08	.22131956-08
MAGN	.27019237-07	.53233716-08

TIME 4 7 FEBRUARY 8 HR 25 MIN 41 SEC TIME-START .36000000 03

GUIDANCE ANALYSIS COEFF.

	XO	YO	ZO	XDOTO	YDOTO	ZDOTO
MVX	.10735268-02	.26463218-03	.19730329-03	.16742982 01	-.48106972 00	-.18685118 00
MVY	-.67982311-03	-.64013987-03	-.13265472-03	-.11454897 01	.13072667 01	.39712089 00
MVZ	-.27104457-03	-.90279429-04	-.49242375-03	-.51332443 00	.42329646 00	.61107844 00

GUIDANCE ANALYSIS COEFF. -- MISS ONLY

	XO	YO	ZO	XDOTO	YDOTO	ZDOTO
MVX	.96553225-03	.45880361-03	.26585106-03	.15622450 01	-.94945855 00	-.40378533 00
MVY	-.79245626-03	-.43762842-03	-.61162693-04	-.12623558 01	.81875973 00	.17086902 00
MVZ	-.31822885-03	-.54432731-05	-.46247427-03	-.56228197 00	.21865096 00	.51629692 00

MIDCOURSE SENSITIVITIES

	X	Y	Z	XDOT	YDOT	ZDOT
M1	.11063375 00	-.53742943 00	-.25576971 00	.89120373 05	-.73384035 05	-.28802852 05
M2	-.35608028-01	.30043127 00	.21855685 00	-.47920477 05	.10686361 05	.84170217 05
M3	.11808343 00	.11243567 01	.59904008 00	-.64478693 04	.12318474 06	.88056923 05

-.66246349 00 -.69091751 00 -.28943934 00

	DELTA V (KM/SEC)	DELTA VC (KM/SEC)
DVX	.20929829-07	.30347327-08
DVY	.14826065-07	-.38376582-08
DVZ	.10033605-07	.22149932-08
MAGN	.27541662-07	.53706068-08

TIME 5 7 FEBRUARY 10 HR 25 MIN 41 SEC TIME-START .48000000 03

GUIDANCE ANALYSIS COEFF.

	XO	YO	ZO	XDOTO	YDOTO	ZDOTO
MVX	.10861021-02	.26434746-03	.19754621-03	.16929074 01	-.47837647 00	-.18453919 00
MVY	-.71133197-03	-.67127245-03	-.14763989-03	-.12005666 01	.13759838 01	.42735191 00
MVZ	-.28415001-03	-.10329410-03	-.50392225-03	-.53727249 00	.45501796 00	.63023958 00

GUIDANCE ANALYSIS COEFF. -- MISS ONLY

	XO	YO	ZO	XDOTO	YDOTO	ZDOTO
MVX	.10073091-02	.47804913-03	.27891254-03	.16300376 01	-.99014796 00	-.42284974 00
MVY	-.79642559-03	-.44048229-03	-.59767164-04	-.12684637 01	.82328886 00	.16998504 00
MVZ	-.32035421-03	-.51013884-05	-.46653563-03	-.56616022 00	.21986663 00	.52073944 00

MIDCOURSE SENSITIVITIES

	X	Y	Z	XDOT	YDOT	ZDOT
M1	.14519854 00	-.40379777 00	-.18351685 00	.88190850 05	-.70063793 05	-.27257600 05
M2	-.52699260-01	.19445344 00	.23283059 00	-.47599134 05	.89563285 04	.82541577 05
M3	.16646598 00	.91008236 00	.51596449 00	-.75077385 04	.11596135 06	.84082213 05

-.64855135 00 -.70041227 00 -.29799964 00

	DELTA V (KM/SEC)	DELTA VC (KM/SEC)
DVX	.21439502-07	.31526719-08
DVY	.15877645-07	-.38714780-08
DVZ	.10640653-07	.22381289-08
MAGN	.28722384-07	.54714626-08

TIME 6 7 FEBRUARY 12 HR 25 MIN 41 SEC TIME-START .60000000 03

GUIDANCE ANALYSIS COEFF.

	XO	YO	ZO	XDOTO	YDOTO	ZDOTO
MVX	.11014453-02	.26341263-03	.19763564-03	.17154681 01	-.47373157 00	-.18112626 00
MVY	-.73873943-03	-.70090471-03	-.16066753-03	-.12489250 01	.14411432 01	.45509307 00
MVZ	-.29484580-03	-.11451887-03	-.51653331-03	-.55755433 00	.48401995 00	.65023474 00

GUIDANCE ANALYSIS COEFF. -- MISS ONLY

	XO	YO	ZO	XDOTO	YDOTO	ZDOTO
MVX	.10431707-02	.49458620-03	.29008196-03	.16882258 01	-.10250867 01	-.43917117 00
MVY	-.80324576-03	-.44501020-03	-.58335319-04	-.12790805 01	.83082792 00	.16945369 00
MVZ	-.32266406-03	-.41647231-05	-.47240268-03	-.57055882 00	.22082235 00	.52705315 00

MIDCOURSE SENSITIVITIES

	X	Y	Z	XDOT	YDOT	ZDOT
M1	.16852991 00	-.34233558 00	-.14974537 00	.87056394 05	-.67402946 05	-.26071460 05
M2	-.64941148-01	.14342848 00	.24284618 00	-.47173327 05	.77593821 04	.80827439 05
M3	.17932970 00	.80356832 00	.47504896 00	-.87640568 04	.10983060 06	.80529642 05
		-.63846156 00	-.70673652 00	-.30477913 00		

	DELTA V (KM/SEC)	DELTA VC (KM/SEC)
DVX	.22102478-07	.32542775-08
DVY	.16942462-07	-.39213022-08
DVZ	.11273206-07	.22757369-08
MAGN	.30044163-07	.55808522-08

TIME 7 7 FEBRUARY 14 HR 25 MIN 41 SEC TIME-START .72000000 03

GUIDANCE ANALYSIS COEFF.

	XO	YO	ZO	XDOTO	YDOTO	ZDOTO
MVX	.11187826-02	.26198919-03	.19758237-03	.17408658 01	-.46761955 00	-.17686865 00
MVY	-.76485432-03	-.73079307-03	-.17310558-03	-.12953006 01	.15067368 01	.48249879 00
MVZ	-.30458990-03	-.12519195-03	-.53023479-03	-.57654281 00	.51264683 00	.67145748 00

GUIDANCE ANALYSIS COEFF. -- MISS ONLY

	XO	YO	ZO	XDOTO	YDOTO	ZDOTO
MVX	.10768446-02	.51012931-03	.30053183-03	.17428596 01	-.10579038 01	-.45445792 00
MVY	-.81218222-03	-.45076195-03	-.56925037-04	-.12930505 01	.84058918 00	.16923371 00
MVZ	-.32525622-03	-.29128151-05	-.47950308-03	-.57556029 00	.22176503 00	.53466631 00

MIDCOURSE SENSITIVITIES

	X	Y	Z	XDOT	YDOT	ZDOT
M1	.18555465 00	-.31023471 00	-.13172704 00	.85779059 05	-.65065494 05	-.25064481 05
M2	-.74218708-01	.11501594 00	.25081923 00	-.46671112 05	.68380781 04	.79049469 05
M3	.17950837 00	.74183940 00	.45167141 00	-.10060706 05	.10428510 06	.77200505 05
		-.63039219 00	-.71141026 00	-.31064631 00		

	DELTA V (KM/SEC)	DELTA VC (KM/SEC)
DVX	.22878104-07	.33500123-08
DVY	.18055253-07	-.39825916-08
DVZ	.11945474-07	.23223696-08
MAGN	.31497526-07	.56988611-08

TIME 8 7 FEBRUARY 16 HR 25 MIN 41 SEC TIME-START .84000000 03

GUIDANCE ANALYSIS COEFF.

	XO	YO	ZO	XDOTO	YDOTO	ZDOTO
MVX	.11377954-02	.26010663-03	.19736740-03	.17686304 01	-.46014836 00	-.17182169 00
MVY	-.79105853-03	-.76190578-03	-.18564829-03	-.13420456 01	.15749605 01	.51071475 00
MVZ	-.31408437-03	-.13594630-03	-.54509664-03	-.59540284 00	.54215102 00	.69421852 00

GUIDANCE ANALYSIS COEFF. -- MISS ONLY

	XO	YO	ZO	XDOTO	YDOTO	ZDOTO
MVX	.11100992-02	.52549179-03	.31081850-03	.17968090 01	-.10903205 01	-.46952050 00
MVY	-.82282625-03	-.45750639-03	-.55518763-04	-.13097245 01	.85214684 00	.16925129 00
MVZ	-.32812222-03	-.14352631-05	-.48759372-03	-.58112046 00	.22274690 00	.54332925 00

MIDCOURSE SENSITIVITIES

	X	Y	Z	XDOT	YDOT	ZDOT
M1	.19903019 00	-.29236611 00	-.12136145 00	.84392898 05	-.62901905 05	-.24156545 05
M2	-.81775195-01	.97606351-01	.25776576 00	-.46108696 05	.60771502 04	.77218069 05
M3	.17414680 00	.70196521 00	.43685685 00	-.11336056 05	.99096463 05	.74005386 05

-.62347598 00 -.71513306 00 -.31601015 00

	DELTA V (KM/SEC)	DELTA VC (KM/SEC)
DVX	.23752559-07	.34448393-08
DVY	.19239907-07	-.40532466-08
DVZ	.12669000-07	.23759881-08
MAGN	.33088693-07	.58258943-08

TIME 9 7 FEBRUARY 18 HR 25 MIN 41 SEC TIME-START .96000000 03

GUIDANCE ANALYSIS COEFF.

	XO	YO	ZO	XDOTO	YDOTO	ZDOTO
MVX	.11583496-02	.25773315-03	.19695655-03	.17985512 01	-.45125514 00	-.16595085 00
MVY	-.81817419-03	-.79490444-03	-.19872695-03	-.13905785 01	.16473119 01	.54049402 00
MVZ	-.32373103-03	-.14717659-03	-.56123048-03	-.61482085 00	.57335856 00	.71880316 00

GUIDANCE ANALYSIS COEFF. -- MISS ONLY

	XO	YO	ZO	XDOTO	YDOTO	ZDOTO
MVX	.11439214-02	.54112711-03	.32125324-03	.18516756 01	-.11232974 01	-.48481205 00
MVY	-.83496368-03	-.46512999-03	-.54087752-04	-.13287597 01	.86528265 00	.16944775 00
MVZ	-.33123645-03	.24301762-06	-.49657219-03	-.58718586 00	.22376675 00	.55293374 00

MIDCOURSE SENSITIVITIES

	X	Y	Z	XDOT	YDOT	ZDOT
M1	.21046568 00	-.28222979 00	-.11516219 00	.82917717 05	-.60836990 05	-.23306919 05
M2	-.88329887-01	.86160598-01	.26419339 00	-.45495780 05	.54182974 04	.75338786 05
M3	.16597702 00	.67392105 00	.42668970 00	-.12561772 05	.94148796 05	.70898713 05

-.61724782 00 -.71826706 00 -.32108808 00

	DELTA V (KM/SEC)	DELTA VC (KM/SEC)
DVX	.24723456-07	.35415202-08
DVY	.20516253-07	-.41323340-08
DVZ	.13454554-07	.24358561-08
MAGN	.34830890-07	.59625451-08

TIME 10 7 FEBRUARY 20 HR 25 MIN 41 SEC TIME-START .10800000 04

GUIDANCE ANALYSIS COEFF.

	XO	YO	ZO	XDOTO	YDOTO	ZDOTO
MVX	.11804149-02	.25481290-03	.19630937-03	.18305655 01	-.44080422 00	-.15917996 00
MVY	-.84681490-03	-.83035450-03	-.21267188-03	-.14419720 01	.17250650 01	.57244994 00
MVZ	-.33381108-03	-.15918601-03	-.57878342-03	-.63529549 00	.60694390 00	.74551228 00

GUIDANCE ANALYSIS COEFF. -- MISS ONLY

	XO	YO	ZO	XDOTO	YDOTO	ZDOTO
MVX	.11789897-02	.55734813-03	.33204771-03	.19085606 01	-.11574955 01	-.50064172 00
MVY	-.84849553-03	-.47358710-03	-.52601211-04	-.13499956 01	.87990024 00	.16977809 00
MVZ	-.33457099-03	.21262376-05	-.50640751-03	-.59370836 00	.22480299 00	.56344433 00

MIDCOURSE SENSITIVITIES

	X	Y	Z	XDOT	YDOT	ZDOT
M1	.22069439 00	-.27670803 00	-.11144343 00	.81365027 05	-.58826872 05	-.22492267 05
M2	-.94289333-01	.78226517-01	.27039421 00	-.44838164 05	.48281172 04	.73414198 05
M3	.15621880 00	.65281382 00	.41926084 00	-.13722296 05	.89375567 05	.67854499 05

-.61142292 00 -.72102597 00 -.32601163 00

	DELTA V (KM/SEC)	DELTA VC (KM/SEC)
DVX	.25794150-07	.36419747-08
DVY	.21903578-07	-.42195740-08
DVZ	.14313434-07	.25018604-08
MAGN	.36742064-07	.61096717-08

Page intentionally left blank

Page intentionally left blank

REFERENCES

1. Bellcomm, Inc., Document No. 63 2001, to E. M. Boughton from T. H. Thompson, dated 22 January 1963. (Conf.)

2. Bellcomm, Inc., Document No. 63 2003, to E. M. Boughton from T. H. Thompson, dated 14 February 1963. (Conf.)

3. Bellcomm, Inc., Document No. 63 2006, to E. M. Boughton from T. H. Thompson, dated 5 March 1963. (Conf.)

4. STL Report No. 9861.2-302, dated 6 February 1963. (Conf.)

5. STL Report No. 9861.2-314, dated 6 March 1963. (Conf.)

6. Bellcomm, Inc., Document No. 63 2009, "Data for Apollo Reference Trajectory Simulations - (Issue 0)", dated 8 April 1963. (Conf.)

7. STL Report, "Lunar Orbit Rendezvous Reference Trajectory Data Package - Issue 0", dated 31 March 1963.

   Volume 1 - Document No. 8408-6005-RC-000 (Conf.)
   Volume 2 - Document No. 8408-6006-RC-000 (Conf.)
   Volume 3 - Document No. 8408-6007-RC-000 (Conf.)
   Volume 4 - Document No. 8408-6008-RC-000 (Conf.)